

**DEPOLYMERIZATION OF LIGNIN OVER
HETEROGENEOUS CATALYST HAVING ACIDIC
FUNCTIONALITY**

A THESIS SUBMITTED TO THE
SAVITRIBAI PHULE PUNE UNIVERSITY

FOR THE DEGREE OF
DOCTOR OF PHILOSOPHY

IN
CHEMISTRY

BY
DEEPA A. K.

Dr. PARESH L. DHEPE
(RESEARCH GUIDE)

**CATALYSIS AND INORGANIC CHEMISTRY DIVISION
CSIR-NATIONAL CHEMICAL LABORATORY**

PUNE 411008

INDIA

NOVEMBER 2014

DECLARATION BY RESEARCH GUIDE

Certified that the work incorporated in the thesis entitled: **“Depolymerization of lignin over heterogeneous catalyst having acidic functionality.”** submitted by Ms. Deepa A. K., for the Degree of *Doctor of Philosophy*, was carried out by the candidate under my supervision at Catalysis and Inorganic Chemistry Division, National Chemical Laboratory, Pune-411008, India. Such material as has been obtained from other sources has been duly acknowledged in the thesis.

Dr. Paresh L. Dhepe
(Research Guide)
Tel. 91-20-25902024
E-mail: pl.dhepe@ncl.res.in

21st November 2014, Pune

DECLARATION BY RESEARCH SCHOLAR

I hereby declare that work reported in the thesis entitled **“Depolymerization of lignin over heterogeneous catalyst having acidic functionality.”** submitted for the *Degree of Doctor of Philosophy* to Savitribai Phule Pune University, has been carried out by me at Catalysis and Inorganic Chemistry Division, National Chemical Laboratory, Pune-411008, India, under the supervision of Dr. Paresh L. Dhepe. The work is original and has not been submitted in part or full by me for any other degree or diploma to this or any other University.

Deepa A. K.

.....DEDICATED

TO MY BELOVED

PARENTS

&

HUSBAND

Acknowledgement

*It gives me immense pleasure to express my sincere gratitude to my supervisor and mentor **Dr. Paresh L. Dhepe** for his excellent guidance, continuous encouragement, and support in achieving this entire endeavour. Wholeheartedly, I am very much grateful to him for motivating me in the field of Catalysis. Without his encouragement and constant guidance, I could not have finished my doctoral degree. Working with him was really a great pleasure and fetched me a lot of learning experience. His tireless attitude has been an impetus for me throughout the course of study. My deepest personal regards are due for him forever.*

My heartfelt thanks to Dr. R. Nandini Devi, Dr. C. V. V. Satyanarayana, Dr. T. Raja and Dr. A. A. Kelkar for their valuable discussions and helping me in every possible way. I sincerely acknowledge the help provided by Dr. Rajamohanan, Dr. Sayam Sen Gupta, Dr. V. Panchagnula, Dr. P. A. Joy, Dr. Patil and Dr. Jayakannan.

I wish to convey my deepest gratitude to Dr. A. P. Singh, Head, Catalysis Division for providing the divisional facilities for my research work.

It gives me great pleasure to thank my labmates Prasenjit, Anup, Sagar, Sandip, Richa, Manisha, Himani, Dr. Ramakanta Sahu, Dr. Atul Prashar, Dr. Manoj, Tanushree, Sanil and Ajay for their kind help and support, invaluable discussions which we shared and helped in maintaining a lively environment in the laboratory.

I would like to express my appreciation to my friends Rajesh, Jijil, Leena, Soumya, Dr. Kala Raj, Sourik, Shubin, Sumona, Priti, Anish, Shoy, Sanjay, Nishita, Kanna, Hanmat, Reji, Joby, Unni, Athira, Anjali, Prajitha, Nivedita, Dr. Debashish, Dr. Anal, Dr. Chandan, Dr. Sumantra, Dr. Basab Dhar, Shyam, Krishanu, Saikat, Prithvi, Subhadeep, Anjan, Arpan, Sankho, Souman, Munmun, Bhavana for their help and support during my doctoral study.

A special thanks to my roommates Vinisha, Bindu, Nisha and Manisha, from whom I received support and encouragement during my doctoral studies. I would like to express my appreciation to my friends Ayisha, Gauri, Hifsu, Christy, Asha, Raj, Nuthan, Nanda, Deepthi and Nidhina for spending wonderful time with them.

It gives me great pleasure to thank my parents, my brother and family members, for their love and unconditional support. I must acknowledge my husband and best friend Anupam without whose love, encouragement and editing assistance, I would not have finished this thesis.

Finally, my thanks are due to Council of Scientific and Industrial Research, Government of India, for awarding the research fellowship, and to Dr. S. Sivaram, former Director and Dr. Sourav Pal, Director, National Chemical Laboratory, to carry out my research work and extending all possible infrastructural facilities, and to allow me to submit this work in the form of a thesis for the award of Ph.D. degree.

.....Deepa

ABSTRACT

Lignocellulosic biomass can act as a good alternative to fossil feedstocks for the production of liquid transportation fuels and chemicals without impacting nation's food supply. Lignin comprises 15-25 % of lignocellulosic biomass and is the only renewable resource that can be efficiently valorized into aromatic monomers, which can be used in the form of fuel additives or octane enhancers and chemicals. Therefore several researches are performed for the direct and efficient conversion of lignin into aromatic monomers. Earlier reports on the depolymerization reactions of lignin were associated with the drawbacks like they either employ homogeneous catalysts for lignin depolymerization or use harsh reaction conditions ($T > 340\text{ }^{\circ}\text{C}$), those may increase the possibility for the formation of degradation products. In previous reports it was also observed that depolymerization of lignin was performed using precious metal catalysts, which increases the capital cost of the reaction. Additionally, most of the earlier studies were done using model compounds instead of using actual lignin substrates. In view of these points, I have focused my studies on developing an efficient method for the depolymerization lignin into aromatic monomers using solid acid catalysts (structured and amorphous) under milder reaction conditions ($T \leq 250\text{ }^{\circ}\text{C}$). Furthermore, in order to upgrade the fuel efficiency of lignin derived aromatic monomers hydrodeoxygenation (HDO) reactions were performed using supported metal catalysts.

Considering the above points, work has been carried out and hence my Ph.D. thesis is divided into 5 chapters.

Chapter 1 discusses about the importance of using lignin as a renewable source of carbon for the production of fuels and chemicals. In this chapter I have discussed about the linkages and functional groups present in lignin and also explained about the various isolation techniques used for lignin isolation from lignocellulosic biomass. Chapter 1 is especially a comprehensive review about the different methods used for depolymerization of lignin. This chapter also gives a brief introduction about various types of solid acid catalysts employed in depolymerization reactions of lignin and also gives an idea why the proposed process is superior over previous reports on depolymerization studies of lignin. Additionally this chapter discusses the previous reports on hydrodeoxygenation studies of lignin derived aromatic monomers and explains the major drawbacks associated with the conventional methods.

Chapter 2A includes the details on characterizations performed on various types of actual lignin substrates using various physico-chemical techniques. This chapter also discusses the details on the isolation of lignin from sugarcane bagasse using organosolv method. Structural and functional properties of all these lignins were studied using MALDI-TOF, GPC, CHNS, ICP-OES, SEM-EDAX, FTIR, NMR (^1H and ^{13}C), UV-Vis and TGA-DTA analysis. Details on the solubilities of lignin in various solvents were also discussed in this chapter.

Chapter 2B discusses about the synthesis and characterization of solid acid catalysts and supported metal catalysts used for the depolymerization reactions of lignin and HDO studies of lignin derived aromatic monomers, respectively. Various physico-chemical techniques were used to study the properties of both solid acids and supported metal catalysts. XRD technique was used to identify the structure, phase purity and crystallinity of the materials and also to determine the crystalline size of metal nanoparticles. NH_3 -TPD was used for acidity measurements of the samples. ICP-OES analysis was performed to determine the elemental composition of the materials. N_2 -sorption studies were performed to determine the textural properties like surface area, pore volume and pore diameter. HRTEM analysis was performed to determine the particle size and morphology of supported metals catalysts.

Chapter 3A discusses the depolymerization of dealkaline lignin substrate into aromatic monomers using various solid acid catalysts. Structured and amorphous solid acid catalysts were employed for depolymerization reactions of lignin. Reactions were performed at $250\text{ }^\circ\text{C}$ with 0.7 MPa N_2 for 30 min. in $\text{H}_2\text{O}:\text{CH}_3\text{OH}$ (1:5 v/v, 30 mL) solvent. The aromatic monomer formation was evaluated using various techniques like GC-FID, GC-MS, HPLC, LC-MS, GPC, MALDI-TOF, CHNS, NMR and FTIR analysis. Quantification of these aromatic monomers were done by injecting calibration standards which were procured commercially and it was found that 90 % of the products extracted using THF solvent from the reaction mixture were confirmed to be aromatic monomers. Among the solid acid catalysts tested, H-USY (Si/Al = 15) was found to be giving maximum amount of aromatic monomers (60 %). But the recycle studies performed over H-USY (Si/Al = 15) catalysts showed a drastic decrease in the activity of the catalyst. This decrease in the catalytic activity of H-USY (Si/Al = 15) was due to poisoning of active sites by Na contamination in dealkaline substrate and also due to the structural deformation happened during the

course of the reaction. Therefore amorphous solid acid catalysts ($\text{SiO}_2\text{-Al}_2\text{O}_3$ (Si/Al = 5.3)) were suggested as a better catalyst for performing further studies on depolymerization of lignin into aromatic monomers.

Chapter 3B discusses the solid acid catalysed depolymerization of six different types of actual lignin substrates into aromatic monomers using amorphous solid acid catalysts ($\text{SiO}_2\text{-Al}_2\text{O}_3$ (Si/Al = 5.3)). It was observed that at a temperature of 250 °C with 0.7 MPa N_2 at RT, in $\text{H}_2\text{O}:\text{CH}_3\text{OH}$ (1:5 v/v, 30 mL) solvent system, at 30 min., 1000 rpm with $\text{SiO}_2\text{-Al}_2\text{O}_3$ (Si/Al = 5.3) catalyst maximum amount of aromatic monomers (58 %) can be obtained. The lignin derived aromatic monomers obtained were isolated in pure form by column chromatography (3 nos.) and were well characterized. From various characterization studies it was understood that $\text{SiO}_2\text{-Al}_2\text{O}_3$ (Si/Al = 5.3) catalyst was also undergoing structural deformation under the reaction conditions employed. It was also observed that the acidic sites of the catalyst were poisoned by Na contamination present in the lignin substrate (dealkaline lignin). Even the amorphous catalysts were undergoing few changes but were still found to be recyclable and gave high yields of aromatic monomers.

Chapter 4 discusses the HDO studies of lignin derived aromatic monomers over supported metal catalysts under similar reaction conditions. Phenol, guaiacol and eugenol substrates were chosen for HDO reactions since they are the true representatives of lignin derived aromatic monomers. From these studies it was understood that irrespective of metal, HDO reactions happens only if the support was acidic. HDO studies were also performed over a physical mixture of model compounds (guaiacol and eugenol), which mimicks the lignin derived aromatic monomer mixture, using supported metal catalysts. These studies will help to develop a suitable supported metal catalyst for the one pot conversion of lignin into hydrocarbon fuels having high efficiency.

Chapter 5 summarizes the observations and gives overall conclusion of the work done. As a whole this thesis describes the solid acid catalysed depolymerization of actual lignin substrates into aromatic monomers under milder reaction conditions and also includes the HDO studies performed on lignin derived aromatic monomers using supported metal catalysts.

TABLE OF CONTENTS

	Page
ACKNOWLEDGEMENT	i
ABSTRACT	iii
LIST OF FIGURES	xiii
LIST OF SCHEMES	xviii
LIST OF TABLES	xix
ABBREVIATIONS/NOTATIONS	xxi
1. INTRODUCTION AND LITERATURE SURVEY	
1.1. INTRODUCTION	1
1.2. BIOMASS AS A RENEWABLE SOURCE OF CARBON	2
1.3. BIO-REFINERY CONCEPT	4
1.4. LIGNOCELLULOSIC BIOMASS	5
1.4.1. Cellulose and hemicellulose	6
1.4.2. Lignin	7
1.5. LIGNIN ISOLATION TECHNIQUES	11
1.5.1. Kraft lignin method	12
1.5.2. Lignosulfonate method	13
1.5.3. Organosolv method	15
1.6. AVAILABILITY OF LIGNIN	18
1.7. VALORIZATION OF LIGNIN	18
1.8. LIGNIN DEPOLYMERIZATION	20
1.8.1. Thermal depolymerization of lignin	20
1.8.1.1. Pyrolysis	20
1.8.1.2. Gasification	21
1.8.2. Chemical depolymerization of lignin	22
1.8.2.1. Base catalysed depolymerization (BCD)	22
1.8.2.2. Acid catalysed depolymerization	23
1.8.2.3. Metal catalysed depolymerization	25
1.8.2.4. Supercritical fluid assisted depolymerization	26

1.8.2.5. Ionic liquid (IL) assisted depolymerization	27
1.8.2.6. Oxidative depolymerization	28
1.8.3. Solid acid catalysts	29
1.8.3.1. Structured solid acid catalysts	29
1.8.3.2. Amorphous solid acid catalysts	32
1.9 HYDRODEOXYGENATION STUDIES OF LIGNIN DERIVED AROMATIC MONOMERS	32
1.10. SCOPE AND OBJECTIVE OF THESIS	35
1.11. REFERENCES	39
2. LIGNIN AND CATALYST CHARACTERIZATION	
2.1. LIGNIN CHARACTERIZATION TECHNIQUES	44
2.1.1. MALDI-TOF mass spectroscopy and GPC analysis	44
2.1.2. CHNS elemental analysis	46
2.1.3. ICP-OES and SEM-EDAX analysis	46
2.1.4. FT-IR Spectroscopy	47
2.1.5. ¹ H and ¹³ C NMR analysis	48
2.1.6. XRD analysis	48
2.1.7. UV-Vis analysis	49
2.1.8. TGA-DTA analysis	49
2.2 CATALYST CHARACTERIZATION TECHNIQUES	50
2.2.1. ICP-OES analysis	50
2.2.2. XRD analysis	51
2.2.3. N ₂ sorption analysis	51
2.2.4. NH ₃ -TPD and CO ₂ -TPD analysis	52
2.2.5. HRTEM analysis	53
2.2.6. ²⁹ Si and ²⁷ Al MAS NMR	53
2A. LIGNIN ISOLATION AND CHARACTERIZATION	
2A.1. INTRODUCTION	54
2A.2. RESULTS AND DISCUSSIONS	56
2A.2.1. Lignin extraction from sugarcane bagasse	56
2A.2.2. MALDI-TOF mass spectroscopy and GPC analysis	57
2A.2.3. CHNS elemental analysis	58

2A.2.4.	ICP-OES and SEM-EDAX analysis	59
2A.2.5.	FT-IR Spectroscopy	62
2A.2.6.	Solid state ¹³ C NMR analysis	65
2A.2.7.	XRD analysis	68
2A.2.8.	UV-Vis analysis	69
2A.2.9.	TGA-DTA analysis	70
2A.2.10.	Solubility of lignin	78
2A.3.	CONCLUSIONS	80
2A.4.	REFERENCES	81
2B.	CATALYST SYNTHESIS AND CHARACTERIZATION	
2B.1.	INTRODUCTION	84
2B.1.1.	Solid acid catalysts	84
2B.1.2.	Supported metal catalysts	87
2B.2.	MATERIALS	88
2B.2.1.	Solid acid catalysts	88
2B.2.2.	Supported metal catalysts	88
2B.3.	SYNTHESIS	88
2B.3.1.	Synthesis of 10 wt % MoO ₃ /SiO ₂	89
2B.3.2.	Synthesis of hydrotalcite (HT)	89
2B.3.3.	Synthesis of supported metal catalysts	89
2B.4.	RESULTS AND DISCUSSIONS	90
2B.4.1.	Solid acid catalysts	90
2B.4.1.1.	XRD analysis	90
2B.4.1.2.	N ₂ sorption analysis	91
2B.4.1.3.	NH ₃ -TPD analysis	93
2B.4.1.4.	ICP-OES analysis	95
2B.4.2.	Supported metal catalysts	96
2B.4.2.1.	XRD analysis	96
2B.4.2.2.	ICP-OES analysis	98
2B.4.2.3.	N ₂ sorption analysis	99
2B.4.2.4.	HRTEM analysis	99
2B.5.	CONCLUSIONS	102
2B.6.	REFERENCES	103

3.	SOLID ACID CATALYSED DEPOLYMERIZATION OF LIGNIN INTO AROMATIC MONOMERS AND ISOLATION OF AROMATIC MONOMERS	
3A.	DEPOLYMERIZATION OF LIGNIN USING STRUCTURED SOLID ACIDS	
3A.1.	INTRODUCTION	104
3A.2.	EXPERIMENTAL	106
3A.2.1.	Materials	106
3A.2.2.	Depolymerization of lignin	106
3A.2.3.	Analysis	107
3A.2.3.1.	GC- FID	108
3A.2.3.2.	GC-TCD	108
3A.2.3.3.	GC-MS	109
3A.2.3.4.	HPLC	109
3A.2.3.5.	LC-MS	109
3A.2.3.6.	GPC Analysis	110
	3A.2.3.6.1. DMF-GPC	110
	3A.2.3.6.2. THF-GPC	110
3A.2.3.7.	NMR analysis	110
3A.2.4.	Yield calculations	110
3A.2.5.	Mass balance calculation	112
3A.2.6.	Substrate/Catalyst (S/C) calculation	114
3A.3.	RESULTS AND DISCUSSIONS	114
3A.3.1.	Evaluation of catalytic activities of various solid acid catalysts in depolymerization of dealkaline lignin reaction	114
3A.3.2.	Confirmation of aromatic monomers formation	117
3A.3.2.1.	GC-FID, GC-MS, HPLC, LC-MS	117
3A.3.2.2.	GPC and MALDI-TOF analysis	121
3A.3.2.3.	CHNS elemental analysis and UV-Vis analysis	123
3A.3.3.	Quantification of aromatic monomers	125
3A.3.4.	Correlation between lignin and aromatic	127

	monomers structures and functional groups	
	3A.3.4.1. FTIR analysis	127
	3A.3.4.2. ¹ H and ¹³ C NMR analysis	128
	3A.3.5. Analysis of gases and reproducibility of catalytic activities	132
	3A.3.6. Comparison of catalytic activities between solid acids and homogeneous acids	132
	3A.3.7. Correlation between the acidity and the activity of solid acid catalysts in dealkaline lignin depolymerization reaction	134
	3A.3.8. Study on reuse, stability and characterization of H-USY catalyst	135
3A.4.	CONCLUSIONS	141
3A.5.	REFERENCES	142
3B.	DEPOLYMERIZATION OF LIGNIN USING AMORPHOUS SOLID ACIDS AND ISOLATION OF AROMATIC MONOMERS	
3B.1.	INTRODUCTION	144
3B.2.	RESULTS AND DISCUSSIONS	144
	3B.2.1. Study on amorphous SiO ₂ -Al ₂ O ₃ catalysts	144
	3B.2.1.1. Effect of lignin substrates	144
	3B.2.1.2. Effect of temperature and pressure	146
	3B.2.1.3. Effect of reaction medium	148
	3B.2.1.4. Influence of reaction time and stirring speed	150
	3B.2.2. Isolation of aromatic monomers by column chromatography	152
	3B.2.3. Depolymerization of various lignin substrates	154
	3B.2.4. Study on reuse, stability and characterization of SiO ₂ -Al ₂ O ₃ catalyst	155
3B.3.	CONCLUSIONS	162
3B.4.	REFERENCES	164
4.	HYDRODEOXYGENATION OF LIGNIN DERIVED	

AROMATIC MONOMERS OVER SUPPORTED METAL CATALYSTS

4.1.	INTRODUCTION	165
4.2.	EXPERIMENTAL	167
4.2.1.	Catalyst synthesis	167
4.2.2.	Hydrodeoxygenation of lignin derived aromatic monomers	167
4.2.3.	Analysis	168
4.2.3.1.	GC-FID	168
4.2.3.2.	GC-MS	169
4.2.4.	Conversion, selectivity and yield calculation	169
4.3.	RESULTS AND DISCUSSIONS	169
4.3.1.	Studies on HDO of phenol	170
4.3.2.	Studies on HDO of guaiacol	172
4.3.2.1.	Catalytic studies using Pd supported catalysts	173
4.3.2.2.	Effect of acidic support on guaiacol HDO reactions	177
4.3.2.3.	Catalytic studies using Ru and Pt catalysts	178
4.3.2.4.	Effect of time on the guaiacol HDO reactions	180
4.3.2.5.	Effect of temperature and pressure on guaiacol HDO reactions	182
4.3.2.6.	Catalyst recyclability	185
4.3.2.7.	Reaction pathway for guaiacol HDO reactions using supported metals	187
4.3.3.	Eugenol HDO studies	188
4.3.3.1.	Catalytic studies over Pd catalysts	189
4.3.3.2.	Catalytic studies over Pt and Ru catalysts	192

4.3.4.	The effect of electron density (deficiency or richness) of metal particles on supports	194
4.3.5.	Hydrodeoxygenation studies of guaiacol-eugenol mixtures	196
4.4.	CONCLUSIONS	197
4.5.	REFERENCES	199
5.	SUMMARY AND CONCLUSIONS	202
	PUBLICATIONS/SYMPOSIA/CONFERENCES	

List of Figures (Fig.)

Fig. 1.1.	Major sources of biomass	3
Fig. 1.2.	Bio-refinery concept for the conversion of biomass	5
Fig. 1.3.	Structure of cellulose and hemicellulose	7
Fig. 1.4.	Main precursors of lignin and their structures in lignin polymer	8
Fig. 1.5.	Major linkages present in lignin	10
Fig. 1.6.	Structure of softwood lignin	11
Fig. 1.7.	Structure of Kraft pine lignin	13
Fig. 1.8.	Mechanism of lignosulfonate formation	14
Fig. 1.9.	Structure of lignosulfonate lignin	15
Fig. 1.10.	Lignin valorization into value added products	19
Fig. 1.11.	Summary on the various processes by which lignin can be transformed into aromatic monomers or gases	21
Fig. 1.12.	Different types of solid acid catalysts	30
Fig. 1.13.	Brönsted and Lewis acid sites in zeolites	31
Fig. 2.1.	Different types of physisorption isotherm	52
Fig. 2A.1.	MALDI-TOF analysis of dealkaline lignin	57
Fig. 2A.2.	SEM-EDAX analysis of lignin	61
Fig. 2A.3a.	FTIR analysis of dealkaline lignin	62
Fig. 2A.3b.	FTIR analysis of organosolv lignin	62
Fig. 2A.3c.	FTIR analysis of alkali lignin	63
Fig. 2A.3d.	FTIR analysis of ORG lignin	63
Fig. 2A.3e.	FTIR analysis of EORG lignin	64
Fig. 2A.3f.	FTIR analysis of bagasse lignin	65
Fig. 2A.4a.	Solid state ^{13}C NMR spectra of dealkaline lignin	66
Fig. 2A.4b.	Solid state ^{13}C NMR spectra of organosolv lignin	66
Fig. 2A.4c.	Solid state ^{13}C NMR spectra of ORG lignin	67
Fig. 2A.4d.	Solid state ^{13}C NMR spectra of EORG lignin	67
Fig. 2A.5.	Liquid ^{13}C NMR of dealkaline lignin in $\text{CD}_3\text{OD}:\text{D}_2\text{O}$ (5:1 v/v) solvent	68
Fig. 2A.6.	XRD pattern of A) organosolv, B) dealkaline, C) ORG,	69

	D) EORG and E) bagasse lignin	
Fig. 2A.7.	UV-Vis analysis of A) organosolv B) dealkaline C) ORG D) alkali E) EORG lignin	70
Fig. 2A.8a.	TGA-DTA analysis of dealkaline lignin in N ₂ and air	73
Fig. 2A.8b.	TGA-DTA analysis of organosolv lignin in N ₂ and air	74
Fig. 2A.8c.	TGA analysis of alkali lignin in N ₂ and air	75
Fig. 2A.8d.	TGA-DTA analysis of ORG lignin in N ₂ and air	76
Fig. 2A.8e.	TGA-DTA analysis of EORG lignin in N ₂ and air.	77
Fig. 2A.8f.	TGA analysis of bagasse lignin in N ₂	78
Fig. 2B.1.	Structure of various types of zeolites adapted from IZA site [Source: Ref. 7]	85
Fig. 2B.2.	Structure of Montmorillonite (K10) clay [Source Ref. 10]	86
Fig. 2B.3a.	XRD pattern of H-USY, H-ZSM-5, H-BEA and H-MOR zeolites	90
Fig. 2B.3b.	XRD pattern of K10 clay, Al pillared clay, SiO ₂ -Al ₂ O ₃ and 10 wt% MoO ₃ /SiO ₂	91
Fig. 2B.4.	NH ₃ -TPD analysis of solid acid catalysts	94
Fig. 2B.5a.	XRD patterns of supported Pd catalysts.	97
Fig. 2B.5b.	XRD patterns of supported Pt catalysts	97
Fig. 2B.5c.	XRD patterns of supported Ru catalysts	98
Fig. 2B.6a.	HRTEM images of supported Pd catalysts	100
Fig. 2B.6b.	HRTEM images of supported Pt catalysts	100
Fig. 2B.6c.	HRTEM images of supported Ru catalysts	101
Fig. 3A.1.	Value addition of lignin	104
Fig. 3A.2.	Batch mode reactor used for depolymerization studies of lignin	107
Fig. 3A.3.	Scheme for the extraction of THF soluble products in dealkaline lignin reactions	111
Fig. 3A.4.	Catalyst evaluation study of dealkaline lignin depolymerization reaction	115
Fig. 3A.5.	GC-MS of the THF soluble products obtained in	116

	dealkaline lignin reaction	
Fig. 3A.6.	Products in the THF soluble mixture of dealkaline lignin reaction identified using GC-MS analysis	117
Fig. 3A.7a.	HPLC analysis of dealkaline lignin reaction mixture	119
Fig. 3A.7b.	GC-FID analysis of dealkaline lignin reaction mixture	120
Fig. 3A.8.	GPC (DMF) for dealkaline lignin	121
Fig. 3A.9.	GPC (DMF) for MeOH soluble reaction mixture	121
Fig. 3A.10.	GPC (THF) for THF soluble products	122
Fig. 3A.11.	UV-Vis analysis of (A) dealkaline lignin in methanol (B) THF soluble products	123
Fig. 3A.12.	UV-Vis analysis of standard compounds of aromatic monomer products of dealkaline lignin depolymerization, dissolved in methanol	124
Fig. 3A.13.	FTIR of dealkaline lignin and products	128
Fig. 3.14.	¹ H NMR of dealkaline lignin and products	130
Fig. 3A.15.	¹³ C NMR of dealkaline lignin and products	131
Fig. 3A.16a.	GC-MS analysis of HCl catalyzed depolymerization of dealkaline lignin.	133
Fig. 3A.16b.	GC-MS analysis of H ₂ SO ₄ catalyzed depolymerization of dealkaline lignin	133
Fig. 3A.17.	Correlation of the formation of aromatic monomers in dealkaline lignin depolymerization with the total acid sites of solid acid catalysts	134
Fig. 3A.18.	Recycle study H-USY catalyst in dealkaline lignin reaction	135
Fig. 3A.19.	NH ₃ -TPD of H-USY (Si/Al = 15) A) fresh B) spent catalyst	136
Fig. 3A.20.	Metal exchanged Brönsted acidic sites of zeolites with metal (Na ⁺) ion	136
Fig. 3A.21.	XRD pattern of H-USY (Si/Al = 15) catalyst, A) fresh B) Na- exchanged	138
Fig. 3A.22.	Recycle study H-USY catalyst in organosolv lignin reaction	139

Fig. 3A.23.	XRD pattern of H-USY (Si/Al = 15) catalyst, A) fresh B) spent-calcined	139
Fig. 3A.24.	²⁹ Si NMR of H-USY (Si/Al = 15) catalyst	141
Fig. 3A.25.	²⁷ Al NMR of H-USY (Si/Al = 15) catalyst	141
Fig. 3B.1.	Catalyst recycle study for organosolv lignin	145
Fig. 3B.2.	Catalyst recycle study for ORG lignin	145
Fig. 3B.3.	Effect of temperature on lignin depolymerization	147
Fig. 3B.4.	Effect of pressure on lignin depolymerization	147
Fig. 3B.5.	Effect of solvent on depolymerization	149
Fig. 3B.6.	Effect of time on depolymerization	151
Fig. 3B.7.	Effect of RPM on depolymerization	151
Fig. 3B.8.	Scheme for the isolation of products using column chromatography from THF soluble mixture of dealkaline lignin reaction	153
Fig. 3B.9.	Effect of various lignin substrates	155
Fig. 3B.10.	Recycle study SiO ₂ -Al ₂ O ₃ catalyst in dealkaline lignin reaction	156
Fig. 3B.11.	XRD pattern of SiO ₂ -Al ₂ O ₃ catalyst, A) fresh B) spent-calcined sample	156
Fig. 3B.12.	Pore size distribution (N ₂ sorption study) of fresh SiO ₂ -Al ₂ O ₃ catalyst	157
Fig. 3B.13.	Pore size distribution (N ₂ sorption study) of spent calcined SiO ₂ -Al ₂ O ₃ catalyst	158
Fig. 3B.14.	NH ₃ -TPD of SiO ₂ -Al ₂ O ₃ A) fresh B) spent	159
Fig. 3B.15.	²⁹ Si MAS NMR of SiO ₂ -Al ₂ O ₃ catalyst A) fresh B) spent	160
Fig. 3B.16.	²⁷ Al MAS NMR of SiO ₂ -Al ₂ O ₃ catalyst A) fresh B) spent	161
Fig. 3B.17.	Morphological changes occurred in SiO ₂ -Al ₂ O ₃ catalyst after lignin depolymerization reaction	162
Fig. 4.1.	Phenol HDO studies over supported metal catalysts	172
Fig. 4.2.	Effect of support on supported Pd catalysts in guaiacol HDO reactions	175

Fig. 4.3.	Effect of temperature on guaiacol HDO reactions using Pd/SA catalyst	182
Fig. 4.4.	Effect of hydrogen pressure on guaiacol HDO reactions using Pd/SA catalyst	184
Fig. 4.5.	Recycle study with (a) Ru/SA and (b) Pd/SA for guaiacol HDO reactions	185
Fig. 4.6.	XRD patterns of Ru/SA catalyst (a) fresh (b) spent	186
Fig. 4.7.	XRD patterns of Pd/SA catalyst (a) fresh (b) spent	186
Fig. 4.8.	Proposed reaction pathway for supported Pd catalysts in guaiacol HDO reactions	187
Fig. 4.9.	Proposed reaction pathway for supported Pt catalysts in guaiacol HDO reactions	188
Fig. 4.10.	Proposed reaction pathway for supported Ru catalysts in guaiacol HDO reactions	188
Fig. 4.11.	Effect of support on supported Pd catalysts in eugenol HDO reactions.	190
Fig. 4.12.	Possible formation of carbenium ion	192
Fig. 4.13.	Eugenol HDO reactions over Ru supported metal catalysts	193
Fig. 4.14.	Eugenol HDO reactions over Pt supported metal catalysts	194
Fig. 4.15.	XPS analysis of Pd/SA (Pd3d) catalyst	195
Fig. 4.16.	XPS analysis of Pd/C (Pd3d) catalyst	195
Fig. 4.17.	Mechanism proposed for ring hydrogenation versus HDO for lignin derived aromatic monomers	199
Fig. 5.1.	Catalyst evaluation study of dealkaline lignin depolymerization reaction	207
Fig. 5.2.	Effect of various lignin substrates	209
Fig. 5.3.	Effect of support on supported Pd catalysts in guaiacol HDO reactions	211

List of Schemes

Scheme 3A.1.	Depolymerization of lignin over solid acid catalysts into aromatic monomers	105
Scheme 4.1.	Hydrodeoxygenation of lignin derived aromatic monomers into hydrocarbons	165
Scheme 4.2.	Possible products formed in HDO of phenol	171
Scheme 4.3.	Possible products formed in HDO of guaiacol	173
Scheme 5.1.	Solid acid catalysed depolymerization of lignin into aromatic monomers and their further hydrodeoxygenation over supported metal catalysts	204

List of Tables

Table 1.1.	Summary on several types of linkages present in lignin	9
Table 1.2.	Functional groups present in softwood and hardwood lignin per 100 C9 units	10
Table 1.3.	Summary of lignin isolation techniques	17
Table 2A.1	GPC analysis of lignin	58
Table 2A.2.	CHNS elemental analysis of lignin	59
Table 2A.3.	ICP-OES and SEM-EDAX of lignin	60
Table 2A.4.	Summary on thermal degradation analysis of various lignin	71
Table 2A.5.	Solubility of lignin in various solvents	79
Table 2B.1.	Structural properties of zeolites used for depolymerization of lignin	84
Table 2B.2.	Summary on N ₂ sorption analysis of solid acid catalysts	92
Table 2B.3.	Summary on NH ₃ -TPD analysis of solid acid catalysts	95
Table 2B.4.	Summary on ICP-OES analysis of solid acid catalysts	96
Table 2B.5.	Summary on the ICP-OES analysis of supported metal catalysts	98
Table 2B.6.	Summary on N ₂ sorption analysis of supported metal catalysts	99
Table 2B.7.	Summary on average particle size and dispersion of supported metal catalysts determined using HRTEM analysis	101
Table 3A.1.	Quantification of monomeric products in dealkaline lignin reaction	126
Table 3A.2.	ICP-OES study of Fresh & Spent H-USY (Si/Al = 15) zeolite	137
Table 3A.3.	ICP-OES and NH ₃ -TPD data for fresh and metal-exchanged catalysts	138
Table 3A.4.	Nitrogen sorption study of Fresh & Spent H-USY (Si/Al	140

= 15) zeolites

Table 3B.1.	Summary on characterization of products isolated by column chromatography	154
Table 3B.2.	NH ₃ -TPD, N ₂ sorption & ICP-OES analysis of fresh and spent SiO ₂ -Al ₂ O ₃	158
Table 4.1.	Role of acidic support on the HDO of guaiacol	177
Table 4.2.	Guaiacol HDO over supported Ru and Pt catalysts	178
Table 4.3.	Time study for guaiacol HDO reactions using various supported metal catalysts	181
Table 4.4.	Effect of temperature on guaiacol HDO reactions using Pd/SA catalyst	183
Table 4.5.	Effect of hydrogen pressure on guaiacol HDO reactions using Pd/SA catalyst	184
Table 4.6.	HDO reactions of guaiacol and eugenol mixture over Pt catalysts	196

List of Abbreviations

AL	γ -Al ₂ O ₃
APR	Alcohol Pulping and Recovery
BCD	Base catalysed depolymerization
BCM	Billion Cubic Meter
BET	Braunauer-Emmett-Teller
BHT	Butylated hydroxyl toluene
BOE	Barrels of oil energy equivalent
CHNS	Carbon, Hydrogen, Nitrogen, Sulfur
DEE	Diethyl ether
DMBQ	2, 6-dimethoxy-1, 4-benzoquinone
DMF	Dimethyl formamide
DMSO	Dimethyl sulfoxide
DOE	Department of Energy
EORG	Etherified organosolv
EDAX	Energy Dispersive X-Ray Analysis
EtOAc	Ethyl acetate
FAU	Faujasite
FER	Ferrierte
FID	Flame ionization detector
FTIR	Fourier Transform Infrared
GC	Gas Chromatography
GC-MS	Gas Chromatography Mass Spectrometry
GPC	Gel Permeation Chromatography
HPLC	High Performance Liquid Chromatography
HRTEM	High Resolution Transmission Electron Microscopy
HT	Hydrotalcite
H-MOR	Mordenite (H-form)
H-USY	Ultra Stable Zeolite Y (H-form)
H-ZSM	Zeolite Socony Mobil (H-form)
HDO	Hydrodeoxygenation
ICP-OES	Inductively Coupled Plasma-Optical Emission Spectrometry

LC-MS	Liquid Chromatography Mass Spectrometry
LPG	Liquefied Petroleum Gas
LALS	Low Angle Light Scattering
MAS NMR	Magic Angle Spinning Nuclear Magnetic Resonance
Mn	Number Average Molecular Weight
MPa	Mega Pascal
MT	Metric Ton
MMT	Million Metric Ton
Mw	Weight Average Molecular Weight
NMR	Nuclear Magnetic Resonance
ORG	Organosolv
P.D	Polydispersity = (Mw/Mn)
RT	Room Temperature
SA	Silica Alumina
RI	Refractive Index
SAC	Strongly Acidic Cation Exchanged Resins
SBA	Santa Barbara Amorphous
SEM	Scanning Electron Microscopy
TCD	Thermal Conductivity Detector
THF	Tetrahydrofuran
TLC	Thin Layer Chromatography
TPD	Temperature Programmed Desorption
TGA-DTA	Thermo Gravimetric Analysis-Differential Thermal Analysis
USDA	US Department of Agriculture
UV-Vis	Ultraviolet-Visible
XRD	X-Ray Diffraction

CHAPTER 1

INTRODUCTION AND LITERATURE SURVEY

1.1. INTRODUCTION

Fossil feedstocks such as crude oil, coal and natural gas are non-renewable forms of energy, derived from dead organisms under high pressures and temperatures. Those are considered as primary source for the generation of energy, chemicals, and materials for our daily needs.¹⁻³ According to a survey done by US Energy Information Administration, in 2007, the primary sources of energy consists of crude oil (36.0 %), coal (27.4 %) and natural gas (23.0 %) which amount for 86.4 % of total energy generation from fossil feedstocks. On the other hand remaining energy can be generated from non-fossil sources, which include hydroelectric (6.3 %), nuclear (8.5 %) and others (geothermal, solar, tidal, wind, waste etc. (0.9 %)).⁴ In case of transportation sector almost 96 % of energy is derived from fossil feedstocks (mainly crude oil). It is estimated that the world's energy consumption is growing approximately at the rate of 2.3 % per year.⁵

Fossil feedstocks can act as a good source for the production of variety of fuels and chemicals. For instance, coal (one of the component of fossil resources) is primarily used as solid fuel to produce electricity and heat by combustion. Also, up on gasification, coal can produce syn-gas (CO and H₂), which can be further converted into transportation fuels such as gasoline, diesel etc. through Fischer Tropch process. Second major component of fossil feedstock is crude oil. In petro-refinery, crude oil can be refined into products like petroleum naptha, gasoline, diesel, asphalt base, heating oil, kerosene and liquefied petroleum gas (LPG). Crude oil can also be used in variety of ways since it contain hydrocarbons of varying molecular masses, lengths, forms (for e.g. paraffins, aromatics, napthenes, alkenes, dienes and alkynes). Third component of fossil feedstock is natural gas, which is a hydrocarbon mixture primarily consisting of CH₄ (70-90 %) along with other alkanes and even lesser percentage of CO₂ (0-8 %), N₂ (0-5 %) and H₂S (0-5 %).⁶

Fossil feedstocks have several advantages like; they are easily available and are capable of producing large amount of energy, fuels and chemicals. But due to rise in population, there is an obvious increase in the rate of consumption of fossil feedstocks. According to Ministry of petroleum and natural gas the annual production of crude oil in India for the year 2013-14 was ca. 37.88 MMT (Million Metric Ton) and the import of crude oil during the period was ca. 185 MMT.⁷ Similarly, natural gas production in India for the year of 2013-14 was ca. 35.406 BCM (Billion Cubic

Meter). Annual report of Indian coal ministry shows that in the year of 2013-14, ca. 565 MMT of coal is produced, with an import of 168.44 MMT.⁸ These information illustrates that there is a huge demand for fossil feedstocks, however there are still few drawbacks which have to be tackled. First drawback is that, fossil fuel reserves are finite, and the current consumption rate is increasing day-by-day because of the higher demand from industrialized countries and emerging economies. This may lead to inevitable depletion of these feedstocks within few decades.⁹ Second drawback is that the consumption of fossil feedstocks leads to net emissions of CO₂ into the atmosphere, which will contribute to global warming and climatic issues due to increase in the earth's surface temperature. It is estimated that combustion of fossil feedstocks can produce ca. 21.3 billion tonnes of CO₂ per year.¹⁰ But from this amount of CO₂ only 10.65 billion tonnes is absorbed by the plants during the natural processes like photosynthesis. Third drawback of fossil feedstocks is the uneven geographical distribution of their reserves, which arises political, economic and security issues worldwide.

Considering above points, it is essential to look for a renewable resource, which is abundant, easily available and also can possibly reduce the global warming issues. In this sense both, US and the EU are stimulating a gradual shift of current fossil feedstock based economy towards a more renewable energy based one, and have established ambitious goals to produce 20 % of fuels and 25 % of chemicals from renewable sources by 2030.^{1-3, 11}

1.2. BIOMASS AS A RENEWABLE SOURCE OF CARBON

Due to depletion in fossil feedstocks and along with an increase in demand it is very important to develop cheap and energy efficient processes for the production of fuels and chemicals. In this respect, biomass is the only current sustainable source of carbon which can generate fuels and chemicals similar to that derived from fossil feedstocks.¹² An important point for utilization of biomass as chemical raw material is its cost. For instance, crude oil price varies from \$ 40 to \$ 80 per barrel (i.e., \$ 7.1–14.2/GJ), which is much higher than the price of lignocellulosic biomass (\$ 0–3/GJ) proving the cost effectiveness of this raw material.¹³⁻¹⁵

Biomass can be defined as “the total mass of living organisms or recently living organisms in a given area or of a given species usually expressed as dry

weight.” It is a resource that can be used for the production of heat, power, fuels and chemicals in addition to the significant contribution for climate change mitigation. Biomass feedstocks include forestry residues, industrial wastes, agricultural crop waste, sewage waste, municipal solid waste, animal residues, sewage wastes etc.¹⁶ (Figure 1.1). Traditionally, biomass feedstocks like forest residues, wood chips, and municipal wastes are used to generate electricity or to produce heat by direct ignition. But since biomass is a good source of carbon, can also be valorized for the production of fuels and chemicals through bio-refinery concept.

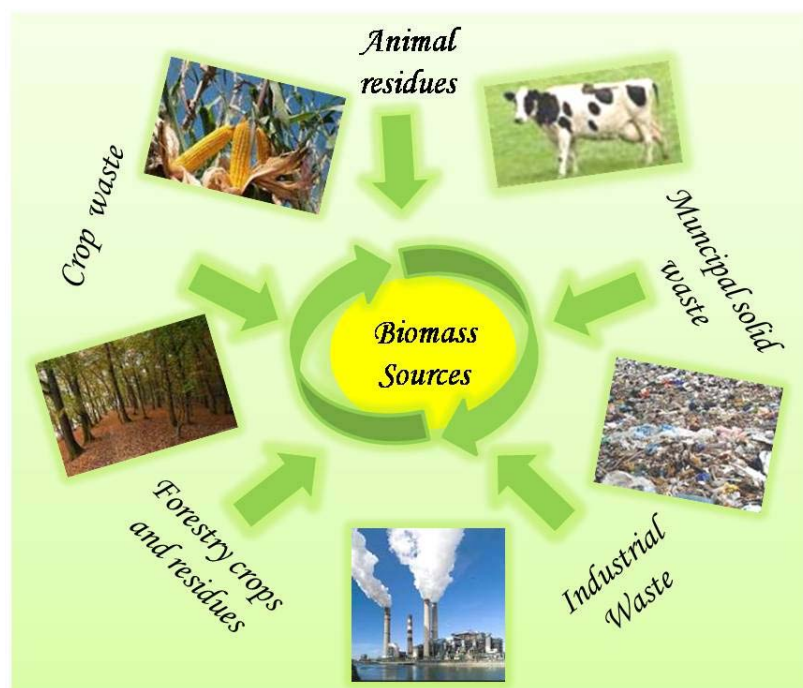


Figure 1.1. Major sources of biomass.

Biomass can be either plant derived or animal derived (chitin, cow dung etc.). Plant derived biomass includes edible (e.g. starch, sugars) and non edible portions (lignocellulosic biomass). Biomass has several advantages over conventional fossil feedstocks which can be listed as follows,

- a) Biomass is a renewable and sustainable source of carbon which is abundantly available. It can be found almost everywhere in the form of trees, seaweed or animal waste.
- b) It can be easily converted into high energy fuels (alcohol or gas) and chemicals, similar to those obtained from fossil feedstocks.

- c) It is less expensive in comparison to other resources such as coal, petroleum and natural gas.
- d) If produced in renewable basis biomass energy can reduce the net CO₂ in the atmosphere (responsible for global warming), as plants absorb it during photosynthesis.
- e) Since biomass has a very low concentration of sulfur it will help to reduce the acid rain phenomenon, which happens when fossil feedstocks are used.

Based on these advantages, biomass can act as a very good alternative for fossil feedstocks.

1.3. BIO-REFINERY CONCEPT

Bio-refinery is a facility similar to petro-refinery, which is meant to produce energy, fuels and chemicals from locally available biomass feedstock instead of using fossil feedstocks¹⁷ (Figure 1.2). In bio-refinery multiple products can be generated from the biomass feedstocks. The fuels generated from the biomass in a bio-refinery can be called as biofuels and can be classified into three categories,

- i. First generation biofuels, are generated from edible biomass. e.g. Bio-ethanol, produced by the fermentation of starch, sucrose etc. and biodiesel produced from fatty acids (oil).
- ii. Second generation biofuels are generated from non edible biomass ranging from lignocellulosics to municipal solid wastes.
- iii. Third generation biofuels are derived from microalgae and cyanobacteria (blue-green algae).

First generation biofuels have few drawbacks like low energy efficiency and those are also not recommended due to food verses fuel debate. The growing impacts on these concerns have increased an interest in developing second generation biofuels produced from non edible lignocellulosic biomass. Lignocellulosic biomass feedstocks include cereal straw, bagasse, forest residues and purpose grown energy crops such as vegetative grasses etc.

Accordingly, this thesis will focus on the valorization of lignocellulosic biomass into fuels and chemicals.

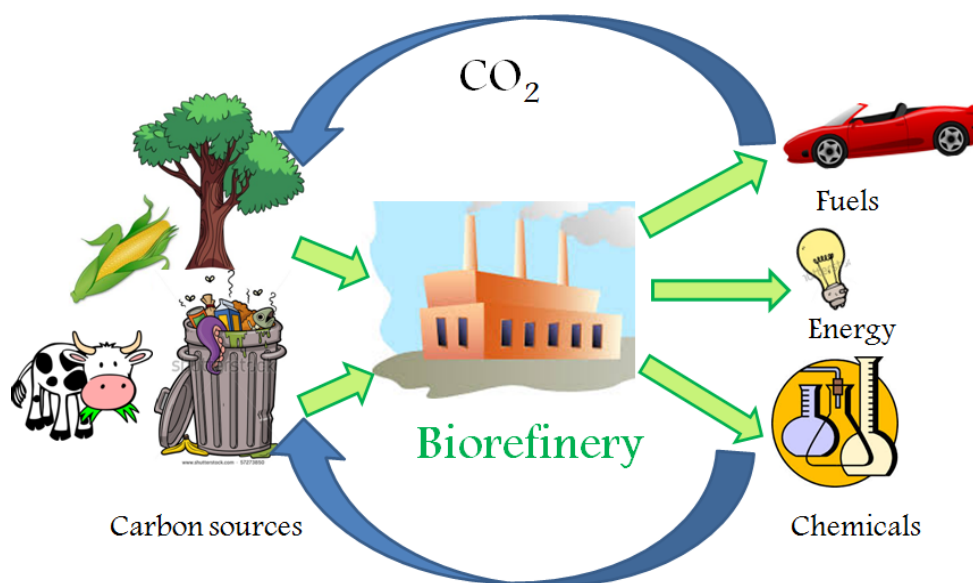


Figure 1.2. Bio-refinery concept for the conversion of biomass.

1.4. LIGNOCELLULOSIC BIOMASS

Lignocellulosic biomass refers to plant derived non edible biomass. The major components of lignocellulosic biomass are cellulose (38-50 %), hemicellulose (23-32 %) and lignin (15-25 %).¹⁸ These components are located within the microfibrils of plant cell wall, where cellulose is surrounded by a matrix made up of hemicellulose and lignin. During photosynthesis process plants produce chemical energy using sunlight, CO₂ and water. This energy is stored in the form of organic compounds like cellulose, hemicellulose and lignin which can be converted into fuels and chemicals as explained under bio-refinery concept. Upon utilization of these products, CO₂ is released in the environment which can be reutilized by plants during its growth, thus resulting in a sustainable CO₂ cycle. But the complete valorization of all three major components of lignocellulosic biomass (cellulose, hemicelluloses and lignin) is extremely difficult. However, before discussing the methods to valorize these components, it is essential to know the classification of lignocellulosic biomass.

Lignocellulosic biomass can be generally classified into 3 categories;

- a. Virgin biomass, which include trees, bushes and grasses.
- b. Waste biomass, which is produced in various sectors like, agriculture (corn stover, bagasse, rice husk, wheat straw, corn cobs etc.), municipality (kitchen waste) and forest.

- c. Energy crops, which include plants grown at lower cost, maintenance and are harvested to make biofuels like bio-ethanol or burnt for energy (e.g. Elephant grass (*Miscanthus*), Switch grass (*Panicum virgatum*)).

In order to consider lignocellulosic biomass as a renewable resource we should know the annual production of this raw material. From a survey done it was understood that world's annual production of lignocellulosic biomass is ca. 1.5×10^{10} MT and India itself produces ca. 623.4 MMT of lignocellulosic biomass annually in the form of crop waste.¹⁹ Also in the survey report prepared by US Department of Agriculture (USDA) it is estimated that the USA can sustainably produce 1.3×10^9 MT of dry biomass per year.²⁰ This much amount of biomass has the energy content of ca. 3.8×10^9 BOE (barrels of oil energy equivalent).¹⁴ It is predicted that approximately 1 billion tons of dry biomass is available annually from fields and forests that can replace 30 % of US annual petroleum consumption.¹⁵ Therefore abundant availability of lignocellulosic biomass makes it a renewable source of carbon, which holds the key to supplying society's basic needs for sustainable production of liquid transportation fuels and chemicals without impacting the nation's food supply.

As discussed above lignocellulosic biomass is mainly composed of cellulose, hemicellulose and lignin. The polysaccharide part of lignocellulosic biomass includes cellulose and hemicellulose and the aromatic part include lignin.

1.4.1. Cellulose and hemicellulose

Cellulose is the most abundant organic homopolymer, which comprises 38-50 % of lignocellulosic biomass. The main building block of cellulose polysaccharide is glucose unit which is linked together through β (1 \rightarrow 4) glycosidic bonds in an orderly fashion. Cellulose is crystalline in nature due to the regular arrangement of glucose units and severe (intra-, inter-molecular and inter-sheet) hydrogen bonding existing between them.²¹ Second largest component of lignocellulosic biomass is hemicellulose, which constitutes 23-32 % of its composition.²¹ Unlike cellulose, hemicellulose is a heteropolymer made up of different C5 (xylose and arabinose) and C6 sugars (glucose, galactose and mannose) linked together through β (1 \rightarrow 4) glycosidic bonds in variable proportions depending on the type of plant from which it is isolated. Structures of cellulose and hemicelluloses are shown in Figure 1.3.

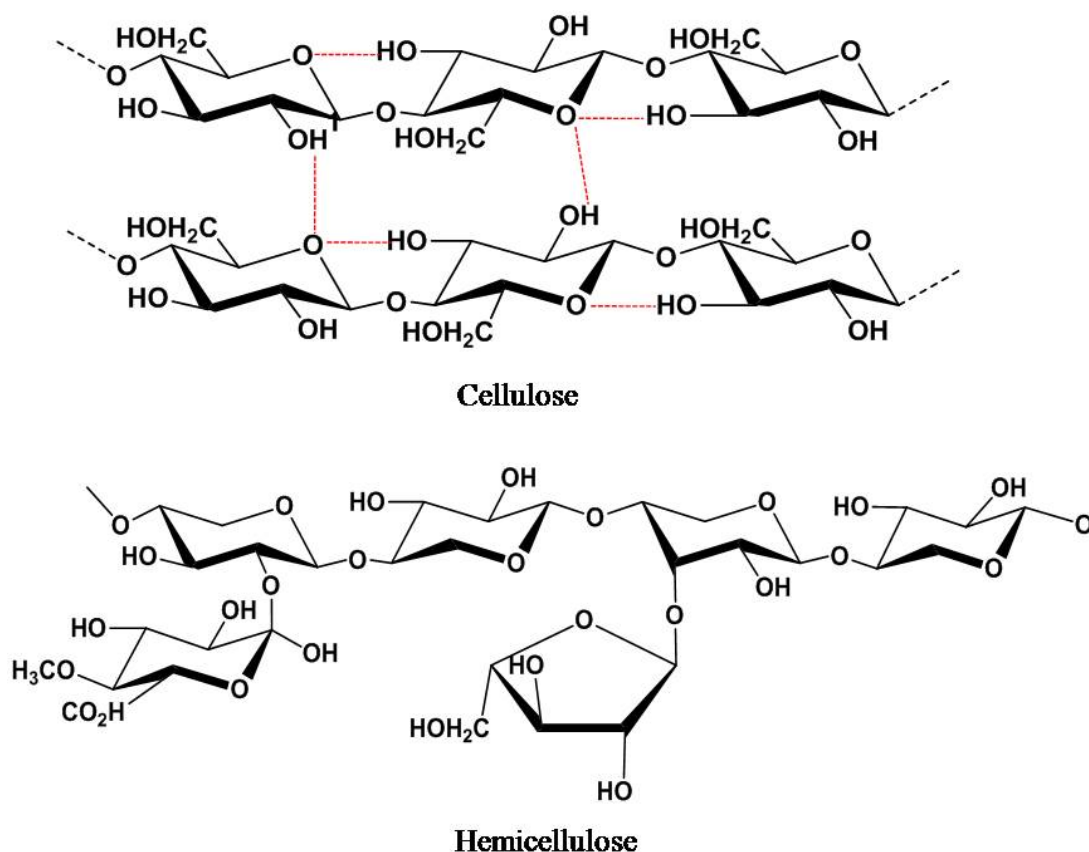


Figure 1.3. Structure of cellulose and hemicellulose.

1.4.2. Lignin

Lignin is the aromatic part of lignocellulosic biomass composition. The term lignin is derived from Latin word '*lignum*' which means wood. Besides cellulose and hemicellulose, lignin one of the major constituents of vascular plants. It fills the space between cellulose and hemicellulose in the secondary cell walls and acts like a resin holding the lignocellulosic matrix together. The covalent linking of lignin with the carbohydrate polymers confers on the plant strength and stiffness and thereby help in its growth.²²

Lignin has an annual production of 20 billion tons²³ and is the only largest biopolymer having 3-dimensional amorphous aromatic network structure. Depending on the wood species, the lignin content in a plant can vary between 15-25 %. The abundance of lignin in lignocellulosic biomass is in the order: softwood > hardwood > grasses. In softwoods the lignin content is typically ca. 27-31 % and in hardwood it is ca. 19-25 % and in grasses it is ca. 17-24 %.²⁴

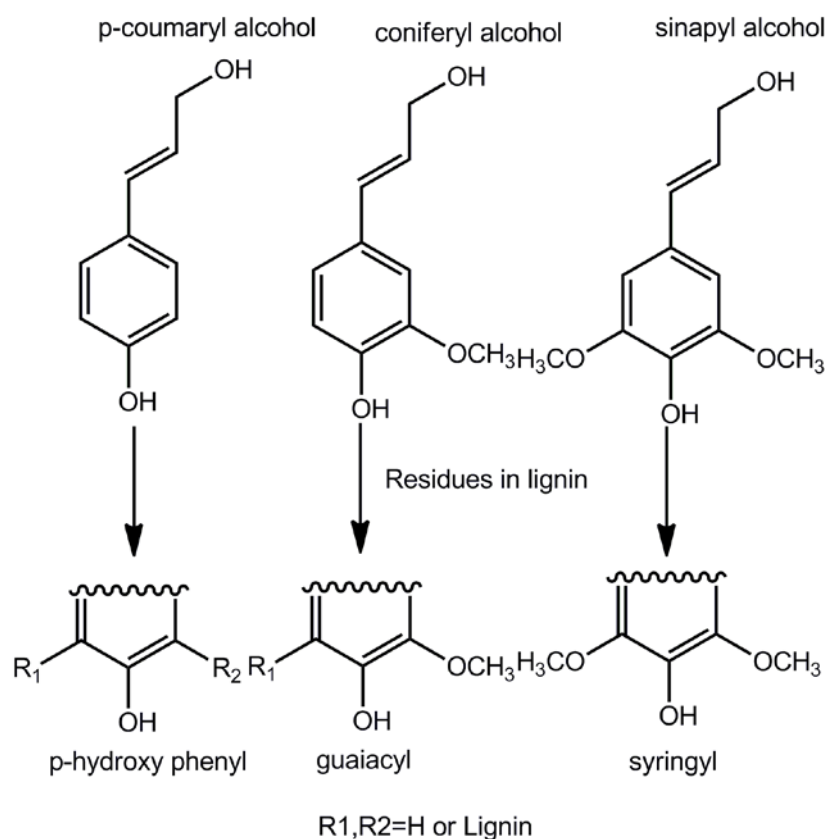


Figure 1.4. Main precursors of lignin and their structures in lignin polymer.

Lignin is a randomly cross-linked aromatic polymer whose exact structure has not been elucidated yet, unlike other biopolymers in lignocellulosic biomass (cellulose and hemicellulose). From various studies it was understood that the formation of lignin in plant cell wall was due to the random polymerization of three aromatic monolignol units (C₉ phenyl propane units) namely, p-coumaryl alcohol (hydroxyphenyl unit), coniferyl alcohol (guaiacyl unit) and sinapyl alcohol (sinapyl unit) (Figure 1.4). The relative composition of these aromatic building units depend on the source from which lignin is isolated. In softwood, 90 % of lignin structure is made of coniferyl alcohol units (guaiacyl units) and in hardwood; lignin is composed of equal amount of coniferyl and sinapyl alcohol units. But in grasses the lignin structure is made up of equal amount of coniferyl and sinapyl alcohols along with 10-20 % p-coumaryl alcohol. The radical polymerization process of these phenyl propane units is initiated by an enzyme catalyzed oxidation of their phenolic hydroxyl groups, resulting in a random cross-linking and building up of the amorphous three-dimensional structure of lignin.²⁵ Typically, when lignin is isolated from

lignocellulosic biomass its structure gets deformed and it complicates the study on the determination of its native structure in plants.

Lignin precursors or building units are linked together with ether linkages (C-O-C) and with carbon-carbon (C-C) linkages. The percentage distribution of these linkages will vary between softwood and hardwood species. β -O-4 is the most prominent and common linkage in all the lignin. It is observed that hardwood lignin has higher amount (60 %) of β -O-4 linkages than softwood lignin (46 %).²⁶ Other major linkages and their composition in lignin are β -5, 5, 5, 5, 4-O-5, β -1, α -O-4 and β - β as shown in Figure 1.5 and Table 1.1. It is also observed that 4-O-5 and α -O-4 aryl ether bonds are less predominant (5-8 %) in both the types of woods. Biphenyl linkages 5-5 (18 %), phenyl coumaran β -5 (11 %), diaryl propane β -1 (7 %) and β - β (2 %) are present in very less amount in both softwood and hardwood lignin.

Table 1.1. Summary on various types of linkages present in lignin

S.No.	Linkage	Softwood lignin (spruce) (%)	Hardwood lignin (birch) (%)
A	β -O-4	46	60
B	α -O-4	6-8	6-8
C	4-O-5	4	6.5
D	β -5	9-12	6
E	5-5	9.5-11	4.5
F	β -1	7	7
G	β - β	2	3
H	others	13	5

Lignin polymer contains several types of functional groups like, alkoxy groups, phenolic hydroxyl groups, benzyl alcohol groups and carbonyl groups and some terminal aldehydic groups on the side chains. Table 1.2 shows the functional groups present per 100 C₉ units of softwood and hardwood lignin.²⁷ These distributions of functional groups vary among different lignin and hence only approximate values are shown here.

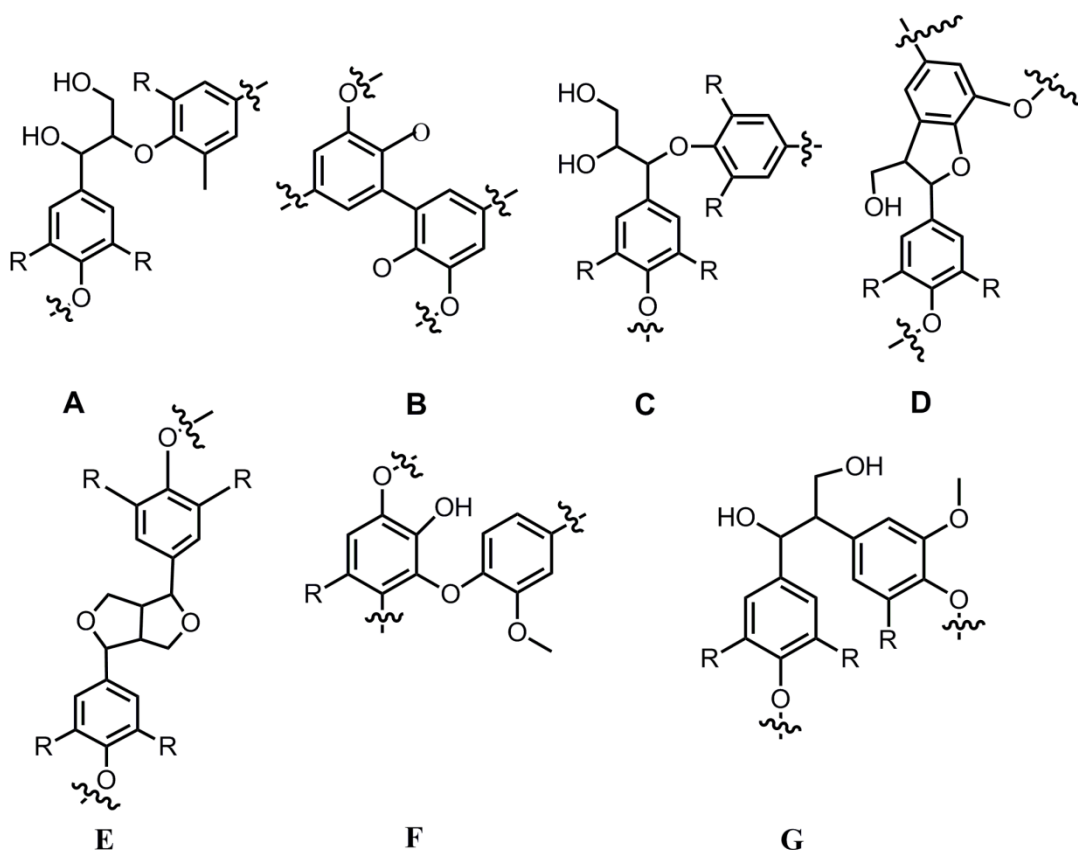


Figure 1.5. Major linkages present in lignin.

Table 1.2. Functional groups present in softwood and hardwood lignin per 100 C9 units

Functional groups	Softwood lignin	Hardwood lignin
Phenolic hydroxyl	15-30	10-20
Aliphatic hydroxyl	115-120	110-115
Methoxyl	92-96	140-160
Carbonyl	10-15	15

In 1950's Freudenberg and co-workers have done fundamental study on the constitution and biosynthesis of lignin.²⁸ Based on several observations, they came up with an early version of the structure of softwood lignin. But later in 1977 Adler presented a structure for lignin which was widely accepted and is referred until today.²⁹ This structure with its main functional groups is schematically depicted in Figure 1.6.

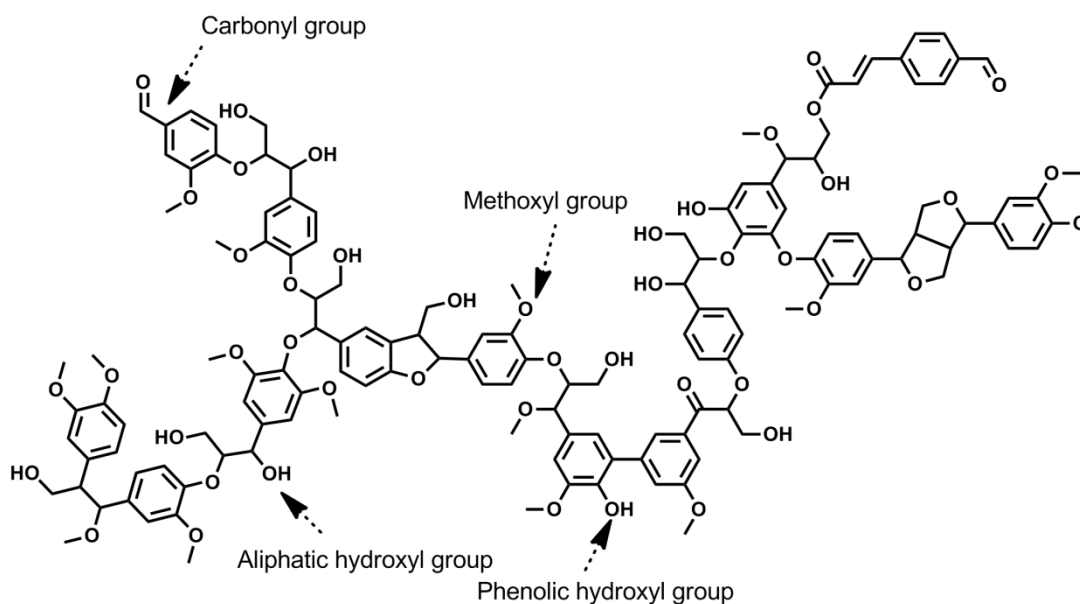


Figure 1.6. Structure of softwood lignin.

But these lignin structures and linkages vary according to the type and origin of the plant from which it is isolated. It also depends on the type of process used for its isolation from plant biomass.

1.5. LIGNIN ISOLATION TECHNIQUES

Pretreatment of biomass is an initial step in the bio-refinery operation. The pretreatment helps in the separation of primary components of lignocellulosic biomass (cellulose, hemicellulose and lignin); also it degrades the polymeric components of biomass to smaller compounds. Depending on the pretreatment (Kraft) process there is a possibility of incorporation of S and metals like Na into the isolated lignin. Thus, the structure, composition and even molecular weight of the isolated lignin is independent on the technique employed for its separation from lignocellulosic biomass.

Pretreatment technologies used to isolate lignin from lignocellulosic biomass can be broadly classified into 4 categories; physical pretreatment (ball milling), solvent fractionation (organosolv process, ionic liquid pretreatment and phosphoric acid fractionation), chemical pretreatment (acidic, alkaline and oxidative) and biological (using fungi) pretreatment.³⁰ Each pretreatment has both merits and demerits. In various lignin pretreatments, different conditions and degradation techniques including temperature, pressure, solvents and pH ranges are used which will alter the composition, chemical structure and linkages in lignin to various extents.

Pretreatment technologies can also be broadly classified into 2 categories. In the first group cellulose and hemicellulose undergoes dissolution but lignin remains insoluble in the form of a solid residue. In the second category lignin is dissolved and separated out. For instance, during bio-ethanol production lignin is obtained as a by-product. Lignin obtained here remains insoluble while cellulose and hemicelluloses remain soluble. Organosolv lignin, Kraft lignin and liginosulfonates isolated come under the second category, where lignin is soluble and is separated out, while cellulose and hemicelluloses remain insoluble. Various types of chemical pretreatments for lignin isolation are summarized below;

1.5.1. Kraft lignin method

The most dominant process used for the lignin extraction is Kraft lignin process or sulfate process, which uses mixture NaOH and Na₂S, known as white liquor with a high pH (range) at a temperature range of 150-180 °C for about 2 h.¹⁷ *Kraft* in German means “strong”. Ragauskas and coworkers have detailed the chemistry surrounding Kraft process including a description of the primary linkages in lignin and the ways in which these linkages are disrupted during this process. One of the main chemical reactions that happen during the Kraft process is the scission of ether bonds by the nucleophilic sulfide (S²⁻) or bisulfide (HS⁻) ions. It is important to note that 5-5 linkages in lignin are highly stable even at high temperatures and hence they typically survived during the Kraft pulping process. During pulping, nucleophilic attack happens on electron deficient conjugated centers and carbonyl structures, while during bleaching electrophilic attack of electron rich centers in aromatic nuclei and unsaturated, ring conjugated side chains occurs.³¹⁻³² It was observed that some new types of functional groups called stilbenes are also introduced during the Kraft pulping process. These groups are formed from the cleavage of alky-aryl ether linkages of phenyl coumaran structures.³³

The number average molecular weight (Mn) of Kraft lignin obtained is typically between 1000 and 3000 gmol⁻¹ and it exhibits a polydispersity (P. D.) typically between 2-4 which can increase up to 8 or 9. An approximate molecular formula depicted for Kraft lignin is C₉H_{8.5}O_{2.1}S_{0.1}(OCH₃)_{0.8}(CO₂H)_{0.2}. Kraft lignin has a major disadvantage of Na and S contamination occurred during the extraction

process where NaOH and Na₂S are used as reagents. A model structure for Kraft pine lignin is presented in Figure 1.7.

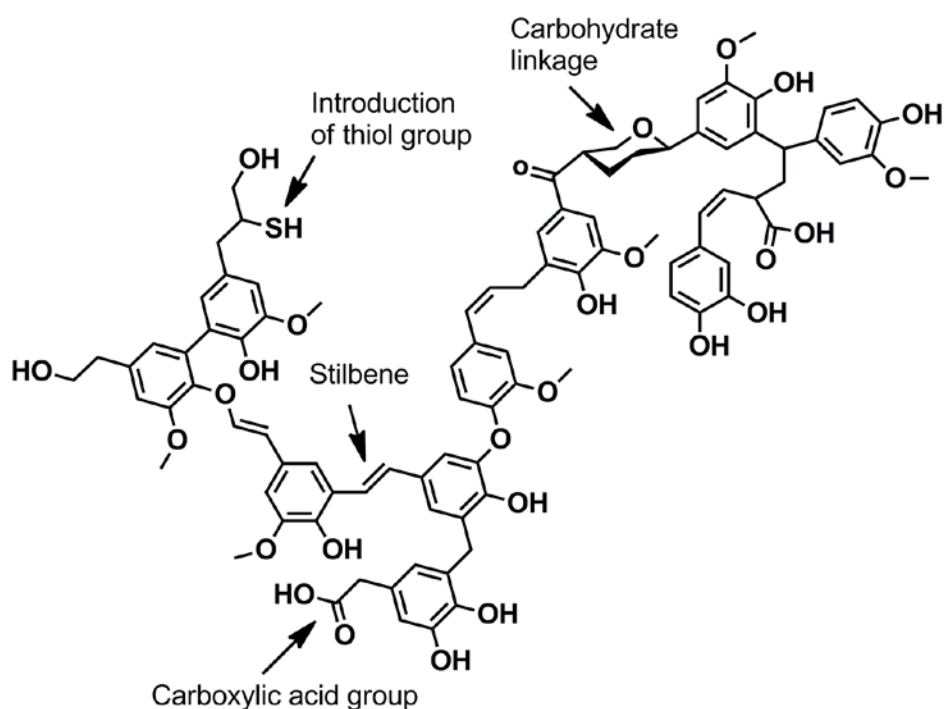


Figure 1.7. Structure of Kraft pine lignin.

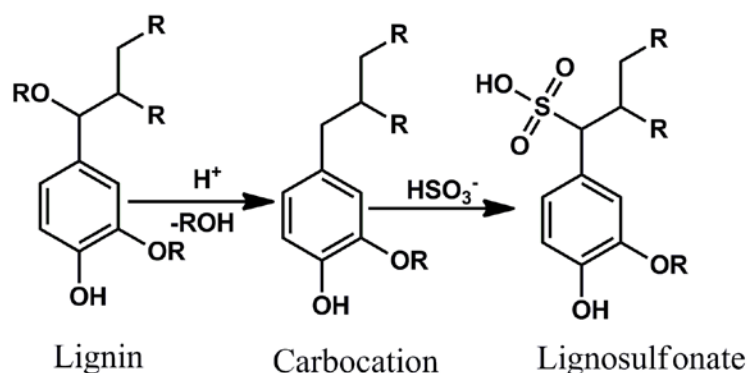
Kraft lignin is produced commercially by MeadWestvaco and LignoBoost Technology, a process owned by Metso Corporation where lignin is extracted from pulp mill black liquor.^{24, 33-34}

1.5.2. Lignosulfonate method

Lignosulfonates also called as lignin sulfonates or sulfite lignins are derived from sulfite pulping of wood by lignosulfonate process. Lignosulfonates are precipitated as calcium or magnesium sulfites from sulfite plants by the addition of lime (CaO or Ca(OH)₂) at 175 °C. This process uses a pH between 2 and 12 depending on the cationic composition of the pulping liquor. Lignosulfonates formed remain dissolved during the process and can be separated out by simple pH adjustment. During this process the acidic cleavage of the ether linkages in lignin occurs in presence of sulfites. The electrophilic carbocation produced during ether cleavage combines with the bisulfate ion to form sulfonates (Equations 1 and 2).³⁵



The primary site for the cleavage in liginosulfonate process is the α -C atom of the propyl side chain attached to the aromatic ring. It was also understood that sulfonation occurs on the side chain, not on the aromatic ring (Figure 1.8).



[where R refers to a wide variety of groups present in lignin]

Figure 1.8. Mechanism of liginosulfonate formation.

Approximately 90-95 % of the liginosulfonates can be obtained by this process. Liginosulfonate lignin obtained is polydisperse in nature and has molecular weight higher than Kraft lignin due to the incorporation of sulfonate groups over the arenes. It was found that softwood derived liginosulfonates have a molecular weight between 1000-1,40000 gmol^{-1} and hardwood derived liginosulfonates have lower molecular weights compared to softwood. An approximate molecular formula of liginosulfonates can be depicted as $C_9H_{8.5}O_{2.5}(OCH_3)_{0.85}(SO_3H)_{0.4}$ for softwood and $C_9H_{7.5}O_{2.5}(OCH_3)_{1.39}(SO_3H)_{0.6}$ for hardwood, respectively. A model structure of liginosulfonate lignin is shown in Figure 1.9.³³

Liginosulfonates are produced commercially by Lignotech with an annual production of ca. 120×10^3 tonnes.¹⁷ Also the worldwide annual production of liginosulfonates from sulfite black liquor is estimated to be ca. 1060×10^3 tonnes.¹⁷

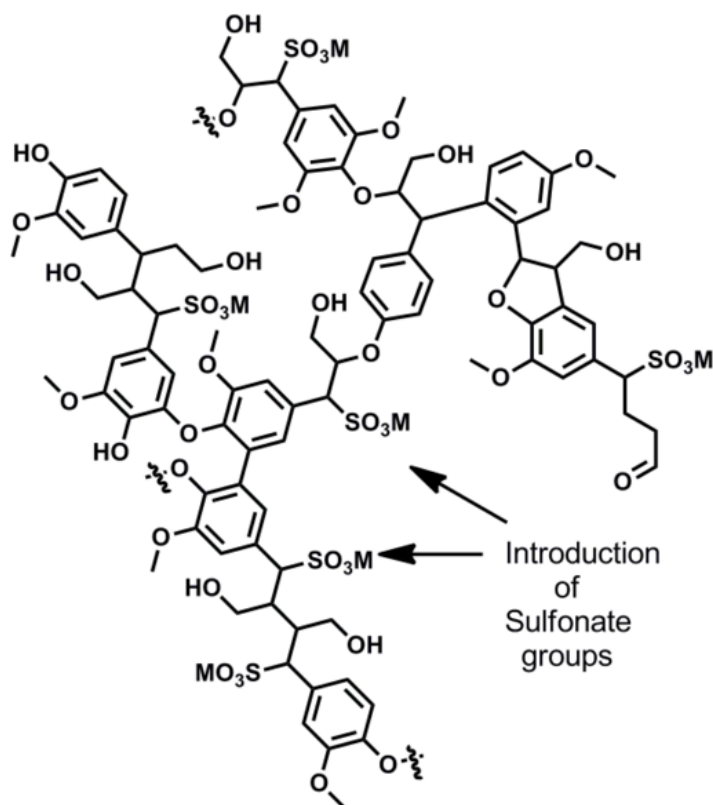


Figure 1.9. Structure of lignosulfonate lignin.

1.5.3. Organosolv method

Organosolv method used to extract lignin from lignocellulosic materials was invented by Theodore Klienert. This method uses organic solvents for the extraction of lignin from lignocellulosic materials at a temperature of 140-220 °C. In organosolv process the hydrolytic cleavage of α -aryl linkages in lignin happen and the fragments formed are soluble in solvent system. Solvents like methanol, ethanol, butanol, ethylene glycol, acetone, formic acid, acetic acid are used for the organosolv extraction. The concentration of solvent in water used for this process ranges from 40-80 %. Acids and alkalis are also used in organosolv process to increase the rate of extraction of lignin. Alcell and organocell process also come under the general category of organosolv method. Alcell process previously known as APR process (Alcohol Pulping and Recovery) uses aqueous ethanol solutions (40-60 % v/v) to delignify wood at temperatures from 180 to 210 °C and 2-3.5 MPa pressure. In organocell process two stage organosolv techniques are employed for lignin extraction. In first stage, 50 % of methanol solution is used as solvent system to extract lignin. During the second stage of the process, NaOH is added at a loading of 30 % wt/wt of dry

wood to perform the complete extraction of lignin. After these steps, lignin extracted in the soluble form (dissolved in organic solvent) is separated out from the solution by precipitation with the addition of H_3PO_4 until the pH is 4.

Organosolv lignin ($2000\text{-}4000\text{ gmol}^{-1}$) has a lower molecular weight compared to other lignin (Kraft lignin or liginosulfonate). Organosolv lignin is insoluble between a pH = 2-4 (acidic) but gets solubilised in basic pH and is also soluble in many polar organic solvents. An approximate molecular formula of organosolv lignin can be depicted as $\text{C}_9\text{H}_{8.53}\text{O}_{2.45}(\text{OCH}_3)_{1.04}$. Among the lignin isolation processes, organosolv method is mostly preferred since it has several advantages over other processes such as,

- a) In this process separate streams of cellulose, hemicellulose and lignin are formed, which is not possible in Kraft method.
- b) Also this process is considered to be environmentally friendly since it does not use sulfides and harsh reaction conditions to isolate lignin when compared to other processes (Kraft and liginosulfonate). As a result the organosolv lignin isolated has no sulfur or metal contamination and is highly pure compared to other lignin isolated.
- c) Organic solvents used for lignin isolation in this process can be recycled by distillation technique. This also reduces water pollution and eliminates the bad odor usually generated during Kraft pulping process, thereby reducing the environmental pollution.

But unfortunately this technique also has few disadvantages like the high expense for the solvent recovery step employed in the case of high boiling solvents. For e.g. Butanol (B.P. = $117\text{ }^\circ\text{C}$) is capable of isolating higher amount of lignin compared to other solvents but its high cost limits its use. Due to low cost and ease in recovery, ethanol (B.P. = $78\text{ }^\circ\text{C}$) is suggested as the most suitable solvent for lignin extraction by organosolv process.

Along with these methods, there are several other methods by which lignin can be isolated like Klason process, Willstätter process, Björkman process, Cellulolytic enzyme process, Pyrolysis process and Steam explosion process. Details on these methods are tabulated in Table 1.3.

Table 1.3. Summary of lignin isolation techniques

Process	Conditions	Remark	Type of lignin
Klason process ³⁶	72 % H ₂ SO ₄ at R.T.	Hydrolysis and solubilisation of cellulose and hemicellulose from extracted wood pulp and lignin remains undissolved.	Klason or sulfuric acid lignin
Willstätter process ³⁷	42 % HCl at low temp.	Wood meal is extracted and hydrolyses to form insoluble lignin residue.	Willstätter lignin
Björkman process ³⁸	(9:1) v/v mixture of dioxane and water	Wood species is ball milled for 48 h in presence of aqueous dioxane in N ₂ atmosphere. Lignin residue is left behind after polysaccharide hydrolysis. 50 % of lignin is isolated still has some carbohydrate impurities.	Milled Wood Lignin (MWL) or Björkman lignin
Cellulolytic enzyme process ³⁹	Cellulolytic enzymes	Cellulolytic enzymes are used to remove carbohydrates prior to aqueous dioxane extraction of ball milled wood meal. This lignin is structurally similar to MWL.	Cellulolytic enzyme derived lignin (CEL)
Pyrolysis process ⁴⁰	High temp. (450 °C) for a short residence time (2 sec.)	No waste formation. But there is a disadvantage of high carbohydrate consumption to fuel up the process. This process produces C9 derived oligomers, other than C8-oligomers compared to other processes.	Pyrolytic lignin
Steam explosion process ⁴¹	Hot steam of 180 to 240 °C under pressure (1-3.5 MPa)	Molecular weight of steam explosion lignin is similar to organosolv lignin.	Steam explosion lignin

1.6. AVAILABILITY OF LIGNIN

Abundant availability of lignin is essential for the efficient and complete valorization into fuels and chemicals. Production of ethanol from cellulosic feedstock is considered as one of the most promising pathways to reduce the dependence on crude oil for the production of liquid fuels. This process, however, produces a large amount of lignin as waste during the separation of cellulose from lignocellulosic matrix by Kraft or sulfite pulping process. Indeed, for each Kg of ethanol produced, about 1-3 Kg lignin is generated as waste. Being the largest fraction of “non carbohydrate” biomass, lignin contributes as much as 15-25 % of the weight and 40 % of the energy content of lignocellulosic biomass. Natural production of lignin is estimated to be around 20 billion tons per year, while paper and pulp industry produces approximately 70 million tons of lignin as by-product during Kraft process.⁴² But even lignin is a very good carbon source, 99 % of this Kraft lignin obtained from paper and pulp industry is burned only for power generation in the recovery boilers.⁴³ Along with Kraft lignin, ca. 1 million tons of lignosulfonates and ca. 10,000 tons of soda lignin are generated from sulfite and soda pulping industries, respectively. Here also majority of lignin is treated as waste.

Therefore, lignin which is a renewable carbon source and abundantly available, if valorized for the production of fuels and chemicals, can significantly increase the carbon economy of lignocellulosic bio-refinery.¹⁷ So it can be concluded that, the aromatic nature and abundant availability makes lignin a renewable and sustainable carbon resource for the production of energy, fuels and chemicals.

1.7. VALORIZATION OF LIGNIN

Lignin has a great potential to be employed as a renewable source of transportation fuels and fine chemicals. In 2007, DOE (Department of Energy) has set a goal to reduce the crude oil derived gasoline consumption by 20 % in the next 10 years.⁴⁴ 10 % of this reduction accounts to be met by fuel efficiency and remaining will come from alternative fuels.⁴⁴ So by 2030 the target placed was to replace 30 % of transportation fuels by biofuels which is equivalent to 60 gallons of biofuels like ethanol or other bio-derived fuels. For the production of this much of biofuels 0.75 billion tons of biomass is required in which 0.225 billion tons (30 % of lignin) will be composed of lignin. So this amount of lignin can be used for the production power,

fuels and chemicals. But in the current situation only heat and power is generated from lignin available. The industrial valorization of lignin into chemicals has been undertaken through two main processes: Noguchi and HRI (Hydrocarbon Research Inc. or Lignol processes).⁴⁵

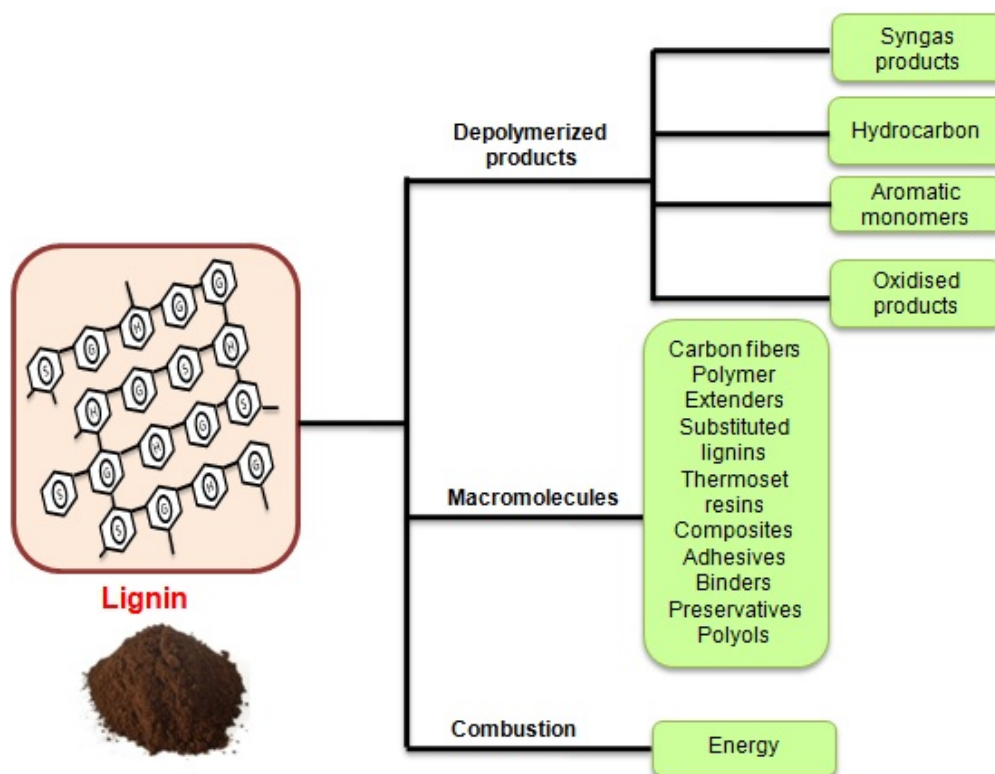


Figure 1.10. Lignin valorization into value added products.

Major applications of lignin can be categorized into three; energy generation by combustion, use of lignin in the form of macromolecule itself and aromatic monomers obtained by depolymerizing lignin, which can be used as fuel additives or platform chemicals (Figure 1.10). Applications of lignin in the form of macromolecule include the synthesis of activated carbon which is capable of absorbing hazardous emissions in air. Lignin can also be used as a substitute for formaldehyde resins, which is banned for its carcinogenic disadvantages. Another application is the use of lignin in the production of low cost carbon fibers, which can replace synthetic polymers like polyacrylonitrile. Next major application of lignin is as a renewable carbon source for the production of aromatic chemicals. By the cleavage of C-C and C-O-C bonds in lignin one can obtain BTX (benzene, toluene, xylene), phenolic products, syn-gas products (methanol, DME, ethanol, mixed alcohols, C1-C7 gases etc.). Also selective oxidation of lignin can produce vanillin which is a flavoring agent. These products can

be used as platform chemicals which can be converted by conventional petrochemical processes to other value added chemicals.

Another important application of lignin is the synthesis of complex aromatic products by the selective cleavage of C-C or C-O-C bonds of lignin. These complex aromatic products truly represent the building blocks of lignin and are difficult to obtain by conventional petrochemical routes. As fossil feedstocks are finite and with increase in cost of theirs, lignin is the only renewable source which can produce high amount of aromatic monomers that can be used as fuels and chemicals. Therefore efficient and one pot conversion of lignin into aromatic monomers is an attractive goal.

1.8. LIGNIN DEPOLYMERIZATION

Various reviews are published over the decades discussing the potential routes for the valorization of lignin into aromatics. Several researches have been done to convert lignin into fuels and chemicals using various processes (Figure 1.11). The primary purpose of lignin depolymerization is to convert complex lignin into aromatic monomers, those can find application as fuels and basic or platform chemicals. We can broadly classify lignin depolymerization methods into thermal and chemical.

1.8.1. Thermal depolymerization of lignin

Gasification and pyrolysis comes under the category of thermal depolymerization.

1.8.1.1. Pyrolysis

It refers to a thermal route to degrade lignin into low molecular weight compounds in absence of O₂ or air. This method is influenced by several factors like feedstock type, heating rate and reaction temperature. Pyrolysis is a promising approach to convert lignin into value added low molecular weight compounds which could be used as biofuels and aromatic chemicals. This process has been commercialized and there are several pyrolysis plants recently built in Wisconsin, US (50 tons of biomass/day); in Vancouver, Canada (10-100 tons of biomass/day) and in Finland (12 tons of biomass/day).⁴⁶ For fast pyrolysis a minimal temperature of 400-450 °C is required to proceed for the decomposition of macromolecule, lignin. Moreover lignin has a thermoplastic behavior which causes trouble for the feeding and specific procedure.⁴⁷

The yield of pyrolytic liquids is ca. 40-60 wt% and gases include ca. 8-20 wt% of lignin. The main composition of pyrolysis liquid is water, unsaturated compounds, aromatic oxygenated compounds (phenols) and char (30-40 wt%). During pyrolysis of lignin polymer, α -O-4 linkage was found to be broken first.⁴⁸ By using non sulphided NiMo/SiO₂-Al₂O₃ and Cr₂O₃/Al₂O₃ the pyrolytic yield can be increased and thereby there is a variation in the composition, which is methoxyphenol products, is replaced by phenols, cresols and xylenols by demethoxylation and hydrodealkylation.⁴⁹ It was also observed that the use of H-ZSM-5 can improve the yield of non-oxygenated aromatics.⁵⁰

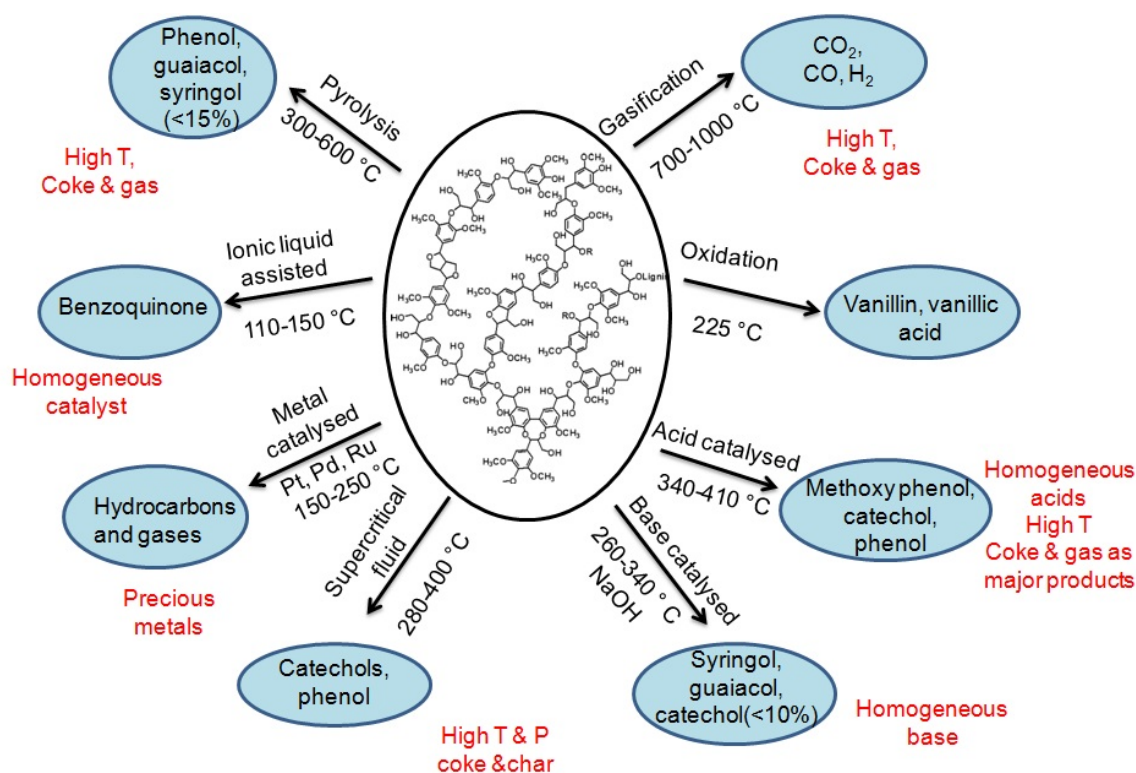


Figure 1.11. Summary on the various processes by which lignin can be transformed into aromatic monomers or gases.

1.8.1.2. Gasification

Gasification represents the conversion of carbonaceous material into gaseous components (syn-gas) which can be used in the form of fuel for power generation. Gasification of lignin produces CO₂, CH₄ and H₂ at 700-1000 °C. There are several studies where gasification of lignin was studied using supercritical water ($T_c = 374.3$ °C and $P_c = 22.1$ MPa). Gasification of alkylphenols as model compounds for lignin

was studied using several supported metal catalysts in supercritical water at 400 °C and Ru metal was reported as an effective catalyst in these reactions.⁵¹⁻⁵² For instance Ru/TiO₂ was used for the gasification of lignin in supercritical water at 400 °C, 3 h with 80 % gas yield.⁵¹⁻⁵² Commercial Ni catalysts were also employed for the gasification of lignin in sub and supercritical water (380-480 °C) to obtain gas yield of 20 % within 1 h.⁵³ Production of H₂ from gasification of was also studied using Ni/MgO catalyst at in supercritical water at 400 °C with a gas yield of 80 %.⁵⁴

1.8.2. Chemical depolymerization of lignin

Generally there are 6 categories of chemical methods used for depolymerization of lignin; (1) Base catalysed (2) Acid catalysed (3) Metal catalysed (4) Supercritical fluids assisted (5) Ionic liquid assisted and (6) Oxidative method.

1.8.2.1. Base catalysed depolymerization (BCD)

BCD process involves depolymerization of lignin using base as catalyst. One of the preliminary studies on base catalysed depolymerization (BCD) of lignin were done on the alkaline degradation of Alcell lignin, a type of organosolv lignin.⁵⁵ The reactions are performed at a temperature range of 200-340 °C for 15-90 min. 0.5-6 wt% of NaOH was used as catalyst in these studies. Results show that temperature is a more important parameter than the reaction time. 10 wt% of DCM soluble products were obtained with a maximum of 4 wt% identified and quantified monomeric products. Later some significant studies were done on the base catalyzed depolymerization (BCD) of lignin in presence of alcoholic base.⁵⁶ They used several types of lignin, including Kraft (Indulin) and organosolv (Repap) lignin. Ethanolic or methanolic KOH at 10 wt% base concentration is typically used for this study. BCD process, at temperature of about 270 °C and an autogeneous pressure of around 14 MPa for about 1-5 min., was the first step and hydrodeoxygenation is considered as the second stage to produce reformulated gasoline. It was observed from GC-MS analysis that drastic changes happens in lignin at 270 °C, but those changes become more pronounced at 290 °C. Also partial oxygen removal occurs by the expulsion of methoxyl groups.

Miller *et al.* studied the use of mixed liquid hydroxides for lignin depolymerization.⁵⁷ The study showed that KOH in supercritical ethanol ($T_c = 241$ °C and $P_c = 6.3$ MPa) at 290 °C can rapidly depolymerize both Kraft and organosolv derived lignin with only 7 % insoluble material remaining after 10 min. Roberts *et*

*al.*⁵⁸ demonstrated that the base catalysed depolymerization products from organosolv lignin vary with the process temperature in aqueous NaOH. It is found that monomer selectivity is maximum (ca.16 wt% syringol, 6 wt % guaiacol, 4 wt % 3, 5-dimethoxy-4-hydroxy acetophenone) between 260 to 280 °C. This process also shows that recovery and recycle of the homogeneous base catalyst is extremely difficult. Few studies were also done using solid base catalysts. In 2014, Beckham *et al.*⁵⁹ have screened heterogeneous solid base supported metal catalysts, 5 wt % Ni/HT at 270 °C for C-O bond cleavage of model compounds that exhibits a common aryl-ether linkage in lignin. They have also shown that 5 wt % Ni-HT catalysts can depolymerize two types of biomass-derived lignin, namely organosolv and ball-milled lignin, which produces alkyl-aromatic products. Solid base catalysts used for lignin depolymerization provides a potentially viable alternative to homogeneous BCD process of lignin.

So in general BCD process is carried out at and above 300 °C and at high pressures from which aromatic monomers like catechol, syringol, guaiacol and its derivatives can be obtained. The mechanism in BCD process is the cleavage of aryl-alkyl bond (β -O-4 bond in lignin), which happens only above 270 °C. Generally the Na⁺ ion present in the base helps to form cation adducts, which then catalyses the formation of 6-membered transition state on β -O-4 bond during the reaction. So the concentration ratio of base or the concentration ratio of lignin to base plays an important role in BCD process. The main disadvantage of BCD process is its harsh conditions and low selectivity towards aromatic monomers. Also soluble base method needs additional step of neutralization. Furthermore this method may cause corrosion to the reactor systems and hence may increase the capital cost of the process.

1.8.2.2. Acid catalysed depolymerization

There are several reports on the acid catalysed depolymerization of lignin. Catalytic upgrading of a lignin derived pyrolysis bio-oil was studied at atmospheric pressure in a continuous, down flow fixed bed reactor using H-ZSM-5 zeolite as an acid catalyst at a temperature range of 340-410 °C.⁶⁰ The objective is to maximize the concentration of hydrocarbon (83 wt %) in the expected organic distillate product. Pyrolysis of softwood (SW) Kraft lignin was examined in the presence of NiCl₂ and H-ZSM-5 zeolite as an additive at 700 °C.⁶¹ The zeolite is shown to improve the

decomposition of aliphatic hydroxyl groups, carboxyl, methoxyl groups, and ether bonds in lignin during pyrolysis. Catalytic fast pyrolysis of alkaline lignin to useful chemicals was reported using zeolite catalysts with different acidity and pore size. Here the catalyst played dual role: in its acid form, it catalytically converted the depolymerized intermediates into desirable and more stable products and its surface prevented repolymerization and coke formation. The yield of liquid and the selectivity to desired products can be controlled by tuning the acidity and pore size of the catalyst.⁶² It was also reported that Kraft lignin can be pyrolysed (500-764 °C) using H-ZSM-5 catalyst with various Si/Al ratios ranging from 25/1 to 200/1, resulting in the formation of 2-5.2 wt% of aromatic hydrocarbons.⁶³ One step thermal conversion of lignin to gasoline range liquid products by pyrolyzing softwood (SW) Kraft lignin at 600 °C was shown using various types of zeolites like MFI (Z), FAU (Y), BEA (B), FER (F) and MOR (M).⁶⁴ Deactivation and regeneration of H-USY zeolite during pyrolysis of alkaline lignin was studied at a 550 °C and 650 °C.⁶⁵

Several homogeneous acids were also tried for lignin depolymerization. Lewis acid catalysts like NiCl₂ or FeCl₃ were used for the depolymerization of Alcell lignin to yield solids, liquids and gaseous products which includes the formation of ether soluble monomers under different reaction conditions. Both the catalysts favour condensation reactions leading to insoluble residues. In these studies a very low temperature of 70-200 °C is used which cannot break the complex structure of lignin into aromatic monomers.⁶⁶ In the literature, 10 wt% of H-COOH with 20-77 wt% ethanol is used for the depolymerization of wheat straw lignin.⁶⁷ The major products obtained in these reactions are methoxy phenol, catechol and phenol. Several other reactions are done in the category of acid catalysed depolymerization of lignin where metal enhancers are included in the depolymerization studies. In acid catalysed depolymerization reactions also β -O-4 linkage in lignin is cleaved, similar to base catalysed reactions. HCOOH and other acids act as hydrogen sources for the formation of H₃O⁺ on β -O-4 linkages or on the cationic aromatic ring. Metallic co-catalysts are also used in this type of studies along with acid catalysts for enhancing the selectivity, but did not reduce the activation energy of the reaction.

Depolymerization of lignin using homogeneous acid catalyst needs an additional step of neutralization and can cause corrosion to the reactor system which may increase the capital cost. Previous reports on lignin depolymerization using solid

acid catalysts especially zeolites also have several disadvantages like they employ harsh reaction conditions, high temperatures ($T \geq 340$ °C) which in turn results in the formation of coke, char and thereby reduces the yield of aromatic monomers. One of the main disadvantages of the existing literatures on acid catalysed depolymerization of lignin is that there are limited reports on the studies involving actual lignin substrate, since in most of the studies model compounds like dimers or trimers are used, which cannot solve the challenges involved in the case of real substrates.^{33, 68}

1.8.2.3. Metal catalysed depolymerization

One of the first reports on metal catalysed depolymerization of lignin was by Harris and co-workers in 1938, where hardwood lignin was treated with hydrogen in presence of copper-chromium oxide catalyst.⁶⁹ This reaction resulted in the hydrogenation of the aromatic ring, forming propylcyclohexanols and methanol. Another early study on lignin hydrogenation involves the use of Raney Ni as catalyst in which syringol and guaiacol are isolated.⁷⁰⁻⁷¹ Pepper *et al.* have done several studies on softwood lignin (spruce wood) using catalysts like Ru/C, Ru/Al₂O₃, Pd/C and Rh/Al₂O₃. It was observed that at 195 °C, 3.5 MPa initial H₂ pressure, Ru/C gave the maximum yield for aromatic monomers like 4-propyl guaiacol and diconiferyl alcohol.⁷² But hardwood lignin (aspen wood) gave corresponding syringyl and guaiacyl compounds with propyl or propanol group, in presence of Rh/C as catalyst. In 1950's Noguchi process was patented for the production of mixture of C6-C9 monophenols (40 wt %) by the hydrogenolysis of lignin.⁷³ The catalyst used for this process was iron (II) sulfide along with a co-catalyst which was a sulfide of at least one metal like Cu, Ag, Sn, Co, Cr, Ni, Zn or Mo. These reactions were done at 250-450 °C and an initial H₂ pressure of 15- 46 MPa.

Since then, many more advances towards catalytic hydrogenolysis of lignin were achieved. Kou *et al.* have reported that lignin can be hydrogenated to yield 46 wt % of monomeric phenols over noble metal catalysts (Pt, Ru, Pd, and Rh supported on activated carbon) under 4 MPa of H₂.⁷⁴ Zhang *et al.* have shown that lignin can be catalytically hydrogenated to guaiacols and syringols at 235 °C under 6 MPa H₂, and has obtained 46 wt% (based on lignin) phenolic compounds.⁷⁵ Other catalysts, such as copper-chromium oxide,⁶⁹ Co-Mo-S/Al₂O₃⁷⁶ activated carbon, alumina or silica-

supported Ru⁷⁷⁻⁷⁹ or Pt⁸⁰⁻⁸¹ have also been reported in hydrogenation of lignin or model compounds to monomeric phenols.

So, in general addition of metal enhancers reduced the activation energy of lignin depolymerization and thereby helped to reduce the reaction temperature. It also increased the selectivity of the process towards aromatic monomers formation. In presence of hydrogen sources like water or ethanol/methanol, C-O and C-C bonds of lignin are cleaved. Metals or other solid acid catalysts provide accessible active sites at the external surface of the catalysts where the reaction occurs. But one of the major drawbacks of metal assisted lignin depolymerization was the catalyst deactivation. In most of the above studies the recyclability of the catalysts is not even mentioned which made it necessary to study the catalyst deactivation in the coming future.

1.8.2.4. Supercritical fluid assisted depolymerization

At conditions near to critical point supercritical fluids can dissolve and depolymerize biomass components like lignin. Supercritical fluids exhibit low viscosity which helps in fast, homogeneous and efficient reaction. There are several examples for supercritical fluids which include carbon dioxide, water, acetone, methanol and ethanol. Depolymerization of lignin model compounds and even actual lignin substrates can be performed in supercritical alcohols like methanol or ethanol at $T > 239\text{ }^{\circ}\text{C}$ and $P > 8\text{ MPa}$. Addition of NaOH and KOH into this system helps to increase the depolymerization of lignin.⁸²⁻⁸³ During this process, solvolysis of C-O-C linkages in lignin structure occurs while the C-C linkages remain stable.

Fang *et al.* have done the depolymerization studies of organosolv lignin in supercritical water. With the addition of phenol, organosolv lignin was completely depolymerized at temperatures between 400-600 °C. The presence of phenol prevented repolymerization and char formation at high pressures up to 10 MPa.⁸⁴ Yield of low molecular weight fraction was increased in supercritical water at 350-400 °C and 25-40 MPa with long reaction time. The water soluble fraction consists of catechol (28.4 %), phenol (7.5 %), m-cresol and p-cresol (7.8 %), o-cresol (3.8 %), suggesting the cleavage of both ether and carbon-carbon bonds.⁸⁵ Additives like phenol and p-cresol suppress the cross linking reactions by the entrapment of reactive fragments like formaldehyde, and capping of active sites (C_{α}) in the lignin structure. Gosselink *et al.* used CO₂/acetone/water supercritical fluid to treat organosolv

hardwood lignin and wheat straw lignin at temperature around 300-370 °C at 10 MPa pressure to obtain syringol and guaiacol as product.⁸⁶

From the earlier reports it was understood that supercritical fluid assisted depolymerization of lignin has advantages like good solubility for organic compounds, high selectivity towards depolymerized products and can be easily separated by solvent extraction method. But they also have disadvantages like they employ high temperature, high pressure for the reactions which increases the capital cost of the process.

1.8.2.5. Ionic liquid (IL) assisted depolymerization

One of the most recent technologies used for depolymerization of lignin is the usage of ionic liquids in the form solvent as well as catalysts.⁸⁷ Ionic liquids are considered as the most popular solvents for the separation of lignin and cellulose from the raw lignocellulosic materials. They are known to have very low vapour pressures and good thermal stability. They have a melting point below 100 °C. By varying the combination of cations and anions the properties of ionic liquids can be altered.

Several studies were done using ionic liquid as solvent in various biomass transformation reactions. Few studies were done to cleave β -O-4 bond in lignin under milder conditions below 250 °C using ionic liquid as catalyst. For both lignin and lignin model compounds ionic liquid with ionic salt exhibited high selectivity for monomer products. Depolymerization studies were performed on organosolv lignin using 1-ethyl-3-methyl imidazolium trifluoro methane sulfonate ([EMIM] [CF₃SO₃]) along with Mn(NO₃)₂ at a temperature of 100 °C and 8.4 MPa pressure.⁸⁸ The main point drawn from the research was that 2, 6-dimethoxy-1, 4-benzoquinone (DMBQ) was obtained as the final and most selective product (11.5 %).

Currently it is proved that ionic liquids can act as both solvent and catalyst, since they are capable of providing hydrogen sources for the catalysed reaction. 1-H-3-methylimidazolium chloride [HMIM][Cl] an acidic ionic liquid was used for the depolymerization of oak wood lignin at temperature range of 110-150 °C thereby cleaving the alkyl aryl linkage present in lignin.⁸⁹ In these reactions ionic liquid behaved both as solvent and catalyst.

Still ionic liquids have several drawbacks like high cost for recovery due to difficulty in the separation⁹⁰ of ionic liquid from the lignin derived molecules because

of π - π interaction between ionic liquid and aromatic moieties.⁹¹ Therefore the use of ionic liquid in lignin depolymerization is very much limited.

1.8.2.6. Oxidative depolymerization

Vanillin is an important product of commercial interest which is mainly obtained by the oxidation of softwood lignin. With an annual consumption of 12000 tons, vanillin is considered as the most widely used flavouring agent in food and perfumes. Until now the only sector where lignin is commercialized is in the production of vanillin by oxidation reactions. This process is relatively simpler when compared to the complicated petrochemical production routes for vanillin. Since 1936, vanillin is produced by alkaline oxidation of liginosulfonates with a yield of ca. 15 %.⁹² For vanillin production from lignin, reactions are generally performed at 160-175 °C under alkaline conditions using a copper catalyst.⁹³ Alkaline oxidation of sugarcane soda lignin was carried out in a continuous fluid bed with $\text{PdCl}_3 \cdot 3\text{H}_2\text{O}/\gamma\text{-Al}_2\text{O}_3$ catalyst at 100-250 °C and 0.2-1 MPa partial oxygen pressure with a yield of vanillin ca. 12 %.⁹⁴⁻⁹⁵ Catalytic lignin oxidation processes giving aromatic aldehydes and acids which do not exceed 10 % on lignin weight basis were also reported.⁹⁶ Several oxidation studies performed over lignin model compounds gave good conversions which will help in developing further strategies for depolymerization of lignin using bio-refinery concept.

Based on the literature reports it was observed that several researches are performed on the valorization of lignin into value added chemicals and fuels. But it can be summarized that most of the processes are using harsh reaction conditions which will result in the formation of higher amount of degradation products (coke, char and gas) and reduces the aromatic monomer formation. Also most of the processes use homogeneous catalysts (acids or bases) or metal catalysts which may increase the capital cost of the reaction. To overcome these drawbacks and to attain efficient and complete valorization of lignin into aromatic monomers, I have preferred to study in the area of acid catalysed depolymerization of lignin into aromatic monomers under milder reaction conditions using various types of solid acid catalysts.

1.8.3. Solid acid catalysts

As mentioned in earlier section (Refer section 1.8.2.2) mineral acids are known to depolymerize lignin.⁶⁶⁻⁶⁷ Hence it was believed that solid acid catalysts can also catalyze this reaction. Processes involving mineral acids as catalysts are associated with problems like toxicity, corrosion and difficult in catalyst separation. Solid acid catalysts facilitate reactions with less waste production and thus have replaced toxic, corrosive, and non recyclable liquid mineral acids in many catalytic applications. Solid acid catalysts can have Brönsted and/or Lewis acidity which can possibly cleave the C-O-C and C-C bonds in lignin. Therefore it was decided to use solid acid catalysts for depolymerization reactions of lignin.

Depolymerization studies of lignin would be performed at $T \leq 250$ °C, so the solid acid catalyst chosen should be stable under this condition. Several types of solid acid catalysts are available (zeolites, silica alumina, supported metal oxides, sulfonated mesoporous silica, clays, ion exchange resins, heteropoly acids etc.) but only a few were particularly selected for depolymerization of lignin. (Figure 1.12) Solid acid catalysts like ion exchange resins (Nafion silica (SAC-13), Amberlyst-15) and heteropoly acids were avoided from employing in lignin studies since these catalysts are known to be unstable above certain temperature ($T < 150$ °C).⁹⁷ In this sense solid acid catalyst like synthetic zeolites and silica alumina appears to be promising catalysts with the obvious advantages compared to other solid acid catalysts with an easy separation from the reaction mixture, hydrothermal stability, shape selectivity, and reusability. Along these, clay catalysts were also studied for depolymerization reactions of lignin due to its heterogeneous behavior and acidic nature. Few of the supported metal oxides were also used since they are also well known for performing acid catalysed reactions over a large variety of substrates.

In general, solid acids used for depolymerization studies of lignin can be classified as structured and amorphous solid acids.

1.8.3.1. Structured solid acid catalysts

Structured catalysts have definite channel structure, pore volume and pore diameter. Structured solid acid catalysts employed in the lignin depolymerization study include zeolites, clays and metal oxides.

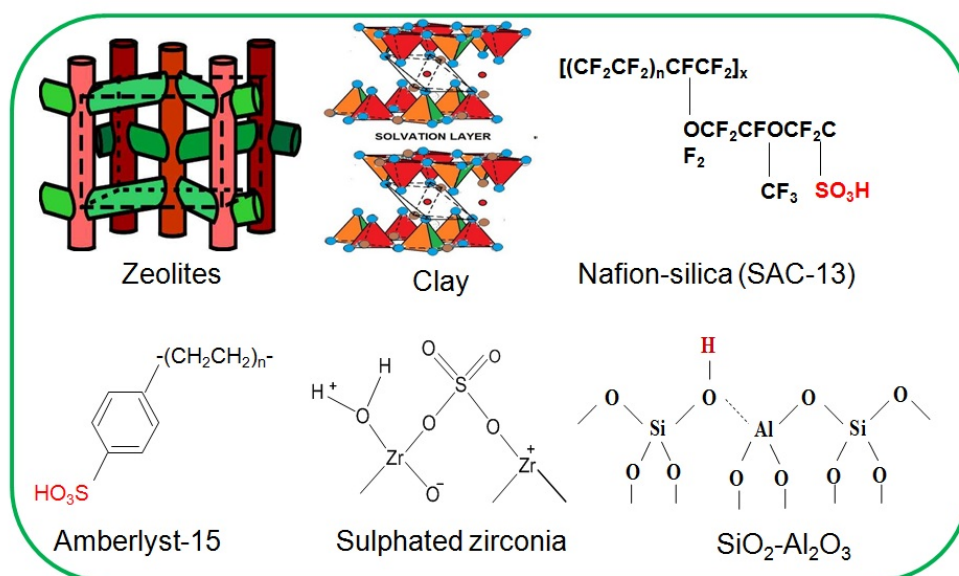
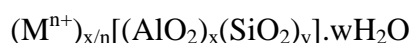


Figure 1.12. Different types of solid acid catalysts.

Zeolites are crystalline aluminosilicates with fully cross linked framework structures made up of corner sharing SiO₄ and AlO₄ tetrahedra, named primary structural units. The term “zeolites” came from a Greek word *zeo* (to boil) and *lithos* (stones); and it was first used by a Swedish mineralogist Cronstedt in 1756.⁹⁸ Zeolites are typically aluminosilicates composed of Si⁴⁺ and Al³⁺. They are formed when some of the Si⁴⁺ is replaced by Al³⁺. For each of the Si⁴⁺ ion replaced by Al³⁺, the charge is balanced by other positive ions such as Na⁺, K⁺ or Ca²⁺ ions. The structural formula of zeolite is based on the crystallographic unit cell represented as,



‘M’ represents the exchangeable cation of valence n and M is a cation generally belonging to group I or II, which can balance the negative charge created by the Al in the structure. ‘M’ is later replaced by NH₄⁺ ion, which on calcination at 550 °C releases NH₃ leaving behind H⁺ ion attached to the framework resulting in the generation of Brönsted acidity in zeolites (Figure 1.13).⁹⁹ Si/Al ratio in zeolites is represented by ‘y/x’ and ‘w’ represents the water present inside the discrete cages and channels of zeolites. In addition to Si⁴⁺ and Al³⁺ other elements can also be present in zeolites, they need not be isoelectronic but should be capable of occupying the framework sites. Si/Al ratio is one of the fundamental characteristics of zeolites

because several properties such as thermal stability, acidity, hydrophobic character are related to it.

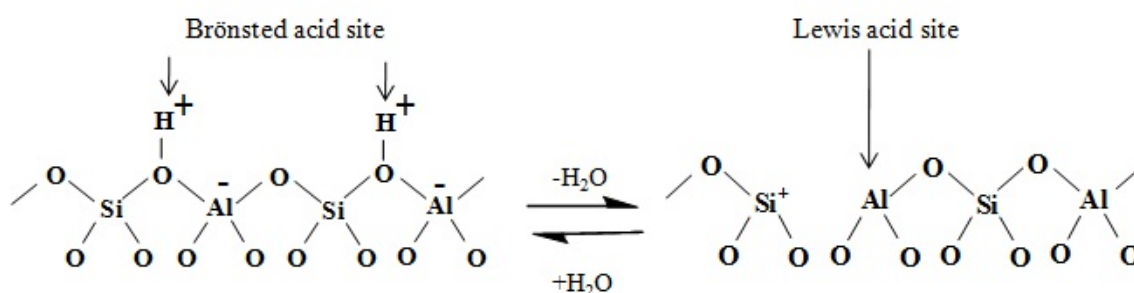
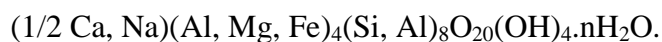


Figure 1.13. Brønsted and Lewis acid sites in zeolites.

According to Lowenstein's rule, Al-O-Al linkages in zeolitic framework are forbidden. As a result all AlO_4 tetrahedrons are linked to four SiO_4 tetrahedron, but a SiO_4 tetrahedron may have five different possible environments like $\text{Si}(0\text{Al},4\text{Si})$, $\text{Si}(1\text{Al},3\text{Si})$, $\text{Si}(2\text{Al},2\text{Si})$, $\text{Si}(3\text{Al},1\text{Si})$ and $\text{Si}(4\text{Al},0\text{Si})$. Si/Al ratio is one of the important parameters which govern the zeolites reactivity.

Another type of solid acid catalyst used for depolymerization studies of lignin is clay. The term clay has been used to either indicate fine particles with a grain size less than $2\ \mu\text{m}$ or minerals belonging to clay minerals group. Clay minerals have received considerable attention in the last couple of years because of their environmental compatibility, low cost, high selectivity, reusability and operational simplicity.¹⁰⁰ Clays are amorphous, pillared or naturally occurring aluminosilicates. Clays were used in 1930's to mid 1960's for catalytic oil refining, but they were later replaced by zeolites. Clay has an aluminosilicate structure which can be compared to a multi-decker ham sandwich. The bread layers represent the extended aluminosilicate sheets where two external tetrahedral silica groups surround internal octahedral alumina groups in a tetrahedral octahedral tetrahedral ('TOT') structure. The ham represents an interlamellar water layer containing dissolved cations. Montmorillonites are a group of TOT-type clays in which isomorphous substitution of some of the octahedral aluminium (III) atoms by magnesium (II) or iron (II) atoms has taken place, with the result that the sheet retains a residual negative charge. The acidity of the ion-exchanged clays is very much influenced by the quantity of water between the sheets.¹⁰¹

The general formula of Montmorillonite clay is



Porosity and stability of clay is improved by pillaring, which leads to materials known as pillared clays (PILC). These materials show increased surface area, pore volume, thermal and mechanical stability and depending on the pillars, improved catalytic activity compared to the parent clays, making them suitable catalysts and adsorbents. Aluminium is the one of the cation used to build up the pillars of the structure, yielding aluminium pillared clay materials (Al-PILCs). Pillared clays have shape selective properties due to their interlayer and interpillar distances which control the diffusion rates of the reactants, reaction intermediates and products.

1.8.3.2. Amorphous solid acid catalysts

Amorphous solid acid catalysts do not have a definite channel structure, pore volume and pore diameter. Amorphous solid acid catalysts employed in the lignin depolymerization study include $\text{SiO}_2\text{-Al}_2\text{O}_3$ and supported metal oxides ($\text{MoO}_3/\text{SiO}_2$). $\text{SiO}_2\text{-Al}_2\text{O}_3$ catalyst possess both Brönsted and Lewis acid sites making it well suited for the use as a support for multifunctional industrial catalysts.¹⁰² $\text{SiO}_2\text{-Al}_2\text{O}_3$ have been directly used as an important acid catalyst in oil refineries and furthermore, have been applied as excellent supports for nanoparticles in many hydrogenation and oxidation reactions. Amorphous solid acid catalyst also includes metal oxides (10 wt% $\text{MoO}_3/\text{SiO}_2$). The electropositivity of the central atom in metal oxide decides whether it is acidic or basic in nature.

1.9. HYDRODEOXYGENATION STUDIES OF LIGNIN DERIVED AROMATIC MONOMERS

Depolymerization of lignin can produce a mixture of aromatic monomers those can be used in the form of fuel additives and octane enhancers.¹⁰³ But the high oxygen content will reduce the efficiency of the fuels derived from these aromatic monomers.¹⁰⁴⁻¹⁰⁸ Therefore they have to be upgraded before using them as fuels. Hydrodeoxygenation (HDO) reactions are considered to be the best method for upgrading the efficiency of fuels obtained from lignin derived aromatic monomers. In this process typically hydrogenation of $\text{C}=\text{C}$, $\text{C}=\text{O}$ bonds and aromatic rings happens along with the removal of oxygen in the presence of H_2 and catalysts.¹⁰⁹ Model

compounds like phenol, guaiacol and eugenol are used for HDO studies since they are the true representative of the lignin derived aromatic monomers. Typically, sulphided CoMo or NiMo catalysts are used as conventional catalysts for HDO reactions.¹¹⁰⁻¹¹³ Reactions using these catalysts are carried out at high H₂ pressures (10–20 MPa) and high temperatures (300–400 °C) for the removal oxygen in the form of water. Even though these sulphided CoMo or NiMo catalysts gave good HDO activity, but those are associated with several drawbacks like coke formation, low water tolerance and sulfur contamination in products/solvents. Due to these reasons several non-sulphided catalysts those can operate at milder reaction conditions (T < 300 °C) were developed for HDO study of lignin derived products.

Typically, non-sulphided HDO catalysts include supported metal catalysts (metal = Fe, Cu, Ni, Mo, Co, W, Re, Pt, Ru, Rh, Pd etc.; support = C, γ -Al₂O₃, H-ZSM-5, SiO₂-Al₂O₃)^{104, 114-118} But it was observed that noble metal (Pt, Pd, Ru, Rh) catalysts were showing better HDO activity when compared to other supported metal catalysts (Fe, Cu, Ni, Co and Mo). So further studies on HDO reactions were mainly carried out using noble metal catalysts. A wide range of supported metal catalysts including Pt, Pd, Ru or Rh metals impregnated on supports like C, γ -Al₂O₃, SiO₂-Al₂O₃, ZrO₂, SiO₂ and CeO₂ were investigated for HDO reactions.^{104, 114, 119-122} Rh,¹¹⁴⁻¹¹⁶ Pt,^{104, 117} Pd,¹¹⁵ Ru^{114, 118} or bimetallic catalysts were also studied in HDO process and exciting results are achieved.

From literature reports it was understood that complete HDO activity with supported metal catalysts can be achieved only when the metal hydrogenation property was combined with an acidic functionality (mineral acid or solid acid).^{115, 121, 123-125} Therefore, further attempts on HDO of lignin model compounds were performed under acidic conditions. For e.g. A bifunctional combination of Pd/C and H₃PO₄ was used for aqueous phase HDO of phenolic bio-oil components (phenols, guaiacols, and syringols) into cycloalkanes at 80 °C and 5 MPa H₂.^{115, 123-125} To overcome the obvious drawbacks associated with the use of homogeneous acids (H₃PO₄), solid acid like, Nafion/SiO₂ was used. But lower thermal stability of Nafion was proven to be disadvantageous.¹²¹ Instead of Nafion/SiO₂, stable solid acids like zeolites (H-ZSM-5, H-BEA) were used in HDO reactions. For instance, HDO of a lignin model compound (propylphenol) was carried using Pd/C and H-ZSM-5 catalysts in aqueous phase at 200 °C and 5 MPa H₂.¹²⁶ It was observed that approximately 90 % of cycloalkanes

were obtained in presence of H-ZSM-5 and Pd/C combination when compared to sulfated zirconia, Amberlyst 15, Nafion/SiO₂, and Cs_{2.5}H_{0.5}PW₁₂O₄₀ catalysts under similar reaction conditions. Attempts were also made to synthesise HDO catalysts by impregnating noble metals directly on to the solid acid support. For e.g. Pt/H-BEA catalyst was prepared and used in the HDO studies of phenol, guaiacol and eugenol compounds at 200 °C and 5 MPa H₂. Furthermore, to avoid the use of acidic supports since those can lead to coke formation, but to achieve HDO activity, Pt/C catalysts were reported at 280 °C and 4 MPa H₂.¹²⁷ In this case dehydration (or oxygen removal) was facilitated by the in situ protons generated from solvent, water (pK_w=11.2 at 280 °C) under the reaction conditions employed. Guaiacol conversions were studied using Pd/C at 350 °C and 4 MPa H₂, benzene as major product (15.3 %). But if the same reactions were performed at 250 °C, 4 MPa H₂, the major product obtained was methoxycyclohexanol (41 %).¹¹⁴ It was also observed that if guaiacol reactions were performed using Pd/Al₂O₃ catalyst at 250 °C, 4 MPa H₂, the products obtained were cyclohexane (19 %) and cyclohexanol (13 %), while for Pd/SA under the same reaction conditions cyclohexane was the major product (41 %).¹¹⁴ From literature reports it was observed that depending on the conditions employed the product distribution was different. For instance, in guaiacol HDO reactions using Ru/HZSM-5 catalyst after 4 h at 200 °C, cyclohexane was obtained as a main product (93 %),¹²⁸ but under the same reaction conditions if Ru/C was used as a catalyst then cyclohexanol was obtained as the final product (70 %).¹²⁹ Also it was observed that if guaiacol HDO is done using Ru/C catalyst at 250 °C the major product observed is methoxycyclohexanol (60 %).¹³⁰ It was also seen that in guaiacol HDO study if a base (MgO) is added along with Ru/C catalyst then at relatively milder reaction condition (160 °C, 2 h) maximum yield for cyclohexanol (80 %) can be obtained.¹³¹ These reports shows that variation in temperature, time and support alters the course of reaction¹³² and there is a lack of systematic study on HDO reactions. Considering this, it is very important to check the activities of different catalysts under similar reaction conditions to illustrate how catalysts will show difference in their HDO activities.

Ultimately from literature reports it was understood that bifunctional catalysts prepared by supporting noble metals on acidic matrices can be a good selection for HDO study of lignin derived compounds. It is evident from the published reports that,

several researches are done in evaluating the catalytic activity of different metals impregnated on different supports for HDO under varying reaction conditions. Since HDO studies of various lignin model compounds using supported metal catalysts were performed under different reaction conditions, a direct comparison of their activities is almost impossible to substantiate which factors are vital in deciding the selectivity towards the products. Therefore I presume that understanding of the catalytic reactions of lignin derived compounds under the same reaction conditions may assist in the better perceptive of the reaction network. It will also help in the development of stable and active HDO catalysts and processes for one pot conversion of lignin into hydrocarbons. Also in order to verify which factors influence the course of reaction further investigations on several parameters like effect of metal, support, temperature, pressure, time etc. on HDO activity has to be performed.

1.10. SCOPE AND OBJECTIVE OF THESIS

Lignin, due to its abundant availability and aromatic nature can be used as a renewable carbon source. Depolymerization of lignin can yield aromatic monomers which can be efficiently valorized to yield fuel additives or octane enhancers, but the complex nature of lignin makes the process extremely complicated.

Earlier, several attempts were made for the transformation of lignin, but most of them are associated with many drawbacks. In earlier reports on depolymerization of lignin, homogeneous catalysts (acids or bases) were employed which may cause corrosion of the reactor systems, needs an additional step of neutralization and furthermore it increases the capital cost of the process. It was also observed that in the processes employing solid acid catalysts for depolymerization of lignin, harsh reaction conditions ($T > 340\text{ }^{\circ}\text{C}$) were used which results in the formation of degradation products (coke, char and gases) instead of achieving good yield for aromatic monomers. Reports on metal assisted depolymerization of lignin showed that compared to other heterogeneous catalysts relatively milder reaction conditions were used in these processes. But one of the drawbacks of the process was that they employ precious metal catalysts with excess of H_2 which was not economically viable and also face a problem of catalyst deactivation during the course of reaction. Additionally, one of the major drawbacks with the conventional processes for depolymerization of lignin was that most of the studies are done using lignin model compounds like dimers

and trimers instead of using actual lignin substrates.

Considering the drawbacks associated with the known methods it is vital to develop a distinct method to convert actual lignin substrates selectively into aromatic monomers under milder reaction conditions ($T \leq 250$ °C) using heterogeneous catalysts. Moreover, it will be advantageous to use solid acid catalysts as they are already known to convert cellulose and hemicellulose into sugars and sugar derivatives. This will ensure that the same type of catalysts once employed along with lignocellulosic materials into the reactor will in a step-by-step manner convert hemicelluloses, cellulose and lignin to value added products. The development of a methodology employing milder conditions and solid acid catalysts for depolymerization of actual lignin substrates will help in the production of maximum amount of aromatic monomers. Furthermore, the hydrodeoxygenation (HDO) study of lignin derived aromatic monomers in presence of supported metal catalysts will help to reduce the oxygen content and upgrade the efficiency of the fuels derived from these products.

By considering above discussions, following are the objectives of my work:

- ✓ Depolymerization of lignin into aromatic monomers, which can be valorized to yield fuel additives or octane enhancers.
 - Use of actual lignin substrates instead of using model compounds like dimers, trimers etc. to study the depolymerization reactions. Six types of actual lignin substrates obtained from various sources will be studied.
- ✓ To study the structural and functional properties of lignin substrates before employed in the depolymerization reactions to obtain aromatic monomers.
 - It is well known that the structure and linkages present in lignin depends on the plant species, plant parts and even the extraction techniques used for the isolation of lignin from lignocellulosic biomass. Therefore lignin used in the study have to be well characterized using techniques like MALDI-TOF and GPC analysis for the determination of molecular weight; NMR and FTIR analysis to

identify the functional groups; CHNS and ICP-OES for elemental analysis; XRD analysis to confirm the amorphous nature and TGA-DTA analysis to study the thermal degradation behaviour of lignin substrates.

- ✓ To employ solid acid catalysts for the depolymerization reactions of lignin into aromatic monomers.
 - Solid acid catalysts which differ in their properties like crystalline or amorphous nature, acid amount, surface area, pore volume and pore diameter will be used to study the depolymerization reactions of lignin into aromatic monomers. This will help in understanding which factors play important role in catalysis.
- ✓ To study the physico-chemical properties of solid acid catalysts using various characterization techniques before used in the depolymerization reactions of lignin.
 - Properties of solid acid catalysts has to studied using techniques like XRD to determine its crystalline or amorphous nature, NH₃-TPD analysis to determine the acid amount (weak and strong), N₂ sorption analysis to determine the surface area, pore volume and pore diameter, ICP-OES to determine the elemental composition.
- ✓ To develop a method for the depolymerization of lignin into aromatic monomers using solid acid catalysts under milder reaction conditions.
 - Depolymerization of lignin over solid acid catalysts will be greener route compared to earlier reports where homogeneous acids were used as catalysts. Additionally, heterogeneous nature of solid acid catalysts will help in their easier recovery and reusability.
 - Milder reaction conditions ($T \leq 250$ °C) will be used for solid acid catalysed depolymerization of lignin, which will suppress formation of degradation products like coke, char and gases.

- Optimization of the reaction conditions (temperature, pressure, time, rpm) will be performed to produce maximum amount of aromatic monomers.
- ✓ Isolation of aromatic monomers obtained after solid acid catalysed depolymerization of lignin using column chromatography.
 - Product isolation using column chromatography will help to obtain pure compounds from complex mixture of aromatic monomers and will also facilitate in the further confirmation of these products.
- ✓ To perform HDO reactions of lignin derived aromatic monomers into hydrocarbons.
 - HDO reactions will help to reduce the oxygen content of lignin derived aromatic monomers and increase the efficiency of fuel derived from it.
 - HDO studies will be performed over phenol, guaiacol and eugenol model compounds since they are true representatives for lignin derived aromatic monomers.
- ✓ HDO studies of lignin derived aromatic monomers over supported metal catalysts.
 - Conventional HDO catalysts have several drawbacks like coke formation and low water tolerance which can be overcome by performing the HDO studies using supported metal catalysts.
 - Noble metals impregnated over acidic, basic and neutral supports will be synthesized by impregnation method. Noble metals are preferred because they are found to be highly active for facilitating hydrogenation reactions. Acidic supports (SA, AL) will be used since they are known to cleave C-O bonds, neutral (C), and basic supports (HT) will help to reduce the coke formation on the catalysts.
- ✓ To study physico-chemical properties of supported metal catalysts using

various characterization techniques before used in HDO study.

- Supported metal catalysts will be characterized using techniques like XRD, N₂ sorption, ICP-OES and HRTEM analysis.
- ✓ Optimization of reaction conditions (temperature, pressure and time) for HDO of lignin derived aromatic monomers will be performed to obtain maximum amount of deoxygenated products.
- ✓ To perform HDO reactions using supported metal catalysts over a physical mixture of model compounds (guaiacol and eugenol) which mimicks lignin derived aromatic monomer mixture.
 - These studies will help to find a best catalytic system for the one pot HDO of lignin into hydrocarbon fuels.

1.11. REFERENCES

1. Simonetti, D. A.; Dumesic, J. A., *ChemSusChem* **2008**, *1*, 725-733.
2. Goswami, D. Y.; Kreith, F., *Handbook of Energy Efficiency and Renewable Energy*. CRC Press: 2007
3. BP Statistical Review of World Energy.
4. *Annual Energy Review 2011*; U.S. Energy Information Administration: 2012.
5. BP Statistical Review of World Energy. <http://spmlib.pdpu.ac.in:8080/jspui/bitstream/123456789/198/1/MPR00036.pdf>.
6. <http://cdn.intechopen.com/pdfs-wm/11439.pdf>.
7. *Indian Petroleum and Natural Gas Statistics*; Government of India, Ministry of Petroleum & Natural Gas: 2012-13.
8. *Annual report 2013-14*; Indian Ministry of Coal: 2014.
9. *World energy, technology and climate policy outlook (WETO) 2030*; European Commission: 2003.
10. Kumar, C. N. K.; Tran, K. C.; Sigurbjornsson, O. F.; Whitlow, J.; Alexander, K. Storage of intermittent renewable as fuel using carbon containing feedstock. May 30, 2013.
11. Directive 2003/30/EC of the European parliament and of the council. http://ec.europa.eu/energy/res/legislation/doc/biofuels/en_final.pdf.
12. Chheda, J.; Huber, G. W.; A., D. J., *Angew. Chem. Int. Ed.* **2007**, *46*, 7164–7183.
13. Huber, G. W.; Iborra, S.; Corma, A., *Chem. Rev.* **2006**, *106*, 4044-4098.
14. Klass, D. L., In *Biomass for Renewable Energy, Fuels, and Chemicals*, Klass, D. L., Ed. Academic Press: San Diego, 1998; pp 1-27.
15. Perlack, R. D.; Wright, L. L.; Turhollow, A. F.; Graham, R. L.; Stokes, B. J.; Erbach, D. C. *Biomass as feedstock for a bioenergy and bioproducts industry: the technical feasibility of a billion-ton annual supply*; U. S. Department of Energy: 2005.
16. Biomass sources. <http://www.dwgreenewables.com/home/#>.
17. Holladay, J. E.; White, J. F.; Bozell, J. J.; Johnson, D. *Top Value Added Chemicals from Biomass: Volume II -Results of Screenings for Potential Candidates from Biorefinery Lignin*; 2007.

18. Gu, T., *Green Biomass Pretreatment for Biofuels Production* Springer: 2013.
19. *Study on availability of Indian biomass resources for exploitation*; Technology Information, Forecasting and Assessment Council (TIFAC).
20. Kim, J.; Yun, S.; Ounaies, Z., *Macromolecules* **2006**, *39*, 4202-4206.
21. Barrett, C. J. *Renewable Liquid Fuels from Catalytic Reforming of Biomass-derived Oxygenated Hydrocarbons*. University of Wisconsin, 2008.
22. Kaplan, D., *Biopolymers from Renewable Resources*. Springer Science & Business Media: p 417.
23. Kaplan, D. L., *Biopolymers from Renewable Resources*. Springer: Berlin, 1998; p 292.
24. Belgacem, M. N.; Gandini, A., *Monomers, Polymers and Composites from Renewable Resources*. Elsevier Amsterdam, 2008.
25. Davin, L. B.; Lewis, N. G., *Curr. Opin. Biotechnol.* **2005**, *16*, 407-415.
26. Adler, E., *Wood Sci. Technol.* **1977**, *11*, 169-218.
27. Hon, D. N.-S., *Chemical Modification of Lignocellulosic Materials*. CRC Press USA, p 384.
28. Freudenberg, K.; Neish, A. C., *Constitution and biosynthesis of lignin*. Springer: 1968 p 129.
29. Adler, E., Lignin chemistry—past, present and future. *Wood Sci. Technol.* **1977**, *11*, 169-218.
30. Mosier, N.; Wyman, C.; Dale, B.; Elander, R.; Lee, Y. Y.; Holtzapple, M.; Ladisch, M., *Bioresour. Technol.* **2005**, *96*, 673-686.
31. Gierer, J., *Wood Sci. Technol.* **1985**, *19*, 289-312.
32. Gierer, J., *Wood Sci. Technol.* **1986**, *20*, 1-33.
33. Zakzeski, J.; Bruijninx, P. C. A.; Jongerius, A. L.; Weckhuysen, B. M., *Chem. Rev.* **2010**, *110*, 3552-3599.
34. Tomani, P., *Cellulose Chem. Technol.*, **2010**, *44*, 53-58.
35. Lin, S. Y.; Lin, I. S., Lignin. In *Ullmann's Encyclopedia of Industrial Chemistry*, Wiley-VCH Verlag GmbH & Co. KGaA: 2000.
36. López, M.; Huerta-Pujol, O.; Martínez-Farré, F. X.; Soliva, M., *Resour., Conserv. Recycl.* **2010**, *55*, 171-181.
37. Wenzl, H. F. J., IV - The Acid Hydrolysis of Wood. In *The Chemical Technology of Wood*, Academic Press: 1970; pp 157-252.
38. Hu, Z.; Yeh, T.-F.; Chang, H.-m.; Matsumoto, Y.; Kadla, J. F., *Holzforschung* **2006**, *60*, 4923-4930.
39. Libby, C. E., *Pulp and paper science and technology. Volume I. Pulp*. Vol. 1.
40. Jiang, X. X.; Naoko, E.; Zhong, Z. P., *Chin. Sci. Bull.* **2011**, *56*, 1417-1421.
41. Li, J.; Gellerstedt, G.; Toven, K., *Bioresour. Technol.* **2009**, *100*, 2556-2561.
42. Pye, E. K., *Industrial Lignin Production and Applications*. In *Biorefineries-Industrial Processes and Products*, Wiley-VCH Verlag GmbH: 2008; pp 165-200.
43. Lora, J., Chapter 10 - Industrial Commercial Lignins: Sources, Properties and Applications. In *Monomers, Polymers and Composites from Renewable Resources*, Gandini, A.; Belgacem, M. N., Eds. Elsevier: Amsterdam, 2008; pp 225-241.
44. *Annual Energy Outlook 2014*; US Energy Information Administration: April 2014.
45. Huibers, D. T. A.; Jones, M. W., *Can. J. Chem. Eng.* **1980**, *58*, 718-722.
46. Czernik, S.; Bridgwater, A. V., *Energy Fuels* **2004**, *18*, 590-598.
47. Kaminsky, W.; Schweers, W.; Schwesinger, H., *Holzforschung* **1980**, *34*, 73-76.
48. Dorrestijn, E.; Laarhoven, L. J. J.; Arends, I. W. C. E.; Mulder, P., *J. Anal. Appl. Pyrolysis* **2000**, *54*, 153-192.
49. Meier, D.; Ante, R.; Faix, O., *Bioresour. Technol.* **1992**, *40*, 171-177.
50. A., M. C.; A., B. A., *Fuel Process. Technol.* **2010**, *91*, 1446-1458.
51. Sato, T.; Osada, M.; Watanabe, M.; Shirai, M.; Arai, K., *Ind. Eng. Chem. Res.* **2003** *42*, 4277-4282.

52. Osada, M.; Sato, O.; Arai, K.; Shirai, M., *Energy Fuels* **2006**, *20*, 2337-2343.
53. Minowa, T.; Zhen, F.; Ogi, T., *J. Supercrit. Fluids* **1998**, *13*, 253-259.
54. Yoshida, T.; Matsumura, Y., *Ind. Eng. Chem. Res.* **2001**, *40*, 5469-5474.
55. Thring, R. W., *Biomass Bioenergy* **1994**, *7*, 125-130.
56. Kadangode, S. M., *Lignin Conversion Into Reformulated Hydrocarbon and Partially Oxygenated Gasoline Compositions*. Department of Chemical and Fuels Engineering, University of Utah: 2001.
57. Miller, J. E.; Evans, L.; Littlewolf, A.; Trudell, D. E., *Fuel* **1999**, *78*, 1363-1366.
58. Roberts, V. M.; Stein, V.; Reiner, T.; Lemonidou, A.; Li, X. B.; Lercher, J. A., *Chem. - Eur. J.* **2011**, *17*, 5939-5948.
59. Sturgeon, M. R.; O'Brien, M. H.; Ciesielski, P. N.; Katahira, R.; Kruger, J. S.; Chmely, S. C.; Hamlin, J.; Lawrence, K.; Hunsinger, G. n. B.; Foust, T. D.; Baldwin, R. M.; Biddu, M. J.; Beckham, G. T., *Green Chem.* **2014**, *16*, 824-835.
60. Sharma, R. K.; Bakhshi, N. N., *Energy Fuels* **1993**, *7*, 306-314.
61. Ben, H.; Ragauskas, A. J., *Energy Fuels* **2011**, *25*, 4662-4668.
62. Ma, Z.; Troussard, E.; van Bokhoven, J. A., *Appl. Catal., A* **2012**, *423*, 130-136.
63. Li, X.; Su, L.; Wang, Y.; Yu, Y.; Wang, C.; Li, X.; Wang, Z., *Front. Environ. Sci. Eng.* **2012**, *6*, 295-303.
64. Ben, H.; Ragauskas, A. J., *RSC Adv.* **2012**, *2*, 12892-12898.
65. Ma, Z.; van Bokhoven, J. A., *ChemCatChem* **2012**, *4*, 2036-2044.
66. Hewson, W. B.; Hibbert, H., *J. Am. Chem. Soc.* **1943**, *65*, 1173-1176.
67. Gasson, J. R.; Forchheim, D.; Sutter, T.; Hornung, U.; Kruse, A.; Barth, T., *Ind. Eng. Chem. Res.* **2012**, *51*, 10595-10606.
68. Park, H.; Kim, J.; Hong, U.; Lee, Y.; Song, J.; Song, I., *Catal. Surv. Asia* **2013**, *17*, 119-131.
69. Harris, E. E.; D'Ianni, J.; Adkins, H., *J. Am. Chem. Soc.* **1938**, *60*, 1467-1470.
70. Brewer, C. P.; Cooke, L. M.; Hibbert, H., *J. Am. Chem. Soc.* **1948**, *70*, 57-59.
71. Pepper, J. M.; Hibbert, H., *J. Am. Chem. Soc.* **1948**, *70*, 67-71.
72. Pepper, J. M.; Lee, Y. W., *Can. J. Chem.* **1969**, *47*, 723-727.
73. Goheen, D. W., Hydrogenation of Lignin by the Noguchi Process. In *Lignin Structure and Reactions*, AMERICAN CHEMICAL SOCIETY: 1966; Vol. 59, pp 205-225.
74. Yan, N.; Zhao, C.; Dyson, P. J.; Wang, C.; Liu, L.-t.; Kou, Y., *ChemSusChem* **2008**, *1*, 626-629.
75. Li, C.; Zheng, M.; Wang, A.; Zhang, T., *Energy Environ. Sci.* **2012**, *5*, 6383-6390.
76. Jongorius, A. L.; Jastrzebski, R.; Bruijninx, P. C. A.; Weckhuysen, B. M., *J. Catal.* **2012**, *285*, 315-323.
77. Wu, A.; Patrick, B. O.; Chung, E.; James, B. R., *Dalton Trans.* **2012**, *41*, 11093-11106.
78. Nichols, J. M.; Bishop, L. M.; Bergman, R. G.; Ellman, J. A., *J. Am. Chem. Soc.* **2010**, *132*, 12554-12555.
79. Patil, P. T.; Armbruster, U.; Richter, M.; Martin, A., *Energy Fuels* **2011**, *25*, 4713-4722.
80. Runnebaum, R. C.; Nimmanwudipong, T.; Block, D. E.; Gates, B. C., *Catal. Sci. Technol.* **2012**, *2*, 113-118.
81. Xu, W.; Miller, S. J.; Agrawal, P. K.; Jones, C. W., *ChemSusChem* **2012**, *5*, 667-675.
82. Miller, J. E. E., L.; Littlewolf, A.; Trudell, D. E., *Fuel* **1999**, *78*, 1363-1366.
83. Minami, E.; Kawamoto, H.; Saka, S., *J. Wood Sci.* **2003**, *49*, 158-165.
84. Fang, Z.; Sato, T.; Smith Jr, R. L.; Inomata, H.; Arai, K.; Kozinski, J. A., *Bioresour. Technol.* **2008**, *99*, 3424-3430.
85. Wahyudiono; Sasaki, M.; Goto, M., *Chem. Eng. Process.: Process Intensification* **2008**, *47*, 1609-1619.
86. Gosselink, R. J. A.; Teunissen, W. r.; van Dam, J. E. G.; de Jong, E.; Gellerstedt, G.; Scott, E. L.; Sanders, J. P. M., *Bioresour. Technol.* **2012**, *106*, 173-177.

87. Wang, H.; Tucker, M.; Ji, Y., *J. Appl. Chem.* **2013**, 2013, 9.
88. Stärk, K.; Taccardi, N.; Bösmann, A.; Wasserscheid, P., *ChemSusChem* **2010**, 3, 719-723.
89. Cox, B. J.; Ekerdt, J. G., *Bioresour. Technol.* **2012**, 118, 584-588.
90. Zhu, S., *J. Chem. Technol. Biotechnol.* **2008**, 83, 777-779.
91. Reading, N. S.; Kevin, D. W.; Steven, D. A., Free Radical Reactions of Wood-Degrading Fungi. In *Wood Deterioration and Preservation*, American Chemical Society: 2003; Vol. 845, pp 16-31.
92. Bjørsvik, H.-R.; Minisci, F., *Org. Process Res. Dev.* **1999**, 3, 330-340.
93. Klinke, H. B.; Ahring, B. K.; Schmidt, A. S.; Thomsen, A. B., *Bioresour Technol.* **2002**, 82, 15-26.
94. Sales, F. G.; Abreu, C. A. M.; Pereira, J. A. F. R., *Braz. J. Chem. Eng.* **2004**, 21, 211-218.
95. Sales, F. G.; Maranhão, L. C. A.; Filho, N. M. L.; Abreu, C. A. M., *Chem. Eng. Sci.* **2007**, 62, 5386-5391.
96. Zakzeski, J.; Jongerius, A. L.; Weckhuysen, B. M., *Green Chem.* **2010**, 12, 1225-1236.
97. Alvino, W. M., *Ind. Eng. Chem. Prod. Res. Dev.* **1980**, 19, 276-281.
98. Cronstedt, A. F., *Kongl. Vetenskaps Acad. Handl.* **1756**, 17, 120 - 123.
99. Ma, Y.; Tong, W.; Zhou, H.; Suib, S. L., *Microporous Mesoporous Mater.* **2000**, 37, 243-252.
100. Ding, Z.; Klopogge, J. T.; Frost, R. L.; Lu, G. Q.; Zhu, H. Y., *J. Porous Mater.* **2001**, 8, 273-293.
101. Uddin, F., *Metall. Mater. Trans. A* **2008**, 39, 2804-2814.
102. Corma, A., *Chem. Rev.* **1995**, 95, 559-614.
103. Deepa, A. K.; Dhepe, P. L. Depolymerization of lignin using solid acid catalysts. U.S. 0302796 A1, November 29, 2012.
104. Gutierrez, A.; Kaila, R. K.; Honkela, M. L.; Slioor, R.; Krause, A. O. I., *Catal.Today* **2009**, 147, 239-246.
105. González-Borja, M. A.; Resasco, D. E., *Energy Fuels* **2011**, 25, 4155-4162.
106. Bykova, M. V.; Ermakov, D. Y.; Kaichev, V. V.; Bulavchenko, O. A.; Saraev, A. A.; Lebedev, M. Y.; Yakovlev, V. A., *Appl. Catal., B* **2012**, 113-114, 296-307.
107. Şenol, O. İ.; Ryymin, E. M.; Viljava, T. R.; Krause, A. O. I., *J. Mol. Catal. A: Chem.* **2007**, 277, 107-112.
108. Bridgwater, A. V., *Biomass Bioenergy* **2012**, 38, 68-94.
109. Marker, T. L. *Opportunities for Biorenewables in Oil Refineries*; 2005.
110. Elliott, D. C., *Energy Fuels* **2007**, 21, 1792-1815.
111. Ryymin, E. M.; Honkela, M. L.; Viljava, T. R.; Krause, A. O. I., *Appl. Catal. A Gen.* **2010**, 389, 114-121.
112. Furimsky, E., *Appl. Catal., A* **2000**, 199, 147-190.
113. Ryymin, E. M.; Honkela, M. L.; Viljava, T. R.; Krause, A. O. I., *Appl. Catal. A Gen.* **2009**, 358, 42-48.
114. Lee, C. R.; Yoon, J. S.; Suh, Y.-W.; Choi, J.-W.; Ha, J.-M.; Suh, D. J.; Park, Y.-K., *Catal. Commun.* **2012**, 17, 54-58.
115. Zhao, C.; He, J.; Lemonidou, A. A.; Li, X.; Lercher, J. A., *J. Catal.* **2011**, 280, 8-16.
116. Lin, Y.-C.; Li, C.-L.; Wan, H.-P.; Lee, H.-T.; Liu, C.-F., *Energy Fuels* **2011**, 25, 890-896.
117. Ardiyanti, A. R.; Gutierrez, A.; Honkela, M. L.; Krause, A. O. I.; Heeres, H. J., *Appl. Catal., A* **2011**, 407, 56-66.
118. Sitthisa, S.; Resasco, D. E., *Catal. Lett.* **2011**, 141, 784-791.
119. Heitner, C.; Dimmel, D. R.; Schmidt, J. A., *Lignin and Lignans: Advances in Chemistry*. CRC Press: Boca Raton, FL, 2010.

120. Zhao, C.; Kou, Y.; Lemonidou, A. A.; Li, X.; Lercher, J. A., *Angew. Chem., Int. Ed.* **2009**, *121*, 4047–4050.
121. Zhao, C.; Kou, Y.; Lemonidou, A. A.; Li, X. B.; Lercher, J. A., *Chem. Commun.* **2010**, *46*, 412–414.
122. Wang, Y.; He, T.; Liu, K.; Wu, J.; Fang, Y., *Bioresour.Technol.* **2012**, *108* 280-284.
123. Zhao, C.; Kou, Y.; Lemonidou, A. A.; Li, X.; Lercher, J. A., *Angew. Chem., Int. Ed.* **2009**, *48*, 3987–3990.
124. Jongerius, A. L.; Bruijninx, P. C. A.; Weckhuysen, B. M., *Green Chem.* **2013**, *15*, 3049–3056.
125. Zhao, C.; Camaioni, D. M.; Lercher, J. A., *J. Catal.* *2012*, 12–23.
126. Zhao, C.; Lercher, J. A., *ChemCatChem* **2012**, *4*, 64–68.
127. Ohta, H.; Kobayashi, H.; Hara, K.; Fukuoka, A., *Chem. Commun.* **2011**, *47*, 12209–12211.
128. Zhang, W.; Chen, J.; Liu, R.; Wang, S.; Chen, L.; Li, K., *ACS Sustainable Chem. Eng.* **2013**, *2*, 683-691.
129. Nimmanwudipong, T.; Runnebaum, R. C.; Block, D. E.; Gates, B. C., *Catal. Lett* **2011**, *141*, 779-783.
130. Ruiz, P. E.; Frederick, B. G.; De Sisto, W. J.; Austin, R. N.; Radovic, L. R.; Leiva, K.; García, R.; Escalona, N.; Wheeler, M. C., *Catal. Commun.* **2012**, *27*, 44-48.
131. Nakagawa, Y.; Ishikawa, M.; Tamura, M.; Tomishige, K., *Green Chem.* **2014**, *16*, 2197-2203.
132. Saidi, M.; Samimi, F.; Karimipourfard, D.; Nimmanwudipong, T.; Gates, B. C.; Rahimpour, M. R., *Energy Environ. Sci.* **2014**, *7*, 103-129.

CHAPTER 2

LIGNIN AND CATALYST

CHARACTERIZATION

2.1. LIGNIN CHARACTERIZATION TECHNIQUES

Characterizations were performed to understand the morphology and properties of lignin. Following are the details on the instruments used for characterization and the methods used sample preparation.

2.1.1. MALDI-TOF mass spectroscopy and GPC analysis

MALDI-TOF (Matrix Assisted Laser Desorption Ionization-Time of Flight) is a soft ionization technique commonly used for the determination of molecular weight of natural and synthetic polymers. In this technique sample is mixed with a matrix, applied on a metal plate and is irradiated with a pulsed laser (UV laser, nitrogen laser). First the matrix is ionized and it transfers protons to the analyte molecule, thus charging the analyte.¹ The commonly used matrices are sinapinic acid (3,5-dimethoxy-4-hydroxycinnamic acid), DHB (2,5-dihydroxy benzoic acid) etc. and their choice for the analysis is simply trial and error.² Number average molecular weight (M_n), weight average molecular weight (M_w), number and nature of repeating units and end group determination can be done using this technique. Even MALDI-TOF technique is well accepted for synthetic polymers, but this technique in the case of lignin polymer is poorly explored. Most of the studies reported are for high mass lignin model compounds, generally commercial lignin like Kraft lignin and synthetic lignin prepared by the enzymatic polymerization of coniferyl alcohol, milled wood lignin etc.³⁻⁴ Generally the MALDI-TOF spectra for lignin samples shows low resolution and less accuracy due to poor ionization of lignin samples. But this technique is a nondestructive one and can possibly reflect the complete composition of lignin samples.

Molecular weight of dealkaline lignin was determined using MALDI-TOF, Voyager DE-STR instrument. It was equipped with a N_2 laser (337 nm, 3 ns pulse, 20 Hz maximum firing rate). The matrix compound used was 2, 5-dihydroxy benzoic acid (DHB). Sample was prepared in methanol with a concentration of 1mgmL^{-1} . Lignin samples ($1\mu\text{L}$) were overlaid onto the matrix ($1\mu\text{L}$) placed on the golden MALDI target plate. Plate was then kept for drying until the solvent was evaporated and then subjected for the analysis.

Another technique used for the molecular weight determination of lignin is gel permeation chromatography (GPC).⁵⁻⁶ In this technique analytes are separated based

on their size or hydrodynamic volume. This process involves passing a solution of macromolecules dissolved in a solvent (THF/ DMF/water) into a column filled with porous beads or gel (PL gel, styragel) which acts as the stationary phase. Commonly used mobile phases or eluents are THF,⁷ DMF,⁸ water⁹ etc. in which polymers should be dissolved at room temperature. The principle of the technique is that, a molecule with smaller hydrodynamic volume penetrates into the porous gel and spends more time in the column while the polymer molecules with larger size cannot enter the pores, hence eluted quickly causing a difference in the retention times. Columns used in GPC analysis can separate only a limited range of molecular weights. If the sample has fractions of wide range of molecular weight it is necessary to use several GPC columns in series in order to do complete separation. In GPC, commonly used detectors are UV, RI and light scattering detector. GPC calibration was commonly done using polystyrene standards.¹⁰ Mn (number average molecular weight) and Mw (weight average molecular weight) and P. D (polydispersity = Mw/Mn) of a polymer can be determined by GPC analysis. If P. D. = 1, it means all the fractions in the polymer have same length and P.D. >1 shows that, the polymer has fractions with unequal lengths. P. D. for typical polymers ranges from 2 to 10.

GPC of dealkaline lignin was performed in VISKOTEK TDA 305-040 TRIPLE DETECTOR ARRAY refractive index (RI), viscometer (VISC), low angle light scattering (LALS), right angle light scattering (RALS) GPC/SEC MODULE. Separations were achieved by three columns (T6000M, GENERAL MIXED ORG 300 X 7.8 mm) with a guard column attached (TGAURD, ORG GUARD COL 10 x 4.6 mm). DMF was used as eluent at 60 °C with a constant flow rate of 1 mLmin⁻¹. GPC samples were prepared at concentrations of 1 mgmL⁻¹. The instrument was calibrated using polystyrene standards.

GPC analysis of organosolv and ORG lignin were performed using Waters GPC, USA; with an autosampler, RI detector and five columns Styragel HT₂, HT₃, HT₄, HT₅, HT₆ linked in series using tetrahydrofuran (THF) as an eluent with a flow rate of 1 mLmin⁻¹. Lignin samples were dissolved in THF (1 mgmL⁻¹) and the samples were filtered using 0.22 µ filter before analysis. Then 50 µL of the filtered solution was injected into the GPC system and was detected using RI detector. Polystyrene standards were used for plotting calibration curve. Data was collected using EmPower Pro software.

2.1.2. CHNS elemental analysis

CHNS elemental analysers provide a means for the rapid determination of carbon, hydrogen, nitrogen and sulphur in organic matrices and other types of materials. They are capable of handling a wide variety of sample types, including solids, liquids, volatile and viscous samples, in the fields of pharmaceuticals, polymers, chemicals, environment, food and energy. The analysers are often constructed in modular form such that they can be set up in a number of different configurations to determine, for example, CHN, CHNS, CNS or N depending on the application. This adaptability allows not only flexibility of operation but also the use of a wide range of sample weights from a fraction of a milligram to several grams (macro-systems). In its simplest form, simultaneous CHNS analysis requires high temperature combustion in an oxygen-rich environment and is based on the classical Pregl-Dumas method.¹¹ This combustion can be carried out under both static conditions i.e. introduction of a set volume of oxygen or dynamic conditions i.e. a constant flow of oxygen for a set period of time. Often, catalysts are also added to the combustion tube in order to aid complete combustion.

Elemental analysis studies were done in Thermo Finnigan, Italy; model EA1112 Series Flash Elemental Analyzer. This analyzer measures the amount of C, H, N and S in samples by rapid combustion of small amounts (1-2 mg) of the sample in pure O₂ (Dumas method or “flash combustion”). The analysis of all elements in the CHNS group was performed simultaneously.

2.1.3. ICP-OES and SEM-EDAX analysis

Inductively Coupled Plasma-Optical Emission Spectrometry (ICP-OES) is one of the most common techniques for the elemental analysis. Its high specificity, multi-element capability and good detection limits result in the use of the technique in a large variety of applications. All kinds of dissolved samples can be analysed, varying from solutions containing high salt concentrations to diluted acids. A plasma source is used to dissociate the sample into its constituent atoms or ions, exciting them to a higher energy level. They return to their ground state by emitting photons of a characteristic wavelength depending on the element present. This light is recorded by an optical spectrometer. When calibrated against standards the technique provides a quantitative analysis of the elements present in the sample.

For ICP-OES analysis, SPECTRO ARCOS Germany, FHS 12 instrument was employed. For the preparation of the samples for ICP analysis, 0.5 g of lignin was weighed in a crucible and then kept in the muffle furnace. Under air, sample was heated to 650 °C for 6 h with a ramp rate of 5 °Cmin⁻¹. It is suggested that during this process, C, H and O will be burned off in the form of CO, CO₂, CH₄ etc. and in the crucible any unburned residues will remain. This residue was then dissolved in Millipore water and subjected to ICP-OES analysis.

To confirm the elements present in lignin samples another technique used was SEM-EDAX.¹²⁻¹³ In this technique sample is irradiated with a source of X-ray, which ejects an electron present in the inner shell and creates a hole. When an electron from a higher energy shell fills this hole, energy is released in the form of X-rays. These X-rays generated are recorded, which is characteristic for particular element. The SEM micrographs of the samples were obtained on a Leo Leica Cambridge UK Model Stereoscan 440 scanning electron microscope, with an electron beam of 5-50 eV. Lignin samples were prepared by mounting on carbon tapes and were analysed.

2.1.4. FT-IR Spectroscopy

Fourier transform infrared (FTIR) spectroscopy deals with the vibration of chemical bonds in a molecule at various frequencies depending on the elements and types of bonds. After absorbing electromagnetic radiation, the frequency of vibration of a bond increases leading to transition between ground state and several excited states. These absorption frequencies represent excitations of vibrations of the chemical bonds and thus are specific to the type of bond and the group of atoms involved in the vibration. The energy corresponding to these frequencies correspond to the mid-infrared region (4000–400 cm⁻¹) of the electromagnetic spectrum. The term Fourier transform (FT) refers to a recent development in the manner in which the data are collected and converted from an interference pattern to an infrared absorption spectrum that is like a molecular "fingerprint".

IR technique has been widely used for the identification of functional groups in lignin.^{12, 14-18} There are about 20 main asymmetric absorption bands, which are typically observed for high molecular weight compounds with irregular structures (Eg. lignin). Lignin analysis was performed on Bruker Optics ALPHA-E spectrometer,

USA; with a universal Zn-Se ATR (attenuated total reflection) accessory in the 600-4000 cm^{-1} region or using a Diamond ATR (Golden Gate).

2.1.5. ^1H and ^{13}C NMR analysis

Nuclear magnetic resonance (NMR) spectroscopy is one of the most powerful tools to investigate the structure and dynamics of a molecular system in liquid phase. Atomic nuclei consisting of odd number of protons and/or neutrons possessing a nuclear spin $I \neq 0$ and consequently a magnetic moment $\mu = \gamma\hbar I$ (γ = gyromagnetic ratio), when placed in a magnetic field of strength B_0 , Zeeman interaction results in quantized orientations of the nuclear magnetic moments. The nucleus can adopt $2I + 1$ Eigen states with energies $E(m) = -m\gamma\hbar B_0$, where $m = (I, I-1, \dots, -I)$. Transitions between neighbouring energy states ($\Delta m = \pm 1$) can be induced by electromagnetic radiation (energy $E = h\nu$) of frequency $\nu_0 = \gamma B_0/2\pi$. The chemical shift interaction arises from secondary local magnetic fields induced by the interaction of the electrons surrounding the nucleus. The induced local field opposes B_0 and hence shields the nucleus under observation. The shielding is spatially anisotropic due to the non spherical electron distribution around the nucleus.

Solid state ^{13}C NMR analysis for lignin was done in Bruker AV300, Germany; at 10 kHz with a pulse program Cp, av and no. of scans were 7642.

Liquid ^1H and ^{13}C NMR of dealkaline lignin was recorded on Bruker Ascend-700 MHz using CD_3OD and D_2O mixture as solvent with TMS as an internal standard. The sample consisted of 70 mg of lignin dissolved in 0.75 mL of CD_3OD and D_2O mixture (5:1 v/v). No. of scans used for ^{13}C NMR were 10376.

2.1.6. XRD analysis

It is well recognised that X Ray Diffraction (XRD), based on wide-angle elastic scattering of X-rays, has been the single most important tool to determine the structure of the materials characterized by the long range ordering. The XRD patterns are obtained by the measurements of the angles at which the X-ray beam is diffracted by the sample. Bragg's equation relates the distance between two hkl planes (d) and angle of diffraction (2θ) as: $n\lambda = 2d\sin\theta$, where λ = wavelength of X-rays, n = an integer known as the order of reflection (h , k , and l represent Miller indices of respective planes). From the diffraction patterns, the uniqueness of mesoporous structures, phase

purity, degree of crystallinity and unit cell parameters of the semi crystalline hybrid materials can be determined. The identification of phase is based on the comparison of a set of reflections of the sample with that of pure reference phases distributed by International Center for Diffraction Data (ICDD). Unit cell parameter of a cubic lattice can be determined by the following equation:

$$a_0 = d_{hkl} \sqrt{(h^2 + k^2 + l^2)},$$

where d = distance between two consecutive parallel planes having Miller indices h , k , and l . XRD broadening analysis has been widely used to characterize supported metal crystallites in the nanoscale. The average size of nanoparticles can be estimated using Debye-Scherrer equation: $D = k \lambda / \beta \cos \theta$, where D = thickness of the nanocrystal, k is a constant, λ = wavelength of X-rays, β = width at half maxima of reflection at Bragg's angle 2θ .

Powder XRD analysis of lignin was performed using PANalytical X'pert Pro, Netherlands; with dual goniometer diffractor. The source of X-ray was $\text{Cu K}\alpha$ (1.5418 Å) radiation with Ni filter and sample scanning was done from a 2θ value of 5 to 90 ° at the rate of 4.3 °min⁻¹.

2.1.7. UV-Vis analysis

UV-Vis analysis deals with the study of electronic transitions between orbitals or bands of atoms, ions or molecules in gaseous, liquid and solid state. Light brown color of wood derives from typical structural units/functionalities of lignin. A study was made to identify the contribution of color in the lignin using UV-Vis analysis.¹⁹⁻²⁰

The chromophores causing the color in lignin were identified by UV-Vis absorption measurements carried out in VARIAN'S Cary 300 UV-Vis spectrophotometer. Samples were prepared in $\text{H}_2\text{O}:\text{CH}_3\text{OH}$ (1:5 v/v) and was analysed in the range of $\lambda = 200\text{-}800$ nm.

2.1.8. TGA-DTA analysis

Thermogravimetric Analysis-Differential Thermal (TGA-DTA) analysis, the change in weight of the sample is measured as a function of temperature or time. TGA-DTA instruments can quantify loss of water, loss of solvent, decarboxylation, pyrolysis,

oxidation, decomposition happening at these temperatures and also the weight % of ash (unburnt residue) obtained after the analysis. TGA instrument consists of a sample pan that is supported by a precision balance. That pan resides in a furnace and is heated or cooled during the experiment. The mass of the sample is monitored during the experiment. A sample purge gas is used to control the sample environment. This gas may be inert or a reactive gas (air) that flows over the sample and exits through an exhaust. Purge gas is used so that the sample only reacts to temperature during decomposition.

TGA analysis for lignin samples were studied using METTLER TOLEDO TGA/SDTA851 series, USA; instrument with a heating rate from room temperature to 1000 °C at a rate of 10 °Cmin⁻¹, to study the complete decomposition. Thermal degradation studies were done in both N₂ and air atmosphere.

2.2. CATALYST CHARACTERIZATION TECHNIQUES

Characterizations were performed to understand the physico-chemical properties of solid acid catalysts and supported metal catalysts. Following are the details on the instruments used for characterization and the methods used sample preparation.

2.2.1. ICP-OES analysis

Elemental composition of solid acids and supported metal catalyst was determined using Inductively Coupled Plasma-Optical Emission Spectroscopy (ICP-OES) technique. Si/Al ratio of zeolites, SiO₂-Al₂O₃ and percentage of metal loading in supported metal catalysts was confirmed by this technique. Details on the principle, instrumentation are already mentioned in section 2.1.3.

In the case of zeolites, 0.05 g was weighed in the polypropylene bottle, to this ca. 2 g of HF was added followed by 2 mL of water and ca. 0.01 g of conc. H₂SO₄. The mixture was heated at 80 °C to remove the excess HF. The resulting mixture is then diluted and made to 50 mL, filtered using 0.22 micron filter and analysed using ICP-OES.

In the case of supported metal catalyst, 0.01g was weighed in the polypropylene bottle and ca.2 mL of aqua regia (conc. HNO₃:HCl = 1:3 molar ratio) was added to it. The mixture was heated at 80 °C, 20 g of water was added and the

solution was recovered. The resulting mixture is then diluted and made to 10 mL, filtered using 0.22 micron filter and analysed using ICP-OES technique.

2.2.2. XRD analysis

XRD analysis of solid acid catalysts and supported metal catalysts was performed. Details on the principle, instrumentation are mentioned in section 2.1.6.

2.2.3. N₂ sorption analysis

Gas adsorption measurements are widely used for determining the surface area pore volume and pore size of porous solid materials. Nitrogen is commonly used as the adsorbate at liquid nitrogen temperature. Typically materials show six types of isotherms. Type I isotherms are given by microporous solids having relatively small external surfaces (e.g. activated carbons, molecular sieve zeolites and certain porous oxides) The reversible Type II isotherm is the normal form of isotherm obtained with a non-porous or macroporous adsorbent. The reversible Type III isotherm are not common, but there are a number of systems (e.g. nitrogen on polyethylene) which give isotherms with gradual curvature and an indistinct Point B. Characteristic features of the Type IV isotherm are its hysteresis loop, which is associated with capillary condensation taking place in mesopores, and the limiting uptake over a range of high relative pressure. Type V isotherm is uncommon; it is related to the Type III isotherm in that the adsorbent-adsorbate interaction is weak, but is obtained with certain porous adsorbents. Type VI isotherm are shown those obtained with argon or krypton on graphitised carbon blacks at liquid nitrogen temperature. Different types of physisorption isotherms are given in Figure 2.1.

Properties like surface area, pore size and pore volume of solid acid catalysts and supported metal catalysts were determined using nitrogen sorption study. Analysis was done in Autosorb 1C Quantachrome, instrument, USA. Prior to the analysis samples were activated in vacuum at 250 °C for 3 h. The specific surface area was determined using BET method, pore size data was obtained using BJH method and pore volume using t-plot method.

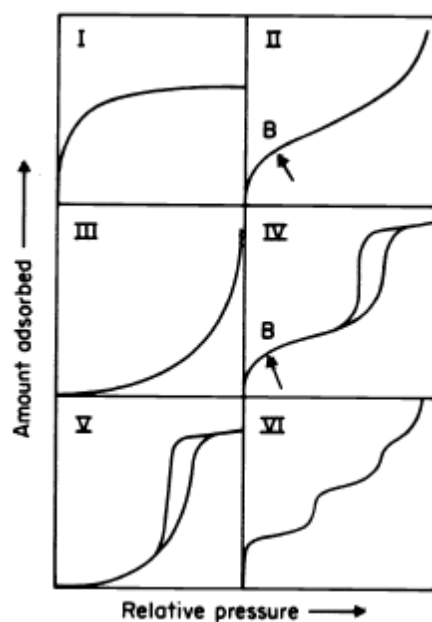


Figure 2.1. Different types of physisorption isotherms.

2.2.4. NH_3 -TPD and CO_2 -TPD analysis

Temperature programmed desorption (TPD) is a technique used to quantify the acidic or basic sites present in the material. Here ammonia (NH_3) is used as a basic probe molecule which is adsorbed on the acid sites and carbon dioxide (CO_2) is acidic probe molecule which adsorbs on the acids sites of the material. With increase in temperature; the probe molecule is desorbed and is recorded using a TCD detector.

Amount of acid sites (strong and weak) present in solid acid catalyst were determined using NH_3 -TPD analysis. Analysis was done in Micromeritics Autochem-2910 model, instrument; USA. Catalyst was activated at a temperature of 500 °C in Helium gas flow (25 mLmin^{-1}) and NH_3 adsorption (30 mLmin^{-1}) was done at 100 °C, desorption was started from 100 to 823 °C at the rate of $10 \text{ }^\circ\text{Cmin}^{-1}$. At lower temperature range (150-350 °C) NH_3 gets desorbed from weak acid sites and at a higher temperature range (350-750 °C) desorption of NH_3 happens from strong acid sites. Density of acid sites can be measured from the quantity of NH_3 desorbed.

CO_2 -TPD was done using Micromeritics AutoChem 2910 instrument. Prior to measurement, samples were activated at 350 °C for 15 min. The adsorption of CO_2 was done at 50 °C and then the sample was kept at 100 °C under Helium gas flow (25 mLmin^{-1}). After this the sample was heated from 100 to 600 °C with a ramping rate of $4 \text{ }^\circ\text{Cmin}^{-1}$.

2.2.5. HRTEM analysis

High Resolution Transmission electron microscopy (HRTEM) is typically used for high resolution imaging of thin sections of solid samples for nanostructural and compositional analysis.

HRTEM images of supported metal catalysts were obtained using FEI TECNAI T30 Model instrument working at an accelerating voltage of 300 kV. Sample was dispersed in isopropanol, sonicated and then a drop of the solution was deposited on grid to take the image.

2.2.6. ^{29}Si and ^{27}Al MAS NMR

For details on principle of the technique refer section 2.1.5.

Solid state ^{29}Si and ^{27}Al MAS NMR spectra were recorded on a Bruker AV300, Germany. Finely powdered fresh and spent catalyst samples were placed in zirconia rotors and spun at 4 kHz for ^{29}Si (no. of scans 2000) and 6 kHz for ^{27}Al (no. of. scans 3454). The chemical shifts were referenced to TMS ($\delta = -82.4$ ppm from TMS) and $[\text{Al}(\text{H}_2\text{O})_6]^{3+}$ ($\delta = 0.0$ ppm) for ^{29}Si and ^{27}Al , respectively.

CHAPTER 2A

**LIGNIN ISOLATION AND
CHARACTERIZATION**

2A.1. INTRODUCTION

Lignin is a 3D amorphous aromatic biopolymer comprising 15-25 % of lignocellulosic biomass.¹⁻³ The main biological role of the lignin in plants is to provide strength and rigidity to the plant, and also to protect the plant tissues from microbial attack. In addition to its biological importance it has a very fundamental role as a renewable feedstock. Also it is one of the major by-products from paper and pulp industry and cellulose to bio-ethanol process. Lignin is formed by the enzymatic polymerization of phenyl propanoid units, coniferyl alcohol, p-coumaryl alcohol and sinapyl alcohol which are linked together by C-C and C-O-C bonds (Refer chapter 1 section 1.4.2).⁴⁻⁶ Lignin structure contains several alkoxy groups, phenolic hydroxyl groups, benzyl alcohol groups, carbonyl groups and some terminal aldehydic groups in the side chains attached to aromatic rings.⁷ It is well known that the structures of lignin and linkages present between several aromatic units, depends on the plant species, plant parts and even the extraction techniques used for the isolation of lignin from lignocellulosic biomass.^{8,9-12} Lignin, due to its abundant availability and having aromatic nature can be industrially very useful for the production of value added chemicals and fuels. Lignin can be depolymerized into aromatic monomers which can be further upgraded via hydrodeoxygenation reactions, to make them suitable to be used as fuel additives.^{8, 13-16}

As mentioned above the properties and structures of lignin are dependent on the linkages and functional groups present in it. Lignin was characterized using various techniques in order to understand their properties. However characterization of lignin is very difficult due to its complex nature, diversity in their source and extraction methods. In my study, for valorization of lignin into aromatic monomers using solid acid catalysts, actual lignin substrates from commercial sources namely, dealkaline, organosolv, alkali; lignin from local industry namely, ORG and EORG; also lignin was isolated by organosolv method, namely bagasse lignin were employed. Therefore before performing the depolymerization study of these lignin, it was decided to study about the structural and functional properties using various physico-chemical techniques. Several techniques like MALDI-TOF (Matrix Assisted Laser Desorption Ionization-Time of Flight) and GPC (Gel Permeation Chromatography) analysis were used for the determination of molecular weight. CHNS elemental, ICP-OES (Inductively Coupled Plasma-Optical Emission Spectroscopy), EDAX (Energy

Dispersive X Ray Analysis) techniques were used for the determination of the elements present in lignin substrate. Functional group analysis was done using NMR (Nuclear Magnetic Resonance) and FTIR (Fourier Transform Infrared) spectroscopy. To know about the crystallinity of the substrate XRD (X Ray Diffraction) was used. Functional group analysis was again performed by UV-Vis technique and the thermal degradation behaviour of lignin was studied using TGA-DTA (Thermo Gravimetric Analysis-Differential Thermal Analysis) analytical techniques.¹⁷

Before proceeding to catalytic runs, solubility of lignin was checked in a wide range of organic solvents (polar to non-polar; polarity index, 0-9). One of the major of the solubility study for lignin substrate was to select a reaction medium for lignin depolymerization and second aim was to select a solvent in which only aromatic monomers (depolymerized products) can be extracted out from the reaction mixture leaving behind the unreacted lignin.

Lignin can be isolated from lignocellulosic biomass using various methods (acid/base (Kraft) hydrolysis, organosolv, pyrolytic, steam explosion methods etc.) (Refer chapter 1, section 1.5). But the isolation of lignin from other wood components (cellulose and hemicellulose) without damaging its structure is a major problem in lignin chemistry. There are several disadvantages associated with the lignin isolation techniques like in the case of acid or base hydrolysis method there is a significant change in the structure of lignin which makes the isolated lignin with a structure, quite different from the native lignin present in the plant tissue.¹⁸ But there other methods which can isolate lignin without undergoing much changes in its structure like, organosolv method (extraction with organic solvents), solvent extraction after extensive grinding (Björkman or milled wood lignin) and the treatment of wood with hydrolytic enzymes in order to remove the polysaccharide associated with it prior to solvent extraction (cellulolytic enzyme lignin).¹⁸ So it is important to choose a suitable isolation method for lignin, where there is not much structural and functional deformation of lignin during the process.

In the study on the depolymerization of lignin using solid acid catalysts organosolv method (organic solvent soluble lignin) was adapted for the isolation of lignin from lignocellulosic biomass (sugarcane biomass) so that the extracted lignin has its characteristics similar to the native lignin in plant. Also organosolv method provides lignin with high purity compared to other (Kraft process, liginosulfonate)

processes. In Kraft process Na_2S and NaOH are typically used as reagents,^{9-10, 19-21} which contaminates lignin with Na and S as impurities. To avoid these contaminations organosolv method was preferred for the isolation of lignin in this study.

2A.2. RESULTS AND DISCUSSIONS

Six types of lignin having different structural and functional properties were employed in the study of lignin depolymerization using solid acid catalysts. Dealkaline lignin (TCI Chemicals, product no. L0045), alkali lignin (Aldrich, product no. 370959) and organosolv lignin (Aldrich, product no. 371017) were purchased and used without any pre-treatment. Along with commercial ones, lignin were collected from local industries, ORG (organosolv lignin) and EORG (organosolv lignin etherified) lignin. Also, by organosolv method lignin was isolated (refer section 2A.2.1) from sugarcane baggase (baggase lignin). Since the source and extraction methods are different, it is obvious that each lignin will differ in their properties. All these lignin were completely characterized using several physico-chemical techniques.

2A.2.1. Lignin extraction from sugarcane bagasse

Among the various methods currently studied for the lignin isolation, the organosolv processes are considered to be very promising. Organosolv processes use either low-boiling solvents (e.g., methanol, ethanol, acetone), which can be easily recovered by distillation, or high-boiling solvents (e.g. ethylene glycol, ethanolamine), which can be used at a low pressure. These procedures produces large amount of high-quality lignin which is relatively pure, primarily unaltered and less condensed than other pretreatment lignin.

In my study the source used for lignin extraction was sugarcane bagasse. Sugarcane bagasse contains 45-55 % cellulose and 20-25 % hemicellulose, 18-24 % lignin, along with 1-4 % ash and < 1 % wax in it.²² Organosolv method was used for lignin extraction.²³ Methanol was used as the organic solvent for the dissolution of lignin. Lignin extraction was performed in reflux condenser set up. 10 g of crushed sugarcane bagasse in 180 mL methanol was heated at 120 °C for 24 h. The mixture was cooled and filtered. In the methanol soluble part (dark brown solution) lignin was extracted. The solid obtained after filtration was also washed with excess methanol to completely remove any lignin present. The entire methanol soluble portion was

collected and concentrated using rotary evaporator and then dried at 60 °C for overnight (16 h); followed by drying under high vacuum (10^{-4} MPa) at 150 °C for 3 h. The solid obtained after drying was weighed. It was observed from that 10 g of sugarcane bagasse 0.45 g of methanol soluble lignin was isolated using organosolv method. The lignin obtained by this process was named as bagasse lignin and was a dark brown in color. To study about the structural and functional properties, bagasse lignin was characterized using XRD, CHNS, TGA-DTA, SEM-EDAX and ICP-OES techniques.

2A.2.2. MALDI-TOF mass spectroscopy and GPC analysis

Molecular weight of lignin is one of the principal properties to be studied in order to understand the reactivity and physical properties of lignin.²⁴⁻²⁶ MALDI-TOF and GPC analysis were used to study about the molecular weight of lignin.

Dealkaline lignin was analysed from the m/z range of 1000-10,000 gmol^{-1} and 10,000-100,000 gmol^{-1} (Figure 2A.1). A broad peak was observed with a peak maximum at ca. 60,000 gmol^{-1} . Broad peaks were observed for dealkaline lignin due to its poor ionization probably due to their poor capability in carrying charge for mass spectrometric detection. From previous reports also it is understood that MALDI-TOF analysis of lignin gives a broad and weak peak with lot of noises due to less ionization of the molecules.²⁷

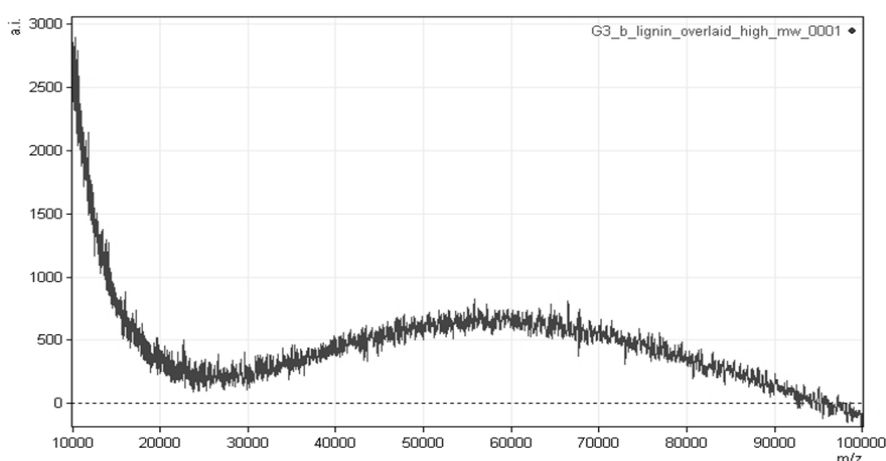


Figure 2A.1. MALDI-TOF analysis of dealkaline lignin.

Molecular weights of dealkaline, organosolv lignin and ORG lignin were also determined by GPC technique (Table 2A.1).²⁸⁻³¹ GPC analysis for dealkaline lignin

was performed in DMF solvent. Dealkaline lignin showed peaks corresponding to molecular weights at $60,000 \text{ gmol}^{-1}$. This data is in correlation with molecular weight ($60,000 \text{ gmol}^{-1}$) obtained from MALDI-TOF analysis. GPC analysis for organosolv and ORG lignin was performed in THF solvent. Organosolv lignin showed $M_n = 2285 \text{ gmol}^{-1}$, $M_w = 4575 \text{ gmol}^{-1}$, P. D. = 2 and ORG lignin showed $M_n = 4177 \text{ gmol}^{-1}$, $M_w = 7059 \text{ gmol}^{-1}$, P. D. = 1.68. P. D. (>1) value for both organosolv and ORG lignin showed that these samples have heterogeneous distribution of fractions having different chain lengths.

Molecular weight of alkali lignin was obtained from Aldrich supplier showing $M_n = 5000 \text{ gmol}^{-1}$, $M_w = 28000 \text{ gmol}^{-1}$ and P. D. = 5.6. From these data it was understood that alkali lignin also shows heterogeneous fractions with different chain lengths. Therefore from molecular weight determination it was understood that all the lignin used in this study have high molecular weights (above 2000 gmol^{-1}) with dealkaline lignin having the highest ($60,000 \text{ gmol}^{-1}$) amongst all. Most of earlier works report the depolymerization studies on dimers/trimers of lignin model compounds,³²⁻³⁸ but in my work I have used actual lignin substrates having very high molecular weight ($60,000 \text{ gmol}^{-1}$).

Table 2A.1. GPC analysis of lignin

Lignin	M.W. (gmol^{-1})		P. D.
	M_n	M_w	
Dealkaline	60,000	-	-
Organosolv	2285	4575	2
ORG	4177	7059	1

2A.2.3. CHNS elemental analysis

CHNS elemental analysis of different types of lignin (dealkaline, organosolv, alkali, ORG, EORG, bagasse) was performed. Since lignin is a polymer having phenolic building units, it was expected to have elements like C, H and O. CHNS elemental analysis revealed that the lignin is composed of 60-65 % C and 5-8 % H, except in case of ORG and bagasse lignin which is made up of 57 % and 51 % of C (Table 2A.2).³⁹⁻⁴⁰ Based on these results, a general (monomer) molecular formula of lignin

was derived and are tabulated in Table 2A.2. S contamination was observed for dealkaline and alkali lignin, as those might have been isolated from lignocellulosic biomass using Kraft method where Na₂S and NaOH were typically used as reagents.^{9-10, 19-21} Typically, all the lignin have the general formula, C_xH_yO_z (x: 7.9-9.0; y: 10-10.62; z: 2.89-4.5) which correlates well with the reported ones.^{8, 41-42}

Table 2A.2. CHNS elemental analysis of various types of lignin

Lignin	C (%)	H (%)	S (%)	Monomer molecular formula
Dealkaline	65	7	1	C ₉ H _{10.62} O _{2.89} S _{0.06}
Organosolv	65	6	0	C ₉ H ₁₀ O ₃
Alkali	61	6	1	C _{8.47} H ₁₀ O _{3.3} S _{0.05}
ORG	57	8	0	C _{8.5} H ₁₀ O ₄
EORG	59	5	0	C ₉ H ₁₀ O ₄
Bagasse	51	7	0	C _{7.9} H _{10.1} O _{4.5}

2A.2.4. ICP-OES and SEM-EDAX analysis

Elemental analysis of different types of lignin (dealkaline, organosolv, alkali, ORG, EORG, bagasse) was determined using ICP-OES technique.⁴³⁻⁴⁴ As expected, the elemental analysis done using ICP-OES and SEM-EDAX characterizations revealed the presence of Na and S in dealkaline and alkali lignin, as those might have been isolated using Kraft method where Na₂S and NaOH were used as reagents (Table 2A.3).¹⁹⁻²¹

It was observed that in dealkaline and alkali lignin 967 ppm and 2333 ppm of Na was present, respectively. Organosolv, ORG, EORG and bagasse lignin does not contain any Na or S as those are isolated by organosolv method where only organic solvents are used, which will result in high purity lignin, free from Na and S.³⁹⁻⁴⁰ By ICP-OES and SEM-EDAX⁴⁵ (Figures 2A) techniques the possibility of presence of other metals (Mg, Ca, K etc.) in lignin, which are required by plant during their growth as nutrients were checked but could not detect their presence, as their concentration if present must be very low.

Table 2A.3. ICP-OES and SEM-EDAX of lignin

Lignin	ICP-OES analysis*		SEM-EDAX of elements
	Na (ppm)	Na(mg)	
Dealkaline	967	29	C, O, Na, S
Organosolv	0	0	C, O
Alkali	2333	70	C, O, Na
ORG	0	0	C, O
EORG	37	1.1	C, O
Bagasse	0	0	C, O, K, Cl

* ICP-OES analysis of 1 g of lignin

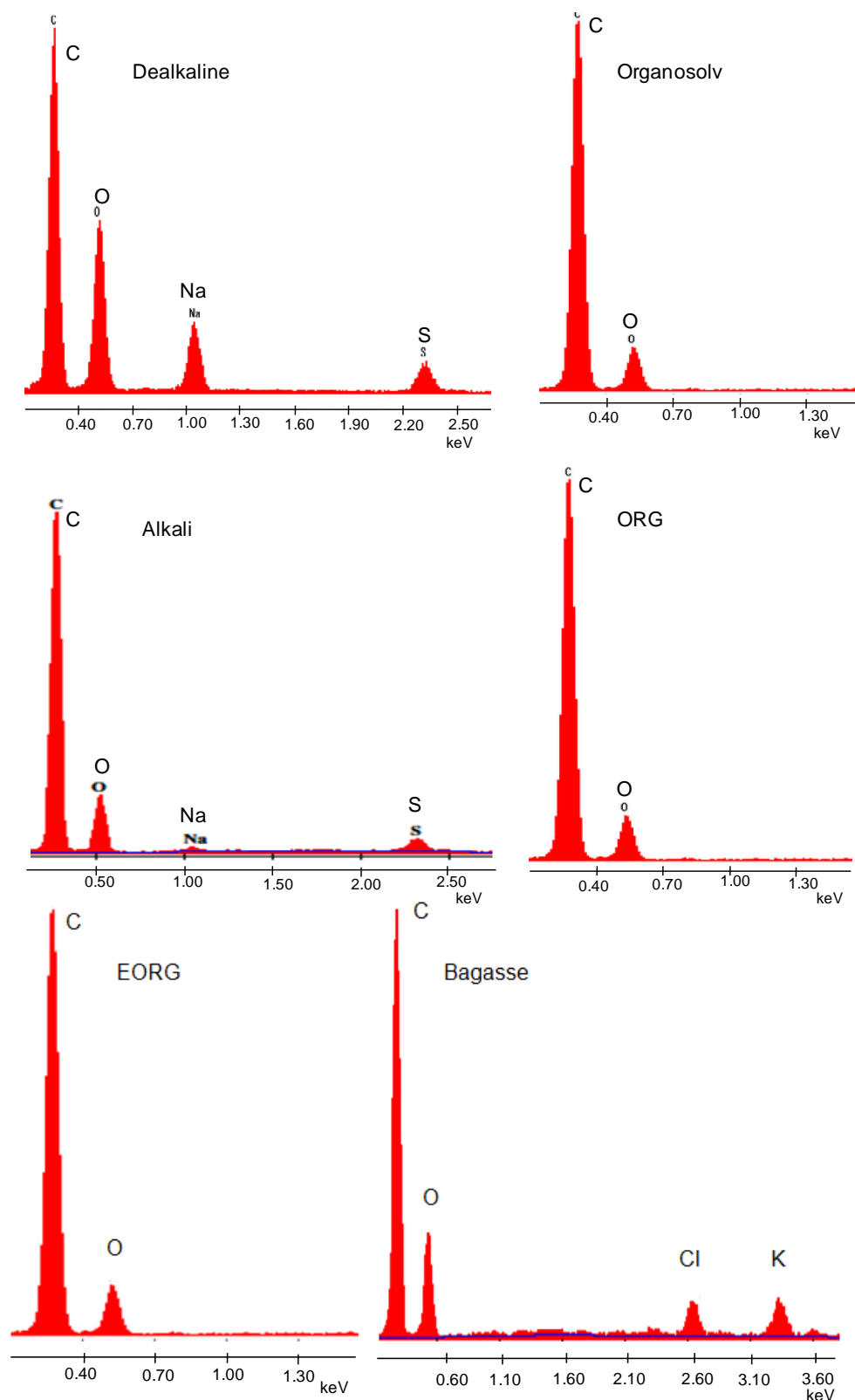


Figure 2A.2. SEM-EDAX analysis of lignin.

2A.2.5. FT-IR Spectroscopy

Functional group analysis of different types of lignin (dealkaline, organosolv, alkali, ORG, EORG, bagasse) were performed using FTIR analysis. All the lignin have similar types and number of functional groups but with different intensities for the peaks depending on the lignin used (Figure 2A.3).⁴⁶⁻⁴⁷

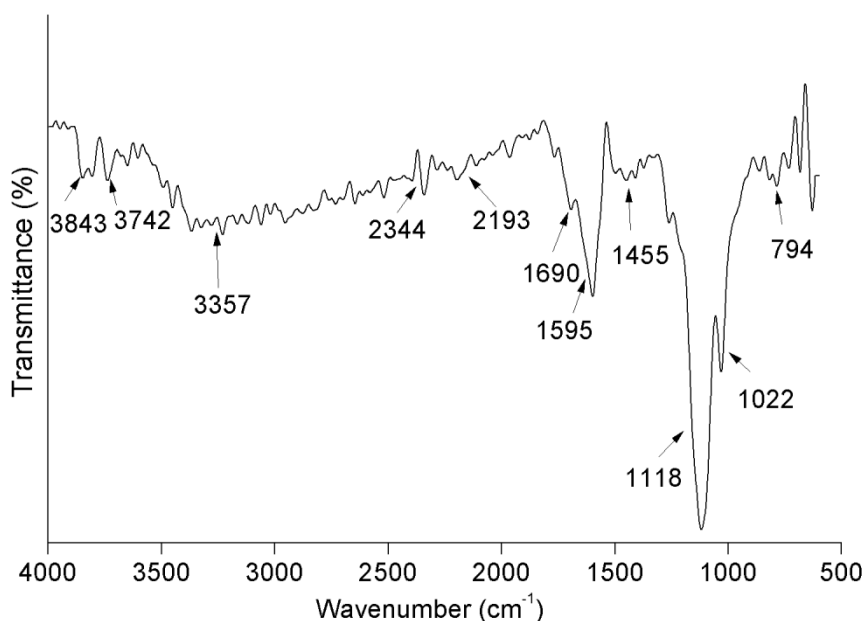


Figure 2A.3a. FTIR analysis of dealkaline lignin.

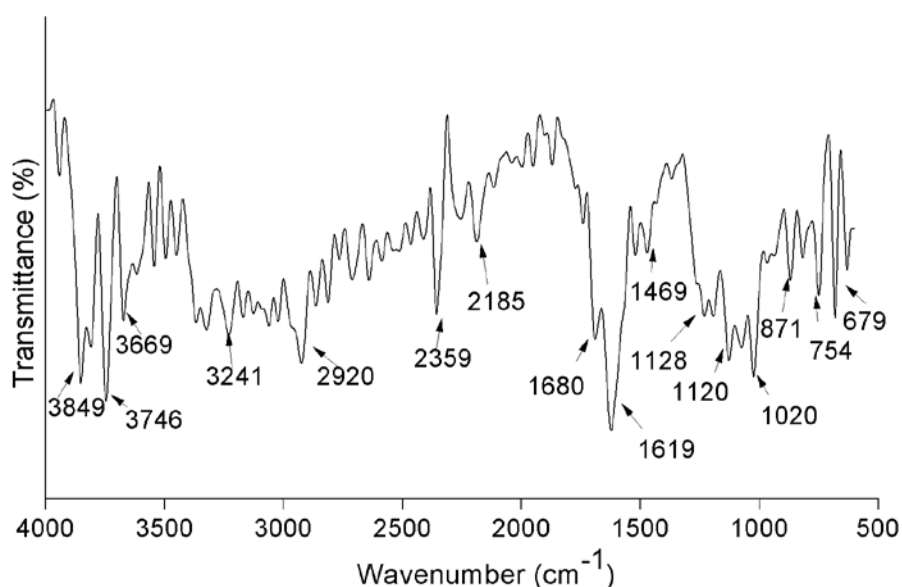


Figure 2A.3b. FTIR analysis of organosolv lignin.

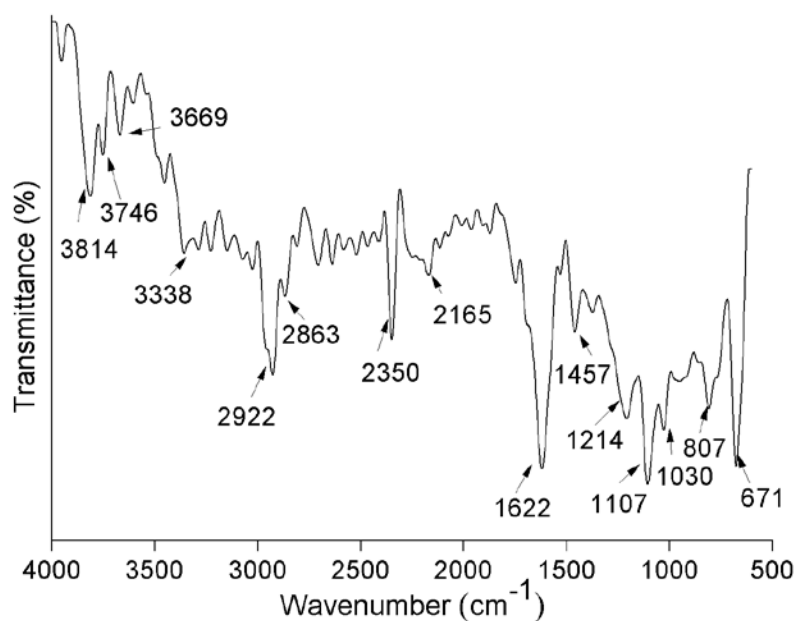


Figure 2A.3c. FTIR analysis of alkali lignin.

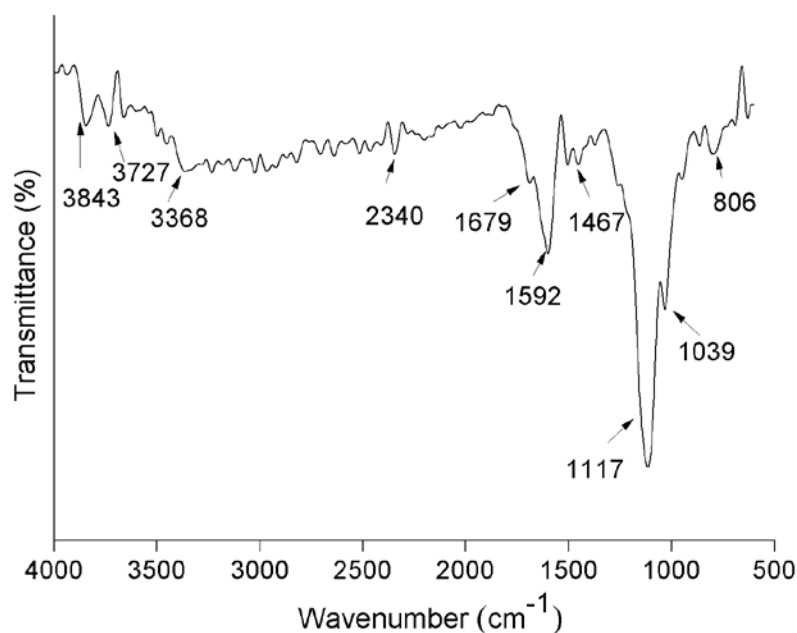


Figure 2A.3d. FTIR analysis of ORG lignin.

A strong broad band was observed in the range of 3200-3600 cm^{-1} for O-H stretching frequency of alcoholic and phenolic hydroxyl groups involved in hydrogen bonding.⁴⁸⁻⁵¹ Sharp bands in the region of 3500-3700 cm^{-1} correspond to free O-H stretching frequency.⁴⁵ In the region of 2850-3000 cm^{-1} , strong bands corresponding to C-H stretching of alkane or alkyl groups can be seen.⁴⁸⁻⁵¹ C-H stretching frequency of alkynes can be observed at 2100-2260 cm^{-1} . Aromatic stretching C-H stretching frequencies (weak to medium bands) are observed at 3000-3100 cm^{-1} and a bunch of

weak bands in the form of “saw tooth” regions are observed at $1700\text{-}2000\text{ cm}^{-1}$ which also corresponds to aromatic rings.⁴⁸⁻⁵¹ Substitutions on aromatic groups are represented by pattern bands in the range of $700\text{-}850\text{ cm}^{-1}$. A strong, broad band in the range of $1670\text{-}1820\text{ cm}^{-1}$ corresponds to C=O stretching frequency of α , β -unsaturated aldehydes. Weak, medium multiple bands between $1400\text{-}1600\text{ cm}^{-1}$ are observed for C=C groups attached to the aromatic ring.⁵² Strong bands in the range of $1000\text{-}1300\text{ cm}^{-1}$ can be assigned to C-O stretching of alkoxy groups/ether linkages/alcohols.⁴⁸⁻⁵¹ These bands are significant in all the lignin which implies that these lignin have higher number of either ether linkages or alkoxy groups. But considering the structure of lignin it is believed that that most of the contribution for these peaks will be coming from ether linkages present in lignin.

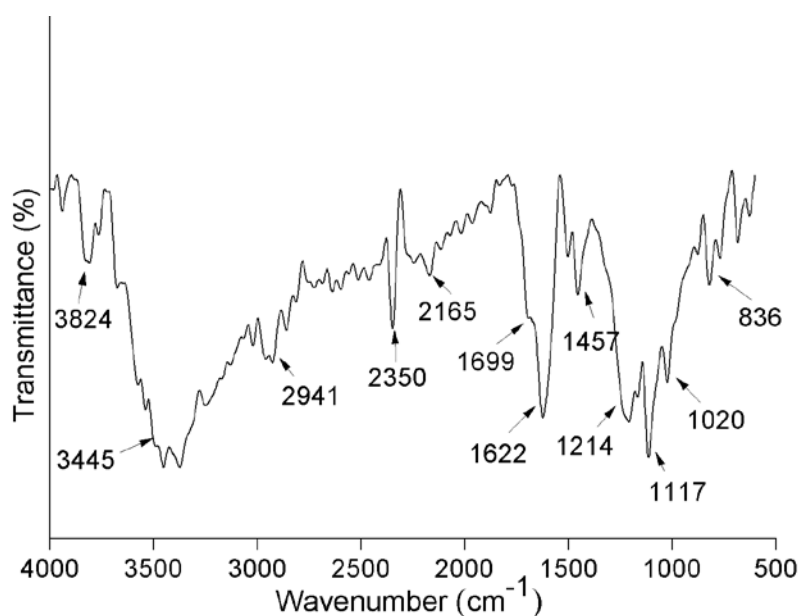


Figure 2A.3e. FTIR analysis of EORG lignin.

Even though the lignin used in my study were having similar functional groups, a careful observation of the IR spectra showed that the intensity of free OH group peaks in the range of $3500\text{-}3700\text{ cm}^{-1}$ and C=C unsaturated groups at 1595 cm^{-1} were found to be highest in organosolv lignin. But the -OH groups involved in hydrogen bonding in the range of $3200\text{-}3600\text{ cm}^{-1}$ was highest in EORG lignin. Another observation was that alkoxy groups or ether linkages were found in abundance for dealkaline lignin rather than any other lignin. This variation in the structure of lignin can be possibly be due to the source of lignin (plant from which it is isolated) and also depends on the types of the techniques used for lignin isolation. So

from IR analysis it was understood that in general all the lignin have aromatic units with methoxyl, hydroxyl, aldehydic, alkyl or alkane substitutions along with a significant amount of ether linkages (β -O-4 linkages).

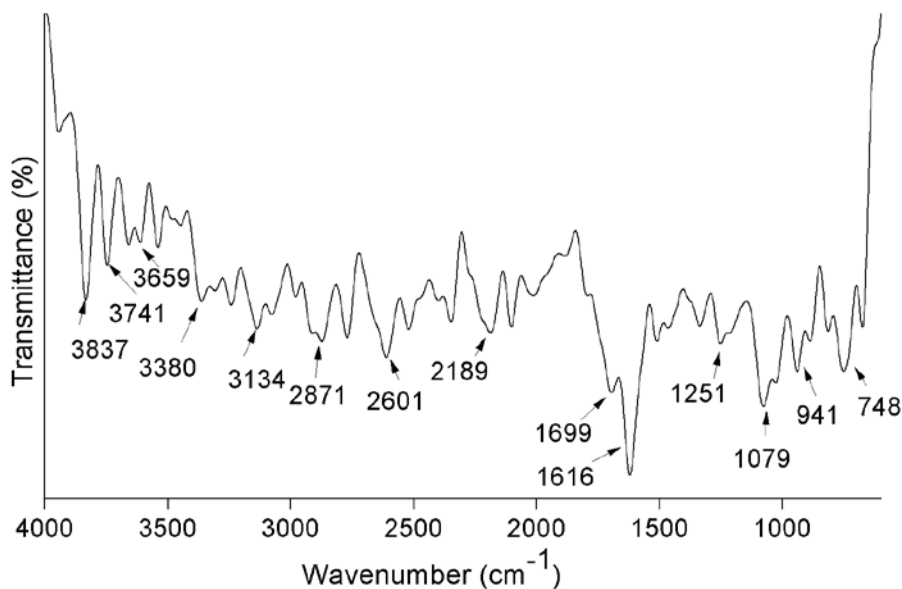


Figure 2A.3f. FTIR analysis of bagasse lignin.

2A.2.6. Solid state ^{13}C NMR analysis

^{13}C NMR characterizations of various lignin disclose the salient features of mainly monolignols and end group distributions. Presence of aromatic rings, ether linkages, unconjugated carbonyl groups, methoxy and alkyl groups etc. in lignin substrate are revealed by this spectroscopic technique.⁵³⁻⁵⁴ Solid state ^{13}C NMR analysis was done for dealkaline, organosolv, ORG, EORG, bagasse lignin (Figure 2A.4). Similar kinds of functional groups were observed in all the samples. Chemical shift at 20-50 ppm corresponding to $\text{CH}_3\text{-CO}$ or R_3CH species are observed. sp^3 carbon appearing next to oxygen ($\text{Ar/R}_2\text{-CH}_2\text{-O}$, $\text{Ar/C}_2\text{-CHO}$, $\text{Ar}_3/\text{R}_3\text{C-O}$) are also seen in the range of 55-90 ppm. An intense peak at 55 ppm common in all lignin, shows that large amount of methoxyl groups are observed attached to the aromatic rings in the lignin structure. Intense peaks observed at 110-150 ppm corresponds to sp^2 carbon ($\text{C}=\text{C}$) in aromatics and alkenes, which shows the aromatic nature of lignin polymer. Few ester groups (Ar/R-CO-R/Ar) are also found in all the lignin in the range of 160-180 ppm. Carbonyl groups (Ar-CHO) are also observed in these lignin in the range of 189-205 ppm.

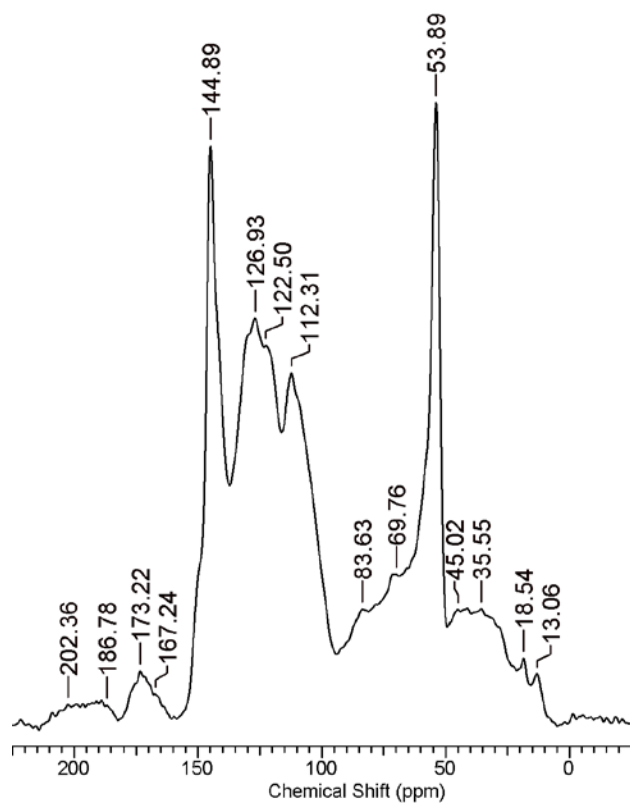


Figure 2A.4a. Solid state ^{13}C NMR spectra of dealkaline lignin.

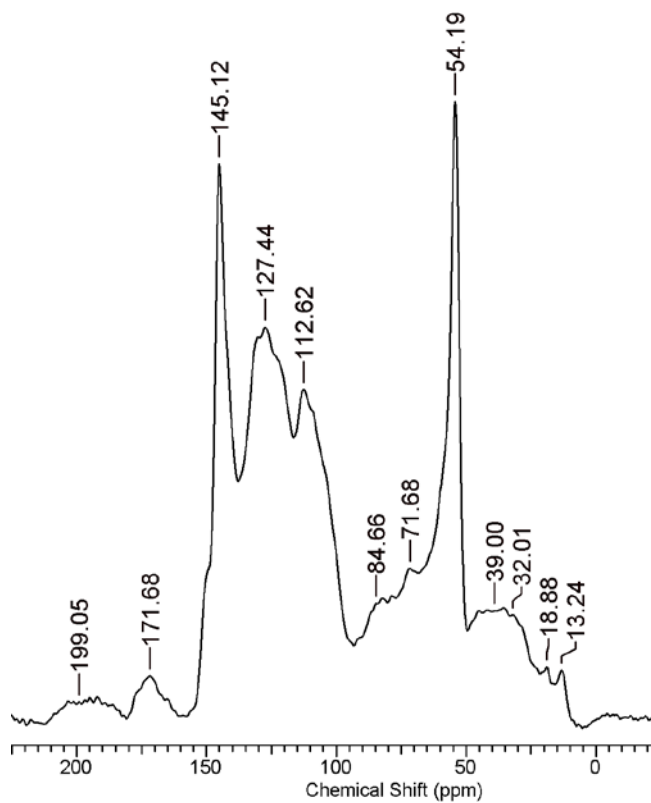


Figure 2A.4b. Solid state ^{13}C NMR spectra of organosolv lignin.

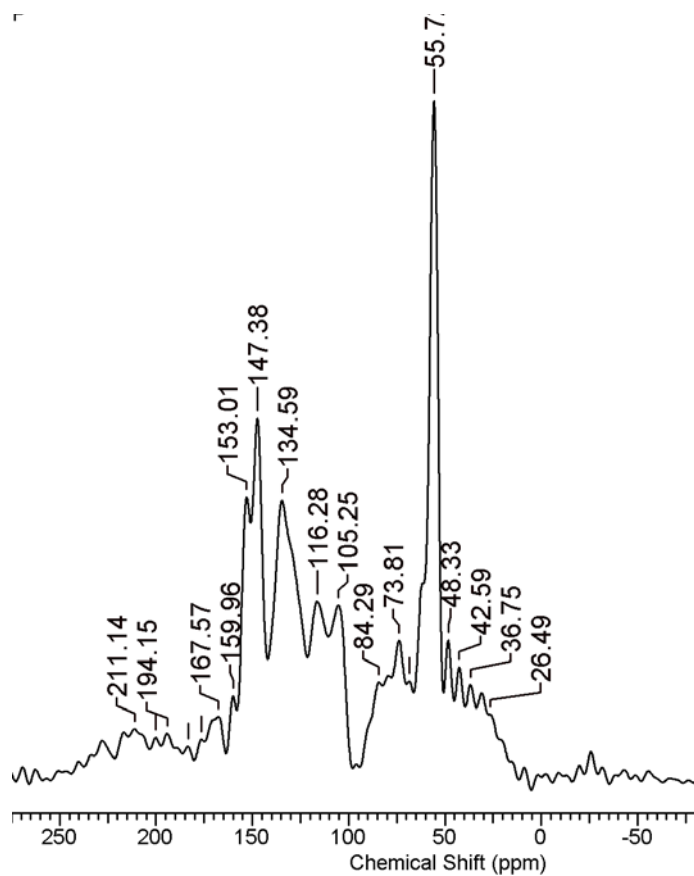


Figure 2A.4c. Solid state ^{13}C NMR spectra of ORG lignin.

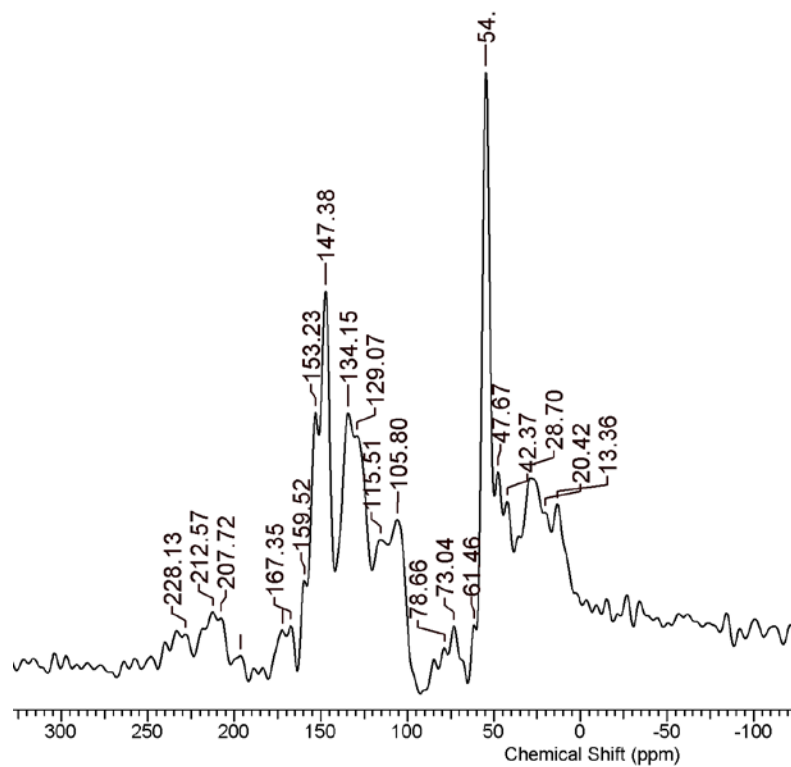


Figure 2A.4d. Solid state ^{13}C NMR spectra of EORG lignin.

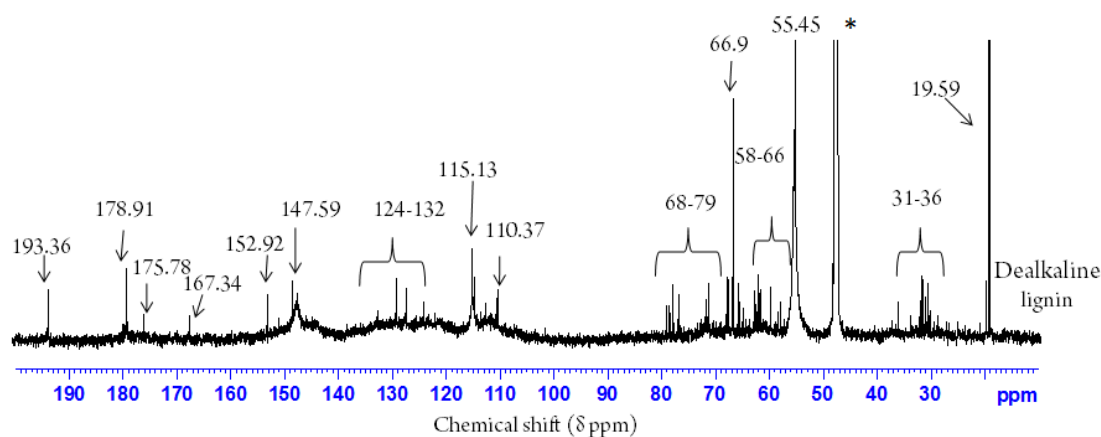


Figure 2A.5. Liquid ^{13}C NMR of dealkaline lignin in $\text{CD}_3\text{OD}:\text{D}_2\text{O}$ (5:1 v/v) solvent.

Liquid ^{13}C NMR was done for dealkaline lignin and data was compared with solid state ^{13}C NMR (Figure 2A.5). Liquid ^{13}C NMR peaks in the range of 20-50 ppm are typically assigned to $\text{CH}_3\text{CO-}$ species or R_3CH species. Observance of peaks at 55-90 ppm is assigned to sp^3 carbon appearing next to oxygen ($\text{Ar/R-CH}_2\text{-O-}$; $\text{Ar}_2/\text{R}_2\text{-CH-O}$; $\text{Ar}_3/\text{R}_3\text{-C-O-}$). It is also discussed that between 30-60 ppm, peak due to $-\text{C}(\text{CH}_3)_3$ are observed. Peaks due to sp^2 carbon ($\text{C}=\text{C}$, 110-150 ppm) in aromatics (125-150 ppm) and alkenes (110-140 ppm) are also clearly visible in the spectra. The peaks between 175-180 ppm are assigned to carbon in esters (Ar/R-CO-R/Ar). Liquid ^{13}C NMR was found to be in good correlation with ^{13}C NMR of dealkaline lignin.

2A.2.7. XRD analysis

XRD analysis was performed for different types of lignin (dealkaline, organosolv, ORG, EORG, bagasse). It is known that lignin is amorphous in nature so it was not expected to observe any sharp peaks representing crystallinity. However; when lignin is separated from lignocellulosic biomass it is possible to be contaminated with the cellulose impurity. It is known that cellulose are crystalline in nature and it shows peaks at $2\theta = 22.5^\circ$ for crystalline cellulose and $2\theta = 17.7\text{-}18.5^\circ$ for amorphous cellulose. In order to detect the presence of cellulose impurity in the lignin sample XRD analysis was performed (Figure 2A.6). XRD pattern showed a broad peak in the range of $10\text{-}30^\circ$ which indicates the amorphous nature of the polymer, which is common in all the lignin and does not indicate amorphous cellulose. But in the case of dealkaline lignin along some additional crystalline peaks were observed. Peaks at 23

$^{\circ}$, 27.9° and 28.7° corresponds to S present in the sample, while peaks at 32° , 48.5° shows the presence of Na. Presence of Na and S in dealkaline lignin was observed since; it may be isolated using Kraft method wherein Na_2S and NaOH are typically used as reagents. S and Na contamination in dealkaline lignin was also detected using ICP-OES and SEM-EDAX analysis (section 2A.2.4).

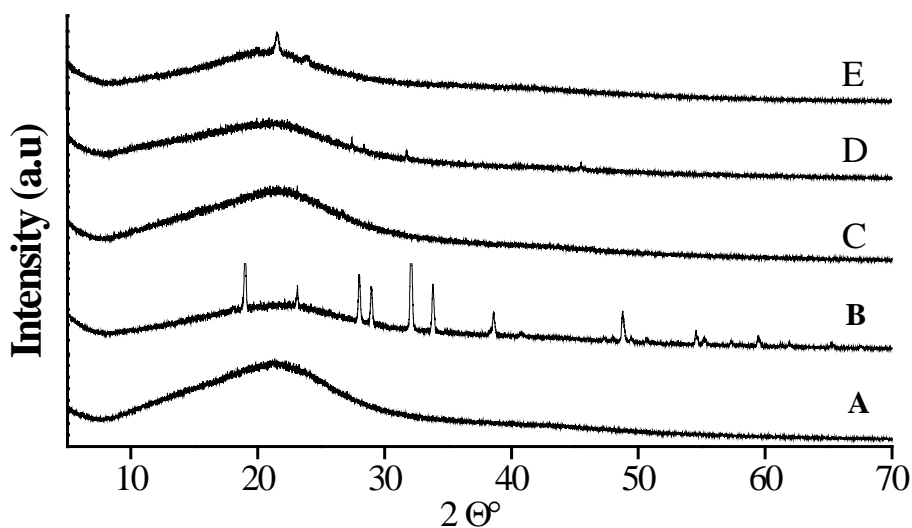


Figure 2A.6. XRD pattern of A) organosolv, B) dealkaline, C) ORG, D) EORG and E) bagasse lignin.

2A.2.8. UV-Vis analysis

The brown color of lignin is due to the presence of chromophores, this was analysed by UV-Vis absorption measurements. Different types of lignin (dealkaline, organosolv, alkali, ORG) were dissolved in methanol: water as solvent and analysed at $\lambda = 200\text{-}800\text{ nm}$ (Figure 2A.7). There were peaks at 280 nm with a shoulder at 230 nm and also a λ value at 312 nm having a shoulder at 340 nm with a gradual decrease in absorption extending towards visible region representing several different chromophores. λ_{max} at 280 nm was common in all lignin and corresponds to $\pi\text{-}\pi^*$ electronic transition in aromatic ring of unconjugated phenolic units, which indicates the presence of free and etherified hydroxyl groups. λ value of 312 nm corresponds to $n\text{-}\pi^*$ transition in lignin units with $\text{C}_\alpha\text{=C}_\beta$ linkages conjugated to the aromatic rings. In the visible region from $400\text{-}600\text{ nm}$ a hump was observed which corresponds to the presence of chromophores in lignin. These chromophores include quinones, carbonyls

in coniferyl aldehyde groups etc. which were also detected using NMR and FT-IR analysis. These characteristics were common for all the lignin employed in the study.

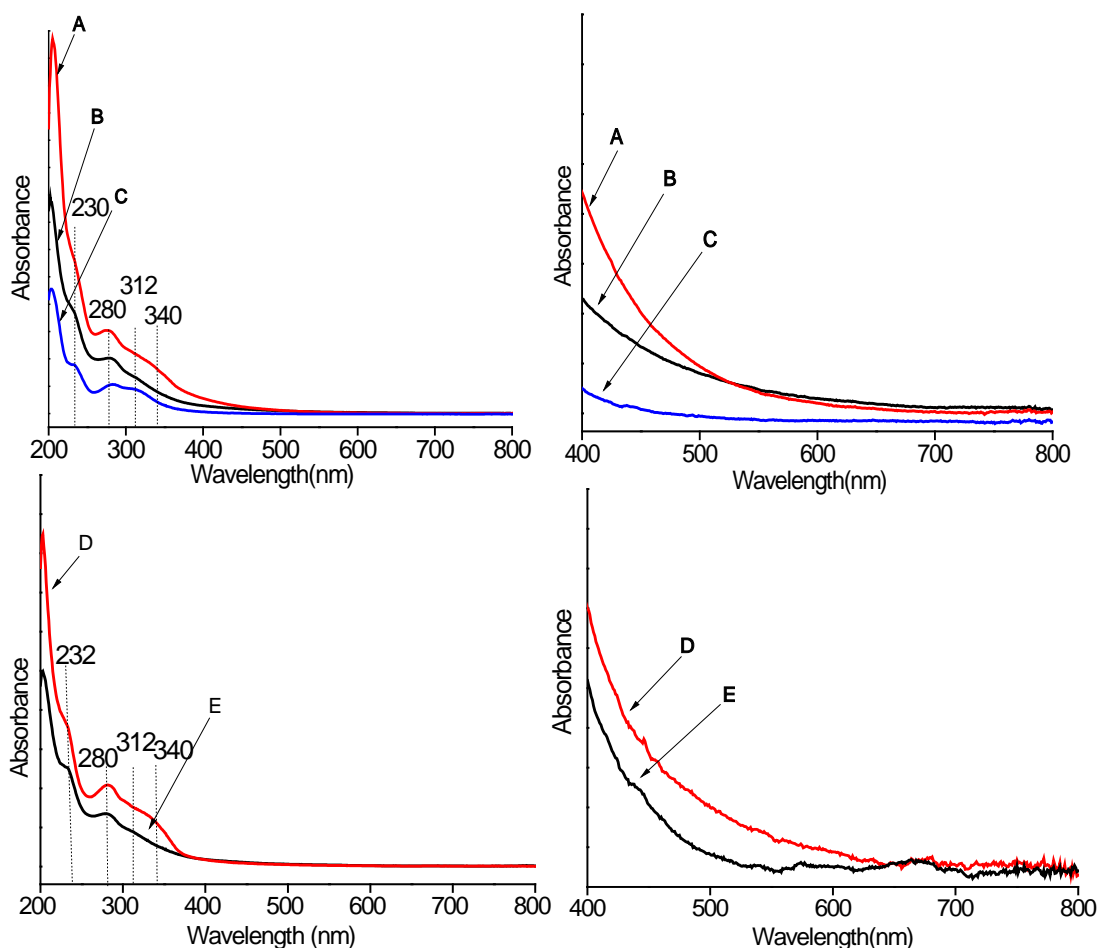


Figure 2A.7. UV-Vis analysis of A) organosolv B) dealkaline C) ORG D) alkali E) EORG lignin.

2A.2.9. TGA-DTA analysis

TGA-DTA analysis of lignin provides information about thermal stability of lignin. Among the components of lignocellulosic materials, lignin is the most thermo-stable component mainly due to the inherent structure of aromatic rings with various branches. Because the reactivity range of lignin is quite wide, the degradation of lignin occurs within a wide temperature range. According to previous reports,⁵⁵⁻⁵⁸ the thermal degradation of lignin could take place in the following steps: 1) cleavage of α - and β -aryl-alkyl-ether linkages occurs between 150 °C and 300 °C; 2) aliphatic side chains start splitting off from the aromatic ring around 300 °C; 3) the carbon-carbon

linkage between lignin structural units is cleaved at 370–400 °C;⁵⁸ decomposition or condensation of aromatic rings is believed to take place at 400–600 °C.⁵⁶ According to the above mentioned literatures, most lignin show their maximum rate of weight loss between 300 °C and 400 °C.⁵⁷

Table 2A.4. Summary on thermal degradation analysis of various lignin

Lignin	TGA (Residue, %)		
	N ₂	Air	H ₂ O (air)
Dealkaline	36	17	11
Organosolv	40	2	0
Alkali	30	2	0
ORG	34	0	0
EORG	36	3	0

Thermal analysis of different types of lignin (dealkaline, organosolv, alkali, ORG, EORG) was performed using TGA-DTA analysis. When TGA study was done until 1000 °C under air atmosphere, it was observed that lignin starts losing weight in the range of 150-450 °C due to the cleavage of α and β -aryl-alkyl-ether linkages. Aliphatic side chains are removed from the aromatic ring around a temperature of 300 °C, and also the carbon-carbon linkage between lignin structural units is also cleaved at 370–400 °C. Also another weight loss was observed in the range of 400-650 °C which may be due to the decomposition of the aromatic rings. (Table 2A.4, Figure 2A.8).

It was also observed that the thermal degradation (TGA-DTA) studies of all the lignin carried out up to 1000 °C in nitrogen atmosphere showed almost 35-40 % of unburnt residues (Table 2A.4, Figures 2A.8). However, when thermal degradation study was carried out in presence of oxygen, minimal quantity (0-3 %) of unburnt residue is observed. But in the case of dealkaline lignin even burnt in air at 1000 °C almost 17 % residue was observed which is in line with the manufactures (TCI Chemicals) specifications.⁴⁵ These studies suggest that in presence of nitrogen (inert atmosphere), carbon in the sample will remain unburnt. However, almost 75 % of carbon was burnt since lignin molecule has ‘O’ and ‘H’ those can help in forming CO

and CH₄. A careful look at molecular formula of lignin reveals that for 9 'C' 10 'H' and 4 'O' are present (section 2A.2.3). It is possible that 4 'C' will be consumed in the form of 4CO molecules and another 2 'C' will get consumed in the formation of 2CH₄ (or 3 'C' as 3CH₄) molecules. However, after the complete use of 'H and 'O' present in the lignin molecule in presence of nitrogen, 3 or 4 'C' will still remain unburnt as coke or char. A quick calculation reveals that this remaining 3 or 4 'C' among 9 'C' gives rise to ca. 30-40 % of residue. This percentage of unburnt residue matches well with the experimental data (Table 2A.4). However, when oxygen is supplied (in presence of oxygen) these entire 'C' are burnt as a result no residue was observed. In the case of dealkaline lignin even in the presence of oxygen, 17 % of ignition residue was observed, which represent some inorganic material, but not Na and S since it covers ca. < 4 % of dealkaline lignin (calculated considering mg of these metals present). The concentration of water in lignin was calculated based on the loss of mass at 150 °C in TGA-DTA analysis.

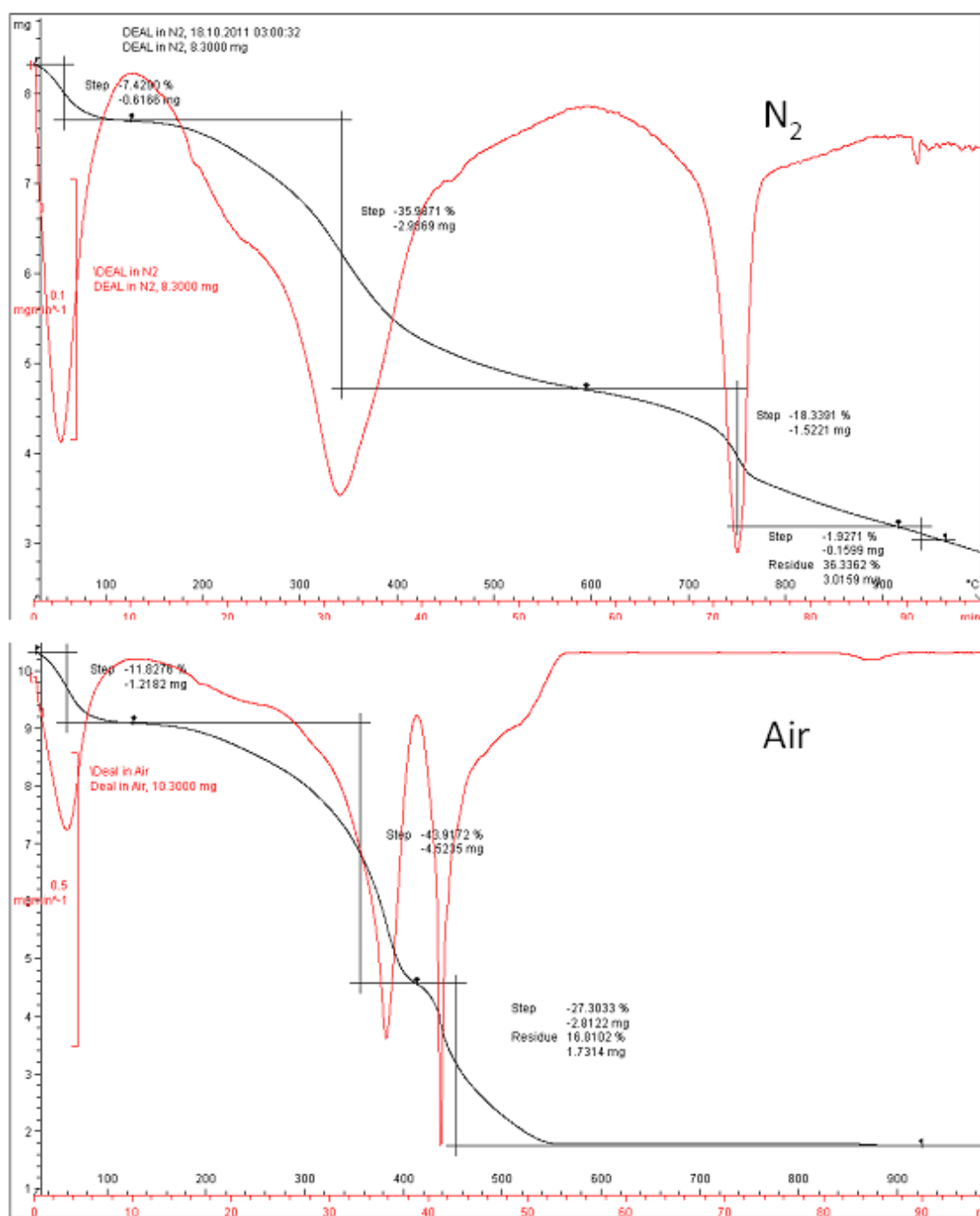


Figure 2A.8a. TGA-DTA analysis of dealkaline lignin in N_2 and air.

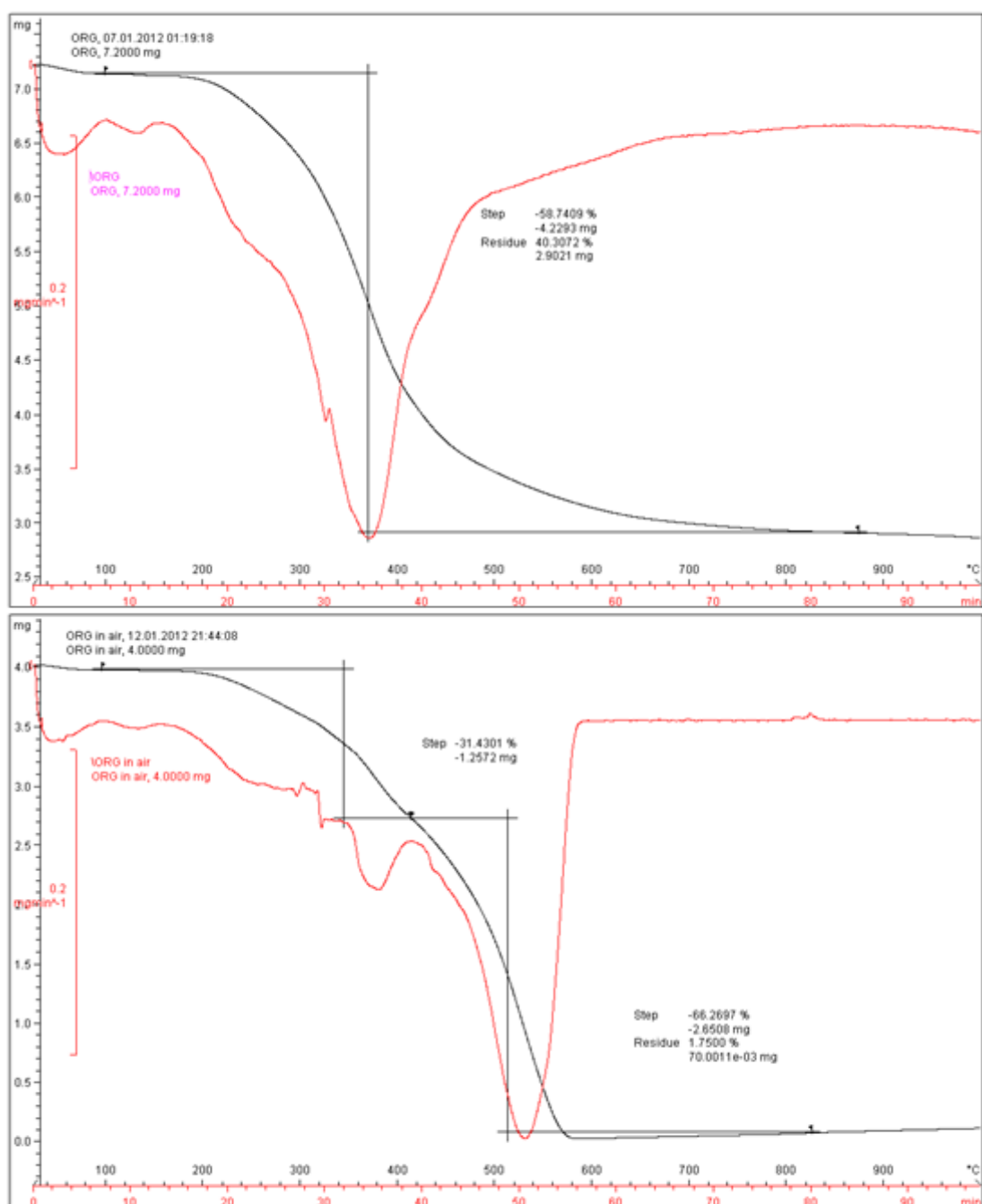


Figure 2A.8b. TGA-DTA analysis of organosolv lignin in N₂ and air.

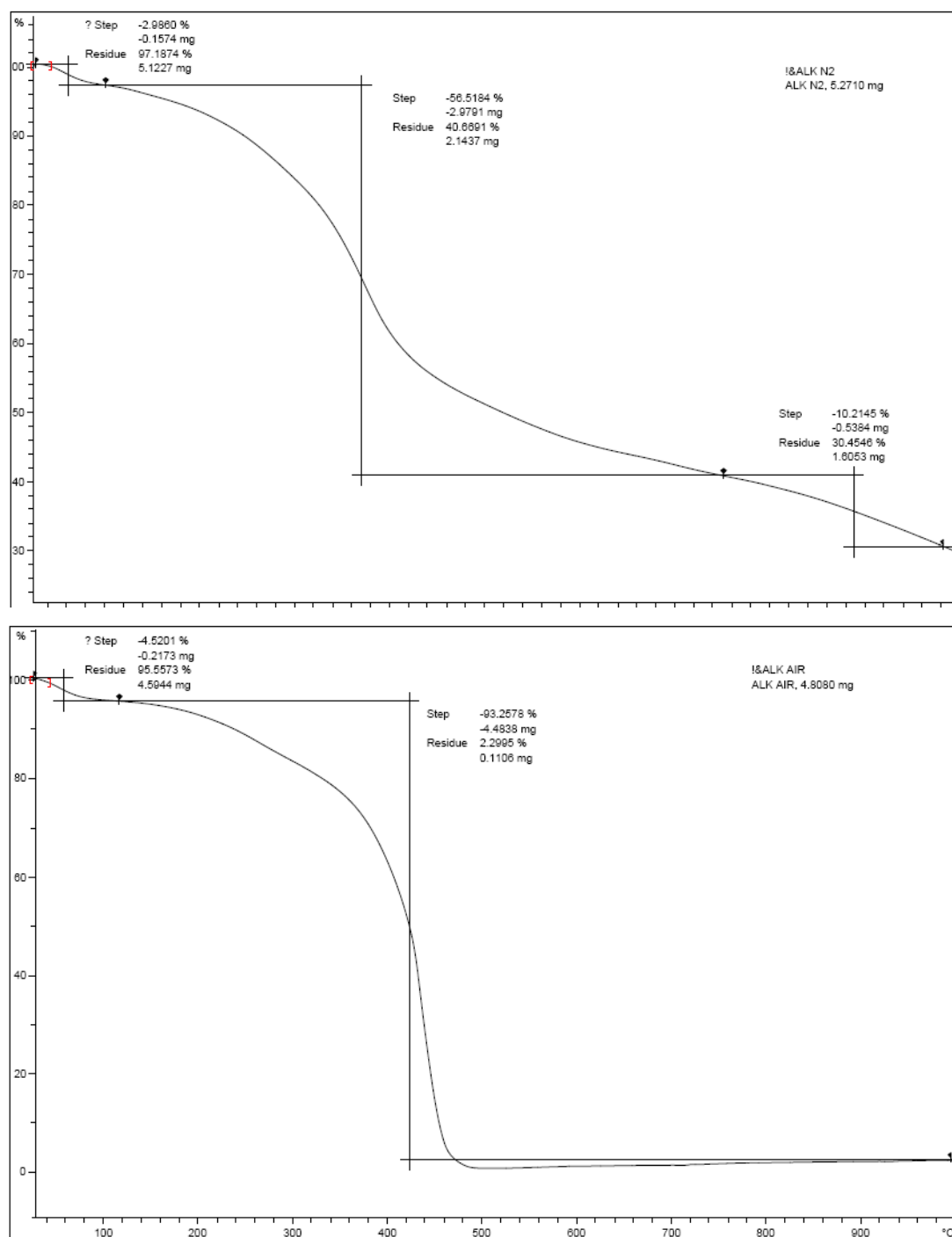


Figure 2A.8c. TGA analysis of alkali lignin in N_2 and air.

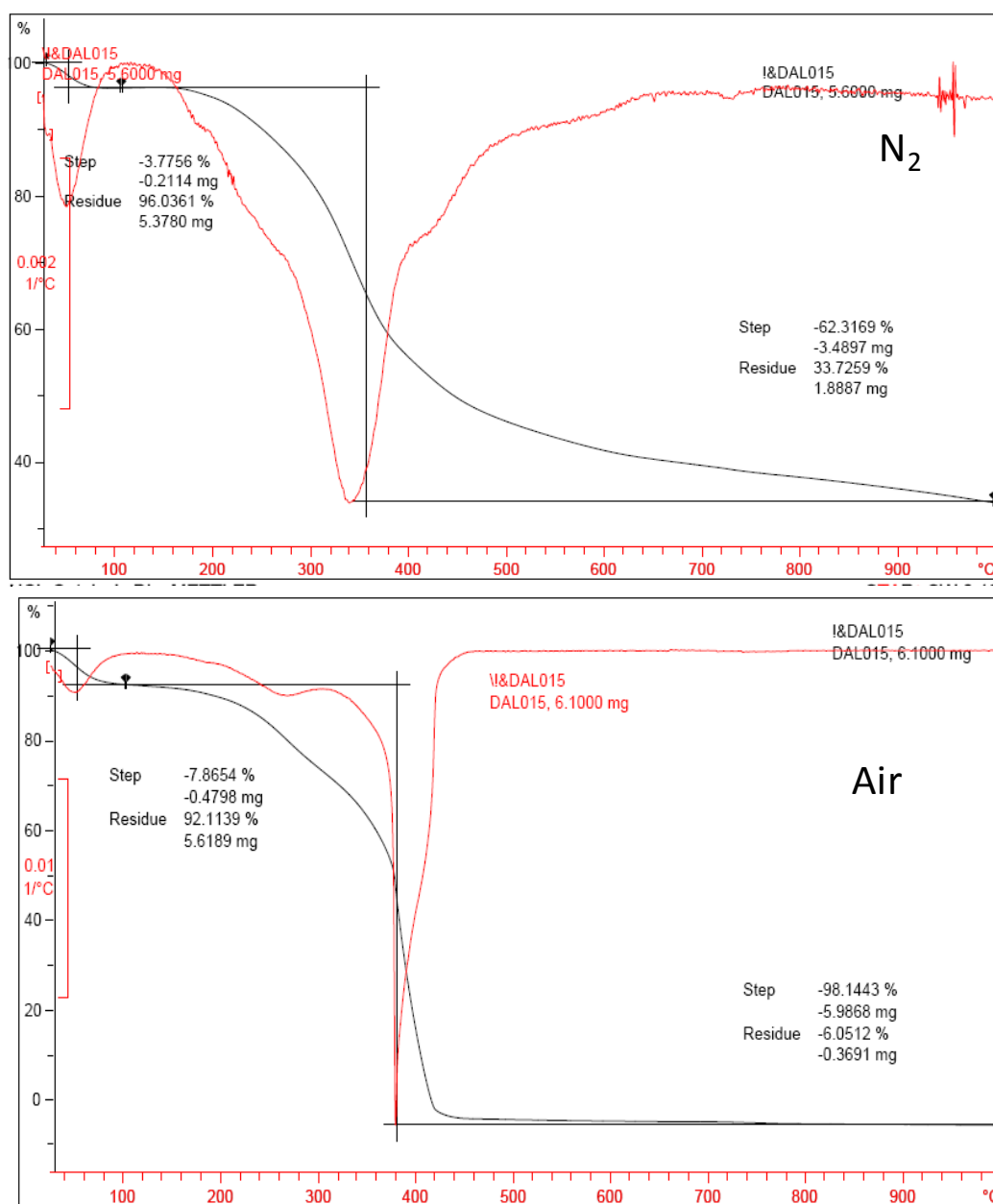


Figure 2A.8d. TGA-DTA analysis of ORG lignin in N₂ and air.

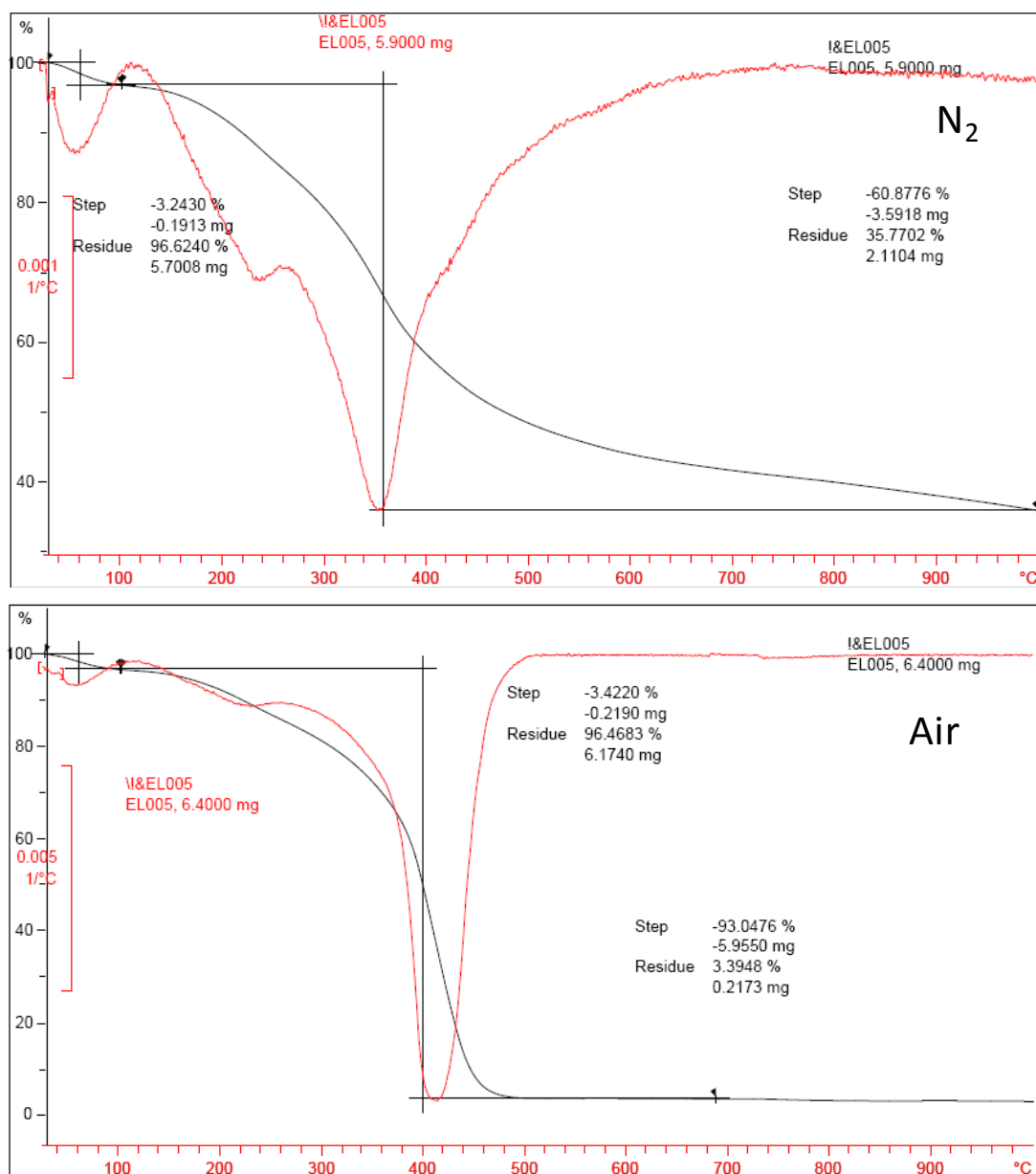


Figure 2A.8e. TGA-DTA analysis of EORG lignin in N₂ and air.

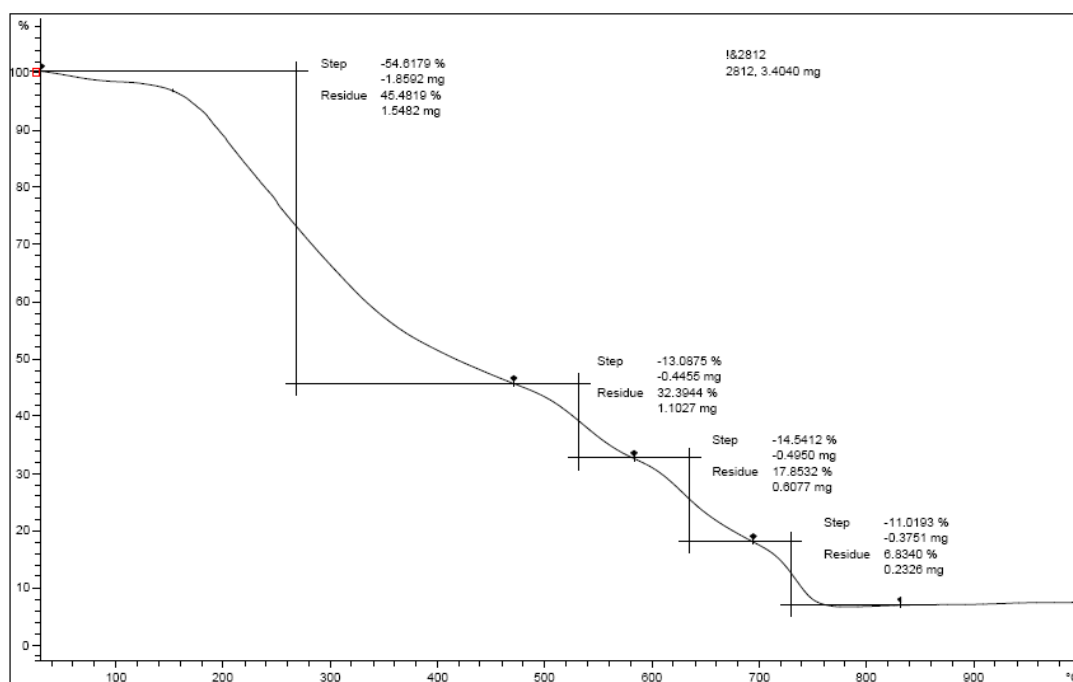


Figure 2A.8f. TGA analysis of bagasse lignin in N_2 .

2A.2.10. Solubility of lignin

Before proceeding to the catalytic runs, solubility of lignin was measured in different solvents and the results are tabulated in Table 2A.5. This study served two purposes namely; (1) selection of suitable reaction medium for the lignin depolymerization reaction and (2) isolation of reaction products from unconverted lignin using suitable solvent in which lignin is not soluble.

Solubility behaviour of lignin is that which should be expected of a polar aromatic polymer with many hydroxyl groups. Lignin fragments of lower molecular weight are more soluble in a wide range of solvents than higher molecular weight components. The solubility of lignin is greater with hydroxylated solvents, e.g., methanol, ethanol, phenol, and water than nonpolar solvents like benzene. Although native lignin behave as an insoluble, three dimensional network but isolated lignin exhibit maximum solubility in solvents including, for e.g. dioxane, acetone, THF, DMF and DMSO. The ability of solvents to dissolve or swell a variety of isolated lignin increases as the hydrogen-bonding capacity of the solvents increase. The solubility of lignin decreases abruptly in alcohols with increasing hydrocarbon chain length. The high association of pure alcohols frequently results in a lower solvent power than expected. The solubility of lignin is greater in the mixture than in either

solvent alone. The hydrogen-bonding capacity of the mixture is greater than that of one individual solvent and often the solubility parameter of the mixture is higher than the pure solvent.⁵⁹

Table 2A.5. Solubility of lignin in various solvents.

Solvent	Polarity index	Lignin ^a (mgmL ⁻¹)					
		Dealkaline	Organo-solv	Alkali	ORG	EORG	Bagasse
Water	9.0	22	Insolb.	Insolb.	Insolb.	Insolb.	Insolb.
Ethanol	5.2	Insolb.	8	5	28	16	10
Methanol	5.1	37	50	50	24	32	50
Acetone	5.1	Insolb.	50	50	1	2	50
Ethyl acetate	4.4	Insolb.	50.	Insolb.	19	Insolb.	Insolb.
Chloroform	4.1	Insolb.	50	40	Insolb.	Insolb.	Insolb.
Tetrahydrofuran	4.0	Insolb.	50	50	50	20	50
Dichloromethane	3.1	Insolb.	Insolb.	Insolb.	Insolb.	Insolb.	Insolb.
Diethyl ether	2.8	Insolb.	Insolb.	Insolb.	Insolb.	Insolb.	Insolb.
Toluene	2.4	Insolb.	Insolb.	Insolb.	Insolb.	Insolb.	Insolb.
Hexane	0.0	Insolb.	Insolb.	Insolb.	Insolb.	Insolb.	Insolb.
Water: Methanol (1:5 v/v)	—	50	50	50	40	26	50

^a50 mg lignin solubilised in 1mL solvent at RT.

Several solvents from polar to nonpolar (polarity index, 0-9) were checked for lignin solubility. Lignin used in the study was found to be insoluble in water thereby showing the hydrophobic nature of the aromatic backbone of lignin structure. From the results it was found that water:methanol (1:5 v/v) mixture would be the best solvent system for carrying out the reactions since in this solvent system all the six different types of lignin have complete solubility. Several other ratios like 1:1 and 1:3

(v/v) of water-methanol were also observed to be suitable to carry out the reactions but, those were not used because literature suggests that in presence of excess amount of water; acid sites can get poisoned and thus will not be available for reactions.⁶⁰⁻⁶¹ In several other solvents like THF, phenol and dioxane also majority of lignin were soluble, but since they were undergoing degradation reactions at reaction temperature ($T \leq 250$ °C), so those solvents were avoided. Considering this, water:methanol, 1:5 (v/v) ratio was used to carry out all the reactions.

2A.3. CONCLUSIONS

Structural and functional properties of lignin depends on the origin, type and age of plant from which it is isolated and also it depends on the methods used for the isolation of lignin. In order to acquire lignin of high purity and to attain a lignin without much structural deformation (having a similar structure to native lignin) organosolv method was used for lignin isolation (bagasse lignin) from sugar bagasse and was characterized using various techniques like XRD, CHNS, TGA-DTA, SEM-EDAX and ICP-OES analysis.

Before performing the depolymerization studies on lignin using solid acid catalysts, it is suitable to do complete characterization of lignin. In my studies six types of lignin namely, dealkaline, organosolv, alkali, ORG, EORG, bagasse lignin were used. Molecular weights of lignin using MALDI-TOF and GPC analysis showed that dealkaline lignin was having the highest molecular weight ($60,000 \text{ gmol}^{-1}$) amongst all other lignin. CHNS elemental analysis revealed that the lignin are composed of 60-65 % C and 5-8 % H, except in case of ORG and bagasse lignin which is made up of 57 % and 51 % of C. S content (ca. 1 %) was observed in dealkaline and alkali lignin possibly due to the type of extraction process (Kraft) used for lignin isolation, where NaOH and Na_2S are used as reagents. ICP-OES and SEM-EDAX showed the presence of Na and S contamination in dealkaline and alkali lignin, which is once again due to the Kraft process employed for lignin extraction. But all other lignin was free of these impurities, since they were isolated using organosolv method. Functional group analyses of these lignin were performed using FTIR and ^{13}C NMR techniques. All the lignin studied here had similar type of functional groups, but with different intensities. Both these techniques confirmed the presence of aromatic units linked together by ether linkages and also showed the presence of

several substituents like hydroxyl, carbonyl, alkyl, methoxyl etc. Amorphous nature of lignin and the absence of crystalline impurities in lignin were confirmed by a single broad peak in XRD analysis. Na and S contamination in dealkaline lignin was also observed in XRD analysis. UV-Vis analysis studied about the chromophores present in lignin and once again confirmed the aromatic nature of lignin by showing the phenolic units at $\lambda = 270$ nm. Thermal degradation study of lignin using TGA-DTA analysis showed the presence of 17 % of ignition residue for dealkaline lignin even after the sample was burnt at 1000 °C in air. Solubility studies of lignin were performed in various solvents and water-methanol, 1:5 (v/v) ratio was chosen as the most suitable solvent for lignin depolymerization studies.

2A.4. REFERENCES

1. Hon, D. N.-S., *Chemical Modification of Lignocellulosic Materials*. CRC Press USA, p 384.
2. E., B. F., *The Chemistry Of Lignin*. New York Academic press: 1952; p 137.
3. Johnson, D. K.; Chornet, E.; Zmierczak, W.; Shabtai, J., *Fuel Chemistry Division Preprints* **2002**, 47, 380-381.
4. Stenius, P., *Forest Products Chemistry* Fapet Oy: p 350.
5. Nagy, M. Biofuels from lignin and novel biodiesel analysis. Georgia Institute of Technology, 2009.
6. Brunow, G.; Lundquist, K.; Gellerstedt, G., Lignin. In *Analytical Methods in Wood Chemistry, Pulping, and Papermaking*, Sjöström, E.; Alén, R., Eds. Springer Berlin Heidelberg: 1999; pp 77-124.
7. El Mansouri, N.-E.; Salvadó, J., *Ind. Crops Prod.* **2007**, 26, 116-124.
8. Zakzeski, J.; Bruijninx, P. C. A.; Jongerius, A. L.; Weckhuysen, B. M., *Chem. Rev.* **2010**, 110, 3552-3599.
9. Avellar, B. K.; Glasser, W. G., *Biomass Bioenergy* **1998**, 14, 205-218.
10. Kim, T. H.; Kim, J. S.; Sunwoo, C.; Lee, Y. Y., *Bioresour. Technol.* **2003**, 90, 39-47.
11. Zhang, Y.-H. P.; Ding, S.-Y.; Mielenz, J. R.; Cui, J.-B.; Elander, R. T.; Laser, M.; Himmel, M. E.; McMillan, J. R.; Lynd, L. R., *Biotechnol. Bioeng.* **2007**, 97, 214-223.
12. Lin, S. Y. L., I. S., *Ullmann's Encyclopedia of Industrial Chemistry*. 5 ed. ed.; VCH: 1990; Vol. 15, p 305.
13. Shabtai, J. S., Zmierczak, W.W., Chornet, E. Process for conversion of lignin to reformulated hydrocarbon gasoline. U.S. Patent 5,959,167, September 28, 1999.
14. Shabtai, J. S.; Zmierczak, W. W.; Chornet, E. Process for conversion of lignin to reformulated, partially oxygenated gasoline. U.S. Patent 6,172,272, January 9, 2001.
15. Deepa, A. K.; Dhepe, P. L. Depolymerization of lignin using solid acid catalysts. U.S. 0302796 A1, November 29, 2012.
16. Holladay, J. E.; White, J. F.; Bozell, J. J.; Johnson, D. *Top Value Added Chemicals from Biomass: Volume II -Results of Screenings for Potential Candidates from Biorefinery Lignin*; 2007.
17. Deepa, A. K.; Dhepe, P. L., *RSC Adv.* **2014**, 4, 12625-12629.
18. Kaplan, D. L., *Biopolymers from renewable resources*. Springer: Germany.
19. Jönsson, A.-S.; Nordin, A.-K.; Wallberg, O., *Chem. Eng. Res. Des.* **2008**, 86, 1271-1280.

20. Stigsson, L.; Lindstrom, C. A method for recovering low sodium content lignin fuel from black liquor. U.S. Patent 8,252,141 B2, August 28, 2012.
21. Jönsson, A.-S.; Wallberg, O., *Desalination* **2009**, *237*, 254-267.
22. Rainey, T. J. A study into the permeability and compressibility of Australian bagasse pulp. PhD, 2009.
23. Pan, X.; Arato, C.; Gilkes, N.; Gregg, D.; Mabee, W.; Pye, K.; Xiao, Z.; Zhang, X.; Saddler, J., *Biotechnol. Bioeng.* **2005**, *90*, 473-481.
24. Yoshida, H.; Mörck, R.; Kringstad, K. P.; Hatakeyama, H., *J. Appl. Polym. Sci.* **1990**, *40*, 1819-1832.
25. Kubo, S.; Uraki, Y.; Sano, Y., *Holzforschung* **1996**, *50*, 144-150.
26. Jeong, H.; Park, J.; Kim, S.; Lee, J.; Ahn, N.; Roh, H., *Fibers Polym.* **2013**, *14*, 1082-1093.
27. Mattinen, M.-L.; Suortti, T.; Gosselink, R.; Argyropoulos, D. S.; Evtuguin, D.; Suurnäkki, A.; de Jong, E.; Tamminen, T., *BioResources* **2008**, 549-565.
28. Ye, Y.; Zhang, Y.; Fan, J.; Chang, J., *Ind. Eng. Chem. Res.* **2011**, *51*, 103-110.
29. Barta, K.; Warner, G. R.; Beach, E. S.; Anastas, P. T., *Green Chem.* **2014**, *16*, 191-196.
30. Xu, W.; Miller, S. J.; Agrawal, P. K.; Jones, C. W., *ChemSusChem* **2012**, *5*, 667-675.
31. Zhu, H.; Chen, Y.; Qin, T.; Wang, L.; Tang, Y.; Sun, Y.; Wan, P., *RSC Adv.* **2014**, *4*, 6232-6238.
32. Park, H.; Kim, J.; Hong, U.; Lee, Y.; Song, J.; Song, I., *Catal. Surv. Asia* **2013**, *17*, 119-131.
33. Amen-Chen, C.; Pakdel, H.; Roy, C., *Bioresour. Technol.* **2001**, *79*, 277-299.
34. Ben, H.; Ragauskas, A. J., *RSC Adv.* **2012**, *2*, 12892-12898.
35. Ma, Z.; van Bokhoven, J. A., *ChemCatChem* **2012**, *4*, 2036-2044.
36. Pandey, M. P.; Kim, C. S., *Chem. Eng. Technol.* **2011**, *34*, 29-41.
37. Wang, H.; Tucker, M.; Ji, Y., *J. Appl. Chem.* **2013**, *2013*, 1-9.
38. Hicks, J. C., *J. Phys. Chem. Lett.* **2011**, *2*, 2280-2287.
39. Delledonne, D.; Buzzoni, R.; Bianchi, D. Process for the conversion of lignin to liquid hydrocarbons. PCT/IB2011/000591, September 29, 2011.
40. Barta, K.; Matson, T. D.; Fettig, M. L.; Scott, S. L.; Iretskii, A. V.; Ford, P. C., *Green Chem.* **2010**, *12*, 1640-1647.
41. Aresta, M. D., A.; Dumeignil, F., *Biorefinery: From Biomass to Chemicals and Fuels*. Walter de Gruyter GmbH & Co KG: Berlin/Boston, 2012; p 446.
42. Saliba, E. O. S.; Rodriguez, N. M.; Piló-Veloso, D.; Morais, S. A. L., *Arq. Bras. Med. Vet. Zootec.* **2002**, *54*, 42-51.
43. Yan, N.; Zhao, C.; Dyson, P. J.; Wang, C.; Liu, L.-t.; Kou, Y., *ChemSusChem* **2008**, *1*, 626-629.
44. Joffres, B.; Lorentz, C.; Vidalie, M.; Laurenti, D.; Quoineaud, A. A.; Charon, N.; Daudin, A.; Quignard, A.; Geantet, C., *Appl. Catal., B* **2014**, *145*, 167-176.
45. <http://www.tcichemicals.com/eshop/en/in/commodity/L0045/>.
46. Carmen, G. B.; Dominique, B.; Gosselink, R. J. A.; Van Dam, J. E. G., *Ind. Crops Prod.* **2004**, 205-218.
47. Sarkanen, K. V.; Ludwig, C. H., *Lignins: occurrence, formation, structure and reactions*. Wiley-Interscience: University of California, 2008.
48. Hergert, H. L., *J. Org. Chem.* **1960**, *25*, 405-413.
49. Roeges, N. P. G., *A Guide to the Complete Interpretation of Infrared Spectral of Organic Structures*. Wiley: Chichester, 1994.
50. Bellamy, L. J., *Advances in infrared group frequencies*. Methuen: 1968.
51. Mantsch, H. H.; Chapman, D., *Infrared spectroscopy of biomolecules*. Wiley-Liss: New York, 1996.
52. Kudzin, S. F.; Nord, F. F., *J. Am. Chem. Soc.* **1951**, *73*, 690-693.
53. Robert, D. R.; Brunow, G., *Holzforschung* **1984**, *38*, 85-90.

54. Capanema, E. A.; Balakshin, M. Y.; Kadla, J. F., *J. Agric. Food Chem.* **2004**, *52*, 1850-1860.
55. Wang, K.; Xu, F.; Sun, R., *Int J Mol Sci.* **2010**, *11*, 2988-3001.
56. Oren, M. J.; Nassar, M. M.; Mackay, G. D. M., *Can. J. Spectrosc.* **1984**, *29*, 10-12.
57. Gardner, D. J.; Schultz, T. P.; McGinnis, G. D., *J. Wood Chem. Tech* **1985**, *5*, 85-110.
58. Balat, M., *Energ. Resour. Part A* **1981**, *30*, 620-635.
59. Horvath, A. L., *J. Phys. Chem. Ref.* **2006**, *35*, 77-92.
60. Li, S.; Zheng, A.; Su, Y.; Zhang, H.; Chen, L.; Yang, J.; Ye, C.; Deng, F., *J. Am. Chem. Soc.* **2007**, *129*, 11161-11171.
61. Okuhara, T., *Chem. Rev.* **2002**, *102*, 3641-3666.

CHAPTER 2B

**CATALYST SYNTHESIS AND
CHARACTERIZATION**

2B.1. INTRODUCTION

As discussed in chapter 1, it is very important to develop a method for the depolymerization of lignin into aromatic monomers using solid acid catalysts.¹⁻² To study the depolymerization reactions of lignin first I have used structured solid acids like zeolites, clays and metal oxides. Along with these amorphous solid acids (non uniform pore structure) like silica alumina and supported metal oxides were also used for the study because they were expected to be stable and recyclable when compared to structured solid acids, under the reaction conditions used for depolymerizing lignin. Also in chapter 1, it was suggested to use stable and recyclable supported metal catalysts for better hydrodeoxygenation (HDO) of lignin derived aromatic monomers.³ Properties of solid acids and supported metal catalysts have to be well studied before employed in reactions.

In this chapter I have discussed about the properties, synthesis procedure and characterization of solid acids used in depolymerization studies of lignin. Also I have discussed about the synthesis and characterization studies done for supported metal catalysts used in HDO of lignin derived aromatic monomers.

2B.1.1. Solid acid catalysts

To avoid the drawbacks associated with the homogeneous catalysts, solid acids were used for the depolymerization of lignin into aromatic monomers.⁴⁻⁵

Table 2B.1. Structural properties of zeolites used for depolymerization study of lignin

Zeolite	Framework	Pore size	Pore diameter (nm)	Ring size	Channel system
H-USY (Si/Al = 15)	FAU	Large	0.74 x 0.74	12	Three dimensional
H-ZSM-5 (Si/Al = 11.5)	MFI	Medium	0.53 x 0.56 0.51 x 0.55	10	Two dimensional
H-MOR (Si/Al = 10)	MOR	Large	0.7 x 0.65	12	One dimensional
H-BEA (Si/Al = 19)	BEA	Large	0.55 x 0.55 0.76 x 0.64	12	Three dimensional

Solid acids have Brønsted and/or Lewis acid sites which can cleave the C-O-C and C-C linkages in lignin to yield aromatic monomers. For this study I purposefully selected certain solid acids which differ in properties like acid amount, surface area, pore volume and pore diameter. Solid acids chosen can be generally classified as structured and amorphous (with non uniform pore structure). Therefore it will help to select a stable and recyclable solid acid catalyst which can yield maximum amount of aromatic monomers from lignin.¹⁻²

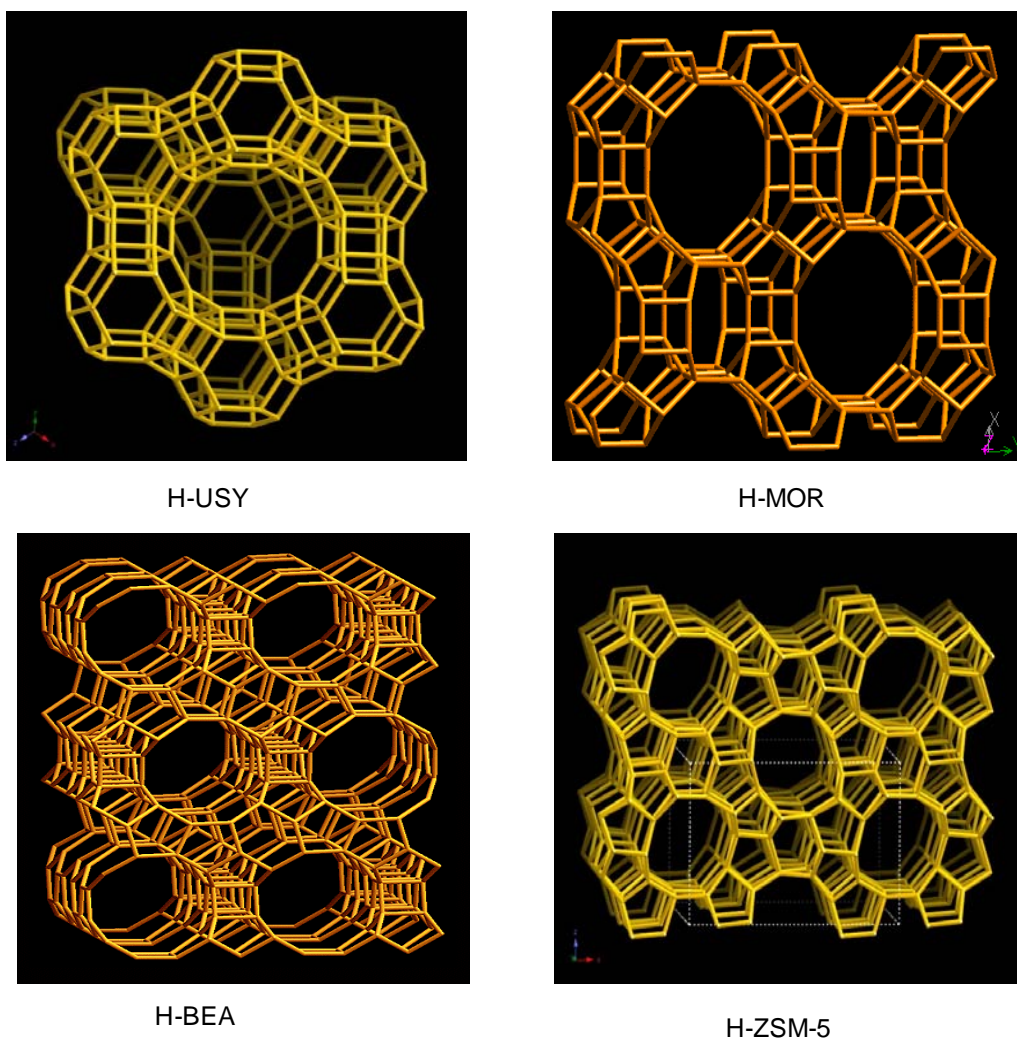


Figure 2B.1. Structure of various types of zeolites adapted from IZA site. [Source: Ref. 7]

Structured solid acids include various types of zeolites, clays and metal oxides. First type is, zeolite which is an aluminosilicate having a microporous structure with a pore diameter less than 2 nm. Several types of zeolites are known today, but I have used particularly H-USY (H-UltrastableY), H-ZSM-5 (H-Zeolite Socony Mobil-5), H-

MOR (H-Mordenite) and H-BEA (H-Beta) type zeolites in my study (Figure 2B.1) because they were already known to be active in hemicellulose depolymerization reactions.⁶ All these zeolites possess both Brønsted and Lewis acid sites which can aid in the cleavage of bonds in lignin. But these zeolites differ in their properties like acid amount, framework type, pore volume, pore diameter etc. (Table 2B.1)⁷ and therefore it is interesting to study their activity in the production of aromatic monomers from lignin.

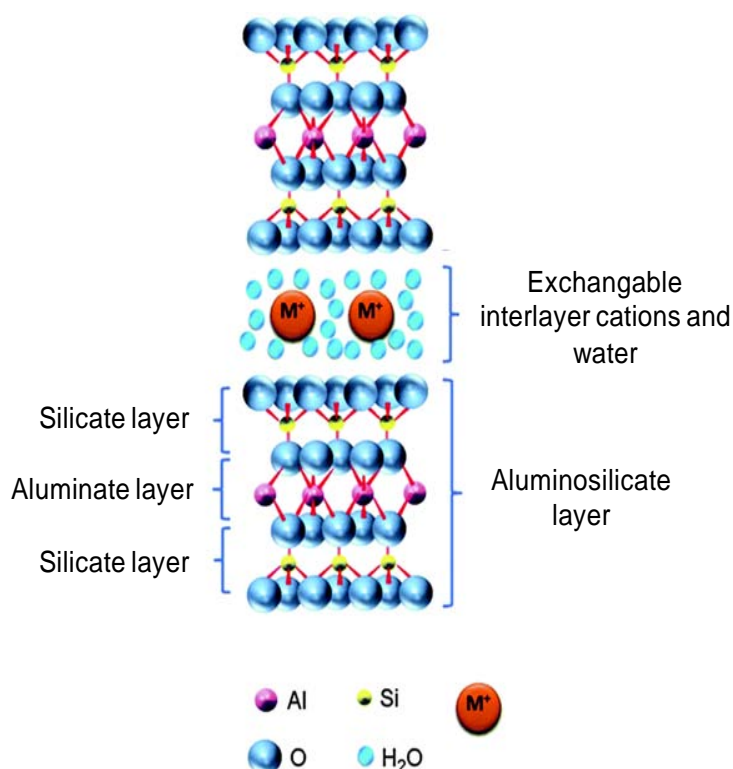


Figure 2B.2. Structure of Montmorillonite (K10) clay [Source Ref. 10].

Second type of structured solid acids used is ‘clay’. Typically clay (eg. Montmorillonite, K10) contain sheets of aluminosilicates,⁸⁻¹⁰ in which each aluminosilicate layer is surrounded by two silicate layers. The space between two aluminosilicate sheets is generally occupied by exchangeable interlayer cations and water which influences the acidity of clay catalyst (Figure 2B.2). Along with simple clay (e.g. Montmorillonite, K10), pillared clay (e.g. Al pillared clay) was also studied since the pillar (Al pillar) present in between the sheets will increase its strength and stability.

Amorphous solid acids were also employed to study on the depolymerization of lignin because there was possibility for the collapse of structure in the case of structured solid acids like zeolites, clays etc. under the reaction condition employed

for depolymerization of lignin ($T = 250\text{ }^{\circ}\text{C}$, $P = 0.7\text{ MPa N}_2$).⁶ Amorphous solids acids used here include $\text{SiO}_2\text{-Al}_2\text{O}_3$ ($\text{Si/Al} = 5.3$) and supported metal oxides like 10 wt% $\text{MoO}_3/\text{SiO}_2$.

Before employing these solid acid catalysts in depolymerization of lignin their properties were studied using various physico-chemical techniques. XRD (X-Ray Diffraction) was used to determine the morphology of the catalysts on bulk level. N_2 sorption studies helped to determine the surface area, pore volume and pore diameter and $\text{NH}_3\text{-TPD}$ (Ammonia-Temperature Programmed Desorption) analysis was used to determine the amount acid sites (strong and weak) present in the catalyst. ICP-OES (Inductively Coupled Plasma-Optical Emission Spectroscopy) analysis was used to determine the Si and Al content in zeolites and $\text{SiO}_2\text{-Al}_2\text{O}_3$ catalyst.

2B.1.2. Supported metal catalysts

Several types of supported metal catalysts were prepared to study the effect of support and metal in HDO reactions.³ They were synthesized using conventional impregnation methods. Noble metals like Pt, Pd and Ru were loaded over acidic ($\text{SiO}_2\text{-Al}_2\text{O}_3$, $\gamma\text{-Al}_2\text{O}_3$), neutral (carbon) and basic (Hydrotalcite) supports. Noble metals were particularly chosen to synthesize supported metal catalysts since they have better activity for HDO reactions than other metals (Refer chapter 1, section 1.9). The main role of support is to help in the better dispersion of metal which help in the formation of highly active smaller nanoparticles. In some cases even supports also shows some additional properties like acidic or basic behavior which can also affect the catalytic activity. So I have chosen acidic ($\text{SiO}_2\text{-Al}_2\text{O}_3$, $\gamma\text{-Al}_2\text{O}_3$), neutral (carbon) and basic (Hydrotalcite) supports for the HDO studies of lignin derived aromatic monomers. These types of supported metals prepared can act as bifunctional catalyst, where metal active sites will facilitate hydrogenation activity and acid sites generated from the supports will help in deoxygenation reactions. After their synthesis, supported metal catalysts were well characterized using various techniques. XRD analysis was performed to detect the metal; N_2 sorption was performed to determine the surface area; HRTEM analysis was employed to determine the average particle size, morphology and dispersion of metal nanoparticles on the supports.

2B.2. MATERIALS

2B.2.1. Solid acid catalysts

Various types of commercial zeolites like H-USY (Si/Al = 15) (CBV-720), NH₄-ZSM-5 (Si/Al = 11.5) (CBV 2314), NH₄-BEA (Si/Al = 19) (CP814C) and NH₄-MOR (Si/Al = 10) (CBV 21A) were supplied by Zeolyst International, USA. Except H-USY zeolite, ZSM-5 (Si/Al = 11.5), BEA (Si/Al = 19) and MOR (Si/Al = 10) (CBV 21A) were typically supplied in their NH₄⁺ form. They were calcined at 550 °C in air at a heating rate of 5 °C min.⁻¹ for 12 h in Muffle furnace and used. Montmorillonite, K10, Al pillared clay, SO₄²⁻/ZrO₂ (99.99 %), SiO₂-Al₂O₃ (Si/Al = 5.3) were purchased from Aldrich and Nb₂O₅ was purchased from Spectrochem. Ammonium heptamolybdate (99 %) was purchased from Loba Chemie, tetraethyl orthosilicate was purchased from Aldrich and ethylene glycol was purchased from s.d. fine.

2B.2.2. Supported metal catalysts

Supported metal catalysts were prepared using noble metals like Pt, Pd and Ru which were loaded over acidic (SiO₂-Al₂O₃ (SA), γ -Al₂O₃ (AL)), neutral (carbon (C)) and basic (Hydrotalcite (HT)) supports. Metal salts like Tetraamine platinum nitrate (99.99 %) was purchased from Alfa Aesar, Ruthenium chloride (RuCl₃, Ru content 45-55 %), and Palladium chloride (PdCl₂, Pd content \geq 99.9 %) were purchased from Aldrich. Supports, SiO₂-Al₂O₃, γ -Al₂O₃, 3 wt% Pt/C and 3 wt% Pd/C were purchased from Aldrich and Carbon (BP2000) used is from Cabot suppliers. Hydrotalcite (HT) support was prepared by co-precipitation method (refer section 2B.3.2). Magnesium nitrate hexahydrate (Mg(NO₃)₂.6H₂O) (99 %) was purchased from Merck, aluminium nitrate nonahydrate (Al(NO₃)₃.9H₂O) was purchased from Thomas Baker, sodium carbonate (Na₂CO₃) (99.5 %) and sodium hydroxide (NaOH) (98 %) were purchased from Loba Chemie.

2B.3. SYNTHESIS

This section includes the synthesis of supported metal oxide (10 wt% MoO₃/SiO₂) which was used as an amorphous solid acid catalyst in the depolymerization studies of lignin. Also this section I have discussed the preparation of hydrotalcite (HT) and supported metal catalysts used for the HDO of lignin derived aromatic monomers.

2B.3.1. Synthesis of 10 wt % MoO₃/SiO₂

10 wt% MoO₃/SiO₂ was synthesized by sol-gel method.¹¹ A calculated amount of ammonium heptamolybdate (corresponding to 10 wt% of Mo) was dissolved in 40 mL ethylene glycol and stirred for half an hour. To which 10 mL tetraethyl orthosilicate was added. The resultant solution was kept under stirring at 80 °C for 5 h. 20 mL water and a 0.5 mL of concentrated nitric acid was added to this solution and kept at 80 °C with continuous stirring until it became thick gel. The gel was then evacuated at 80 °C for 5 h with a rotary evaporator and further dried at 150 °C for 6 h under vacuum (10⁻⁴ MPa). As-synthesized material obtained was calcined at 650 °C for 5 h in air (20 mLmin⁻¹). 10 wt% MoO₃/SiO₂ thus obtained was characterized using XRD, NH₃-TPD and ICP-OES analysis.

2B.3.2. Synthesis of hydrotalcite (HT)

Hydrotalcite (Mg/Al = 3) was synthesized by co-precipitation method.¹² NaOH was used to maintain the pH, while Na₂CO₃ was used as a carbonate source. For the synthesis of catalyst by co-precipitation method, an aqueous solution 'A' (37.5 mL) of Mg(NO₃).6H₂O (0.279 mol) and Al(NO₃)₃.9H₂O (0.093 mol) was slowly added into an aqueous solution 'B' (37.5 mL) of NaOH (0.4375 mol) and Na₂CO₃ (0.1125 mol) under vigorous stirring over a period of 2 h. Solution pH was maintained between 8 and 10 by the addition of NaOH. White precipitate solution obtained after mixing solutions 'A' and 'B' was kept in an autoclave at 80 °C for 16 h. Precipitate was then washed with deionised water until pH became neutral. Solid thus obtained was then dried at 80 °C for 18 h under vacuum (10⁻⁴ MPa). As-synthesized material thus obtained was calcined at 350 °C in air for 8 h to obtain HT (Mg/Al = 3).

2B.3.3. Synthesis of supported metal catalysts

Supported metal catalysts were prepared by conventional impregnation method.¹³⁻¹⁴ Before synthesis of catalysts, supports were evacuated at 150 °C for 6 h in vacuum (10⁻⁴ MPa). An aqueous solution of metal precursor (corresponding to 2-3.5 wt% loading on support) was added to the support suspended in water. The solution was stirred for 16 h at room temperature. Water was removed by rotary evaporator and powder obtained was dried in oven at 60 °C for 16 h. Further it was dried under vacuum (10⁻⁴ MPa) at 150 °C for 6 h and was subjected for calcinations in a tubular

furnace in O₂ flow (20 mLmin⁻¹) and then reduced in H₂ (20 mLmin⁻¹) at 400 °C for 2 h. After synthesis these catalysts were characterized using XRD, ICP-OES, N₂ sorption and HRTEM techniques.

2B.4. RESULTS AND DISCUSSIONS

Properties of solid acid catalysts were studied using XRD, N₂ sorption, NH₃-TPD and ICP-OES analysis. Supported metal catalysts were also characterized using XRD, N₂ sorption, HRTEM, ICP-OES techniques.

2B.4.1. Solid acid catalysts

2B.4.1.1. XRD analysis

Wide angle X-ray analysis of structured solid acids like zeolites (H-USY (Si/Al = 15), H-ZSM-5 (Si/Al = 11.5), H-BEA (Si/Al = 19) and H-MOR (Si/Al = 10)), clays (K10 and Al pillared) and amorphous catalysts like SiO₂-Al₂O₃, 10 wt % of MoO₃/SiO₂ was performed in a 2θ range of 5-90 ° at a scan rate of 4.3 °min⁻¹ (Figures 2B.3a and 2B.3b).

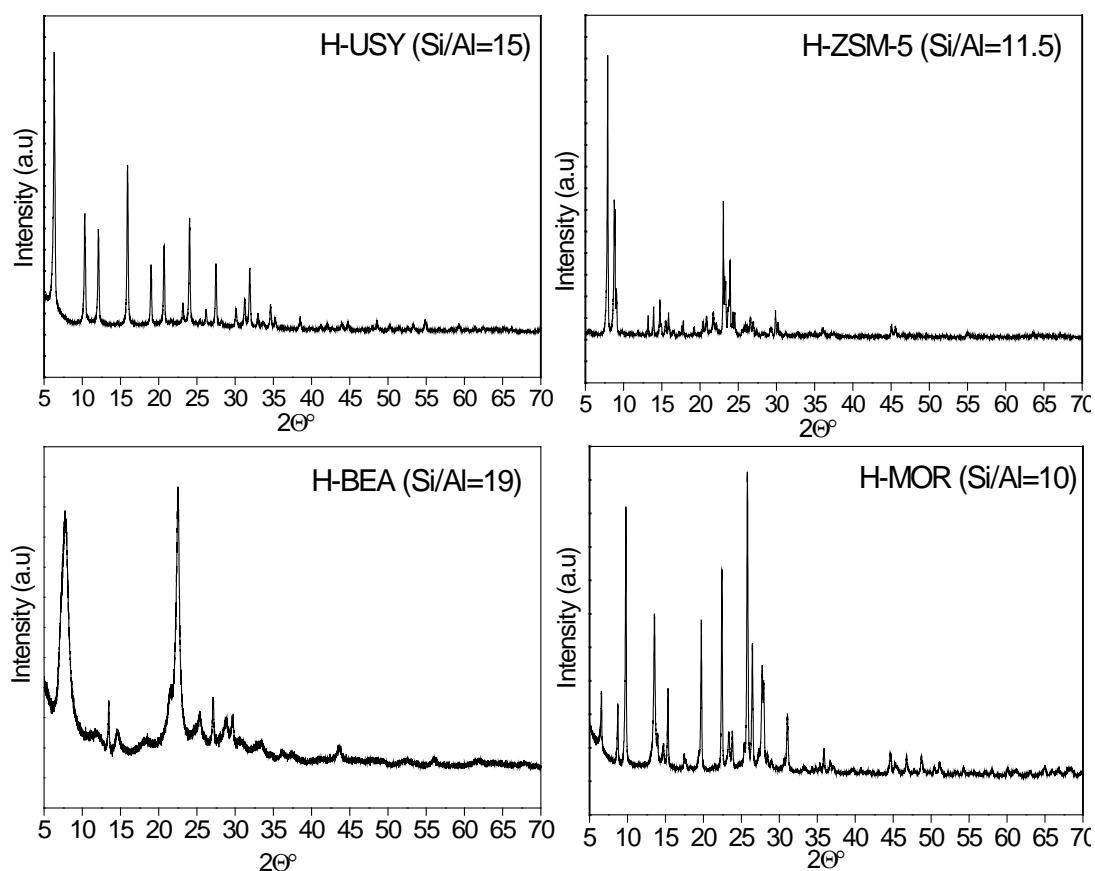


Figure 2B.3a. XRD pattern of H-USY, H-ZSM-5, H-BEA and H-MOR zeolites.

In the case of zeolites and clays sharp peaks were observed in the XRD diffraction pattern, which confirmed the crystalline nature of these materials. But in the case of solid acids like $\text{SiO}_2\text{-Al}_2\text{O}_3$, and 10 wt % $\text{MoO}_3/\text{SiO}_2$ a single broad peak was observed in the range of $15\text{-}35^\circ$ which confirmed the amorphous nature of the material. In the case of 10 wt % $\text{MoO}_3/\text{SiO}_2$, Mo peaks were not visible this was because during the preparation of these catalysts by sol gel method there is possibility of incorporation of the Mo species into silica framework/homogeneous dispersion.

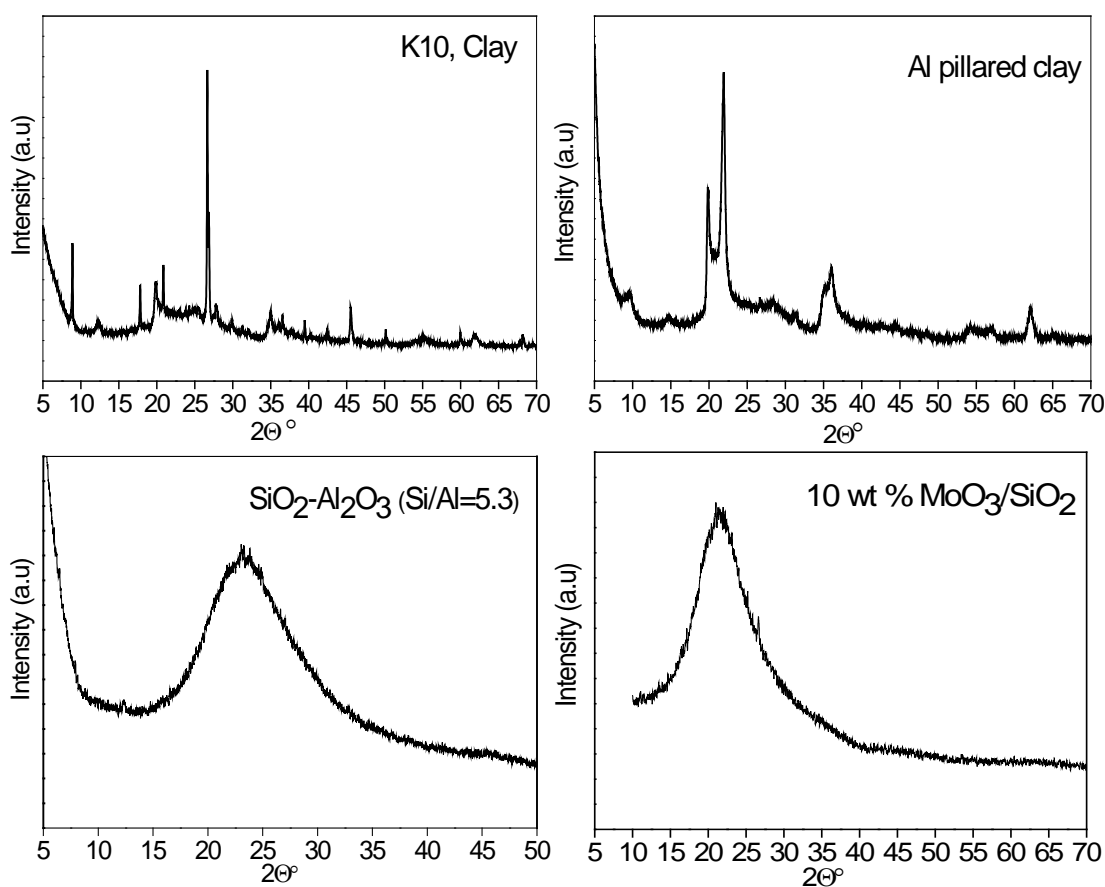


Figure 2B.3b. XRD pattern of K10 clay, Al pillared clay, $\text{SiO}_2\text{-Al}_2\text{O}_3$ and 10 wt% $\text{MoO}_3/\text{SiO}_2$.

2B.4.1.2. N_2 sorption analysis

BET surface area, pore volume and pore diameter of solid acid catalysts used for lignin depolymerization reactions were determined using N_2 sorption analysis. Results are summarized in Table 2B.2.

From N_2 sorption analysis it was observed that among the solid acid catalysts, H-USY ($\text{Si}/\text{A} = 15$) was having the highest surface area of $873 \text{ m}^2\text{g}^{-1}$. It was also understood that among the zeolites, surface area and pore volume decreased in the

order: H-USY (Si/Al = 15) >H-BEA (Si/Al = 19) >H-MOR (Si/Al = 10) >H-ZSM-5 (Si/Al = 11.5). Zeolites showed a pore diameter (D) of < 2 nm which confirmed its the microporous nature and is in good correlation with the literature.¹⁵ Both K10 and Al pillared clays have almost similar surface area ca. 250 m²g⁻¹ but differ in their pore volume, 0.3 cm³g⁻¹ and 0.18 cm³g⁻¹ respectively. In the category of amorphous solid acids, SiO₂-Al₂O₃ (Si/Al = 5.3) showed a surface area of 532 m²g⁻¹ and largest pore diameter of 4.9 nm indicating that catalyst has mesoporous nature. 10 % MoO₃/SiO₂ synthesized by sol gel method has a surface area of 148 m²g⁻¹, SO₄²⁻/ZrO₂ and Nb₂O₅ showed very low surface area ca. < 100 m²g⁻¹. It was expected that the solid acid having high surface area (H-USY (Si/Al = 15)) might show better catalytic activity than others.

Table 2B.2. Summary on N₂ sorption analysis of solid acid catalysts.

Catalyst	N ₂ sorption		
	BET surface area ^a (m ² g ⁻¹)	V ^b (cm ³ g ⁻¹)	D ^c (nm)
H-USY (Si/Al = 15)	873	0.45	0.75
H-ZSM-5 (Si/Al = 11.5)	423	0.22	0.60
H-BEA (Si/Al = 19)	761	0.34	0.60
H-MOR (Si/Al = 10)	528	0.22	0.59
SO ₄ ²⁻ /ZrO ₂	84	0.02	5.7
Nb ₂ O ₅	115	nd	nd
Clay (K10)	246	0.3	nd
Al pillared clay	250	0.18	nd
SiO ₂ -Al ₂ O ₃ (Si/Al = 5.3)	532	0.82	4.90
10 wt% MoO ₃ /SiO ₂	148	nd	nd

^a Brunauer–Emmett–Teller (BET), ^b Pore volume, ^c Pore diameter, nd-not determined.

2B.4.1.3. NH₃-TPD analysis

NH₃-TPD analysis was performed to quantify the total acid amount and their distribution (strong and weak) present in the solid acid catalysts. (Figure 2B.4 and Table 2B.3). In this technique, NH₃ was used as basic probe molecule which is adsorbed on the acid sites of the catalyst. After removing of physisorbed NH₃ molecules by passing an inert gas (Argon gas) at 50 °C, temperature was increased from 100 °C at a of 10 °Cmin⁻¹ up to maximum of 800 °C. It was observed that while heating at lower temperature range (150-350 °C) NH₃ gets desorbed from weak acid sites and at a higher temperature range (350-750 °C) desorption of NH₃ happens from strong acid sites. The amount of NH₃ molecules desorbed corresponds to the amount of acid sites present in the catalyst.

It was observed that for all the zeolites analysed both strong and weak acid sites are present and among zeolites H-MOR (Si/Al = 10) was found to be having the highest amount acid sites (1.15 mmolg⁻¹). For zeolites the total acidity decreased in the order: H-MOR (Si/Al = 10) >H-ZSM-5 (Si/Al = 11.5) >H-BEA (Si/Al = 19) >H-USY (Si/Al = 15). For clays total acid amount was ca. 0.35-0.42 mmolg⁻¹. For SO₄²⁻/ZrO₂ and Nb₂O₅ total acidity was ca. 0.45 and 0.30 mmolg⁻¹ respectively. SiO₂-Al₂O₃ (Si/Al = 5.3) catalyst had an acid amount of ca. 0.63 mmolg⁻¹. MoO₃/SiO₂ synthesized by sol gel method had the least amount of acid sites, ca. 0.09 mmolg⁻¹ which corresponds to only weak acid sites.

Therefore from NH₃-TPD analysis data it was understood that the solid acids selected for lignin depolymerization had various amounts of strong and weak acid sites which may have an effect in the depolymerization of lignin into aromatic monomers.

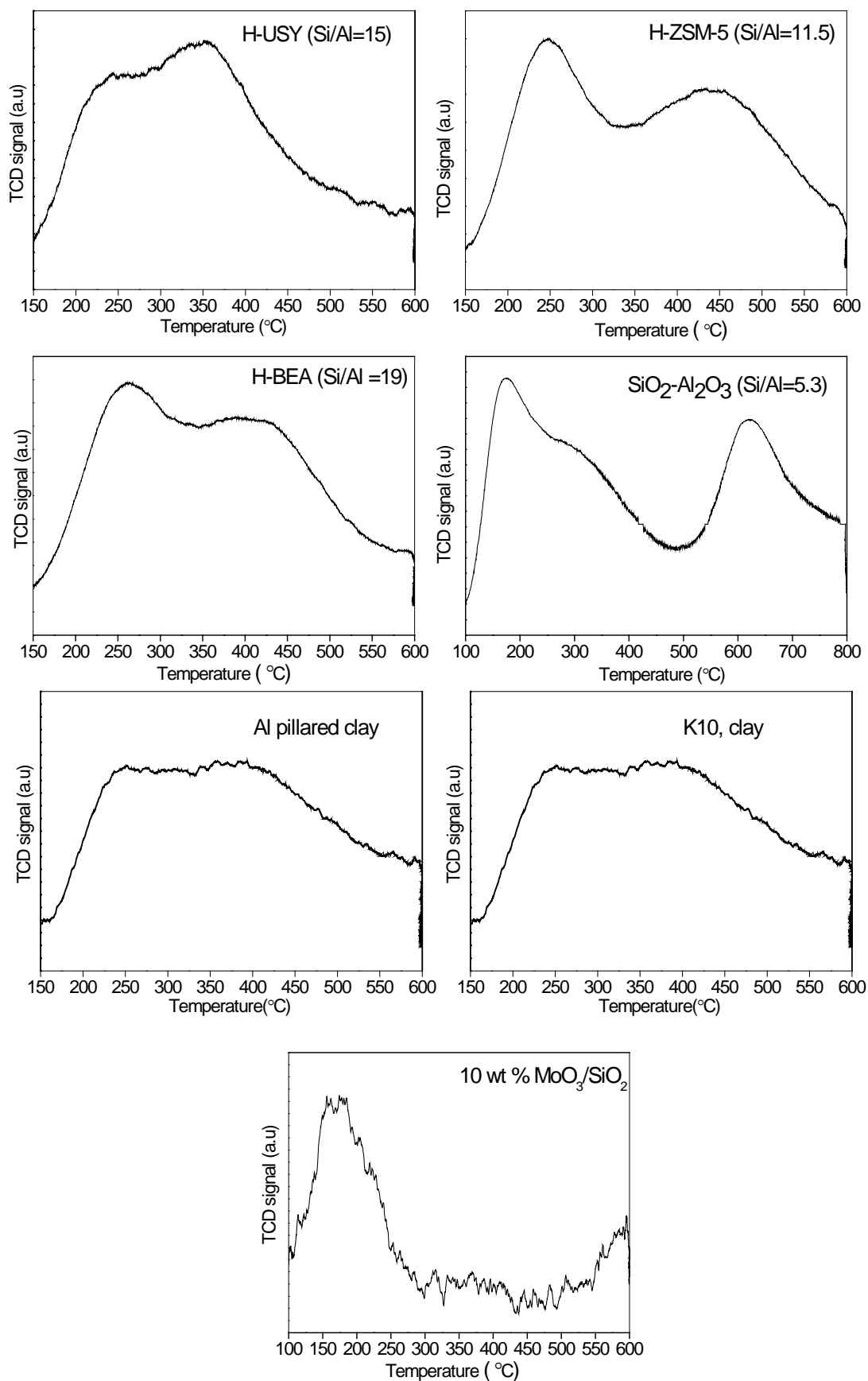


Figure 2B.4. NH₃-TPD analysis of solid acid catalysts.

Table 2B.3. Summary on NH₃-TPD analysis of solid acid catalysts

Catalyst	NH ₃ -TPD		
	Weak acid sites ^a (mmolg ⁻¹) (150-350 °C)	Strong acid sites (mmolg ⁻¹) (350-750 °C)	Total acidity (mmolg ⁻¹)
H-USY (Si/Al = 15)	0.06	0.49	0.55
H-ZSM-5 (Si/Al = 11.5)	0.37	0.61	0.98
H-BEA (Si/Al = 19)	0.25	0.66	0.91
H-MOR (Si/Al = 10)	0.5	0.65	1.15
SO ₄ ²⁻ /ZrO ₂	0.05	0.4	0.45
Nb ₂ O ₅	0.30	--	0.30
Clay (K10)	0.09	0.33	0.42
Al pillared clay	0.05	0.30	0.35
SiO ₂ -Al ₂ O ₃ (Si/Al = 5.3)	0.17	0.46	0.63
10 % MoO ₃ /SiO ₂	0.09	--	0.09

2B.4.1.4. ICP-OES analysis

ICP-OES analysis was performed to determine the Si/Al ratio of zeolites and SiO₂-Al₂O₃ and to determine the percentage of Mo loading on the MoO₃/SiO₂ prepared by sol gel method. Details are summarized in Table 2B.4.

Si/Al ratios obtained were found be similar to the ratio given by the supplier (Zeolyst International). Additionally it was found that the theoretical and actual loading of Mo present in MoO₃/SiO₂ was found to be 10 wt% and 9.0 wt% respectively.

Table 2B.4. Summary on ICP-OES analysis of solid acid catalysts

Catalyst	Si/Al ratio ^a	Si/Al ratio ^b
H-USY	15	14.9
H-ZSM-5	11.5	11.3
H-BEA	19	19.1
H-MOR	10	9.8
SiO ₂ -Al ₂ O ₃	5.3	5.2

^aFrom supplier, ^bICP-OES analysis

Catalyst	Mo loading (wt %)	
	Theoretical	Actual
MoO ₃ /SiO ₂	10	9.0

2B.4.2. Supported metal catalysts

2B.4.2.1. XRD analysis

Wide angle X-ray analysis was performed for bare supports as well as supported metal catalysts in a 2θ range of $5-90^\circ$ with a scan rate of 4.3°min^{-1} (Figures 2B.5a, 2B.5b, 2B.5c).

From the 2θ values formation of the metal nanoparticles was confirmed. Pd (JCPDS File No. 87-0638) showed diffraction patterns at 2θ values 40° (111), 46° (200) and 68° (220). In case of Pd on various supports XRD pattern showed a slight variation. For of Pd/C and Pd/HT catalyst Pd peaks were too broad and less intense which indicates the smallest size nanoparticle when compared to Pd/SA and Pd/AL catalysts. Pt catalysts (JCPDS File No. 04-0802) showed a diffraction pattern at 2θ values 39° (111), 46° (200) and 67° (220). For Pt/C catalysts, Pt metal peaks were almost not visible which indicates that on C support, Pt forms the smallest particles compared to Pt/SA, Pt/AL and Pt/HT. XRD of Ru (JCPDS file No. 6-663) catalysts showed a diffraction pattern at 2θ values 42° (002) and 44° (101). Also we can observe few peaks for RuO₂ at 58° in all the Ru catalysts.

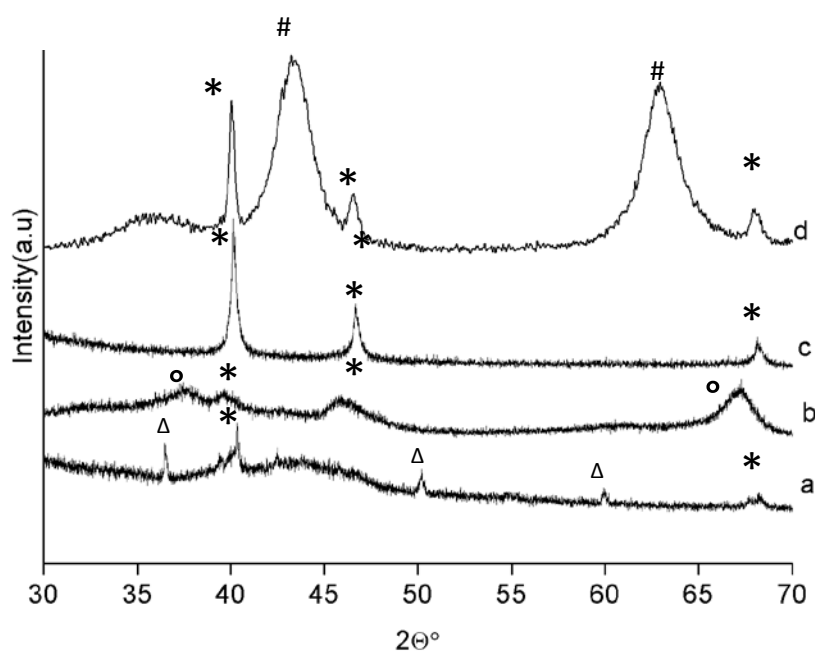


Figure 2B.5a. XRD patterns of supported Pd catalysts. (a) Pd/C (b) Pd/AL (c) Pd/SA (d) Pd/HT, where * indicates Pd metal, Δ indicates 'C' support, \circ indicates AL support and # indicates HT support.

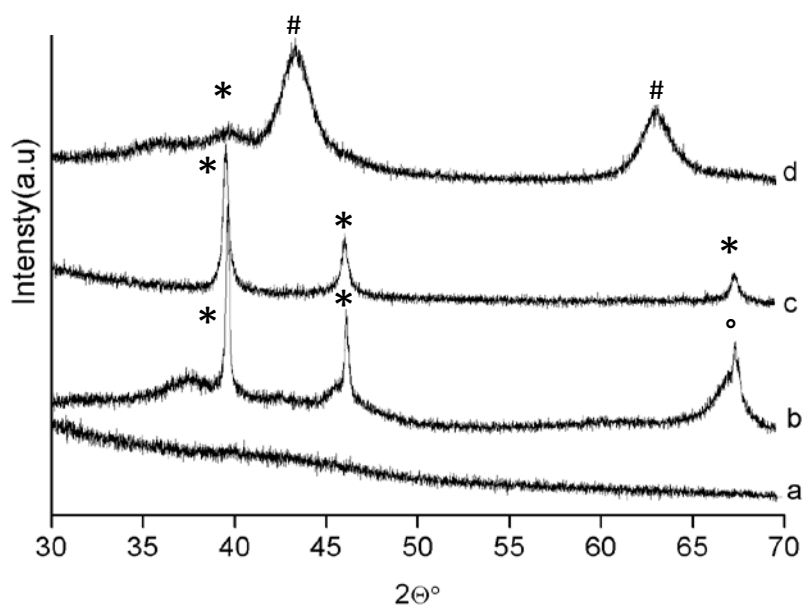


Figure 2B.5b. XRD patterns of supported Pt catalysts (a) Pt/C (b) Pt/AL (c) Pt/SA (d) Pt/HT, where * indicates Pt metal, \circ indicates AL support and # indicates HT support.

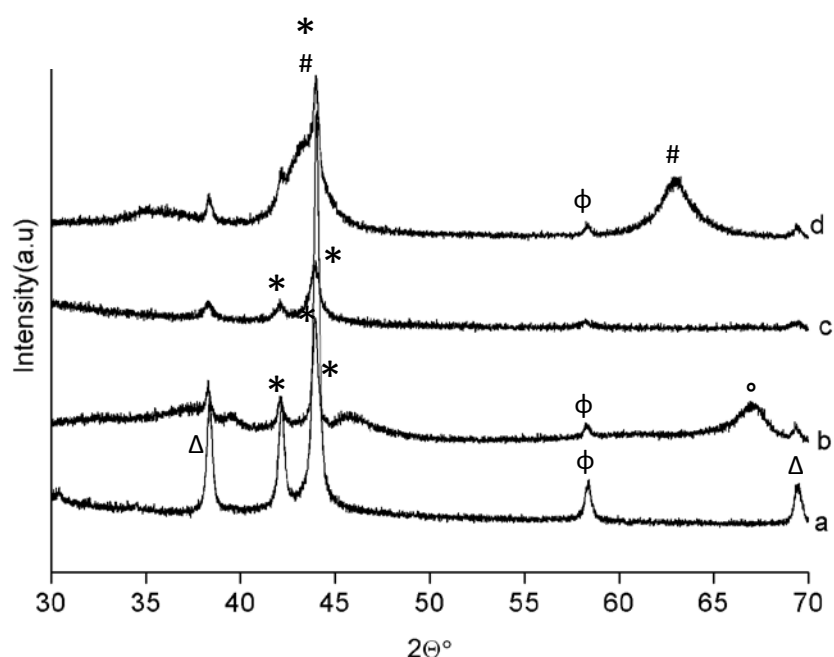


Figure 2B.5c. XRD patterns of supported Ru catalysts (a) Ru/C (b) Ru/AL (c) Ru/SA (d) Ru/HT, where * indicates Ru metal and ϕ indicates RuO_2 , Δ indicates C support, $^\circ$ indicates AL support, # indicates HT support.

2B.4.2.2. ICP-OES analysis

Supported metal catalysts were prepared by impregnation method. Percentage of metal loading on supports was determined by ICP-OES analysis (Table 2B.5). Loading of Pd, Pt and Ru metal on SA, AL, C and HT was found to be ca. 3 wt%. Along with these compositions, 3.5 wt% of Pt/AL and 2 wt% Pt/SA were also prepared which was confirmed by ICP-OES analysis.

Table 2B.5. Summary on the ICP-OES analysis of supported metal catalysts

Catalyst	Theoretical (wt%)	Actual (wt%)	Catalyst	Theoretical (wt%)	Actual (wt%)
Pd/C	3	3	Pt/SA	2	2
Pd/AL	3	3	Pt/HT	3.5	3.2
Pd/SA	3	2.8	Ru/C	3	3
Pd/HT	3	2.9	Ru/AL	3	2.8
Pt/C	3	3	Ru/SA	3	3.1
Pt/AL	3.5	3.3	Ru/HT	3	2.9

2B.4.2.3. N₂ sorption analysis

BET surface area of supported metal catalysts along with the bare supports was determined using N₂ sorption analysis. Higher the surface area of the support better would the dispersion of metal nanoparticles loaded on it. Typically it was observed that after metal loading, the surface area of support was found to be decreased. Results are summarized in Table 2B.6.

Table 2B.6. Summary on N₂ sorption analysis of supported metal catalysts

Catalyst	BET surface area ^a (m ² g ⁻¹)	Catalyst	BET surface area ^a (m ² g ⁻¹)
Carbon (C)	1000	Pt/C ^c	1500
γ-Al ₂ O ₃ (AL)	154	Pt/AL	174
SiO ₂ -Al ₂ O ₃ (SA)	532	Pt/SA	510
Hydrotalcite (HT)	250	Pt/HT	159
Pd/C ^b	1400	Ru/C	850
Pd/AL	122	Ru/AL	123
Pd/SA	500	Ru/SA	490
Pd/HT	187	Ru/HT	165

^a N₂ sorption study, ^{b,c} supplied by Aldrich

2B.4.2.4. HRTEM analysis

HRTEM analysis of Pd, Pt and Ru catalysts on SA, AL, C and HT was performed (Figures 2B.6a, 2B.6b, 2B.6c). Average particle size and percentage of dispersion of metal nanoparticles was calculated using this technique. Results are summarized in Table 2B.7.¹⁶ Pd, Pt and Ru loaded on C supports were having the highest percentage of dispersion (ca. 20 %) among all the supported metal catalysts prepared. This was obvious since high surface area of C support have facilitated the better dispersion of metal on it.

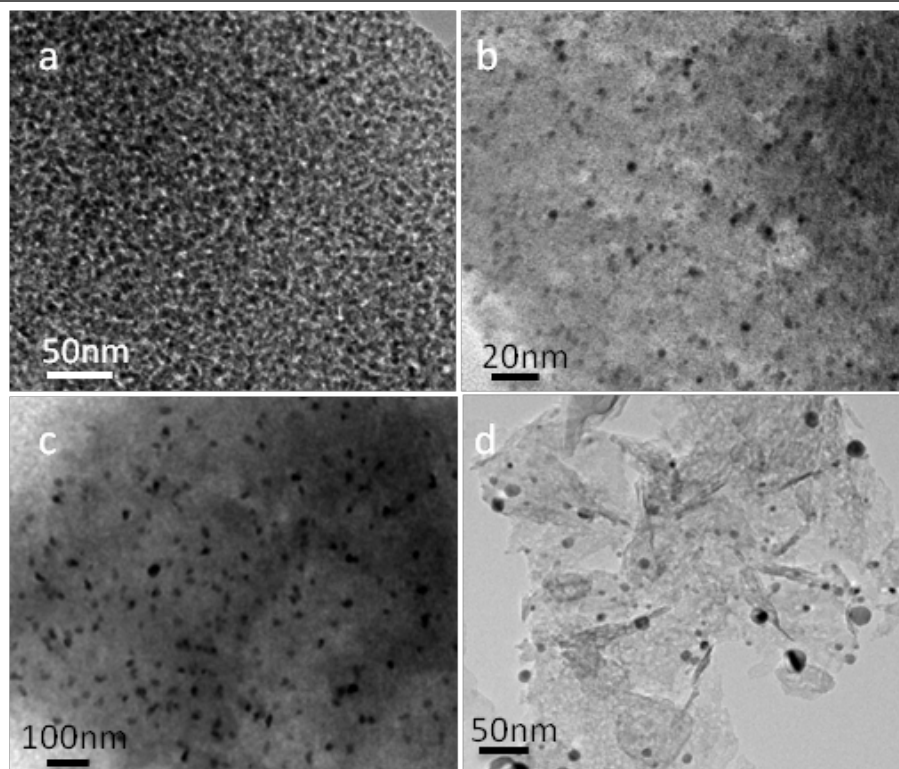


Figure 2B.6a. HRTEM images of supported Pd catalysts (a) Pd/AL (b) Pd/C (c) Pd/SA (d) Pd/ HT.

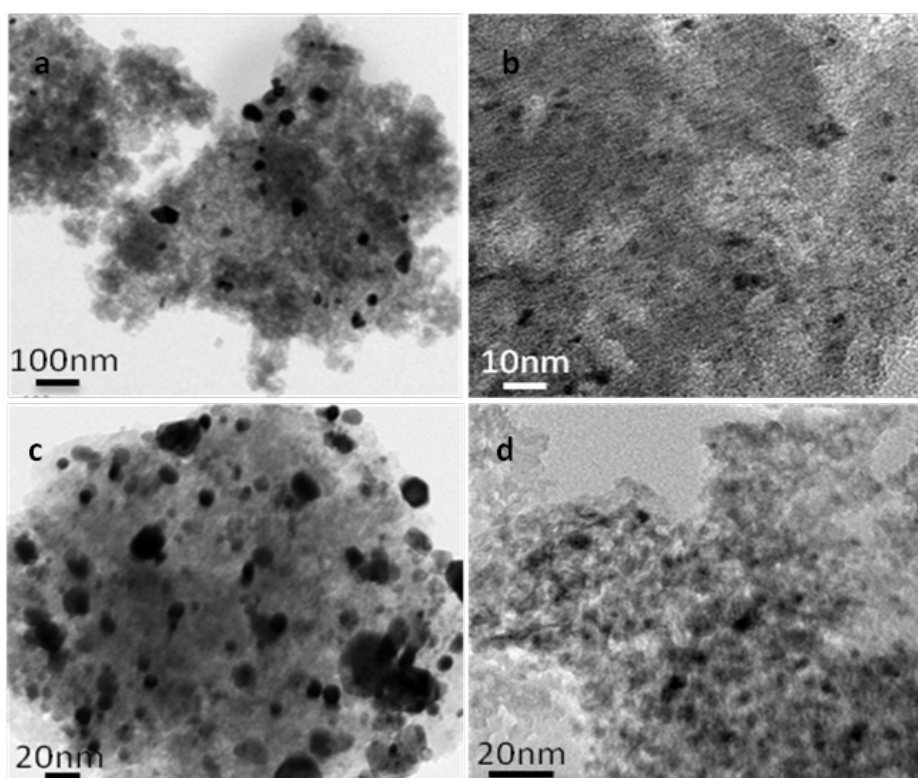


Figure 2B.6b. HRTEM images of supported Pt catalysts (a) Pt/AL (b) Pt/C (c) Pt/SA (d) Pt/HT.

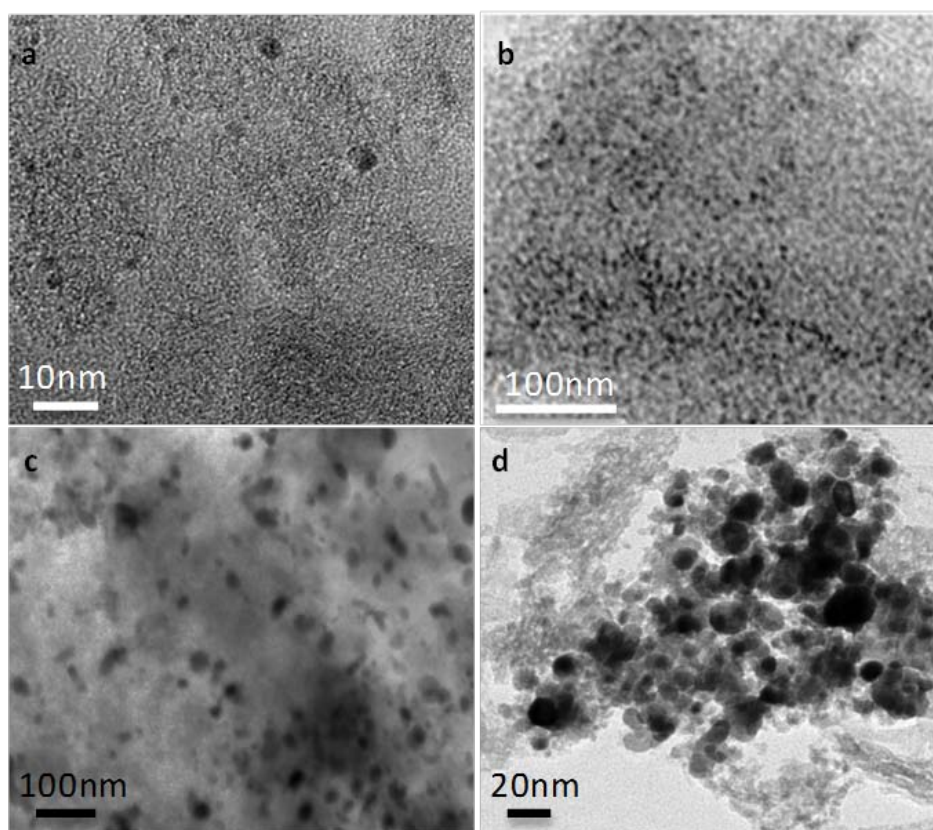


Figure 2B.6c. HRTEM images of supported Ru catalysts (a) Ru/C (b) Ru/AL (c) Ru/SA (d) Ru/HT.

Table 2B.7. Summary on average particle size and dispersion of supported metal catalysts determined using HRTEM analysis

Catalyst	Average particle size (nm)	Dispersion (%)	Catalyst	Average particle size (nm)	Dispersion (%)
Pd/C	5	25	Pt/SA	8	5
Pd/AL	10	12	Pt/HT	3	18
Pd/SA	20	8	Ru/C	3	21
Pd/HT	15	10	Ru/AL	22	10
Pt/C	3	22	Ru/SA	15	15
Pt/AL	15	8	Ru/HT	16	10

2B.5. CONCLUSIONS

For acid catalysed depolymerization of lignin into aromatic monomers structured as well as amorphous solid acids catalysts were used. Particularly structured solid acids like zeolites, clays and metal oxides were selected, since they were found to be capable of depolymerizing cellulose and hemicellulose. Moreover, amorphous solid acids like silica alumina and supported metal oxide (10 wt % $\text{MoO}_3/\text{SiO}_2$) were used with anticipation that they retain their stability when compared to structured solids under the reaction conditions employed for lignin studies. Synthesis of 10 wt% $\text{MoO}_3/\text{SiO}_2$ was performed by sol gel method. This chapter also discusses about the synthesis and characterization of supported metal catalysts used in the HDO reactions. These supported metal catalysts were prepared by impregnation method. They include 2-3.5 wt% of Pt, Pd, Ru metals loaded on SA, AL, C and HT support. Various physico-chemical techniques were used to study the properties of both solid acids and supported metal catalysts. XRD analysis confirmed the crystalline or amorphous nature of solid acids. In the XRD pattern of supported metal oxide (10 wt % $\text{MoO}_3/\text{SiO}_2$) it was observed that metal peaks were not visible since well there was a homogeneous distribution of metal oxide species on the support surface during its synthesis by sol gel method. Metal nanoparticles loaded on supports were detected by XRD analysis of supported metals synthesized by impregnation method. To quantify the amount of acids sites (strong and weak) present, NH_3 -TPD analysis was performed for solid acids. It was observed that among the solid acids used H-MOR (Si/Al = 10) was having the highest amount of total acid sites (1.15 mmol g^{-1}) and for $\text{MoO}_3/\text{SiO}_2$ prepared by sol gel method showed the least amount of total acid sites (0.09 mmol g^{-1}) when compared all other solid acids employed in the study. ICP-OES analysis confirmed the Si/Al ratio of commercial zeolites and $\text{SiO}_2\text{-Al}_2\text{O}_3$ catalysts and it was found to be in good correlation with the suppliers. Metal loading in catalysts like $\text{MoO}_3/\text{SiO}_2$ and supported metals were also confirmed using ICP-OES analysis. N_2 sorption analysis was performed to determine the surface area, pore volume and pore diameter of solid acids and supported metals. It was observed that among the solid acids used H-USY (Si/Al = 15) was found to be having highest surface area ($873 \text{ m}^2\text{g}^{-1}$). It was also observed that metals loaded on carbon supports exhibited high surface area and therefore showed high percentage of dispersion (ca. 20 %) which was

confirmed using HRTEM analysis. Hence Pt, Pd, Ru on C support can be expected to show high activity compared to other supported metals.

In summary, chapter 2B discusses details of synthesis and characterizations done for solid acids and supported metal catalysts. It helped to understand their various physico-chemical properties which will be very helpful while performing depolymerization and HDO studies with solids acids and supported metal catalysts, respectively.

2B.6. REFERENCES

1. Deepa, A. K.; Dhepe, P. L., *RSC Adv.* **2014**, *4*, 12625-12629.
2. Deepa, A. K.; Dhepe, P. L. Depolymerization of lignin using solid acid catalysts. U.S. 0302796 A1, November 29, 2012.
3. Deepa, A. K.; Dhepe, P. L., *ChemPlusChem* **2014**, DOI: 10.1002/cplu.201402145.
4. Tanabe, K.; Misono, M.; Hattori, H., *New Solid Acids and Bases*. Elsevier Science: 1990; p 364.
5. Lin, K.; Ma, B.; Sun, Y.; Liu, W., *Bioresour. Technol.* **2014**, *167*, 133-136.
6. Sahu, R.; Dhepe, P. L., *ChemSusChem* **2012**, *5*, 751-761.
7. Database of zeolite structure. http://izasc.ethz.ch/fmi/xsl/IZA-SC/ftc_fw.xsl?db=Atlas_main&lay=fw&-max=25&STC=BEA&-find.
8. Bergaya, F.; Theng, B. K. G.; Lagaly, G., *Handbook of Clay Science* Elsevier: 2006.
9. Gil, A.; Korili, S. A.; Trujillano, R.; Vicente, M. A., *Pillared Clays and Related Catalysts*. Springer: 2010; p 550.
10. Ng, S.; Plank, J., *J. Plank, Cem. Concr. Res.* **2012**, *42*, 847-854.
11. Suzuki, K.; Hayakawa, T.; Shimizu, M.; Takehira, K., *Catal Lett* **1995**, *30*, 159-169.
12. Salomão, R.; Milena, L. M.; Wakamatsu, M. H.; Pandolfelli, V. C., *Ceram. Int.* **2011**, *37*, 3063-3070.
13. Gerhard, W., *Nanostructured Materials*. Elsevier: 2009; p 367.
14. Campelo, J. M.; Luna, D.; Luque, R.; Marinas, J. M.; Romero, A. A., *ChemSusChem* **2009**, *2*, 18-45.
15. <http://www.zeolyst.com/home.aspx>.
16. Ashcroft, A. T.; Cheetham, A. K.; Harris, P. J. F.; Jones, R. H.; Natarajan, S.; Sankar, G.; Stedman, N. J.; Thomas, J. M., *Catal. Lett.* **1994**, *24*, 47-57.

CHAPTER 3

SOLID ACID CATALYSED DEPOLYMERIZATION OF LIGNIN INTO AROMATIC MONOMERS AND ISOLATION OF AROMATIC MONOMERS

CHAPTER 3A

**DEPOLYMERIZATION OF
LIGNIN USING STRUCTURED
SOLID ACIDS**

3A.1. INTRODUCTION

Lignocellulosic materials, due to their renewability and profuse availability (ca. 1.8 trillion tons of annual production)¹ have generated immense interest in recent years in the production of chemicals, fuels and energy under the bio-refinery concept.²⁻⁶ Lignin is an aromatic biopolymer which is abundantly present in all lignocellulosic materials (15-20 %) and also excess amount of lignin is available from cellulose to ethanol process and from pulp and paper industries, but this excess amount of lignin is mainly used only for power generation. This assures an abundant supply of lignin and thus it becomes crucial to valorize lignin into value added aromatic monomers to substantially augment the prospects of cellulose to ethanol process. By 2030 US, EU and many other countries have set a goal to employ lignocellulosic materials as an alternative for fossil feedstock in the production of fuels and chemicals.⁷ To achieve these aims, it is obvious to develop a method for the efficient valorization of lignin. Considering that lignin is the only natural source of aromatics in the form of cross-linked 3-D amorphous phenolic polymer, it would be natural and desirable to make aromatics based value added chemicals and fuel additives from it. Several review articles have well discussed various methods of lignin valorization into value-added aromatic monomers and also the challenges involved in the present methods.⁷⁻⁹ From the literatures it is well understood that it is vital to develop newer, efficient and greener methods for the depolymerization of lignin into aromatic monomers. In short, due to aromatic nature and abundant availability, lignin is considered as a renewable source for the production of value added chemicals and fuels (Figure 3A.1).



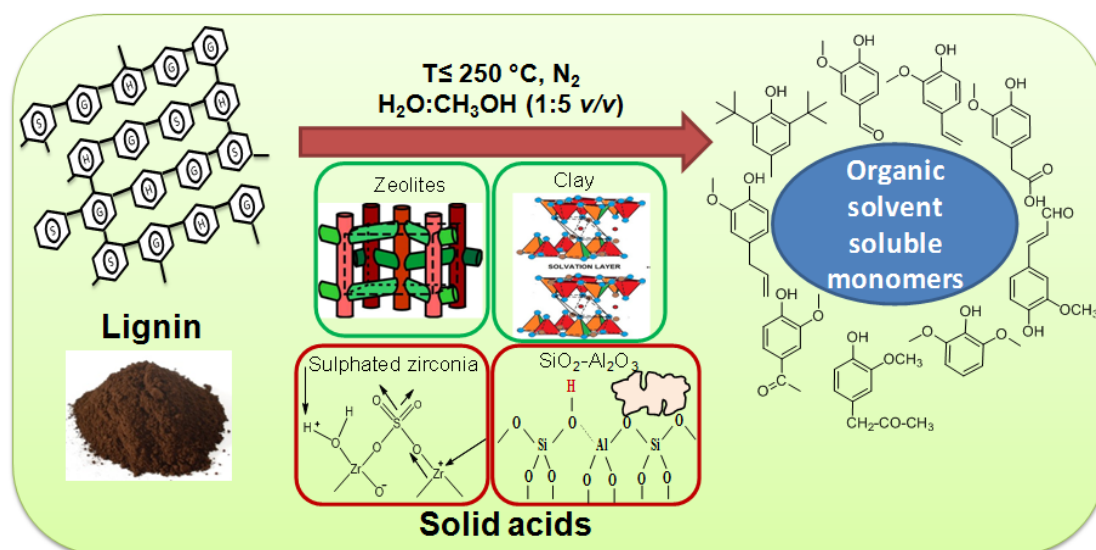
Figure 3A.1. Value addition of lignin.

There are several existing methods for the depolymerization of lignin (Refer Chapter 1, section 1.8) but as per best of my knowledge there are no reports on the solid acid catalysed depolymerization of lignin to obtain aromatic monomers under mild reaction conditions ($T \leq 250$ °C). So here, I am showing for the first time that lignin can be depolymerized into aromatic monomers using only solid acid catalysts

under milder reaction conditions. Details on these are discussed in this chapter.

In all the previous reports on the depolymerization of lignin involving acid catalysts, mostly pyrolysis technique is used and a careful study of these reports reveal that in all these reactions, high temperatures (340-750 °C) are employed.¹⁰⁻¹⁵ Moreover, involvement of high temperatures invariably along with the formation of gases (CO₂, CH₄) shows the presence of coke and char, hence lower yield for the aromatic monomers is achieved. In most of the earlier known literature reports^{8, 14-19} model compounds like dimers or trimers are used. The catalytic results obtained for lignin model compounds cannot be reproduced when actual lignin substrates are used, since lignin has a very complicated structure and also contain several impurities compared to model compounds^{7, 13-20} which can adversely affect the activity of the catalyst.

In this thesis I have presented study on the depolymerization of 6 different types of actual lignin substrates (dealkaline, organosolv, alkali, ORG, EORG and bagasse lignin). These lignins were obtained from various sources and were selectively depolymerized into aromatic monomers in presence of solid acid catalysts (Scheme 3A.1). The reactions were performed under inert atmosphere, at relatively milder reactions when compared to earlier reports ($T \leq 250$ °C), thereby avoiding the formation of degradation products like coke, char or gases.



Scheme 3A.1. Depolymerization of lignin over solid acid catalysts into aromatic monomers.

3A.2. EXPERIMENTAL

3A.2.1. *Materials*

Dealkaline lignin (TCI Chemicals, product no. L0045), alkali lignin (Aldrich, product no. 370959), organosolv lignin (Aldrich, product no. 371017) were purchased and used without any pre-treatment. ORG and EORG lignin were obtained from local industries. Bagasse lignin was isolated in the laboratory by organosolv method (Refer chapter 2A, section 2A.2.1). Zeolites, H-USY (Si/Al = 15), H-ZSM-5 (Si/Al = 11.5), H-MOR (Si/Al = 10), H-BEA (Si/Al = 19) were obtained from Zeolyst International. Prior to use, zeolites were calcined at 550 °C for 16 h in air flow (30 mLmin⁻¹). SiO₂-Al₂O₃ (Aldrich, Si/Al = 5.3, product no. 343358), K10 clay and Al pillared clay (Aldrich), niobium pentoxide (Spectrochem) were also purchased. Various aromatic monomers (vanillin, methyl vanillate, guaiacyl acetone, eugenol, acetosyringone, acetoguaiacone, homovanillic acid, transconiferyl aldehyde, vinyl guaiacol, butylated hydroxy toluene (BHT)) were purchased from Aldrich, Alfa Aesar, TCI chemicals and were used as received.

Solvents like methanol (99.9 %, LOBA Chemie), ethanol (99 %, Changshu Yangyuan Chemical Co., Ltd, China), tetrahydrofuran (99.8 %, LOBA Chemie), ethyl acetate (99.9 %, LOBA Chemie), chloroform (99.8 %, LOBA Chemie), diethyl ether (99.5 %, LOBA Chemie), hexane (99 %, LOBA Chemie) and dichloro methane (99.8 %, LOBA Chemie) were purchased and used as received. NaCl (Merck), H₂SO₄ (98.5-97 %) (Merck), HCl (37 %) (Merck), and HF (48 %) (Merck) were also obtained and used as received. Distilled water was used in all the experiments.

3A.2.2. *Depolymerization of lignin*

Reactions were carried out in 100 mL and 300 mL batch reactor (high temperature and high pressure Parr autoclaves) (Figure 3A.2). Lignin (0.5 g) dissolved in H₂O:CH₃OH (1:5 v/v, 30 mL) solvent along with the catalyst (0.5 g) was charged in the autoclave. The autoclave was flushed at least 3 times with N₂ and was filled with 0.7 MPa N₂ at room temperature (RT). Initially, the rpm was kept at 100 and after attaining the desired reaction temperature (200-250 °C) it was increased to 500 rpm/1000 rpm and this was considered as the starting time of the reaction. After the reaction, reactor was cooled to RT and gas was released. Catalyst was separated out by centrifugation, washed thoroughly with CH₃OH in order to remove any adsorbed lignin or products

on the catalyst. The reaction mixture ($\text{H}_2\text{O}:\text{CH}_3\text{OH}$ (1:5 v/v, 30 mL) was directly injected in GC-FID and GC-MS after filtering through syringe filter (0.22 micron, 13 mm nylon) to remove suspended particles, if any. From the reaction mixture, solvent was removed by rotary evaporator. After the removal of solvent, solids obtained were dried at 60 °C in oven for overnight (16 h). Afterwards these solids were kept at 150 °C under vacuum (10^{-4} MPa) for 2 h. This treatment could possibly remove completely the solvent (water or methanol) present in the solid recovered. Then the resulting solid was weighed. The recovered solid obtained contains unconverted lignin and depolymerized products (monomers, dimers, oligomers). In order to separate the aromatic monomers from this mixture, various organic solvents such as tetrahydrofuran (THF), chloroform (CHCl_3), ethyl acetate (EtOAc), and diethyl ether (DEE) were used depending on the type of lignin employed in the study. The % of aromatic monomer or organic solvent soluble products was calculated based on the solid recovered after evaporating the respective solvents (refer section 3A.2.4).



Figure 3A.2. Batch mode reactor used for depolymerization studies of lignin.

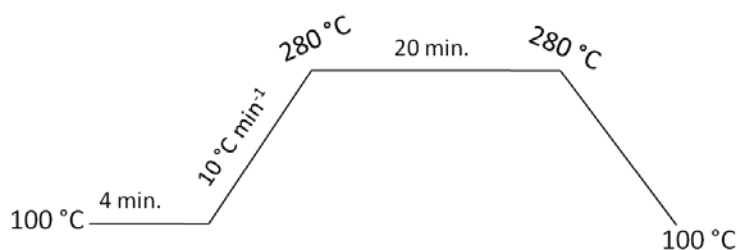
3.A.2.3. Analysis

Analysis of the reaction mixture and the organic solvent soluble products were performed using Gas Chromatography-Flame Ionization Detector (GC-FID), GC-Mass (GC-MS), High Performance Liquid Chromatography (HPLC), Gel Permeation

Chromatography (GPC) (DMF and THF), Nuclear Magnetic Resonance (NMR) (^1H and ^{13}C), elemental analysis (CHNS), Matrix Assisted Laser Desorption Ionization Time of Flight (MALDI-TOF) and Inductively Coupled Plasma Optical Emission Spectroscopy (ICP-OES) and Fourier Transform Infrared Spectroscopy (FTIR) analysis.

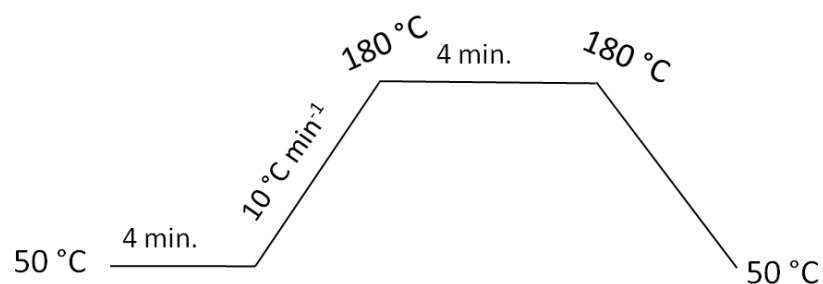
3.A.2.3.1. GC- FID

Products present in the reaction mixture was analyzed using Varian 3800 model GC, Netherland equipped with a capillary column (CPSIL 8CB, 5 % phenyl 95 % dimethyl polysiloxane, 0.25 mm i.d. x 30 m length) and also Agilent Gas Chromatograph (GC) equipped with a capillary column (HP-5, 5 % phenyl 95 % dimethyl polysiloxane, 0.32 mm x 50 m) with flame ionization detector (FID). N_2 was used as a carrier gas, H_2 was used for flame and air as oxidizer, carrier gas flow = 0.6 mLmin^{-1} , injector temperature used was 275°C and detector temperature used was 280°C . Splitmode injector (40:1) was used for sample delivery. Column oven program used was as follows,



3.A.2.3.2. GC-TCD

The gas released from the reactor after the lignin depolymerization reaction was analysed (online sampling was done) using Chemito 8610 model GC, with thermal conductivity detector (TCD) and is equipped with Porapack Q column (2 mm i.d. x 2.74 m length) to detect the formation of any products like CO , CO_2 , CH_4 , dimethyl ether (DME) etc. under the reaction conditions. The injector temperature used was 50°C and detector temperature was 150°C . Column oven program used was as follows,



3.A.2.3.3. GC-MS

The molecular weight of the aromatic products present in the reaction mixture was determined using Varian 3800 GC-MS, (Saturn 2000 MS) equipped with VF-5 capillary column (5 % phenyl 95 % dimethyl polysiloxane) (0.25 mm i.d. x 30 m length). Helium with a flow rate of 0.6 mLmin⁻¹ was used as carrier gas. Column oven program is similar to that used for GC-FID. From the m/z values observed in the fragmentation pattern and also matching it with NIST (version 05) library present in GC-MS, the molecular weights of the corresponding compounds were determined.

3.A.2.3.4. HPLC

Reaction mixture was analysed using Agilent make High Performance Liquid Chromatography (HPLC, 1200 Infinity series) system equipped with autosampler, C18 column (4.6 mm i.d x 0.25 m length, 30 °C) and refractive index (RI) detector (40 °C). CH₃OH:H₂O:Acetic acid (40:58:2 v/v) was used as a mobile phase with a flow rate of 0.8 mLmin⁻¹. The identification of compounds in the reaction mixture was done by injecting standards.

3.A.2.3.5. LC-MS

Reaction mixture was analyzed using Thermo Scientific system (Model no. Q Extractive), C18 column (4.6 mm i.d. x 0.15 m length) and mass detector (Orbitrap analyzer). Reverse phase system was used with CH₃OH:H₂O (40:60 v/v) as mobile phase and pumped at a flow rate of 0.5 mLmin⁻¹. Oven temperature was set at 30 °C and an electron source ionization ion source was used for the analysis.

3.A.2.3.6. GPC Analysis

3.A.2.3.6.1. DMF-GPC

Analysis of dealkaline lignin and MeOH soluble reaction mixture was performed in Viskotek TDA 305-040 model GPC system. Triple detector array was used, refractive index (RI), viscometer (VISC), low angle light scattering (LALS), right angle light scattering (RALS). Separations were achieved by three columns (T6000M (3 no.s), GENERAL MIXED ORG; 7.8 mm i.d. x 0.3 m length) and one guard column (TGAURD, ORG GUARD COL; 4.6 mm i.d. x 0.1 m length). DMF was used as eluent with a constant flow rate of 1 mLmin⁻¹. Column and detector temperature was kept at 60 °C. GPC samples were prepared at a concentration of 10 mgmL⁻¹ and 0.1 mL volume was injected into the instrument.

3.A.2.3.6.2. THF-GPC

GPC analysis of the THF soluble products of dealkaline lignin depolymerization reaction was performed using VISKOTECH VE 1122 pump, Viscotek VE 3580 RI detector) and Viscotek VE 3210 UV/Vis detector with THF as an eluent with a constant flow rate of 1 mLmin⁻¹. Separations were achieved by GMH-HR-H column. Column and detector temperature was kept at 30 °C. GPC samples were prepared at concentrations of 1 mgmL⁻¹ and 0.1 mL volume was injected into the instrument. Polystyrene standards were used for calibration.

3.A.2.3.7. NMR analysis

¹H and ¹³C NMR of dealkaline lignin and products was recorded on Bruker Ascend-700 MHz using CD₃OD and D₂O mixture. TMS was used as internal standard for the analysis. 70 mg of lignin or products were dissolved in 0.75 mL of CD₃OD and D₂O mixture (5:1 v/v) and analysed. No. of scans used for ¹H, ¹³C NMR were 200 and 10376, respectively.

3A.2.4. Yield calculations

After the separation of the catalyst by centrifugation, the reaction mixture was analyzed in GC-FID. The reaction solvent (H₂O:CH₃OH (1:5 v/v, 30 mL)) was removed using rotary evaporator. Now the solid recovered contain both monomeric products, oligomers and unreacted lignin. To separate the products from lignin, the

solid was dissolved in various organic solvents such as tetrahydrofuran, chloroform, ethyl acetate or diethyl ether for the analysis (Figure 3A.3). The choice of these solvents for the extraction of the products was done based on the solubility of lignin (Refer chapter 2A, section 2A.2.10, Table 2A.5). Since particular lignins are not soluble in the above solvents, the products will be extracted out leaving behind those lignins.

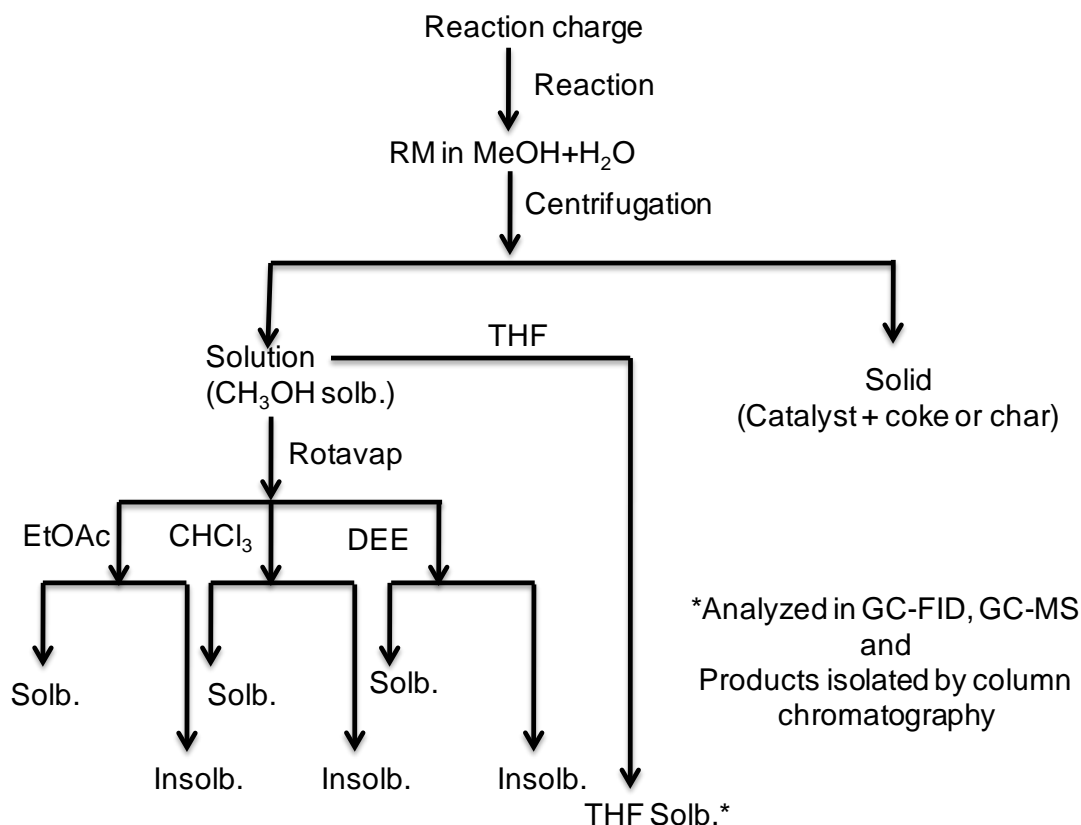


Figure 3A.3. Scheme for the extraction of THF soluble products in dealkaline lignin reactions. Similarly for organosolv lignin, diethyl ether (DEE); for alkali/EORG/bagasse lignin ethyl acetate (EtOAc) and for ORG, chloroform (CHCl_3) was used for solubilizing the products.

Dealkaline lignin contains 11 % moisture, so if 0.5 g of the dealkaline lignin is taken, then it contains 0.055 g (11 %) of moisture in it, (TCI Chemicals)²¹ which is also supported by the TGA-DTA studies done on the this lignin (Refer chapter 2A, Figure 2A.8a). From TGA-DTA analysis of dealkaline lignin performed at 1000 °C in air, 17 % of unburnt residue (inorganic residue/ash) was observed. Therefore if 0.5 g of dealkaline lignin is weighed, 0.085 g is inorganic residue. So the actual weight of dealkaline lignin charged is only 0.36 g (0.5 – (0.055 + 0.085 g)). So the calculation

has to be done based on this information. All other lignins employed in the study are completely free of moisture, so the weight of the substrate charged is 0.5 g itself.

The % of aromatic monomer was calculated based on the weight of solid recovered from the above solvents.

For dealkaline lignin, THF soluble aromatic monomers yield (%)

$$= \frac{\text{Weight of THF soluble solid}}{\text{Lignin charged}} \times 100$$

For organosolv lignin, DEE soluble aromatic monomers yield (%)

$$= \frac{\text{Weight of diethyl ether soluble solid}}{\text{Lignin charged}} \times 100$$

For alkali lignin/EORG/bagasse lignin, EtOAc soluble aromatic monomers yield (%)

$$= \frac{\text{Weight of EtOAc soluble solid}}{\text{Lignin charged}} \times 100$$

For ORG lignin CHCl_3 soluble aromatic monomers yield (%)

$$= \frac{\text{Weight of } \text{CHCl}_3 \text{ soluble solid}}{\text{Lignin charged}} \times 100$$

3.A.2.5. Mass balance calculation

Mass balance (%) =

$$\frac{\text{Wt. of methanol soluble solid} + \text{Wt. of solid deposited on the catalyst}}{\text{Wt. of lignin charged}} \times 100$$

Based on the above calculations, the actual weight of dealkaline lignin charged is only 0.4450 g (0.5-0.055 g moisture). So the calculation has to be done based on this information.

For instance, in the case of dealkaline lignin the mass balance calculation can be done as follows,

Reaction conditions: dealkaline lignin (0.5 g), Solid acid catalyst (0.5 g), $\text{H}_2\text{O}:\text{CH}_3\text{OH}$ (1:5 v/v), 250 °C, 30 min., 500 rpm, 0.7 MPa N_2 at RT.

Solid charged before the reaction

Dealkaline lignin = 0.4450g (0.5 g - 0.055 g of moisture)

Catalyst amount = 0.5 g Total solid charged= (0.4450 g +0.5 g) = **0.9450 g**

Solid and liquid recovery was done by centrifugation after the reaction.

Solid recovered after the reaction

Total solid recovered= 0.6327 g (catalyst + solids)

Solid deposited on the catalyst = total solid recovered – catalyst charged

$$= 0.6327 - 0.5000 \text{ g} = \mathbf{0.1327 \text{ g}}$$

Solid deposited on the catalyst after the reaction can be coke or char.

After the recovery of the catalyst, the (methanol + water) soluble portion of the reaction mixture was subjected to rotary evaporator to remove the solvent. After drying it in drying oven at 60 °C for overnight (16 h) and then in vacuum (10^{-4} MPa) for 2 h, the recovered solid was weighed. The solid now contains unreacted lignin and products.

Weight of (methanol + water) soluble solid = 0.2903 g

Based on the above observations, the mass balance for the lignin charged was calculated using the formula,

$$\text{Mass balance} = \frac{0.2903 + 0.1327}{0.4450} = \mathbf{95 \%}$$

Similar calculation were done for all the reactions and a mass balance of 90±5 % is observed for the lignin depolymerization reactions catalyzed by solid acids.

To ensure that there is no contribution of solvent in weight of solid the following precautions were taken:

The reaction mixture liquid (H₂O:CH₃OH (1:5 v/v, 30 mL) after separation of catalyst, was subjected to rotary evaporator to remove the solvents. The solid obtained thereafter was dried at 60 °C in oven for overnight (16 h). Afterwards the solid was kept at 60 °C under vacuum (10^{-4} MPa) for 2 h. This treatment could completely remove the solvents present in the solid. Then the resulting solid was weighed. Now the weight calculated does not include the solvent weight.

To ensure that no volatile products have escaped during the rotary evaporation the following precautions were taken

After the rotary evaporator the solvent (H₂O:CH₃OH (1:5 v/v, 30 mL) collected in the collection flask was analyzed by GC-FID. Except peak for methanol no other peak(s) was observed in the GC-FID chromatograph. In order to assure that no volatile products are escaped, 3 ice traps were used during rotator evaporation process. This observation helped to confirm that during the process of solvent removal no products are lost.

3A.2.6. Substrate/Catalyst (S/C) calculations

The average molecular weight of monomeric lignin unit was taken as 166 (based on the monomer molecular formula, C₉H₁₀O₃ derived, Refer Chapter 2A, Section 2A.2.3, Table 2A.2)

Acid amount of H-USY (Si/Al=15) catalyst = 0.55 mmol g⁻¹

0.5 g (substrate)/166 = 3.012 x 10⁻³ mol (3.012 mmol)

0.5 g (catalyst loading) x 0.55 = 0.275 mmol

S/C (mol basis) = 3.012/0.275 = **10.95**

3A.3. RESULTS AND DISCUSSIONS

3A.3.1. Evaluation of catalytic activities of various solid acid catalysts in depolymerization of dealkaline lignin reaction

Typically, zeolites (H-USY (Si/Al = 15), H-MOR (Si/Al = 10), H-BEA (Si/Al = 19), H-ZSM-5 (Si/Al = 11.5), clays (K10, Montmorillonite; Al pillared), and metal oxides (SiO₂-Al₂O₃, Nb₂O₅, sulphated zirconia, MoO₃/SiO₂) were used as catalysts. The catalytic reactions were done in batch mode autoclaves with varying reaction parameters. The work up procedure, analysis of reaction mixtures by GC-FID, GC-TCD, GC-MS, HPLC, LC-MS, GPC, NMR, FTIR and calculations are described in section 3A.2.3, Figure 3A.3.

Initially the activity of solid acid catalysts was evaluated in the depolymerization of the dealkaline lignin, which has the highest molecular weight (60,000 gmol⁻¹) amongst all the 6 types of lignins and was also contaminated with Na and S (Refer chapter 2A, Table 2A.2). The depolymerization reactions of dealkaline lignin were carried out using various solid acid catalysts at 250 °C for 30 min. and the results are illustrated in Figure 3A.4. Under the reaction conditions without catalyst only 10 % of aromatic monomers were formed but when solid acid catalysts were used the yield for aromatic monomers increased to 60 % (THF soluble products).

Among the solid acid catalysts, zeolites (H-USY, H-ZSM-5, H-MOR, H-BEA) having definite structure (pore diameter, pore volume, channel structure) showed the highest activity for aromatic monomers formation (40-60 % yield). Most of the other catalysts (Clay, MoO₃/SiO₂, SiO₂-Al₂O₃) gave aromatic monomers yield of 25-40 %.

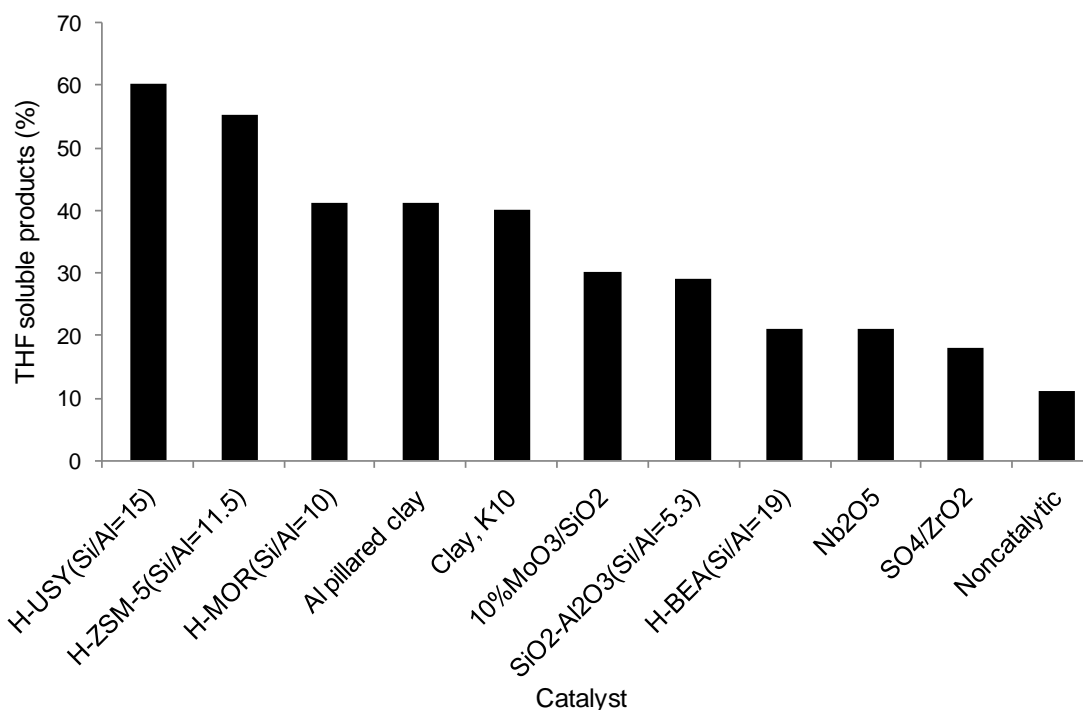


Figure 3A.4. Catalyst evaluation study of dealkaline lignin depolymerization reaction. Reaction conditions: dealkaline lignin (0.5 g), catalyst (0.5 g), H₂O:CH₃OH (1:5 v/v, 30 mL), 250 °C, 30 min., 500 rpm, 0.7 MPa N₂ at RT.

After the reaction, solvent (water + methanol) was removed by rotary evaporator and from the obtained semi-solid part containing aromatic monomers and unreacted lignin, selectively aromatic products were extracted using THF solvent (Figure 3A.3). For the extraction of aromatic monomers, THF was used, since dealkaline lignin was insoluble in this solvent. This precaution helped in avoiding contamination of lignin in the products.

Efforts were taken to check the effect of total acid amount on the catalytic activity (Figure 3A.4) but, could not draw an exact correlation. Similarly, efforts were put in drawing parallels between activity and other properties (surface area, pore volume, pore diameter, Refer chapter 2B, Table 2B.2) of catalysts but it was difficult to arrive at any definite conclusion because of complexity of reactions in terms of which bonds (C-C/C-O-C) in lignin were interacting with catalytically active sites

(Brönsted/Lewis acid sites) under the reaction conditions. But it can be suggested that since no correlations can be drawn to the satisfaction, it implies that under reaction conditions catalysts are probably undergoing changes those alter the catalyst properties. THF extracted products were identified using GC-FID and GC-MS (Figures 3A.5, 3A.6) and it was found out that most of the products are aromatic monomers having m/z of 152-220 gmol^{-1} .

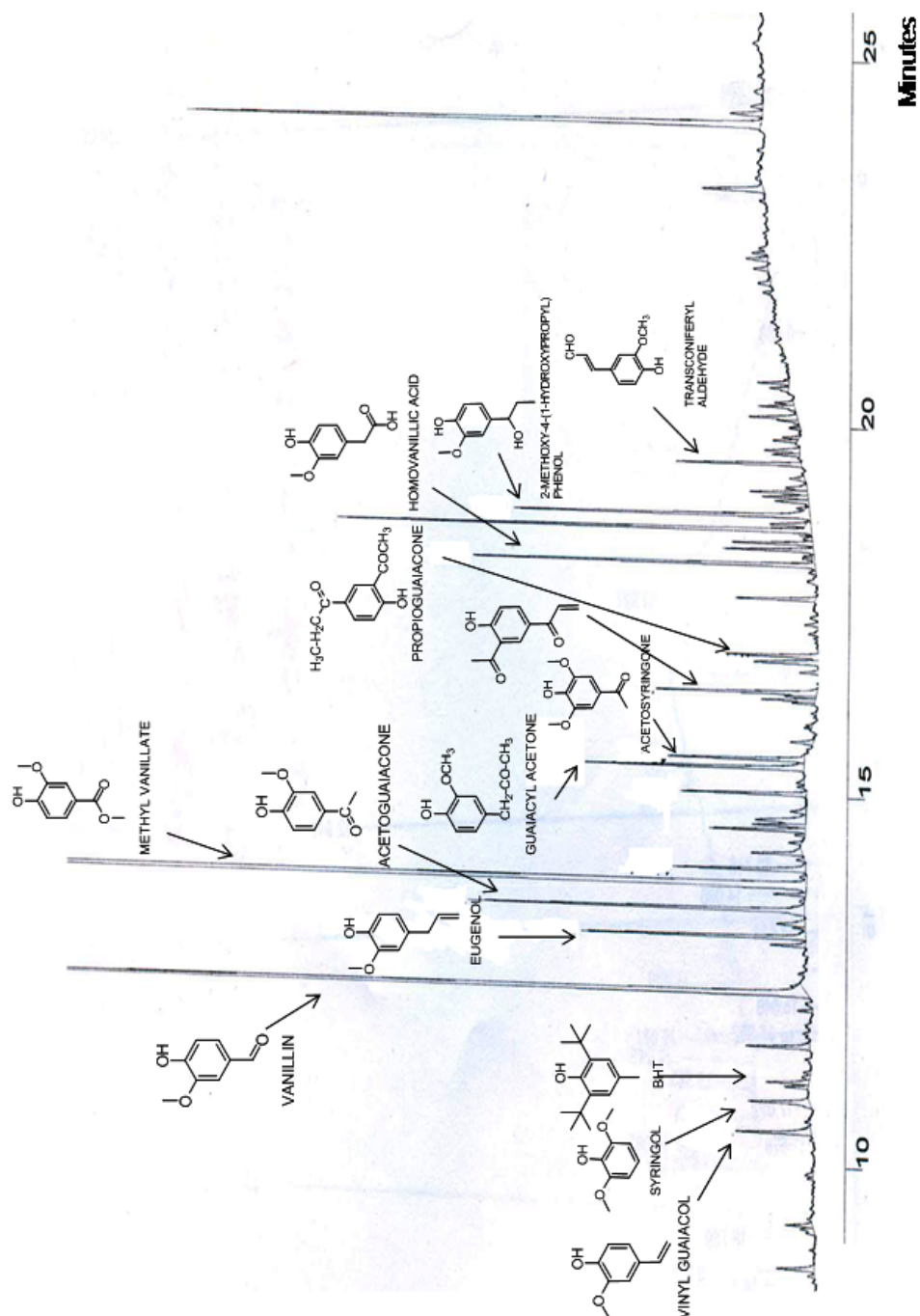


Figure 3A.5. GC-MS of THF soluble products obtained in dealkaline lignin reaction.

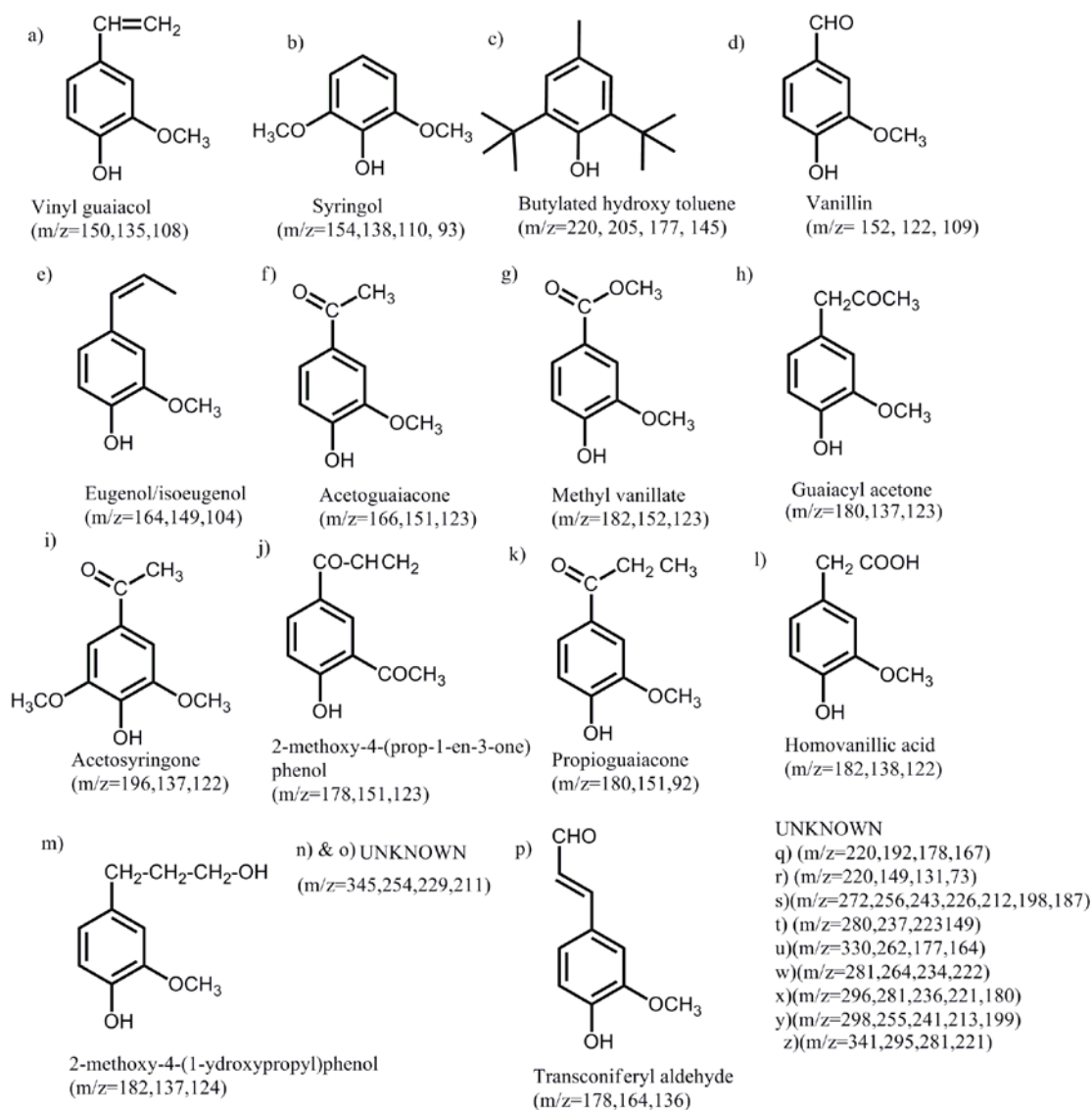


Figure 3A.6. Products in the THF soluble mixture of dealkaline lignin reaction identified using GC-MS analysis.

3A.3.2. Confirmation of aromatic monomers formation

3A.3.2.1. GC-FID, GC-MS, HPLC, LC-MS

The primary characterization of organic solvent soluble products (aromatic monomers) was done using GC-FID and GC-MS techniques. But, there might be a possibility of breaking down the lignin derived organic solvent (THF) and reaction solvent ($\text{H}_2\text{O}:\text{CH}_3\text{OH}$ (1:5 v/v) soluble oligomeric products during GC-FID and GC-MS analysis into aromatic monomers (as temperatures used for analysis are higher than the reaction temperature, refer section 3A.2.3.1 and 3A.2.3.3 for GC-FID and

GC-MS).²² To nullify this effect, samples were analyzed by HPLC and LC-MS techniques (refer section 3A.2.3.4 and 3A.2.3.5). HPLC profile obtained for reaction mixture is presented in Figure 3A.7a. The products observed in HPLC analysis are similar to those identified using GC-FID and GC-MS techniques (Figure 3A.7b). But peaks for few of the aromatic monomers are found to be overlapping in HPLC analysis (Figure 3A.7a). Also from LC-MS analysis it was confirmed that oligomeric products were not formed instead only aromatic products can be observed after the depolymerization reaction of dealkaline lignin over solid acid catalysts.

Further, GC-FID analysis was also carried out at lower temperatures than the reaction temperature (250 °C), to see the effect of temperature on the decomposition of any oligomeric species. Oven program used was, 100 °C (hold time, 4 min.) → 5 °C min⁻¹ ramp rate → 150 °C (hold time, 2 min.) → 5 °C min⁻¹ ramp rate → 200 °C (hold time, 10 min.), injector temperature (200 °C), detector temperature (200 °C) were used which were lower than the reaction temperature of 250 °C. During this study also similar peaks were observed when GC-FID and GC-MS was done under the normal conditions (refer section 3A.2.3.1, 3A.2.3.3).

These results imply that the majority of the products formed under the reaction conditions are aromatic monomers and under GC-FID and GC-MS conditions employed in this study, products do not undergo any degradation. Several literatures on lignin depolymerization reactions have shown the aromatic monomer products obtained which are in good correlation with the products shown here for solid acid catalysed reaction of lignin.^{7, 23}

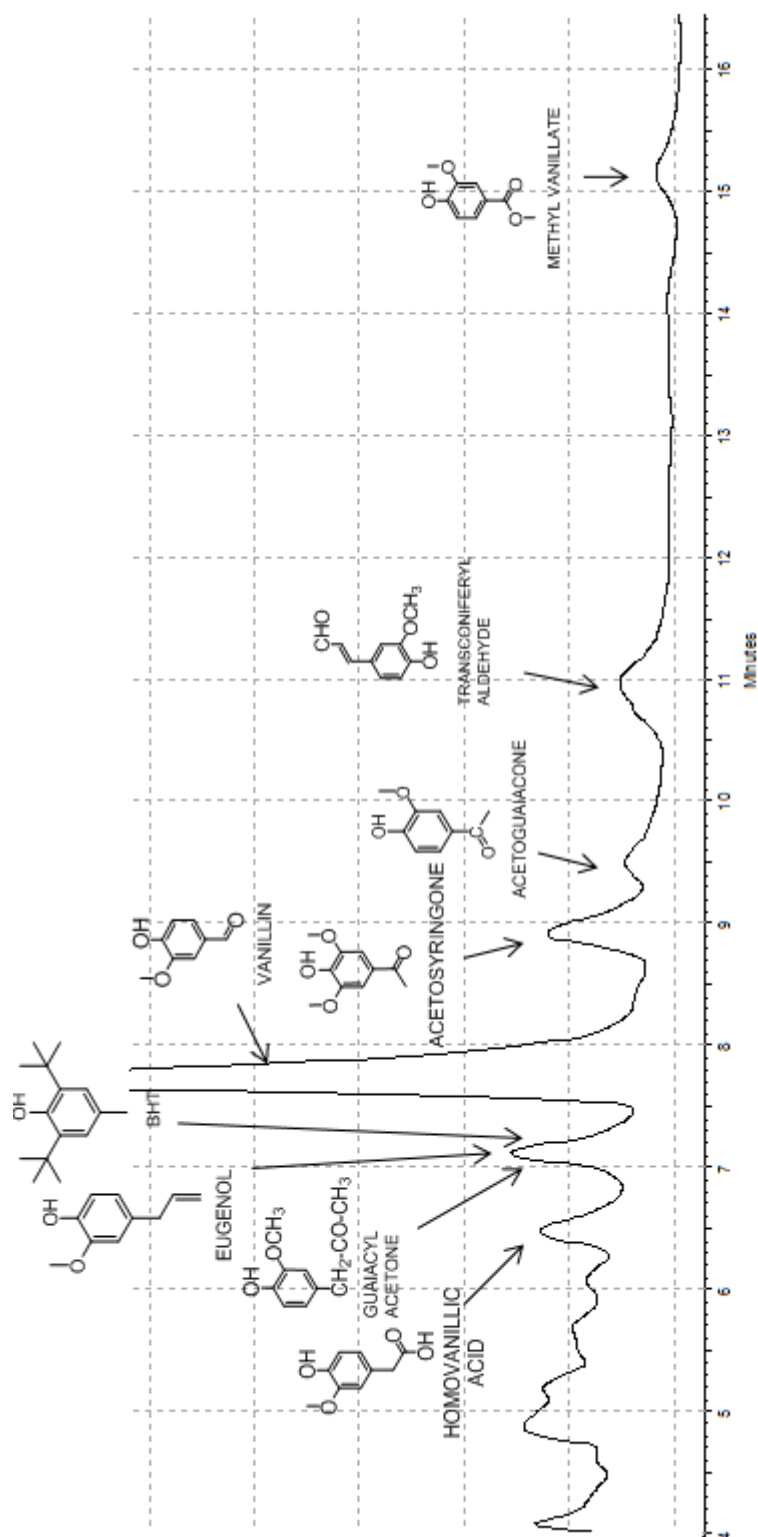


Figure 3A.7a. HPLC analysis of dealkaline lignin reaction mixture.

Reaction conditions: dealkaline lignin (0.5 g), SiO₂-Al₂O₃ (0.5 g), H₂O:CH₃OH (1:5 v/v), 250 °C, 30 min., 500 rpm, 0.7 MPa N₂ at RT.

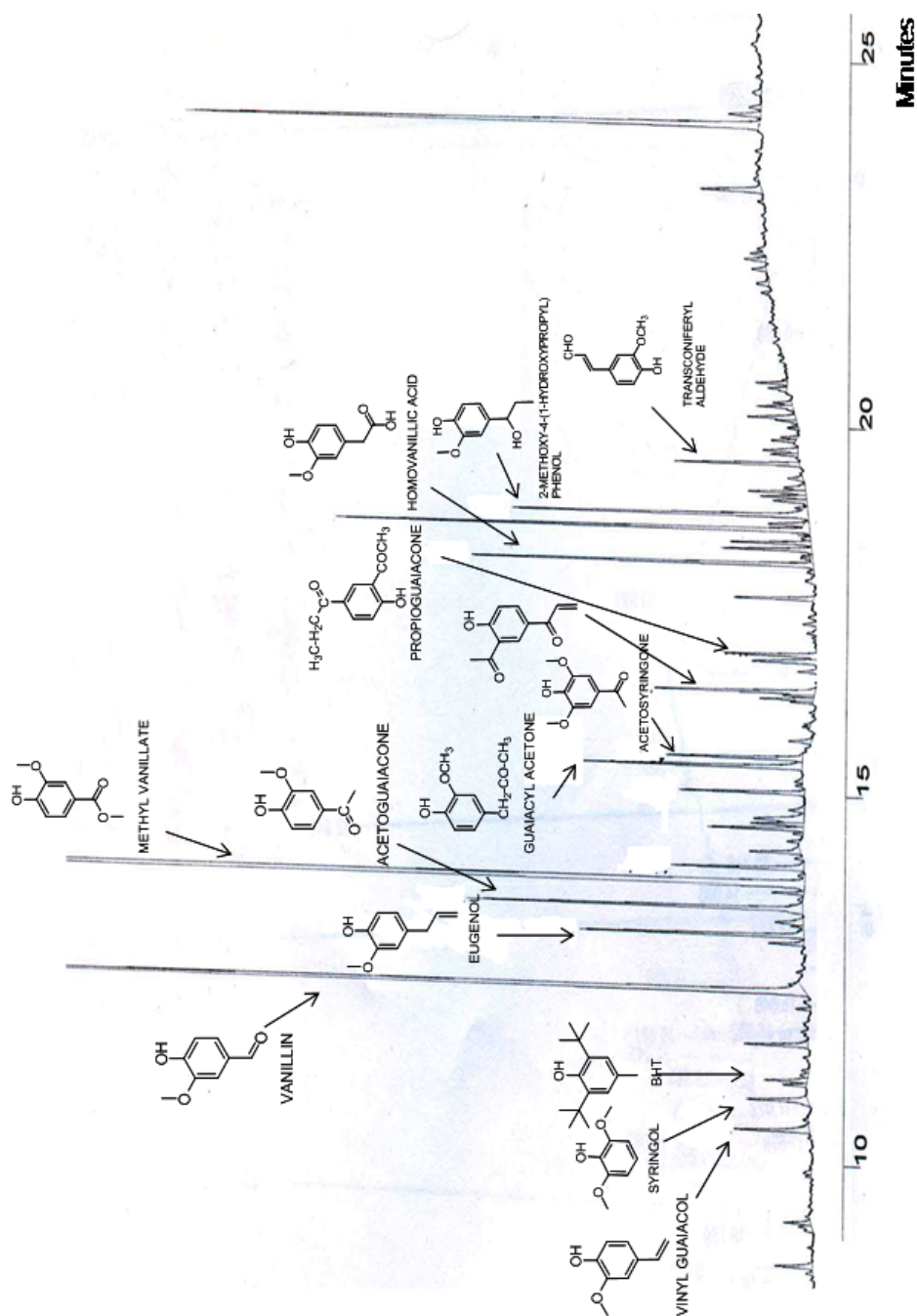


Figure 3A.7b. GC-FID analysis of dealkaline lignin reaction mixture.

Reaction conditions: dealkaline lignin (0.5 g), $\text{SiO}_2\text{-Al}_2\text{O}_3$ (0.5 g), $\text{H}_2\text{O}:\text{CH}_3\text{OH}$ (1:5 v/v), 250 °C, 30 min., 500 rpm, 0.7 MPa N_2 at RT.

3A.3.2.2. GPC and MALDI-TOF analysis

To confirm the formation of aromatic monomers and also to verify the status of the residual lignin (if any) GPC analysis was employed. In previous reports also researchers have used this technique to study the residual lignin and products obtained after depolymerization.²⁴⁻²⁵

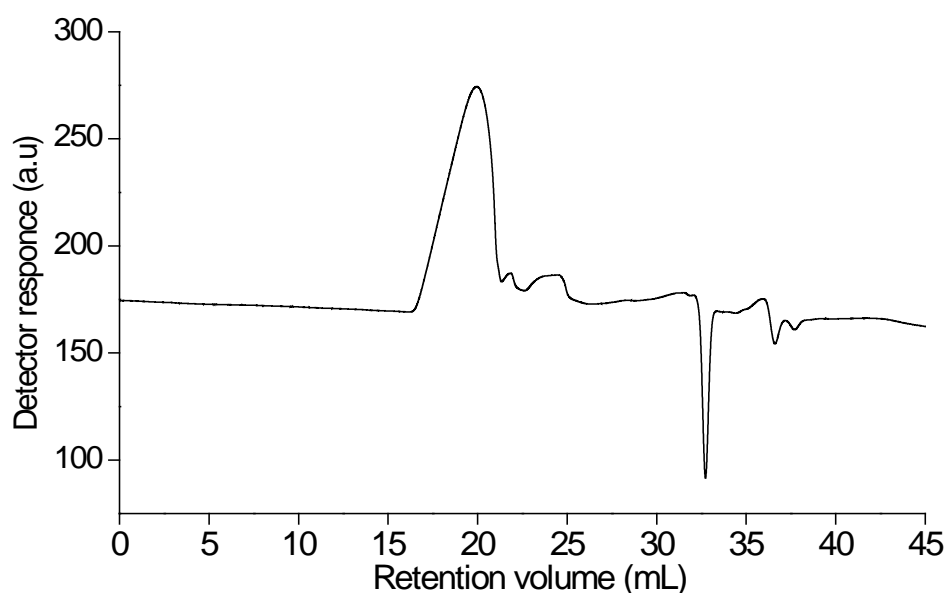


Figure 3A.8. GPC (DMF) for dealkaline lignin.

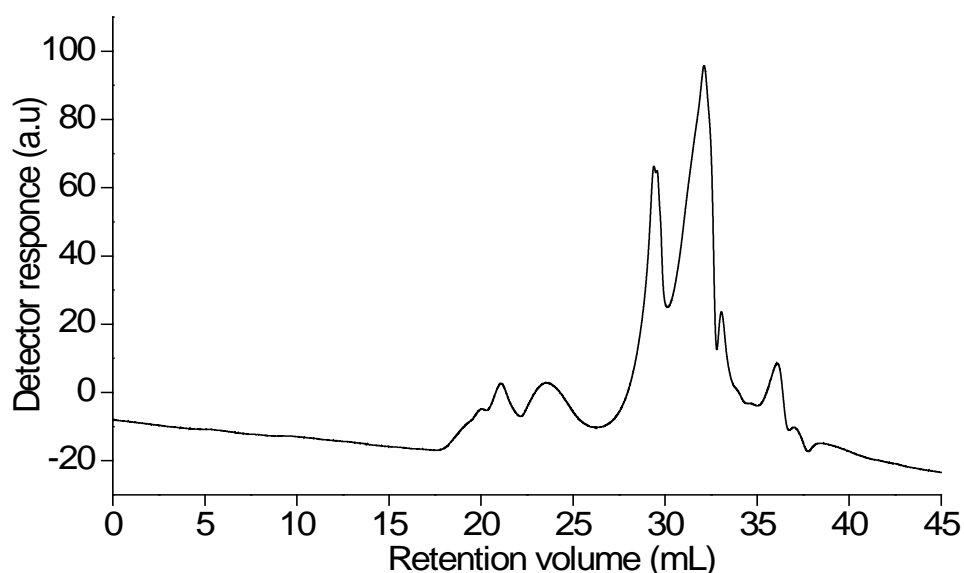


Figure 3A.9. GPC (DMF) for MeOH soluble reaction mixture.

GPC analysis was performed for three samples namely; dealkaline lignin, methanol soluble reaction mixture (dealkaline lignin reaction) and THF soluble products (dealkaline lignin reaction) (Refer section 3A.2.3.6). Dealkaline lignin dissolved in DMF was analyzed on DMF-GPC and a peak with a molecular weight of

ca. $60,000 \text{ gmol}^{-1}$ was observed indicating that high molecular weight (Figure 3A.8) of dealkaline lignin.

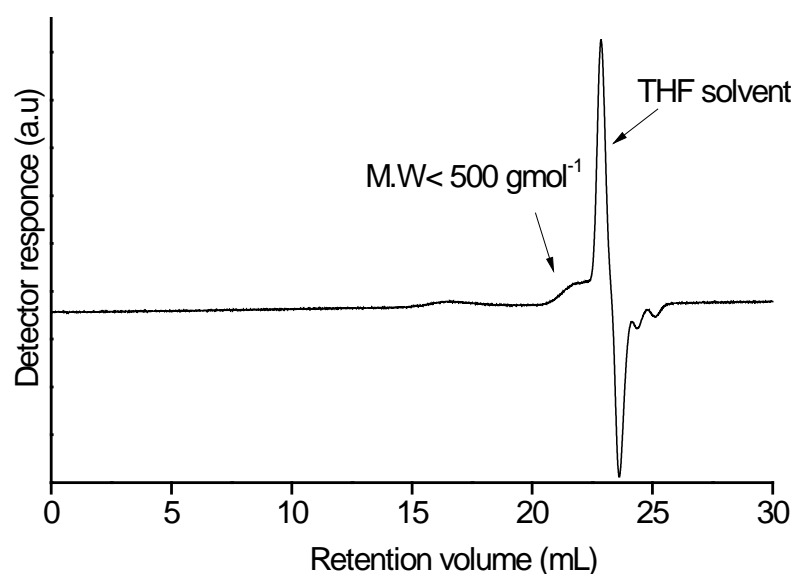


Figure 3A.10. GPC (THF) for THF soluble products.

MALDI-TOF analysis also showed an average molecular weight of $60,000 \text{ gmol}^{-1}$ (Refer chapter 2A, Figure 2A.1) for dealkaline lignin. In the case of methanol soluble reaction mixture (Figure 3A.9), peak was observed almost overlapping with the eluting solvent (DMF) peak and thus it is suggested that this peak must be arising due to presence of low molecular weight (ca. $< 500 \text{ gmol}^{-1}$) products. In the case of methanol soluble reaction mixture, there was no peak in the high molecular weight region which implies that the lignin is converted into products having low molecular weight. GPC study performed for THF soluble products also confirmed that there is no contribution from high molecular weight products (oligomeric species) in the THF soluble fraction (Figure 3A.10). Since, in this sample also the compounds were eluting along with the solvent (THF) indicates that the products have molecular weight $< 500 \text{ gmol}^{-1}$. In GPC analysis of methanol soluble reaction (Figure 3A.9) mixture and THF soluble products, compounds with a molecular weight ca. $< 500 \text{ gmol}^{-1}$ was observed, which can be well related with the unknown peaks observed in GC-MS with having molecular weight $300\text{-}600 \text{ gmol}^{-1}$ (Figure 3A.5). Therefore GC-FID, GC-MS, HPLC and LC-MS results are in good correlation with GPC results. To further confirm the products formed are aromatic monomers, methanol soluble reaction mixture and THF soluble products were also analyzed by MALDI-TOF technique to verify that no high molecular weight fragments ($1000\text{-}10,000 \text{ gmol}^{-1}$) are formed.

3A.3.2.3. CHNS elemental analysis and UV-Vis analysis

Elemental analysis of methanol + water soluble products showed presence of C (67 %) and H (6 %), this matches well with the elemental analysis of lignin (Refer chapter 2A, Table 2A.2; C = 65 % and H = 7 %, dealkaline lignin) indicating that almost no loss of any functional groups even after depolymerization reaction. However, slight increase in C content and reduction in H content implies that addition of carbon in the structure might be possible. The molecular formula thus calculated for products with the help of CHNS analysis, ($C_{9.5}H_{11}O_3$) almost matches with that for dealkaline lignin ($C_9H_{10.62}O_{2.89}S_{0.06}$). The absence of 'S' (containing functional group) in product (dealkaline lignin has 1 % presence of S, Refer chapter 2A, Table 2A.2) can be due to either adsorption of it on catalyst or it ('S' containing product) is insoluble in THF solvent in which products are extracted. Therefore CHNS analysis showed that no functional groups are lost during depolymerization.

To further prove that in this work mainly aromatic monomers are formed as products, UV-Vis spectroscopy analysis of the THF soluble products was done.

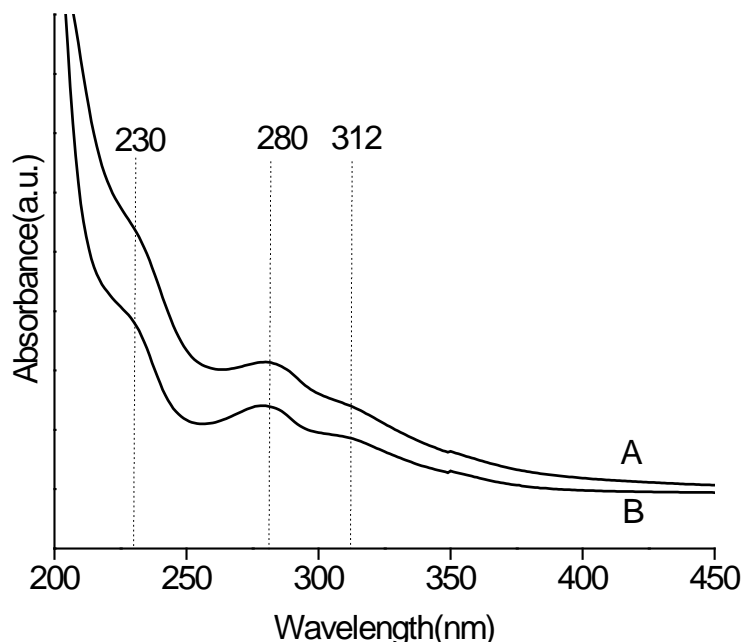


Figure 3A.11. UV-Vis analysis of (A) dealkaline lignin in methanol (B) THF soluble products (THF soluble solid was redissolved in methanol).

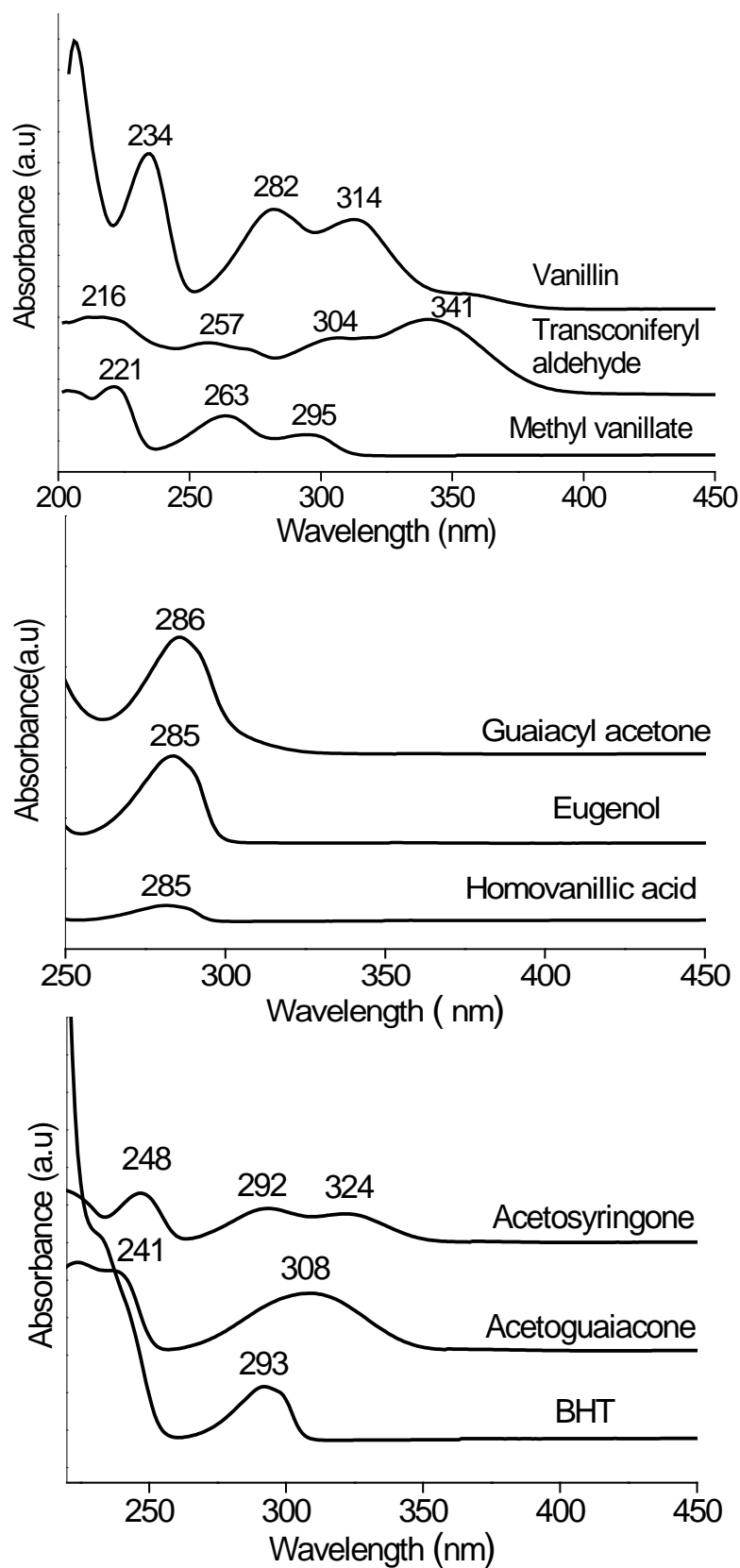


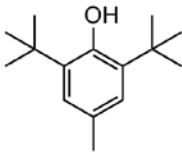
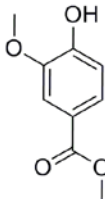
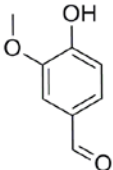
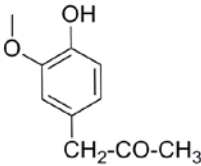
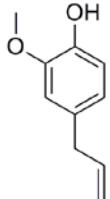
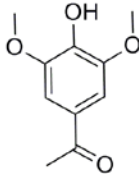
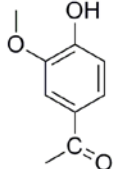
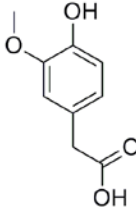
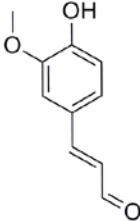
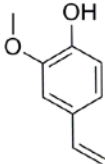
Figure 3A.12. UV-Vis analysis of standard compounds of aromatic monomer products of dealkaline lignin depolymerization, dissolved in methanol.

It is known that absorption bands due to aromatics (such as benzene, phenol) appear between 200 and 350 nm because of π/π^* transitions. Figure 3A.11 shows the similar UV-Vis pattern for both lignin (dissolved in methanol) and reaction mixture (dissolved in methanol). Also the UV-Vis analysis of the standard compounds (procured commercially) representing the aromatic monomers obtained was carried out (Figure 3A.12). The results suggest that reaction mixture contains aromatic products as absorption bands in the range of 200–350 nm. It is also known that if polycyclic aromatic compounds are formed then absorption bands shifts to longer wavelengths (secondary bands can come after 300 nm. For e.g. in naphthalene band appears at ca. 340 nm). Since in the reaction mixture it is not possible to see absorption bands at such a higher wavelength it is assumed that only aromatic monomers are formed. Although, it would be very difficult to come to any tangible conclusion based on mere UV-Vis analysis since many parameters (conjugation, electron withdrawing/donating groups, solvent effect etc.) play a role in deciding location of absorption bands. UV-Vis spectroscopy analysis of the THF soluble products was done but since it is a complex mixture of similar type of aromatic monomers, this technique was not quite suitable for the identification of exact products formation.²⁶

3A.3.3. Quantification of aromatic monomers

The products obtained with all the catalysts remained almost same nonetheless the quantity obtained was altered. To quantify the formation of aromatic monomers GC-MS identified aromatic compounds were commercially procured and were injected on GC-FID and GC-MS to draw calibration curves. From the calibration curve drawn ca. 90 % of THF soluble products were quantified as aromatic monomers (Table 3A.1) in the depolymerization of dealkaline lignin using H-USY catalyst. This information confirms the fact that oligomeric products formed do not contribute > 10% of total yields. Moreover, besides matching the retention times (of standards and THF soluble products obtained in reaction) on GC-FID and GC-MS (Figure 3A.5), the fragmentation patterns obtained in GC-MS for THF soluble products were also matched with the commercially procured samples.

Table 3A.1. Quantification of monomeric products in dealkaline lignin reaction

Compounds identified	Quantity	Compounds identified	Quantity
 BHT	2 %	 METHYL VANILLATE	8 %
 VANILLIN	30 %	 GUAIACYL ACETONE	24 %
 EUGENOL	1 %	 ACETOSYRINGONE	2 %
 ACETOGUAIACONE	3 %	 HOMOVANILLIC ACID	10 %
 TRANSCONIFERYL ALDEHYDE	6 %	 VINYL GUAIACOL	3 %

Reaction conditions: dealkaline lignin (0.5 g), SiO₂-Al₂O₃ (0.5 g), H₂O:CH₃OH (1:5 v/v), 250 °C, 30 min., 500 rpm, 0.7 MPa N₂ at RT.

3A.3.4. Correlation between lignin and aromatic monomers structures and functional groups

3A.3.4.1. FTIR analysis

In literatures it was observed that IR technique was employed to study the structural changes happening in lignin after depolymerization. In order to arrive at a correlation between the structure of starting material (lignin) and aromatic monomers formed FTIR analysis of dealkaline lignin and THF soluble products was performed. As observed from Figure 3A.13, the dealkaline lignin showed an intense peak at 1118 cm^{-1} for C-O stretch assigned to alcohols, esters and ethers.²⁷⁻²⁹ Based on the structure of lignin these peaks can be assigned to ether and alcohol groups. In the range of $700\text{--}850\text{ cm}^{-1}$ peak due to aromatic C-H “oop” are expected. The peaks at 1022 and 1265 cm^{-1} can be assigned to C-O stretch in alkoxy functional group. The peaks for -OH in phenol can also appear in the range of $1150\text{--}1250\text{ cm}^{-1}$. Typically, from $1450\text{--}1600\text{ cm}^{-1}$ multiple peaks for C=C stretch in aromatics (in ring) are observed and in the spectrum for dealkaline lignin peaks could be seen at 1455 and 1595 cm^{-1} with several other weak peaks. Observance of peak at 1690 cm^{-1} can be due to C=O stretch in α,β unsaturated aldehyde or ketone. IR spectrum for THF soluble products (Figure 3A.13) showed peaks due to C-H bending “oop” in the range of $700\text{--}850\text{ cm}^{-1}$. In the spectrum for THF soluble products the intensity of peaks at 1022 and 1265 cm^{-1} due to alkoxy groups has increased indicating an increase in -OCH₃ groups in products after lignin depolymerization. The retention of peak at 1107 cm^{-1} though with lower intensity indicates that the few of the products still have ether bonds or alcohol groups. Based on the results obtained in my work, I suggest that this peak is mainly due to alcoholic groups. Appearance of peak at 1372 cm^{-1} due to sp³ C-H bending/rock implies showed the presence of alkyl groups. The intensities of the peaks from 1450 to 1600 cm^{-1} again emphasize that the aromatic nature is intact in the products. A very intense peak at 1708 cm^{-1} can be assigned to C=O stretch in α,β unsaturated aldehydes (or ketons). The new peak appearing at 2852 cm^{-1} is attributed to the presence of C-H stretch in aldehyde group. Moreover, another peak at 2924 cm^{-1} can be due to C-H stretch in alkanes/alkyl groups. Broad peak observed at 3395 cm^{-1} confirmed the presence of Ar(C)-OH bond which is formed by the cleavage of Ar(C)-O-Ar bonds in dealkaline lignin. Overall, it can be clearly seen that increase in the intensities for peaks of -OCH₃, -CHO and -CH₃ groups and decrease in the intensity

for ether bond ($1118\text{-}1107\text{ cm}^{-1}$) explains that lignin undergoes depolymerization reaction and gives rise to monomers which have functional groups as mentioned above.²⁷ Similar results were observed in the case of all other lignins (organosolv, alkali, ORG, EORG and bagasse lignin). Table 3A.1 summarizes the products formed in dealkaline lignin depolymerization reaction (from GC-MS, LC-MS) with different functional groups which is in good correlation with the IR data.

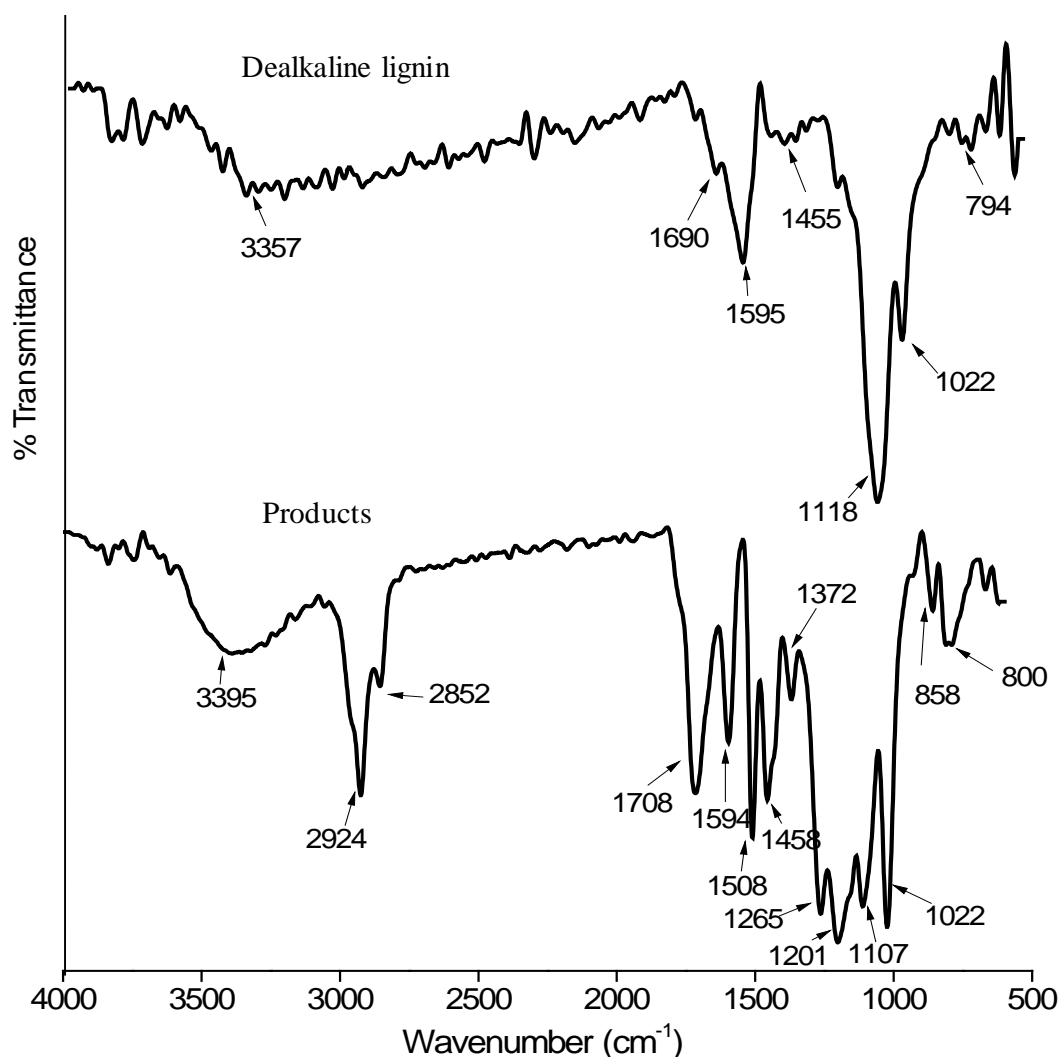


Figure 3A.13. FTIR of dealkaline lignin and products.

3A.3.4.2. ^1H and ^{13}C NMR analysis

^1H and ^{13}C NMR study (700 MHz, refer section 3A.2.3.7) was performed to study more about the presence of functional groups in dealkaline lignin and THF soluble products obtained after depolymerization. ^1H NMR spectra for both, dealkaline lignin and products are presented in Figure 3A.14. As seen, most of the peaks present in

lignin are retained in the products however, with variation in the intensities. Peaks for primary, secondary and tertiary alkyl groups are observed around 0.8-1.70 ppm [Ar-C(CH₃)₃ proton at 1.4 ppm] in both dealkaline lignin and THF soluble products.³⁰⁻³² Appearance of peak at 2.06, 2.16 and 2.56, 2.61 ppm can be assigned to the proton α to carbonyl group (Ar-CO-CH₃) or benzylic proton (Ar-CH₃) or ester (Ar/R-CH₂-COOR/Ar) groups. Ester groups can be observed (Ar/R-COO-CH₂R/Ar) at 3.9 ppm.³² A new peak present in products at 3.71 ppm is due to the substitution of -O-CH₃ in the aromatic ring. Peaks due to aromatic protons are appearing between 6.5-8.5 ppm. The intensity of the peak corresponding to aldehydic protons (9.67 and 9.74 ppm) was found to be increased in products compared to dealkaline lignin.³¹ Increase in the intensity of methoxy groups and aldehyde groups peaks observed in ¹H NMR analysis is in line with the IR data and eventually confirms products listed in Table 3A.1 formed after depolymerization of lignin.

¹³C NMR spectra recorded for both, dealkaline lignin and products are presented in Figure 3A.15. As observed, all the peaks observed in lignin sample are retained in the products also, which indicates that the overall structure of lignin (and substituents) is retained after depolymerization. At 20-50 ppm CH₃CO- species or R₃CH species can be observed.³³⁻³⁴ Observance of peaks at 55-90 ppm is assigned to sp³ carbon appearing next to oxygen (Ar/R-CH₂-O-; Ar₂/R₂-CH-O-; Ar₃/R₃-CO-).³⁴³⁵ It is also discussed that between 30-60 ppm, peak due to -C(CH₃)₃ can be observed. In the case of products a new peak was observed at 54.02 ppm in ¹³C NMR, which is similar to the peak observed at 3.7 ppm in ¹H NMR for the same sample. Both these peaks correspond to the formation of -O-CH₃ groups in products formed after depolymerization of dealkaline lignin.

Peaks due to sp² carbon (C=C, 110-150 ppm) in aromatics (125-150 ppm) and alkenes (110-140 ppm) are clearly visible in both the spectra. In ¹³C NMR of dealkaline lignin at 175-180 ppm peaks due to ester groups (Ar/R-CO-R/Ar) can be observed and it is found that in products the intensity of these peaks was reduced. This is obvious because during lignin depolymerization these ester bonds are cleaved. At the same time peak intensity for 192-193 ppm due to aldehyde (Ar/R-CO-H) is found to be increased in products compared to lignin. These observations also align well with the ¹H NMR and IR data. The absence of peak at 167.34 ppm in products

corresponding to ester groups indicate that under reaction conditions breaking of C-O bond is possible.

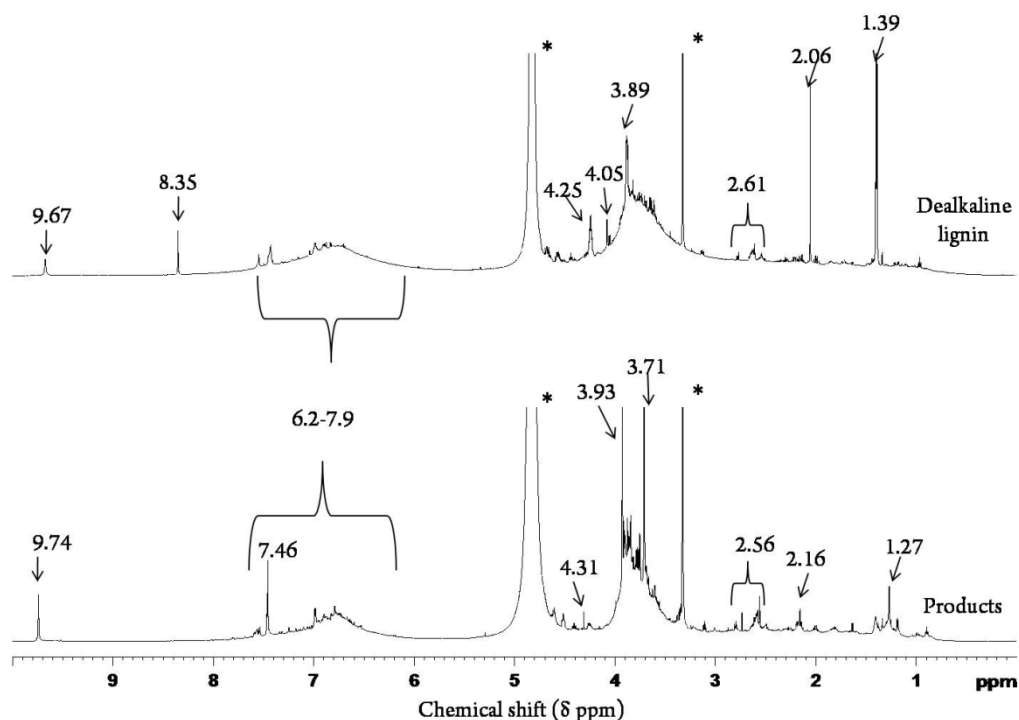


Figure 3A.14. ^1H NMR of dealkaline lignin and products (*Peaks due to solvent).

It is important to bring attention to the fact that in GC, HPLC (Figure 3A.7) analysis also similar types of compounds are detected (Table 3A.1). Few small peaks present in NMR spectra must be arising from various substitutions on aromatic rings (lignin and products) but due to complex structure of lignin it would be very difficult to assign all the peaks (due to varying environment chemical shifts will vary). Similar results were obtained for all other lignins (organosolv, alkali, ORG, EORG and bagasse lignin). All these studies helped to establish the fact that the few functional groups present in lignin and its aromatic nature is retained in products and identification of products can be achieved with the help of IR and NMR spectroscopic techniques along with GC-FID, GC-MS, HPLC and LC-MS characterizations. Additionally, it is confirmed that due to cleavage of several linkages in lignin (ether, C-C) products have higher number of hydroxyl (-OH) and methoxy (-OCH₃) groups. It is also important to note here that insertion of these groups is possible since solid acid catalysts are known to catalyse hydrolysis and methanolysis reactions.

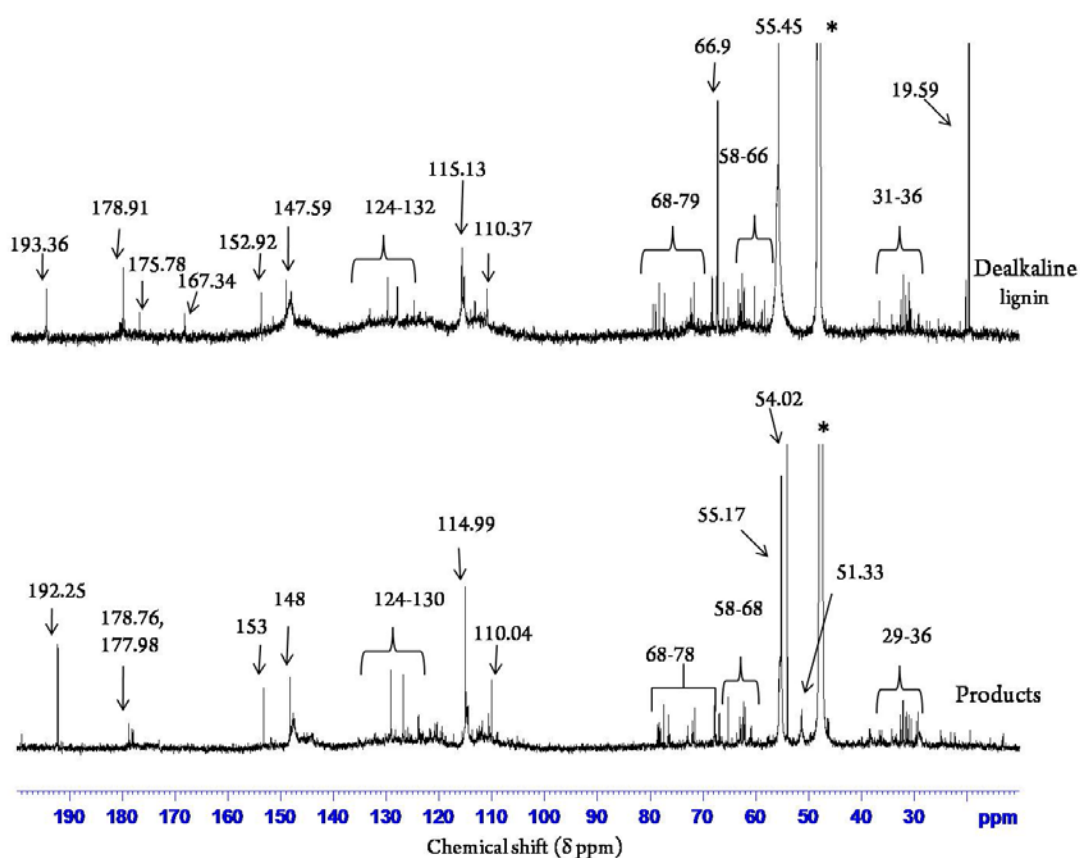


Figure 3A.15. ^{13}C NMR of dealkaline lignin and products (*Peaks due to solvent).

Under the reaction conditions (250 °C, 30 min., 500 rpm, 0.7 MPa N_2 at RT) formation of BHT (Butylated hydroxy toluene, Table 3A.1), an aromatic monomer having tertiary butyl groups was observed. IR (1372, 2924 cm^{-1}), ^1H NMR (1.39 ppm) and ^{13}C NMR (30-60 ppm) data suggest the formation of this compound in the products. The mechanism behind the formation of BHT from lignins was not completely understood, but based on earlier reports the formation of BHT after lignin depolymerization can be possible and also show that this product is stable under the reaction condition.³⁶⁻³⁹ Stability of BHT at 250 °C (30 min., 500 rpm, $\text{SiO}_2\text{-Al}_2\text{O}_3$) and it was observed that only < 5 % BHT undergoes conversion to yield unknown products (not detected on GC-FID) indicating that the product is stable under the reaction conditions.

Therefore it is concluded that in the methodology described here for lignin depolymerization using solid acid catalysts, the products retain the characteristics of lignin substrate molecule. However, it should be noted here that though most of the products are identified as aromatic monomers from various techniques employed in this work, still it is difficult to assess the exact structure, since most of the products

have two or more substituents in the aromatic ring and hence there is a possibility of formation of isomers (which are difficult to separate on GC-FID or GC-MS or HPLC or LC-MS and identify from fragmentation profiles and spectroscopic techniques).

3A.3.5. Analysis of gases and reproducibility of catalytic activities

To check whether under reaction conditions any gaseous products are formed, the gas released from the reactor was analyzed (online sampling was done) using GC-TCD (refer section 3A.2.3.2). However, gaseous products like CO, CO₂, CH₄, H₂, C₂-C₄ were not detected. These observations indicate that the lignin conversion reactions are selective towards the formation of aromatic monomers. Interestingly, in all the reactions 90 ± 10 % (wt. basis) mass balance (refer section 3A.5) was obtained. To check the reproducibility of results, care was taken to carry out all the reactions for 2 or 3 times. An error of ± 3 % was observed in obtaining the THF soluble products (wt. basis) and the peak intensities and areas under the peak were also within the analysis limits of ± 4 %. These results prove that under reaction conditions employed (250 °C; 30 min; water:methanol, 1:5 v/v, 30 mL) to depolymerize dealkaline lignin having 60,000 gmol⁻¹ molecular weight, solid acid catalysts can yield aromatic monomers with 25-60 % yield.

3A.3.6. Comparison of catalytic activities between solid acids and homogeneous acids

The activity of solid acid catalysts in the depolymerization of lignin was compared with homogeneous acids like HCl and H₂SO₄ under similar reaction conditions (with an initial pH of 2; 250 °C; 30 min; water:methanol = 1:5 v/v, 30mL) and ca. 29 % and 39 % of THF soluble products was observed respectively for HCl and H₂SO₄. But the THF soluble products obtained in the homogeneous acid catalysed reactions were not all aromatic monomers, which were confirmed by GC-FID and GC-MS analysis (Figure 3A.16). Few products with m/z value 152, 166 corresponding to aromatic monomers, were also observed in the non catalytic reaction. Along with this, m/z values of 220, 252, 234, 270 which corresponds to higher molecular weight fragments were also observed. So it can be concluded that homogeneous acids like HCl or H₂SO₄ depolymerizes dealkaline lignin to give mainly dimers or oligomers as

products, instead of giving aromatic monomers as major products under the above reaction conditions.

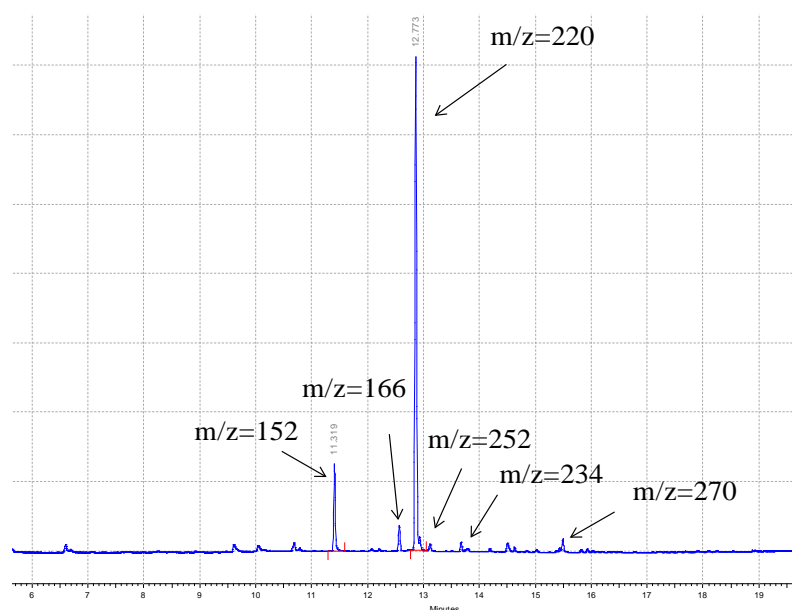


Figure 3A.16a. GC-MS analysis of HCl catalyzed depolymerization of dealkalinized lignin. Reaction conditions: dealkalinized lignin (0.5 g), Acid (pH = 2), H₂O:CH₃OH (1:5 v/v), 250 °C, 30 min., 500 rpm, 0.7 MPa N₂ at RT. Products are extracted in THF solvent.

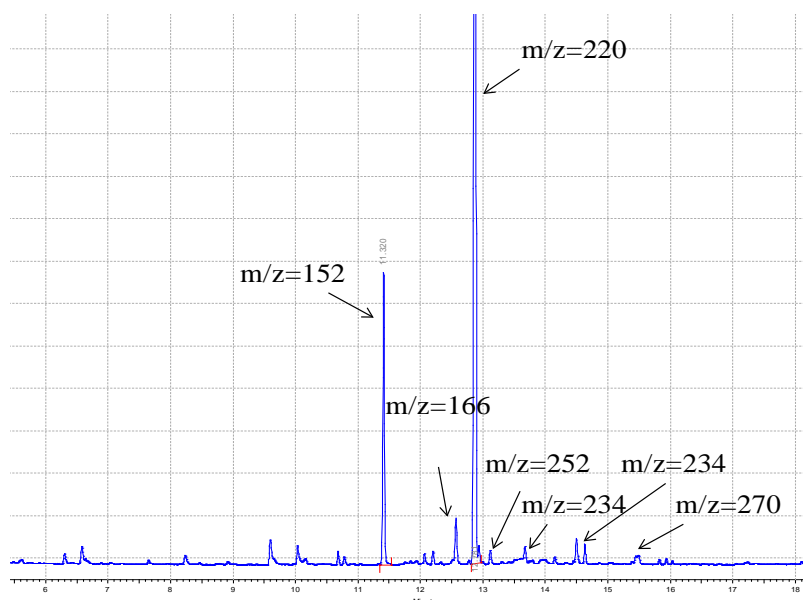


Figure 3A.16b. GC-MS analysis of H₂SO₄ catalyzed depolymerization of dealkalinized lignin. Reaction conditions: dealkalinized lignin (0.5 g), Acid (pH = 2), H₂O:CH₃OH (1:5 v/v), 250 °C, 30 min., 500 rpm, 0.7 MPa N₂ at RT. Products are extracted in THF solvent.

3A.3.7. Correlation between the acidity and the activity of solid acid catalysts in dealkaline lignin depolymerization reaction

From the dealkaline lignin reaction it was observed that in the category of zeolites (H-USY (Si/Al = 15), H-BEA (Si/Al = 19), H-ZSM-5 (Si/Al = 11.5) and H-MOR (Si/Al = 10)). H-USY was giving maximum amount of aromatic monomers (60 %). To study why among the solid acid catalysts, H-USY was giving the higher amount of aromatic monomers; a plot was drawn with total acid sites in zeolites against the % of aromatic monomers formed in dealkaline lignin reaction (Figure 3A.17). A regular trend was observed (Figure 3A. 17) (if neglect H-BEA), as total number of acid sites increases the activity of the catalyst to form aromatic monomers is decreased. H-MOR having the highest amount total acid sites (1.15 mmol g^{-1}) gave only 40 % aromatic monomers and H-ZSM-5 having only 0.98 mmol g^{-1} of total acid sites, as expected gave 55 % of aromatic monomers. H-USY having the least amount of total acid sites (0.55 mmol g^{-1}) gave the highest amount of aromatic monomers (60 %).

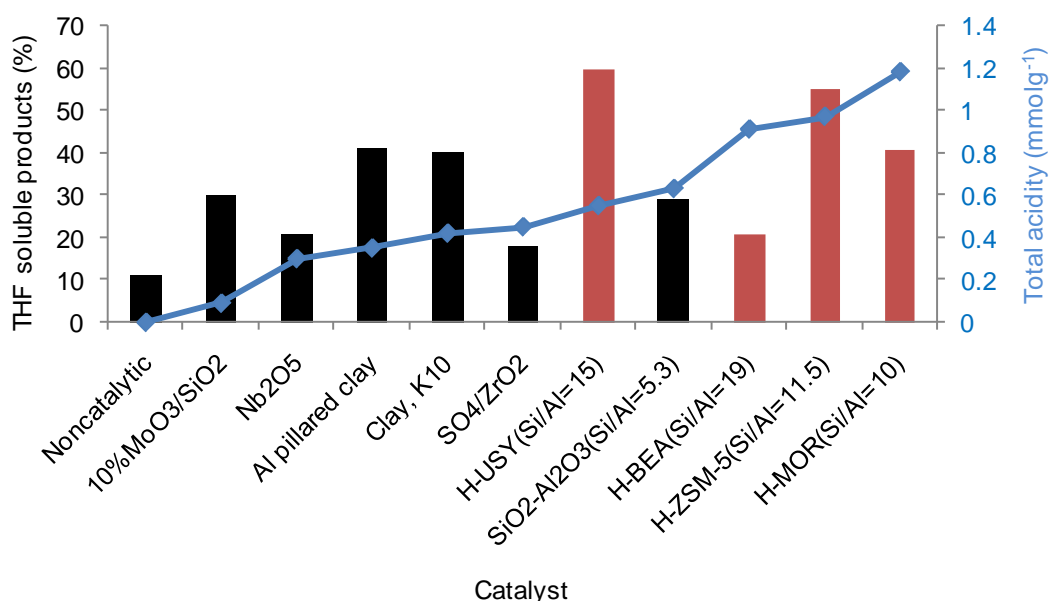


Figure 3A.17. Correlation of the formation of aromatic monomers in dealkaline lignin depolymerization with the total acid sites of solid acid catalysts. Reaction conditions: dealkaline lignin (0.5 g), catalyst (0.5 g), H₂O:CH₃OH (1:5 v/v), 250 °C, 30 min., 500 rpm, 0.7 MPa N₂ at RT. Products are extracted in THF solvent.

H-BEA zeolite was having an acid amount (0.91 mmol g^{-1}) similar to H-ZSM-5, but gave only 21 % of aromatic monomers. This was expected, since XRD and ²⁹Si and ²⁷Al NMR of H-BEA zeolite showed a complete structural collapse of this catalyst

after the reaction. It was also observed during workup of a reaction that the amount of coke and char formation (based solid deposited on the catalyst) was found to be increased when the catalyst was having higher amount of total acid sites. Therefore as the amount of total acid sites increases the selectivity towards the formation of aromatic monomers was reduced.

3A.3.8. Study on reuse, stability and characterization of H-USY catalyst

Amongst all the solid acid catalysts evaluated in the depolymerization of dealkaline lignin reaction since H-USY catalyst gave (Figure 3A.4) the highest aromatic monomers formation (60 %), further studies were done with this catalyst. To test the stability of catalyst H-USY, recycle studies were done after washing the catalyst recovered from earlier run with water:methanol (1:5 v/v, 60 mL) and then drying it (at 60 °C, overnight in drying oven) and further calcine it at 550 °C for 10 h in air.

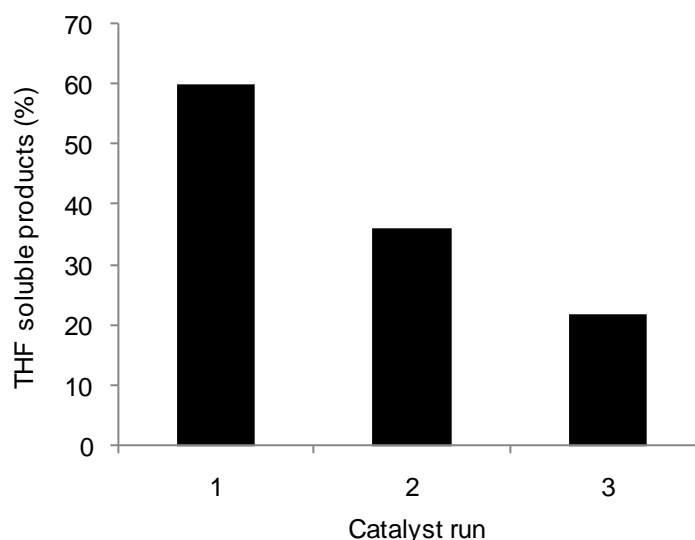


Figure 3A.18. Recycle study H-USY catalyst in dealkaline lignin reaction. Reaction conditions: dealkaline lignin (0.5 g), catalyst (0.5 g), H₂O:CH₃OH (1:5 v/v), 250 °C, 30 min., 500 rpm, 0.7 MPa N₂ at RT. Products are extracted in THF solvent.

In the 1st run THF soluble products yield was 60 %, which was decreased to 36 % in the 2nd run and in the 3rd run the catalyst gave only 22 % yield thereby showing a drastic decrease in the activity of the catalyst (Figure 3A.18). This decrease in the catalytic activity can be expected, since dealkaline lignin contains ca. 29 mg of Na (per 1 g of lignin) which can possibly poison the Brönsted acid sites present in the H-

USY catalyst. In this way activity of the solid acid catalyst in each successive runs was prone to decrease.

To check this hypothesis, fresh and spent H-USY catalysts were subjected to NH_3 -TPD study. The results indicate that compared to 0.55 mmol g^{-1} acid amount present in fresh catalyst, spent catalyst showed 0.05 mmol g^{-1} of acid amount. Moreover, complete loss of strong acid sites was observed in spent catalysts (Figure 3A.19). This result was in line with the consideration that Na may poison the catalytically active site (Figure 3A.20). For the investigation on whether this loss of acid sites was due to Na contamination, fresh and spent catalysts were subjected to ICP-OES characterization. The results indicate (Table 3A.2) that on spent catalyst (19 mg) higher amount of Na was present compared to fresh catalyst (0.46 mg). A quick calculation suggests that with increase in Na content by 18.54 mg (0.8060 mmol) on spent catalyst, it is capable of killing all the acid sites. Again this information helps in suggesting that possible contamination of acid sites by Na might be the reason behind loss in activity.

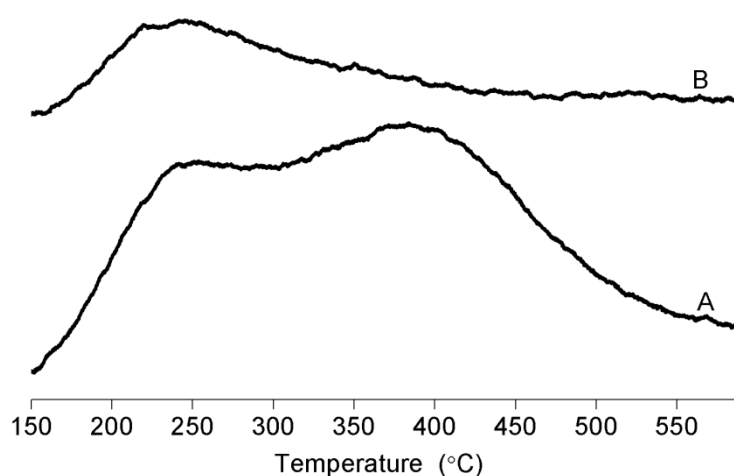


Figure 3A.19. NH_3 -TPD analysis of H-USY (Si/Al=15) A) fresh B) spent.

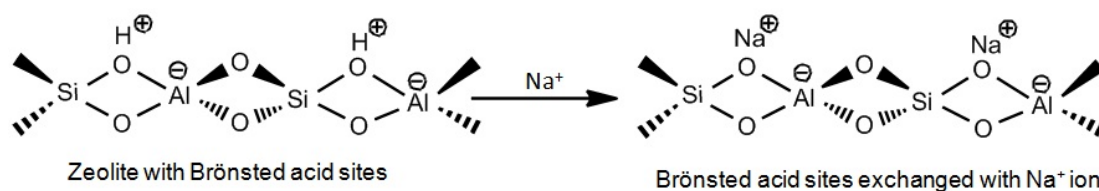


Figure 3A.20. Metal exchanged Brønsted acidic sites of zeolites with metal (Na^+) ion.

Table 3A.2. ICP-OES study of fresh and spent H-USY (Si/Al = 15) zeolite

H-USY (Si/Al = 15)	Si/Al ratio Actual	Si/Al ratio Obs.	Na content (mg/0.5 g catalyst)
Fresh	15	14.7	0.46
Spent	--	14.2	19

To study about the catalyst poisoning, metal-exchange study for H-USY (Si/Al=15) catalyst was carried out at 60 °C using 240 ppm of Na concentration.⁴⁰ It should be noted here that on 1 g of lignin in 60 mL solvent contain 29 mg of Na is present which accounts for 480 ppm of Na, based on this calculation 1 g lignin in 60 mL solvent (H₂O:CH₃OH (1:5 v/v, 60 mL) was charged for the reaction (i.e. in reaction 480 ppm Na is charged). So for metal exchange study 240 ppm metal salt solution (50 % of actual) was used. Fresh and metal-exchanged catalysts were characterized by XRD, ICP-OES and NH₃-TPD analysis. XRD patterns of fresh and metal-exchanged catalysts showed no detectable change in the peak positions, which emphasizes the fact that just stirring of catalyst in water at 60 °C and after the metal exchange treatment, morphology of the zeolites was retained (Figure 3A.21). ICP-OES and NH₃-TPD data for fresh and metal-exchanged catalysts are presented in Table 3A.3. The presence of Na can be clearly seen on the catalyst after the metal exchange treatment however its concentration was too low (0.218 g). This might lead to decrease in the acid amount for treated catalysts. NH₃-TPD analysis revealed that in case of H-USY catalysts, acid amount decreased to 0.46 mmolg⁻¹ (0.06 mmolg⁻¹ weak acid sites and 0.40 mmolg⁻¹ strong acid sites) from 0.55 mmolg⁻¹ (fresh) after metal exchange study at 240 ppm. Therefore strong acid sites were reduced during metal exchange study. From this study it can be claimed that the presence of Na in lignin has an effect on catalyst deactivation. Contrary to these results however in lignin reaction work, a large decrease in acid amount was observed which points out to fact that under lignin reaction conditions (250 °C) along with catalyst poisoning by Na metal, some other changes are also happening to the catalyst due to which it loses acid sites. Subsequently, to check the theory of Na contaminating the acid sites, H-USY catalyzed depolymerization of organosolv lignin was carried out.

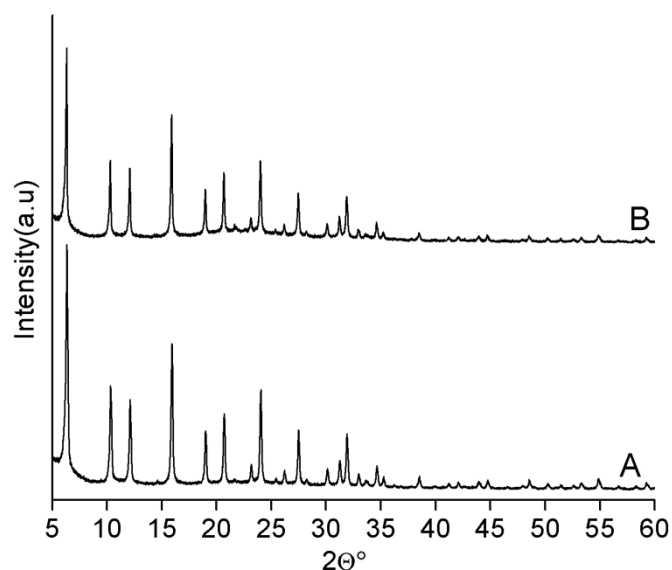


Figure 3A.21. XRD pattern of H-USY (Si/Al = 15) catalyst, A) fresh B) Na-exchanged.

Table 3A.3. NH₃-TPD and ICP-OES data for fresh and metal-exchanged catalysts

H-USY (Si/Al = 15)	NH ₃ -TPD		ICP-OES	
	Total acidity (mmol g ⁻¹)	Si/Al ratio Actual	Si/Al ratio Obs.	Na content (g/1 g catalyst)
Fresh	0.55	15	14.9	0.001
Spent	0.46	--	14.7	0.218

As observed from ICP-OES and SEM-EDAX analysis (Refer chapter 2A, Table 2A.3), organosolv lignin is free of Na and S contaminants and hence, it was expected that H-USY used in these reactions will show repeated activity in recycle runs (as there will be no poisoning of acidic sites by Na). But in these reactions also H-USY catalyst (recycled in a similar fashion as was done in case of dealkaline substrate) showed decrease in the catalytic activity in repeated runs by ca. 70 % (Figure 3A.22). ICP-OES analysis of spent H-USY catalyst was performed but could not find any increase in Na content on spent catalyst (0.46 mg or 15 ppm) compared to fresh catalyst (0.46 mg or 15 ppm). However, when spent catalyst from organosolv reaction was analyzed by NH₃-TPD technique decrease in acid amount was observed.

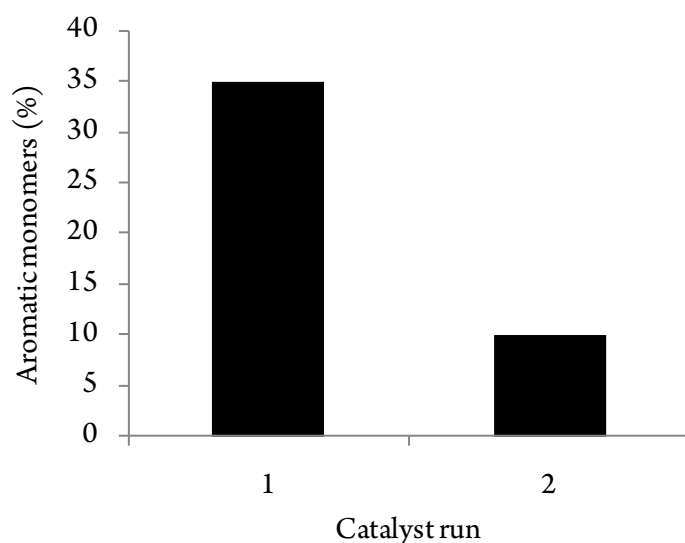


Figure 3A.22. Recycle study H-USY catalyst in organosolv lignin reaction.

Reaction conditions: organosolv lignin (0.5g), H-USY (0.5g), H₂O:CH₃OH (1:5 v/v), 250 °C, 30 min., 500 rpm, 0.7 MPa N₂. Products extracted using DEE.

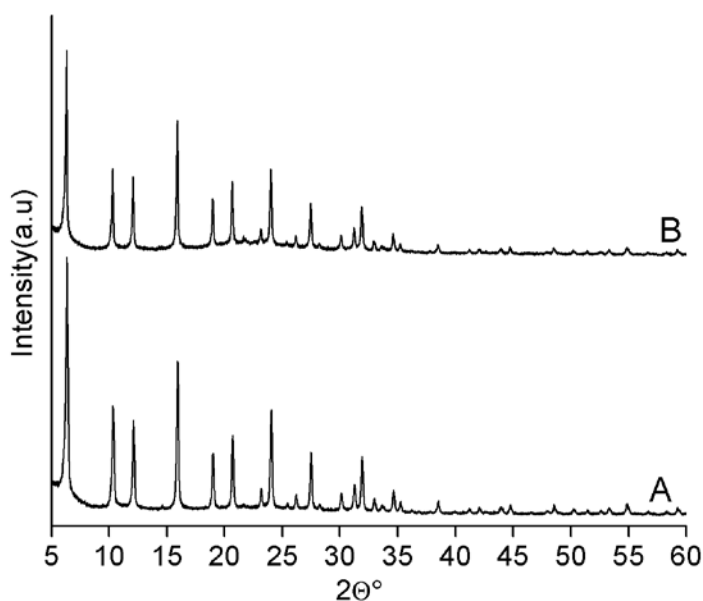


Figure 3A.23. XRD pattern of H-USY (Si/Al = 15) catalyst, A) fresh B) spent-calcined.

To understand then the reason behind the decrease in the activity, H-USY catalyst was characterized in detail using various techniques (XRD, ²⁹Si and ²⁷Al NMR and N₂ sorption study). XRD analysis of spent H-USY (Figure 3A.23) catalyst showed a slight decrease in the intensity of the peaks which implies that the crystallinity of a material has decreased slightly. ²⁹Si and ²⁷Al NMR spectra obtained

for fresh and spent catalysts (Figures 3A.24 and 3A.25) showed that environment around Si and Al has changed thus indicating that catalyst has undergone some structural deformation during the course of reaction. But from ICP-OES analysis of fresh and spent catalysts, the Si/Al ratio remained constant in both the samples (14.9 for fresh and 14.7 for spent). This implies that the catalyst, H-USY is undergoing some structural changes without the leaching of Si and Al. N₂ sorption studies (Table 3A.4) of the spent H-USY catalyst showed a reduction in the surface area of the catalyst from 873 m²g⁻¹ (fresh) to 303 m²g⁻¹ (spent), decrease in pore volume from 0.45 cm³g⁻¹ (fresh) to 0.14 cm³g⁻¹ (spent) and increase in pore diameter from 0.75 nm (fresh) to 1.51 nm (spent). All these characterizations support the fact that the structured solid acid catalysts (having definite pore and channel structure) like H-USY even though capable of giving a very high yield for aromatic monomers (ca. 60 %), are not stable under the reaction conditions.

Table 3A.4. N₂ sorption study of fresh and spent H-USY (Si/Al=15) zeolites

H-USY (Si/Al=15)	BET SA ^a (m ² g ⁻¹)	V ^b (cm ³ g ⁻¹)	D ^c (nm)
Fresh	873	0.45	0.75
Spent	303	0.14	1.51

^a Braunauer–Emmett–Teller (BET) surface area, ^b Pore volume, ^c Pore diameter

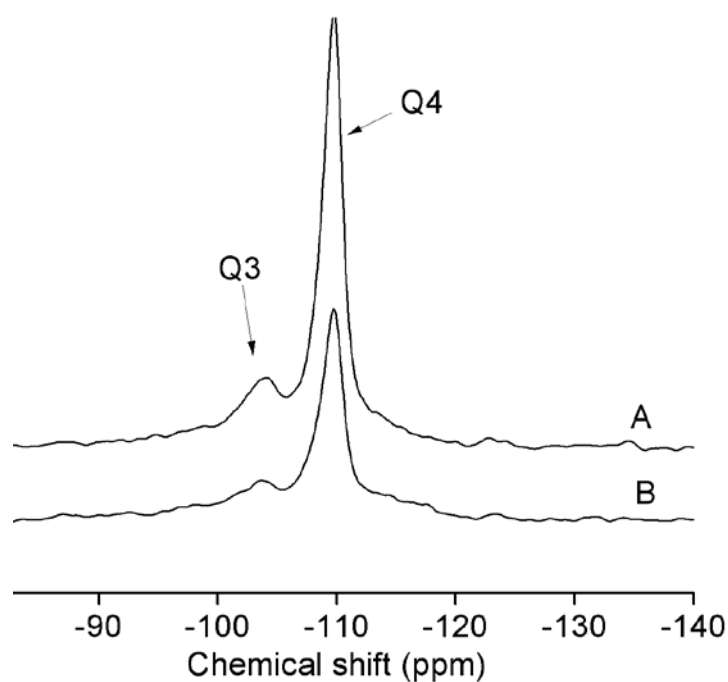


Figure 3A.24. ^{29}Si NMR of H-USY (Si/Al = 15) catalyst A) fresh B) spent-calcined.

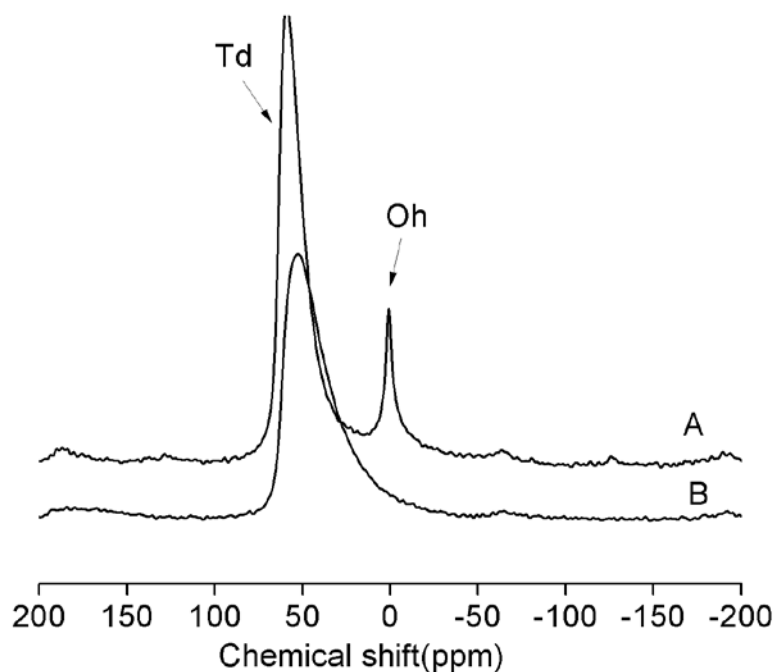


Figure 3A.25. ^{27}Al NMR of H-USY (Si/Al = 15) catalyst A) fresh B) spent-calcined.

3A.4. CONCLUSIONS

In chapter 3A, depolymerization of dealkaline lignin over solid acid catalysts was studied. Various types of solid acid catalysts (structured and amorphous) were

evaluated for the depolymerization reactions for dealkaline lignin substrate. Among the catalysts tested H-USY (Si/Al = 15) was found to be giving highest amount of aromatic monomers (60 %). The aromatic monomer formation was evaluated using various techniques like GC-FID, GC-MS, HPLC, LC-MS, GPC, MALDI-TOF and CHNS analysis. Quantification of these aromatic monomers were done by injecting calibration standards which were procured commercially and it was found that 90 % of the products extracted using THF solvent from the reaction mixture were confirmed to be aromatic monomers. Also FTIR and NMR (^1H and ^{13}C) analysis were done to assign a correlation between lignin and aromatic monomers structure. Catalytic activities of solid acids were compared with homogeneous acids, which showed the formation of large amount of oligomeric products when homogeneous acids were used as catalyst for lignin depolymerization reaction. Correlation between acidity and activity of solid acid catalysts were determined and it was found that as the acidity increases there is a possibility of degradation reactions (char, coke and gas) instead of giving aromatic monomer products. Study on reusability, stability and characterization of H-USY catalyst was checked using XRD, NH_3 -TPD, ICP-OES, N_2 sorption, ^{29}Si and ^{27}Al NMR techniques. After all these characterizations it was concluded that structured solid acids (zeolites, clay etc) were losing their catalytic activity due to the structural deformation happening. So amorphous solid acid catalysts ($\text{SiO}_2\text{-Al}_2\text{O}_3$) can be suggested as a better catalyst for lignin depolymerization reactions.

3A.5. REFERENCES

1. McKendry, P., *Bioresour Technol.* **2002**, *83*, 37-46.
2. Bartholomew, C. H.; Farrauto, R. J., *Fundamentals of Industrial Catalytic processes.* 2006; p 909.
3. Huber, G. W.; Iborra, S.; Corma, A., *Chem. Rev.* **2006**, *106*, 4044-4098.
4. Perlack, R. D.; Wright, L. L.; Turhollow, A. F.; Graham, R. L.; Stokes, B. J.; Erbach, D. C. *Biomass as feedstock for a bioenergy and bioproducts industry: the technical feasibility of a billion-ton annual supply*; U. S. Department of Energy: 2005.
5. Román-Leshkov, Y.; Chheda, J. N.; Dumesic, J. A., *Science* **2006**, *312*, 1933-1937.
6. Sun, Y., Cheng, J., *Bioresour. Technol.* **2002**, *83*, 1-11.
7. Zakzeski, J.; Bruijninx, P. C. A.; Jongerijs, A. L.; Weckhuysen, B. M., *Chem. Rev.* **2010**, *110*, 3552-3599.
8. Pandey, M. P.; Kim, C. S., *Chem. Eng. Technol.* **2011**, *34*, 29-41.
9. Langan, P.; Gnanakaran, S.; Rector, K. D.; Pawley, N.; Fox, D. T.; Cho, D. W.; Hammel, K. E., *Energy Environ. Sci.* **2011**, *4*, 3820-3833.
10. Sharma, R. K.; Bakhshi, N. N., *Energy Fuels* **1993**, *7*, 306-314.
11. Ben, H.; Ragauskas, A. J., *Energy Fuels* **2011**, *25*, 4662-4668.
12. Ma, Z.; Troussard, E.; van Bokhoven, J. A., *Appl. Catal., A* **2012**, *423*, 130-136.

13. Li, X.; Su, L.; Wang, Y.; Yu, Y.; Wang, C.; Li, X.; Wang, Z., *Front. Environ. Sci. Eng.* **2012**, *6*, 295-303.
14. Ben, H.; Ragauskas, A. J., *RSC Adv.* **2012**, *2*, 12892-12898.
15. Ma, Z.; van Bokhoven, J. A., *ChemCatChem* **2012**, *4*, 2036-2044.
16. Park, H.; Kim, J.; Hong, U.; Lee, Y.; Song, J.; Song, I., *Catal. Surv. Asia* **2013**, *17*, 119-131.
17. Amen-Chen, C.; Pakdel, H.; Roy, C., *Bioresour. Technol.* **2001**, *79*, 277-299.
18. Wang, H.; Tucker, M.; Ji, Y., *J. Appl. Chem.* **2013**, *2013*, 1-9.
19. Hicks, J. C., *J. Phys. Chem. Lett.* **2011**, *2*, 2280-2287.
20. Park, P., M. P.; Kim, C. S., *Chem. Eng. Technol.* **2011**, *34*, 29-41.
21. <http://www.tcichemicals.com/eshop/en/in/commodity/L0045/>.
22. Owen, B. C.; Hauptert, L. J.; Jarrell, T. M.; Marcum, C. L.; Parsell, T. H.; Abu-Omar, M. M.; Bozell, J. J.; Black, S. K.; Kenttämaa, H. I., *Anal. Chem.* **2012**, *84*, 6000-6007.
23. Pecina, R.; Burtscher, P.; Bonn, G.; Bobleter, O., *Fresenius' Z. Anal. Chem.* **1986**, *325*, 461-465.
24. Ye, Y.; Zhang, Y.; Fan, J.; Chang, J., *Ind. Eng. Chem. Res.* **2011**, *51*, 103-110.
25. Toledano, A.; Serrano, L.; Labidi, J., *Fuel* **2014**, *116*, 617-624.
26. Deepa, A. K.; Dhepe, P. L., *RSC Adv.* **2014**, *4*, 12625-12629.
27. Shabaka, A. A.; Nada, A. M. A.; Fadly, M., *J. Mater. Sci.* **1990**, *25*, 2925-2928.
28. Stuart, B. H., *Infrared Spectroscopy: Fundamentals and Applications* Wiley: USA, 2004.
29. Smith, B. C., *Fundamentals of Fourier Transform Infrared Spectroscopy*. CRC Press: 2011.
30. Balci, M., In *Basic ¹H- and ¹³C-NMR Spectroscopy*, Elsevier Science: Amsterdam, 2005; pp 3-8.
31. Keeler, J., *Understanding NMR spectroscopy*. Wiley: 2010.
32. Bruch, M., *NMR Spectroscopy Techniques*. Marcel Dekker Inc.: USA, 1996.
33. Stothers, J., *Carbon-13 NMR Spectroscopy*. Academic Press: London, 1972.
34. Balci, M., 13 - ¹³C Chemical Shifts of Organic Compounds. In *Basic ¹H- and ¹³C-NMR Spectroscopy*, Balci, M., Ed. Elsevier Science: Amsterdam, 2005; pp 293-324.
35. Solutions to Exercises. In *Basic ¹H- and ¹³C-NMR Spectroscopy*, Balci, M., Ed. Elsevier Science: Amsterdam, 2005; pp 407-411.
36. Burgess, C. E. C., D. J.; Horvath, J. R. , *Prepr. Pap. - Am. Chem. Soc., Div. Fuel Chem.* **2002**, *47*, 376-379.
37. Erdocia, X.; Prado, R.; Corcuera, M. Á.; Labidi, J., *Frontiers in Energy Research* **2014**, *2*.
38. Lou, R.; Wu, S.-b.; Lv, G.-j., *J. Anal. Appl. Pyrolysis* **2010**, *89*, 191-196.
39. Lou, R.; Wu, S.-B., Lv, G.-J. , *BioResources* **2010**, *5*, 827-837.
40. Bhaumik, P.; Deepa, A. K.; Kane, T., *J.Chem.Sci* **2014**, *126*, 373-385.

CHAPTER 3B

**DEPOLYMERIZATION OF
LIGNIN USING AMORPHOUS
SOLID ACIDS AND ISOLATION
OF AROMATIC MONOMERS**

3B.1. INTRODUCTION

Based on various characterization techniques like XRD, N₂ sorption, ²⁹Si and ²⁷Al NMR, NH₃-TPD, ICP-OES analysis in chapter 3A, it was confirmed that structured solid acid catalysts lost their catalytic activity due to the morphological changes happening during the reactions. It was also observed that few of the Brønsted acidic sites present in the catalysts got exchanged with the Na metal ion contamination present in the lignin substrate (dealkaline lignin), thereby reducing the activity of the catalyst.¹ Based on these studies it was decided that amorphous solid acid catalysts (SiO₂-Al₂O₃) would be better choice than structured solid acid catalysts for lignin depolymerization reactions. As observed from the Chapter 3A, Figure 3A.4, SiO₂-Al₂O₃ catalysts gave only 29 % of aromatic monomers under the following reaction conditions; 250 °C, 0.7 MPa N₂, H₂O:CH₃OH (1:5 v/v, 30 mL), 30 min., 500 rpm. But it was expected that after the optimization of reaction conditions SiO₂-Al₂O₃ can behave equally efficient and more stable than to structured solid acid catalysts.

3B.2. RESULTS AND DISCUSSIONS

3B.2.1. Study on amorphous SiO₂-Al₂O₃ catalysts

3B.2.1.1. Effect of lignin substrates

As mentioned earlier in chapter 3A since structured catalysts were not stable under reaction conditions, further studies were continued using amorphous solid acid catalyst like SiO₂-Al₂O₃ (Si/Al = 5.3). First the stability of the SiO₂-Al₂O₃ (Si/Al = 5.3) catalyst in the depolymerization of organosolv and ORG lignin was checked by subjecting the catalyst to recycle studies (before next run, catalyst recovered from earlier run was washed with methanol (60 mL), dried in oven at 60 °C overnight (16 h) and calcined in air at 550 °C for 12 h). As known from chapter 2A, characterization of lignin substrates using techniques like CHNS, ICP-OES and SEM-EDAX analysis showed that both organosolv and ORG lignin substrates do not contain Na or S and hence if there would be any decrease in the activity then it would be only because of morphological changes happening in the catalyst. The catalytic results for these substrates are illustrated in Figures 3B.1, 3B.2 and as seen, SiO₂-Al₂O₃ catalyst gave similar activity (33-35 % for organosolv and 59-60 % for ORG lignin) in all 3 recycle runs.

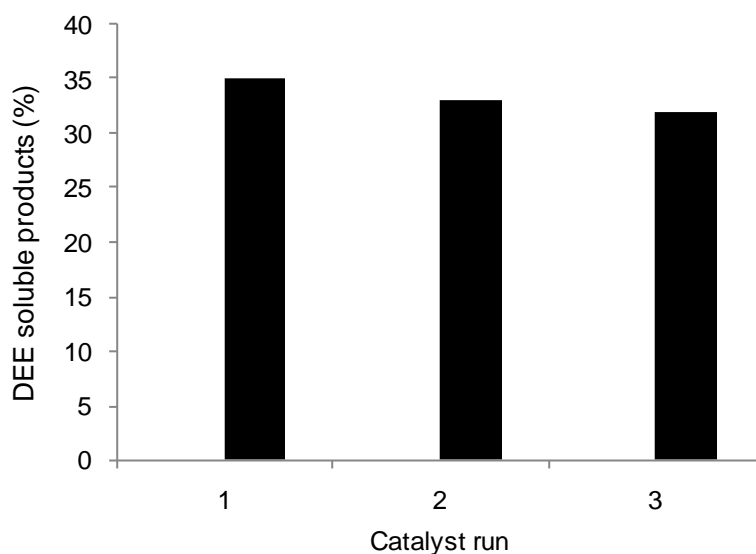


Figure 3B.1. Catalyst recycle study for organosolv lignin. Reaction conditions: organosolv lignin (0.5 g), SiO₂-Al₂O₃ (0.5 g), H₂O:CH₃OH (1:5 v/v, 30 mL), 250 °C, 30 min., 1000 rpm, 0.7 MPa N₂.

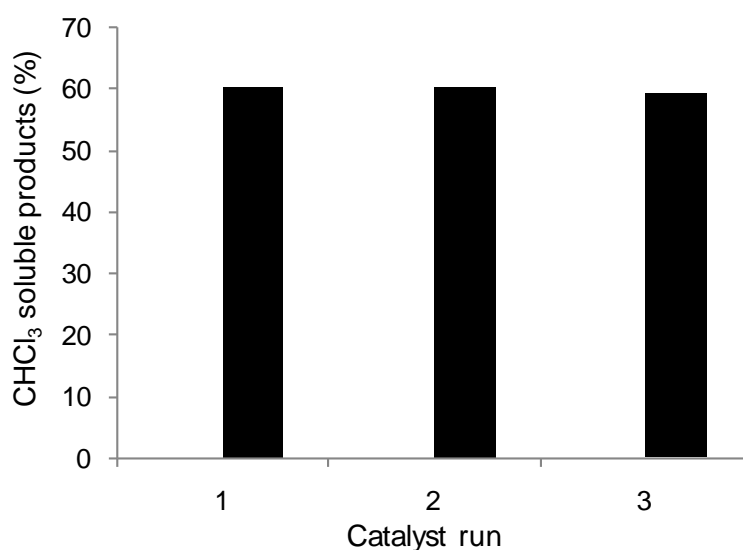


Figure 3B.2. Catalyst recycle study for ORG lignin. Reaction conditions: ORG lignin (0.5 g), SiO₂-Al₂O₃ (0.5 g), H₂O:CH₃OH (1:5 v/v, 30 mL), 250 °C, 30 min., 1000 rpm, 0.7 MPa N₂.

In these reactions, DEE and chloroform were used to extract the products obtained in organosolv lignin and ORG lignin reactions, respectively (Refer chapter 3A, Figure 3A.3) since both these substrates are soluble in THF solvent (Refer chapter 2A, Table 2A.5 which is used for extracting products in dealkaline lignin reaction. Interestingly, SiO₂-Al₂O₃ gave 35 % yield for aromatic monomers in minimum 3 runs when organosolv lignin with molecular weight of 4575 gmol⁻¹ (Chapter 2A, Table

2A.1) was used as a substrate. When ORG lignin with a molecular weight of 7059 g mol^{-1} (Chapter 2A, Table 2A.1) was used, $\text{SiO}_2\text{-Al}_2\text{O}_3$ gave 60 % of aromatic monomers. These results are contradictory to earlier studies with H-USY where decrease in activity in the reactions with organosolv lignin was observed (Refer chapter 3A, Figure 3A.22). Therefore, the results obtained with $\text{SiO}_2\text{-Al}_2\text{O}_3$ have encouraged me to work on this catalyst.

3B.2.1.2. Effect of temperature and pressure

As shown in Chapter 3A, Figure 3A.4, $\text{SiO}_2\text{-Al}_2\text{O}_3$ catalyst was capable of converting dealkaline lignin to yield 29 % of aromatic monomers at 250 °C within 30 min. when stirring was maintained at 500 rpm. To improve the yields of aromatic monomers obtained from dealkaline lignin with $\text{SiO}_2\text{-Al}_2\text{O}_3$ as a catalyst, reaction temperatures were altered (Figure 3B.3). Since earlier reported works on depolymerization of lignin were done at higher temperatures (> 340 °C), it was first decided to carry out reactions at temperatures higher than 250 °C. When reaction temperature was increased to 270 °C, decrease in the aromatic monomer yield (15 %) was observed which was due to the formation of degradation products such as char (visible by black color THF insoluble solid). This reveals that solid acid catalysts are highly active and with increase in temperatures those help in the degradation of products. To avoid degradation of products and enhance the depolymerization activity, reaction temperatures were reduced to 230 °C and 215 °C and again lower yields were obtained (25 % and 1 %) which confirmed that 250 °C is optimum temperature for this reaction.

Further, the role of pressure was investigated (Figure 3B.4) by charging 0.1 or 0.7 MPa pressures of N_2 in the autoclave at room temperature (RT) and reactions were performed at 250 °C for 30 min. in $\text{H}_2\text{O}:\text{CH}_3\text{OH}$ (1:5 v/v, 30 mL). With an initial N_2 pressure of 0.7 MPa, 29 % yield was possible; it decreased to 24 % when 0.1 MPa of N_2 was charged. This indicates a possible dependence of activity on overall final pressures which were found to be 7.5 MPa with 0.7 MPa N_2 charged at RT compared to 6.5 MPa in the case when 0.1 MPa of N_2 was charged at RT.

Reactions were also performed at lower temperature and pressure. When $\text{SiO}_2\text{-Al}_2\text{O}_3$ catalysed depolymerization of dealkaline lignin was carried out at 215 °C with 0.7 MPa N_2 at RT only 1 % yield was achievable. However, under this condition final pressure of only 4.0 MPa was observed.

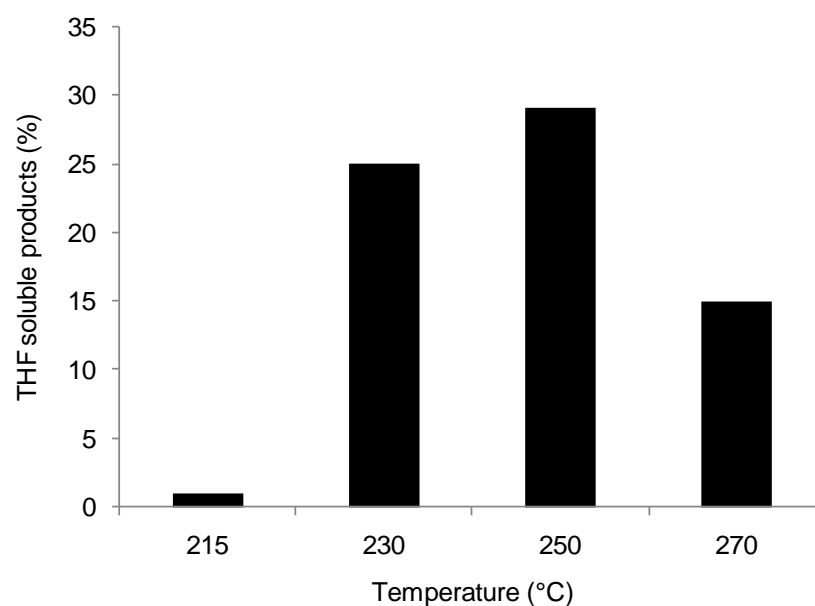


Figure 3B.3. Effect of temperature on lignin depolymerization. Reaction conditions: dealkaline lignin, SiO₂-Al₂O₃, H₂O:CH₃OH (1:5 v/v, 30 mL), 215-270 °C, 30 min., 500 rpm, 0.7MPa N₂.

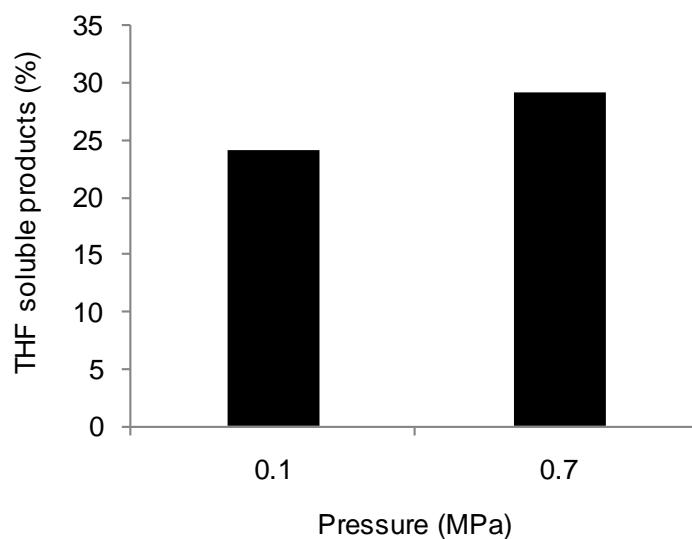


Figure 3B.4. Effect of pressure on lignin depolymerization. Reaction conditions: dealkaline lignin, SiO₂-Al₂O₃, H₂O:CH₃OH (1:5 v/v, 30 mL), 250 °C, 30 min., 500 rpm, 0.1- 0.7 MPa N₂.

To investigate whether increasing the final pressure from 4.0 MPa to 7.0 MPa will help to achieve higher yields at 215 °C, 2.5 MPa of N₂ (at RT) was charged instead of 0.7 MPa N₂ (at RT) and performed the reaction at 215 °C for 30 min. In this reaction, final pressure reached to 7.0 MPa however no increase in yield was achieved (1 %). This emphasizes that both temperature and pressure are important parameters in

these reactions and that 250 °C and 7.5 MPa of final pressure are required to achieve the maximum yields. At this juncture, the question arises whether methanol attains at least a sub-critical state under these reaction conditions (250 °C, 7.5 MPa) since T_c (critical temperature) and P_c (critical pressure) of methanol are 239.2 °C and 8.1 MPa, respectively and whether this affects the reactions dynamics leading to better yields. However, when the reaction was carried out at 250 °C with final pressure of 6.5 MPa (0.1 MPa at RT), almost similar yield (24 %) as that for 250 °C (29 %) with final pressure of 7.5 MPa is obtained. This indicates that methanol, even if present in sub-critical condition is not playing any significant role.

3B.2.1.3. Effect of reaction medium

In several earlier studies it was shown that the depolymerization of lignin also depends on the solvent used in the reaction. For e.g. it is shown that in the depolymerization of Kraft lignin the effect of methanol and water:methanol (1:1) was studied using H-ZSM-5 catalyst NaOH as cocatalyst at 220 °C.² Another report shows that THF was used as solvent for lignin depolymerization into aromatic monomers at 250 °C using MgO as catalyst. In these reactions THF acted as excellent lignin dissolution medium and also it exhibited a promotion effect to the MgO catalyst thereby increasing the monomer yield to 13.2 %.³ A series of hydrogen donating solvents like glycerol, tetralin, isopropanol and formic acid were used for the lignin depolymerization by hydrogenolysis in presence of 10 % Ni on Al-SBA-15 as catalyst.⁴ Considering the above reports it was important to study the effect of solvent used as reaction medium on the conversion of lignin. It was found that reaction done using only water as solvent did not proceed may be due to lower final pressure (5.0 MPa at 250 °C). From the earlier discussions (Refer section 3B.2.1.2) it is evident that final pressure of at least 6.5 MPa is required to achieve ca. 24 % yield of aromatic monomers. Moreover, as observed from Table 2A.5 dealkaline lignin was not completely soluble in water which may hamper the reaction rate. With water:methanol and water:ethanol solvent systems similar product yields (29 %) are obtained (Figure 3B.5). Subsequently water to methanol ratios (v/v) was varied from 1:5 (29 % yield) to 1:1 (22 % yield) to 5:1 (1 % yield) but the best result was obtained only with 1:5 ratio (29 %). This was due to the fact that when water concentration was increased the final pressures were decreased (7.5 MPa at 1: 5 v/v; 6.0 MPa at 1:1 v/v and 5.2 MPa at 5:1

v/v water to methanol ratios). Besides these studies on water:methanol solvent system, other solvents such as phenol, acetone, THF, dioxane were used in the reaction as literature reports use of these solvents in the depolymerization of lignin.⁵⁻⁷

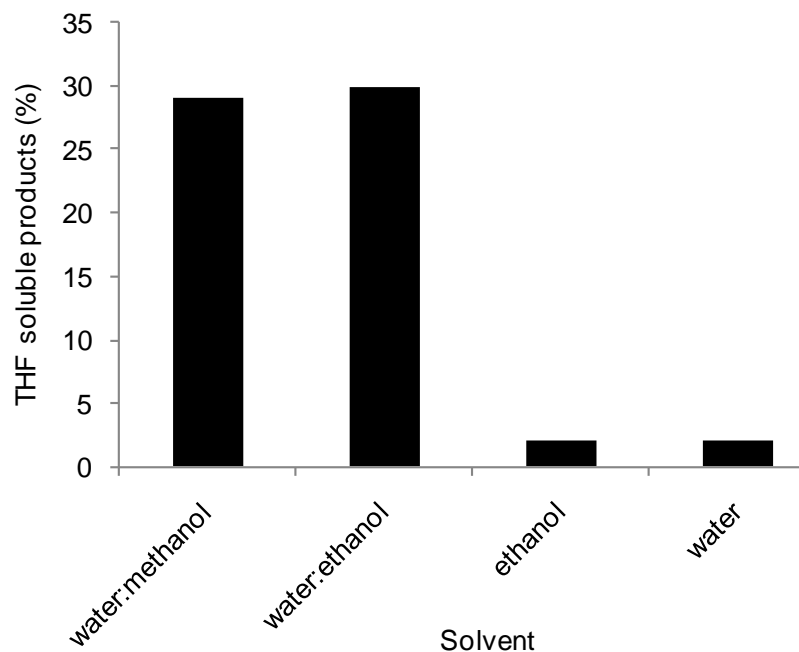


Figure 3B.5. Effect of solvent on depolymerization. Reaction conditions: dealkaline lignin, SiO₂-Al₂O₃, Solvent: (30 mL), 250 °C, 30 min., 500 rpm, 0.7MPa N₂.

It is also mentioned in the literature that phenol can act as capping agent to avoid the repolymerization of aromatic products and thus improve the aromatic product selectivity.⁸⁻⁹ In my work repolymerization products are not expected since milder conditions are used than the reported reaction conditions in which phenol is used.¹⁰ Solubility of dealkaline lignin in these solvents (phenol, acetone, THF, dioxane) was checked and found that it is almost completely soluble in all solvents (50 mgmL⁻¹). Before using these solvents in the reaction, the stability of these solvents at 250 °C for 60 min. in presence of SiO₂-Al₂O₃ catalyst was checked and found out that all the solvents undergo self decomposition reactions and form various products which were detected on GC-FID. Due to this reason reactions were not performed in these solvents. Since the final pressures will be very high (> 8.0 MPa), reactions were not done using only methanol as a solvent. This is because the reactor set up used for lignin depolymerization reactions had a limitation of working up to maximum pressure of 10 MPa. Moreover, from safety point of view it is not advisable to mix

methanol and solid acid catalysts at high temperatures since methanol undergoes dehydration reaction in presence of an acid catalyst forming highly volatile dimethyl ether as product¹¹⁻¹³ which will increase the pressures beyond the reactor limits. It was also reported that coupling reactions of lignin fragments are possible with $\text{CH}_3\text{O}\cdot$ and $\text{CH}_3\cdot$ radicals produced from methanol during acid catalysed formation of dimethyl ether.¹⁴ To check the formation of dimethyl ether, reaction of water:methanol (1:5 v/v) system with solid acid catalysts (H-USY) was performed at 250 °C for 30 min. in presence of 0.7 MPa of N_2 . The gas phase (N_2) was analyzed using GC-TCD and the reaction mixture was analyzed using GC-FID, but no trace of DME was observed during the analysis. So in this work, with the addition of water along with methanol even in presence of solid acid catalysts it is believed that DME formation can be suppressed.

3B.2.1.4. Influence of reaction time and stirring speed

After narrowing down the reaction conditions for the depolymerization of dealkalinized lignin with $\text{SiO}_2\text{-Al}_2\text{O}_3$ as catalyst to obtain higher product yields at 250 °C and 0.7 MPa N_2 pressure (RT) using water:methanol (1:5 v/v) all the further reactions were carried out under similar conditions. To improve the yields and to make amorphous $\text{SiO}_2\text{-Al}_2\text{O}_3$ catalyst also to be equally efficient like zeolites to obtain aromatic monomers, reactions were carried out for 90 min. instead of usual 30 min. (Figure 3B.6). In this reaction, a very high yield of 56 % was achieved for aromatic monomers. Further increase in time duration (120 min.) did not improve the yields (58 %), but, formation of char was observed in minor amount (visibly by black color solid).

Effect of mass transfer limitations was explored by varying the stirring speed to improve the catalyst-substrate interactions. Stirring rate of 500 rpm gave yield of 29 % (30 min.) which could be enhanced to 58 % (30 min.) by increasing the stirring rate to 1000 rpm. However, further increase in stirring rate (1200 rpm) did not yield any better results.

To improve the yields and to make amorphous $\text{SiO}_2\text{-Al}_2\text{O}_3$ also to be equally efficient to zeolites, reaction was carried out for 90 min. and a very high yield of 56 % was achieved (Figure 3B.7). Further increase in time duration (120 min.) did not improve the yields (56 %), and in this case, formation of char is observed due to

degradation reactions. From all these studies it could be concluded that the best condition to obtain maximum amount of aromatic monomers (60 %) is to perform the reaction for 30 min. with a stirring speed of 1000 rpm.

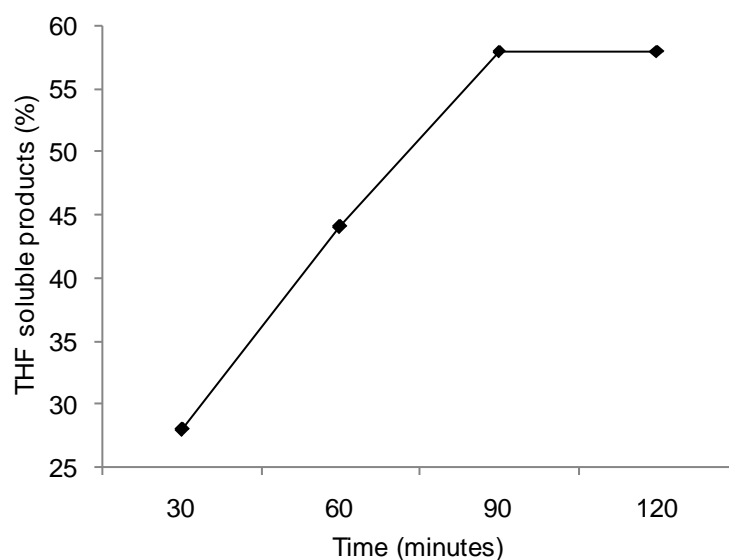


Figure 3B.6. Effect of time on depolymerization. Reaction conditions: dealkaline lignin, $\text{SiO}_2\text{-Al}_2\text{O}_3$, $\text{H}_2\text{O}:\text{CH}_3\text{OH}$ (1:5 v/v, 30 mL), 250 °C, 30-120 min., 500 rpm, 0.7 MPa N_2 .

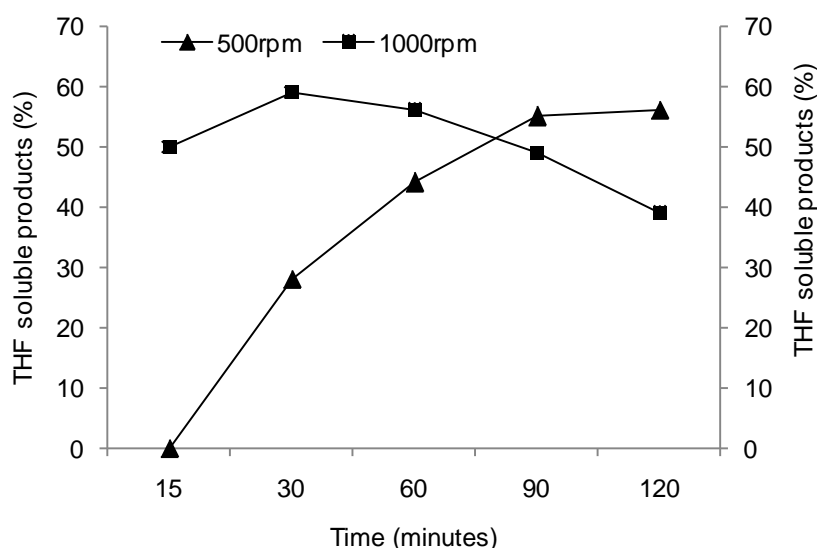


Figure 3B.7. Effect of RPM on depolymerization. Reaction conditions: dealkaline lignin, $\text{SiO}_2\text{-Al}_2\text{O}_3$, $\text{H}_2\text{O}:\text{CH}_3\text{OH}$ (1:5 v/v, 30 mL), 250 °C, 15-120 min., 500-1000 rpm, 0.7 MPa N_2 .

3B.2.2. Isolation of aromatic monomers by column chromatography

Once optimization of reaction conditions (250 °C, 0.7 MPa N₂, H₂O:CH₃OH (1:5 v/v, 30 mL), 30 min., 1000 rpm) with amorphous SiO₂-Al₂O₃ catalyst for depolymerization of dealkaline lignin was achieved, I undertook the task of identifying and isolating the products obtained after lignin depolymerization reaction. From the complex mixture of aromatic monomers, pure compounds were isolated and characterized so that these aromatic monomers which were detected (GC-FID, GC-MS, HPLC, LC-MS) can be once again confirmed. As shown in Chapter 3A, Figures 3A.7 (HPLC and GC-FID profile) and tabulated in Table 3A.1 (for quantification of products) most of the products were identified as aromatic monomers. Next, the fact that it is a difficult task to isolate those in pure form from the products mixture, especially in the case of lignin conversions hardly needs emphasizing.¹⁵⁻¹⁷ However, I undertook this work of separating aromatic monomers using column chromatography technique and 3 products namely; vanillin, methyl vanillate and butylated hydroxy toluene (BHT) in pure form were isolated successfully.

Column chromatography was done for the isolation of monomers from the THF soluble mixture (dealkaline lignin reaction) with silica gel (230-400 mesh) as stationary phase and n-hexane with various concentrations of EtOAc was used as the mobile phase. A column of length 30 cm was filled with silica gel in n-hexane. To increase the flow rates of the mobile phase through the column, air pump was used which helps the mobile phase to flow at a faster rate. Two separate column chromatography were done for the isolation of compounds. From THF soluble components the solid obtained was extracted using excess DCM in order to separate few of the compounds from the complex mixture. DCM extracted products was loaded in the first column (Figure 3B.8). TLC (Thin layer chromatography) was checked before choosing the solvent composition of the mobile phase and found that in solvent composition of 25 % EtOAc in hexane few of the compounds were found to be separating. So 25 % EtOAc in hexane was used as a mobile phase for DCM extract products. Two compounds namely vanillin and methyl vanillate were isolated using this composition. Second column was loaded with the hexane soluble products obtained by the extraction from DCM soluble product mixture (Figure 3B.8). Now the hexane soluble fraction contain fewer number of compounds compared to DCM soluble fraction. TLC helped to choose the mobile phase as 5 % EtOAc in hexane for

hexane soluble portion of products. By this column butylated hydroxy toluene (BHT) was isolated from the hexane soluble fraction. Compounds isolated from both the columns were characterized using GC-FID, GC-MS, $^1\text{H-NMR}$ and CHNS analysis (Table 3B.1), which are identical to the aromatic monomers detected in the methanol soluble reaction mixture and THF soluble products.

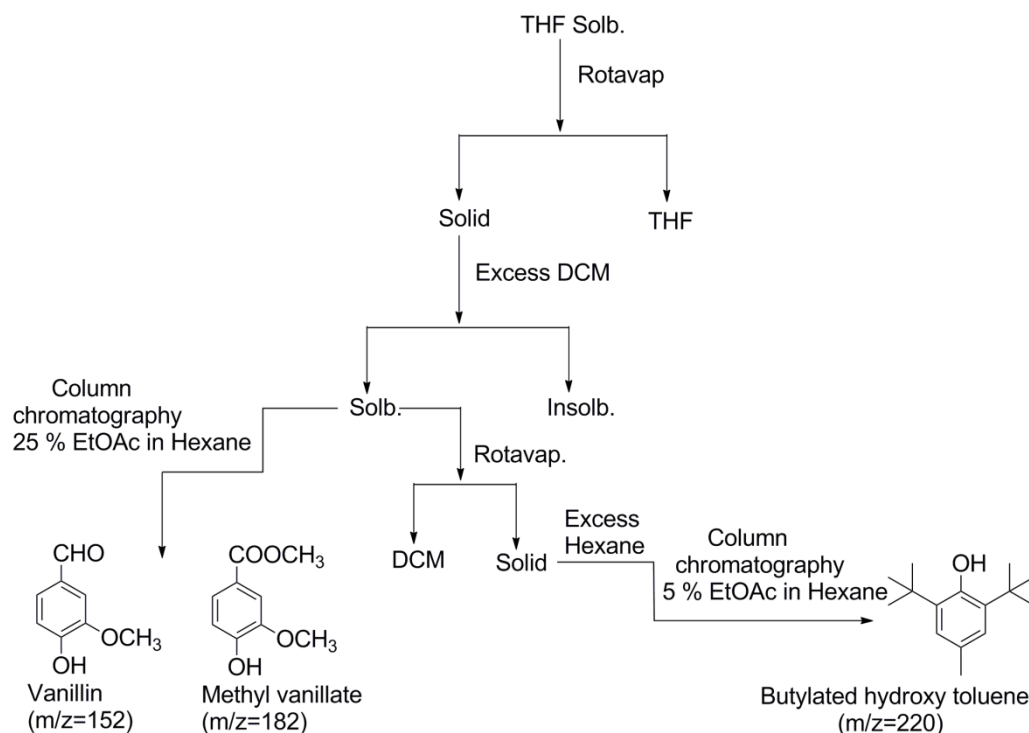


Figure 3B.8. Scheme for the isolation of products using column chromatography from THF soluble mixture of dealkaline lignin reaction.

Pure products formed in the solid acid catalysed depolymerization of other lignin (organosolv, alkali, ORG, EORG, bagasse) were also isolated by similar process of column chromatography.

Table 3B.1. Summary on characterization of products isolated by column chromatography

Product	GC-MS (m/z)	CHNS		¹ H NMR (δ ppm)
		Theoretical	Observed	
Vanillin	152, 122, 109	C=63 %, H=5.2 %	C=62 %, H=5 %	3.9 ppm (s, 3H) corresponds to CH ₃ -group, 7.2, 7.33, 7.38 ppm (s, 1H) corresponds to aromatic protons and 9.76 ppm (s, 1H) corresponds to -CHO group.
Methyl vanillate	182, 152, 123	C=59 %, H=5.4 %	C=59%, H=5 %	3.82 ppm (s, 3H), 3.8 9ppm (s, 3H) corresponds to CH ₃ -group, 7.19 ppm, 7.42, 7.48 ppm (s, 1H) corresponds to aromatic protons.
Butylated hydroxy toluene (BHT)	220, 205, 177, 105	C=81.8 %, H=10.9 %	C=82 %, H=11 %	1.35 ppm (s, 18H) CH ₃ group attached to tertiary carbon, 2.2 ppm (s, 3H) corresponds to CH ₃ -group attached to aromatic carbon, and 6.9 ppm (s, 2H) corresponds to aromatic protons.

3B.2.3. Depolymerization of various lignin substrates

After the optimization of the reaction conditions for the depolymerization of dealkaline lignin (250 °C, water:methanol=1:5 v/v, SiO₂-Al₂O₃, 30 min., 1000 rpm, nitrogen 0.7 MPa at RT) various other lignin substrates like, alkali lignin, bagasse lignin, ORG and EORG were evaluated under similar conditions. Figure 3B.9 shows that except for organosolv lignin, all other lignin gave organic solvent soluble aromatic monomers with 52-60 % yield. It is important to note here that these results clearly prove that using this catalytic system it is able to convert lignin from various sources with diverse physical and chemical properties as mentioned in Chapter 2A, section 2A.2 Also, it is important to state here that for different lignin different

solvents were used for the extraction of products formed (Refer chapter 3A, Table 3A.1, Figure 3A.7) taking into account solubility of lignin in solvents. This was done to avoid any contamination from lignin getting dissolved in the solvent (if used same solvent in all the reactions with different lignin for work-up then there is a possibility of lignin also getting soluble in the solvent). Products obtained after lignin depolymerization was extracted using organic solvents; THF for dealkaline lignin, DEE for organosolv lignin, EtOAc for alkali/EORG/bagasse lignin and CHCl_3 for ORG lignin.

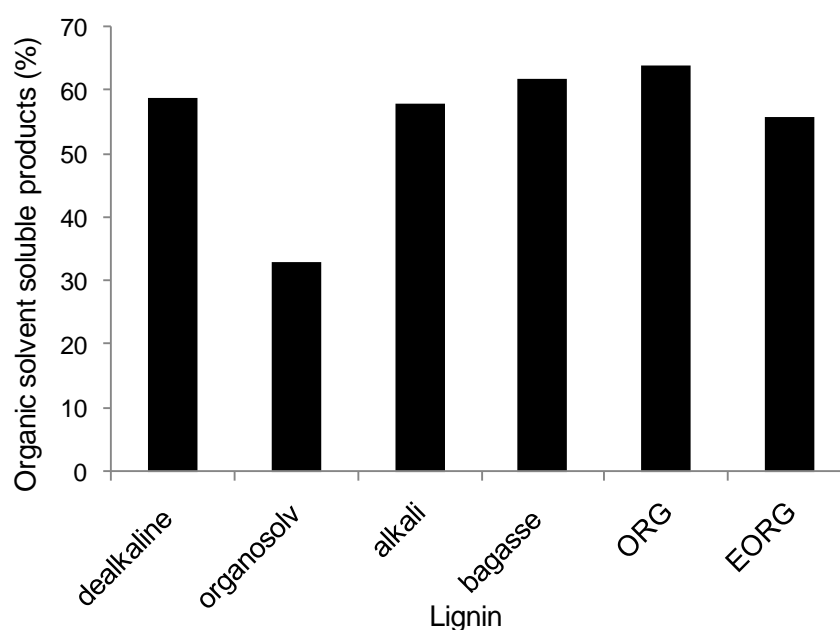


Figure 3B.9. Effect of various lignin substrates. Reaction conditions: Lignin (0.5 g), $\text{SiO}_2\text{-Al}_2\text{O}_3$ (0.5 g), $\text{H}_2\text{O}:\text{CH}_3\text{OH}$ (1:5 v/v, 30 mL), 250 °C, 30 min., 1000 rpm, 0.7 MPa N_2 at RT. Products are extracted in THF for dealkaline lignin, in DEE for organosolv lignin, in EtOAc for alkali/EORG/bagasse lignin and CHCl_3 for ORG lignin.

3B.2.4. Study on reuse, stability and characterization of $\text{SiO}_2\text{-Al}_2\text{O}_3$ catalyst

In the catalyst recyclability study, $\text{SiO}_2\text{-Al}_2\text{O}_3$ was recovered from the reaction mixture, washed (with water:methanol, 60 mL), dried overnight (16 h) in oven, calcined in air (550 °C, 12 h) and then subjected to next reaction. It is found out that with organosolv and ORG (Figures 3B.1, 3B.2) lignin similar yield (ca. 35 % for organosolv and ca. 60 % for ORG lignin) could be obtained minimum up to 3 runs. But in the case of dealkaline lignin catalyst was not recyclable. In the 1st run product

yield was almost 57 %, in the 2nd run the yield decreased to 33 %, after 3rd run catalyst became inactive (Figure 3B.10). This showed that for dealkaline lignin substrate even the amorphous catalyst couldn't be recycled. This happened since dealkaline lignin contains Na and S as impurities (Refer chapter 2A, Table 2A.2 and Table 2A.3) which may poison the catalytically active sites and also due to the morphological changes happening in the catalyst under the reaction conditions employed.

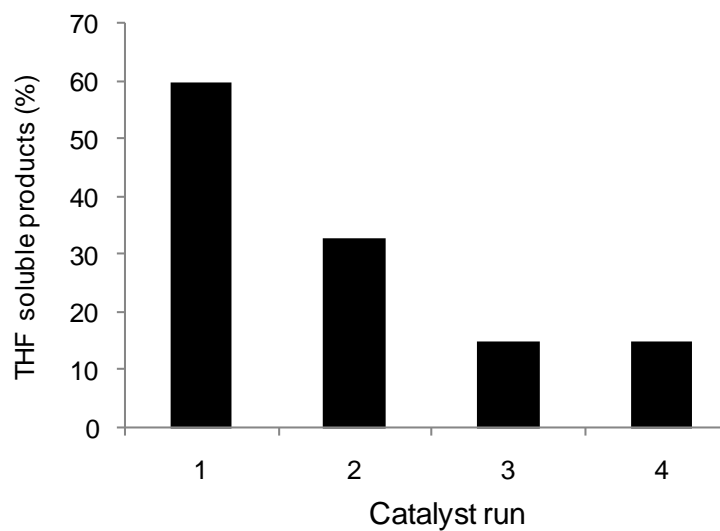


Figure 3B.10. Recycle study $\text{SiO}_2\text{-Al}_2\text{O}_3$ catalyst in dealkaline lignin reaction. Reaction conditions: dealkaline lignin, $\text{SiO}_2\text{-Al}_2\text{O}_3$, $\text{H}_2\text{O}:\text{CH}_3\text{OH}$ (1:5 v/v, 30 mL), 250 °C, 30 min., 1000 rpm, 0.7 MPa N_2 .

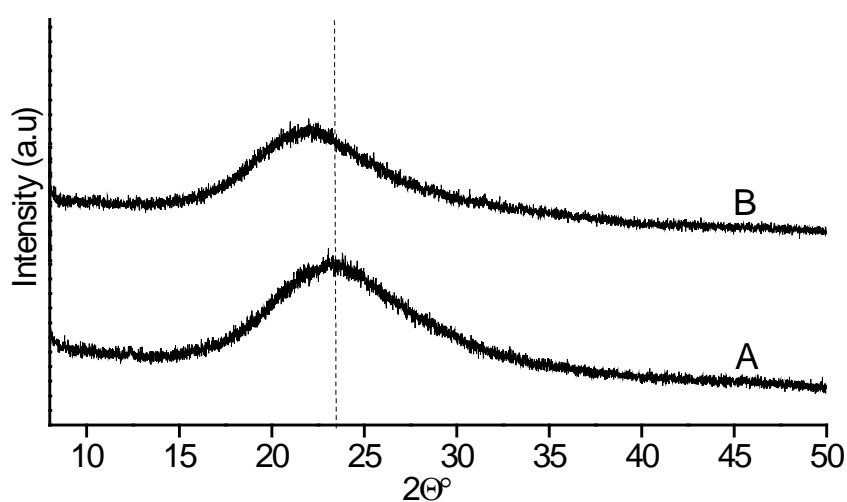


Figure 3B.11. XRD pattern of $\text{SiO}_2\text{-Al}_2\text{O}_3$ catalyst, A) fresh B) spent-calcined sample.

To study about the reason behind the deactivation of spent $\text{SiO}_2\text{-Al}_2\text{O}_3$ catalyst in dealkaline lignin reactions, several characterizations were done. Spent $\text{SiO}_2\text{-Al}_2\text{O}_3$ was calcined in air ($550\text{ }^\circ\text{C}$, 12 h) and then characterized. From XRD analysis (Figure 3B.11) it was found that there was a minor shift in the broad peak (23 °) towards lower 2θ value (21.7 °), which represents an increase in the pore diameter of the spent catalyst. This was further supported by N_2 sorption studies (Figure 3B.12, Table 3B.2); an increase in the pore diameter of the spent catalyst from 4.9 nm to 11 nm was observed (Figure 3B.13). A significant decrease in surface area from 532 to $221\text{ m}^2\text{ g}^{-1}$ and decrease in pore volume from 0.83 to $0.65\text{ cm}^3\text{ g}^{-1}$ was also observed in the case of spent $\text{SiO}_2\text{-Al}_2\text{O}_3$. These observations show that even the amorphous catalyst was undergoing several morphological changes during lignin depolymerization reactions.

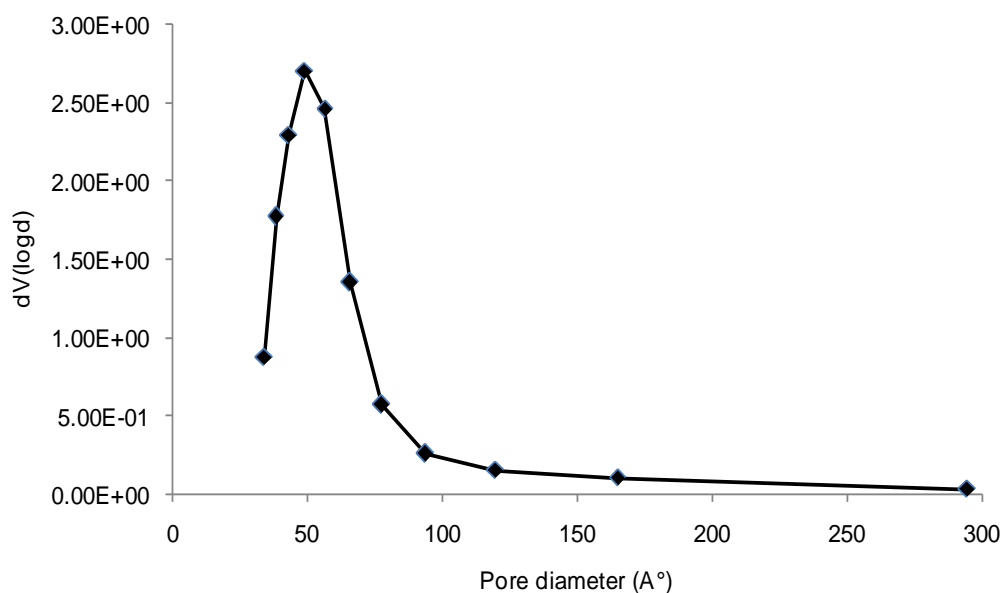


Figure 3B.12. Pore size distribution (N_2 sorption study) of fresh $\text{SiO}_2\text{-Al}_2\text{O}_3$ catalyst.

From $\text{NH}_3\text{-TPD}$ (Table 3B.2, Figure 3B.14) analysis it was observed that the total acidity of the spent $\text{SiO}_2\text{-Al}_2\text{O}_3$ was decreased (0.29 mmol g^{-1}) when compared to the fresh catalyst (0.63 mmol g^{-1}). From TPD profiles it was clear that both strong ($510\text{-}790\text{ }^\circ\text{C}$) and weak acid ($100\text{-}450\text{ }^\circ\text{C}$) sites were reduced during the reaction unlike in H-USY where strong acid sites were completely disappeared (Figure 3B.14). This reduction in acidity corresponds to 26.5 mg of Na present in the spent catalyst, which has poisoned the Brönsted acid sites present in the $\text{SiO}_2\text{-Al}_2\text{O}_3$ by getting exchanged with them. But it was found from ICP-OES analysis that, only a part of Na present in the spent $\text{SiO}_2\text{-Al}_2\text{O}_3$ is exchanged with Brönsted acid sites, as (18.2 mg

Na) 0.79 mmol Na/0.5g catalyst (1.58 mmol g^{-1}) is capable of killing all the acidic sites present in the catalyst (Table 3B.2). This can explain why spent catalyst could lose ca. 15 % activity in dealkaline lignin reaction.

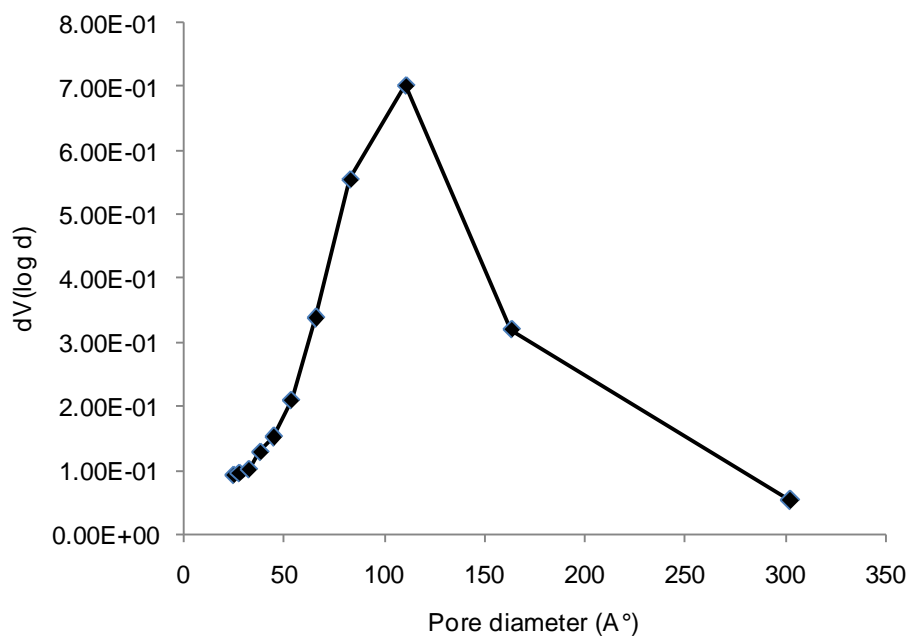


Figure 3B.13. Pore size distribution (N_2 sorption study) of spent calcined $\text{SiO}_2\text{-Al}_2\text{O}_3$ catalyst.

Table 3B.2. NH_3 -TPD, N_2 sorption and ICP-OES analysis of fresh and spent $\text{SiO}_2\text{-Al}_2\text{O}_3$ (Si/Al = 5.3)

$\text{SiO}_2\text{-Al}_2\text{O}_3$	$\text{NH}_3\text{-TPD (mmol g}^{-1}\text{)}$			N_2 sorption			ICP-OES		
	Total acidity	Strong acid sites [510-790 °C]	Weak acid sites [100-450 °C]	BET-SA (m^2g^{-1})	Pore size (nm)	Pore vol. (cm^3g^{-1})	Si/Al ratio Actual	Si/Al ratio Obs.	Na (mg)
Fresh	0.63	0.46	0.17	532	4.90	0.83	5.30	5.50	8.3
Spent	0.29	0.21	0.08	221	11.00	0.65	-	5.20	26.5

On the other hand when other lignin (ORG, EORG, organosolv) are used as substrate, spent $\text{SiO}_2\text{-Al}_2\text{O}_3$ catalyst did not show any Na contamination and it gave similar activity in recycle runs. However, loss of few acid sites is observed with these substrates due to the fact that, during reaction, catalyst morphology was slightly changing and thus few of the acid sites might be buried or are inaccessible. Similar phenomenon was observed during the study of H-USY catalysts used dealkaline lignin depolymerization (Refer chapter 3A, section 3B.2.4).

To probe further, solid state ^{29}Si MAS (Figure 3B.15) and ^{27}Al MAS NMR (Figure 3B.16) of the fresh and spent $\text{SiO}_2\text{-Al}_2\text{O}_3$ catalysts were taken. ^{29}Si NMR of fresh $\text{SiO}_2\text{-Al}_2\text{O}_3$ catalyst showed $\text{Q}^4[\text{Si}(0\text{Al})]$ species at -110.8 ppm, $\text{Q}^3[\text{Si}(1\text{Al})]$ species at -102.6 ppm, $\text{Q}^2[\text{Si}(2\text{Al})]$ species at -93.57 ppm chemical shift values. It is similar to the spectrum reported previously.¹⁸⁻²² But in the spent calcined $\text{SiO}_2\text{-Al}_2\text{O}_3$ catalyst a single broad peak was observed, where mainly $\text{Q}^4[\text{Si}(0\text{Al})]$ species at -107 ppm was predominant, but other species like $\text{Q}^3[\text{Si}(1\text{Al})]$ and $\text{Q}^2[\text{Si}(2\text{Al})]$ were not visible. This result shows that in the spent $\text{SiO}_2\text{-Al}_2\text{O}_3$ catalyst there is change in the Si environment, which may be one of the reasons for the slight reduction in catalytic activity of even amorphous $\text{SiO}_2\text{-Al}_2\text{O}_3$ catalyst during the course of lignin depolymerization reaction.

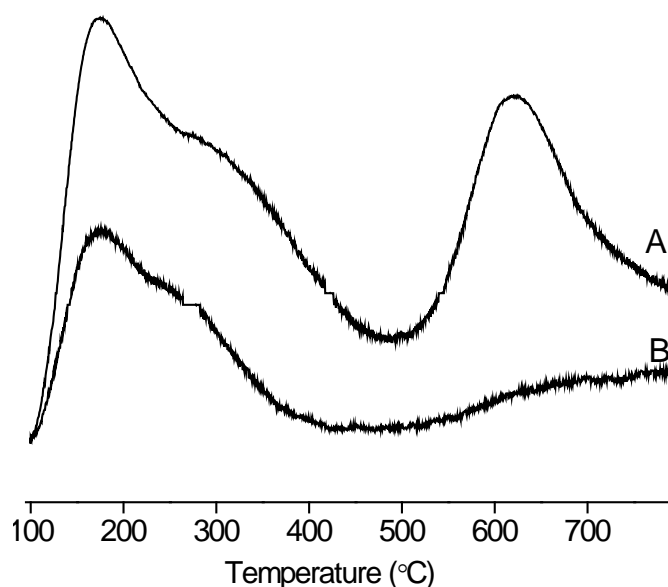


Figure 3B.14. NH_3 -TPD of $\text{SiO}_2\text{-Al}_2\text{O}_3$ catalyst A) fresh B) spent.

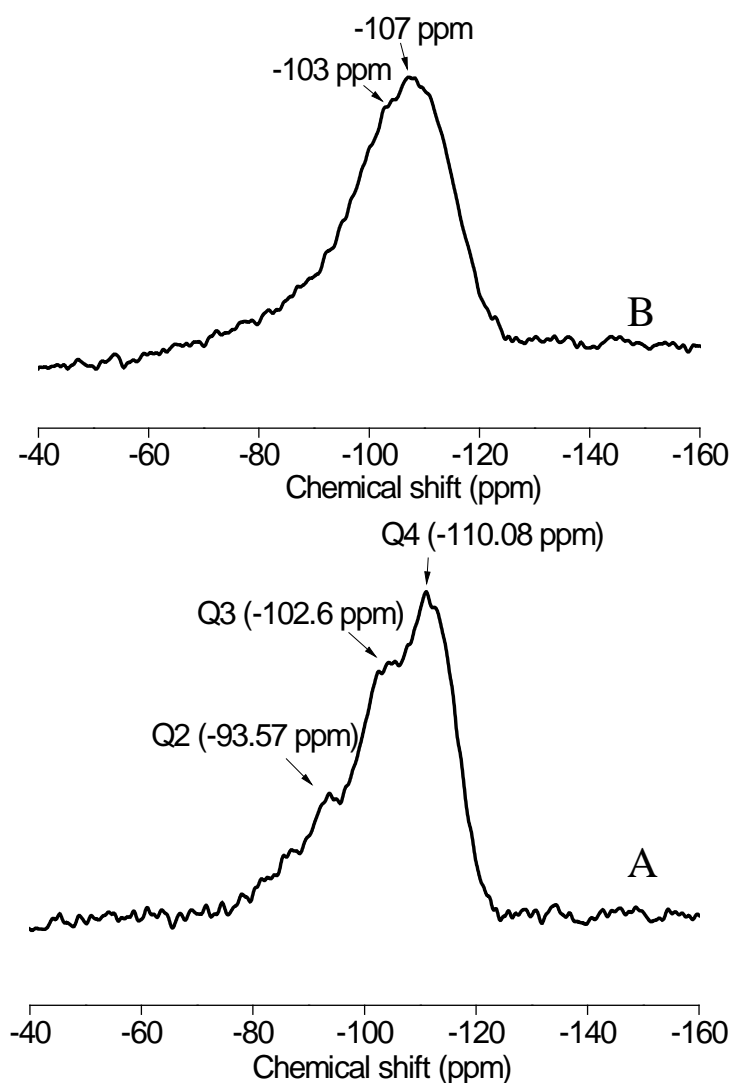


Figure 3B.15. ^{29}Si MAS NMR of $\text{SiO}_2\text{-Al}_2\text{O}_3$ catalyst A) fresh B) spent.

In ^{27}Al NMR of fresh $\text{SiO}_2\text{-Al}_2\text{O}_3$ catalyst at 51.15 ppm tetrahedral (Td) and at -0.99 ppm octahedral (Oh) Al species were observed which were in good correlation with the literature reports.¹⁸⁻²³ But in spent catalyst, ^{27}Al NMR showed broadening of Td Al peak when compared to fresh catalyst. This indicates that the few of Al has changed its coordination by getting removed from the framework to form extra framework species. NMR studies reveal that after the Al extraction, environment around Si will alter and it may form more Si-O-Si bonds. This will give rise to Q^4 species at the expense of Q^2 and Q^3 species.

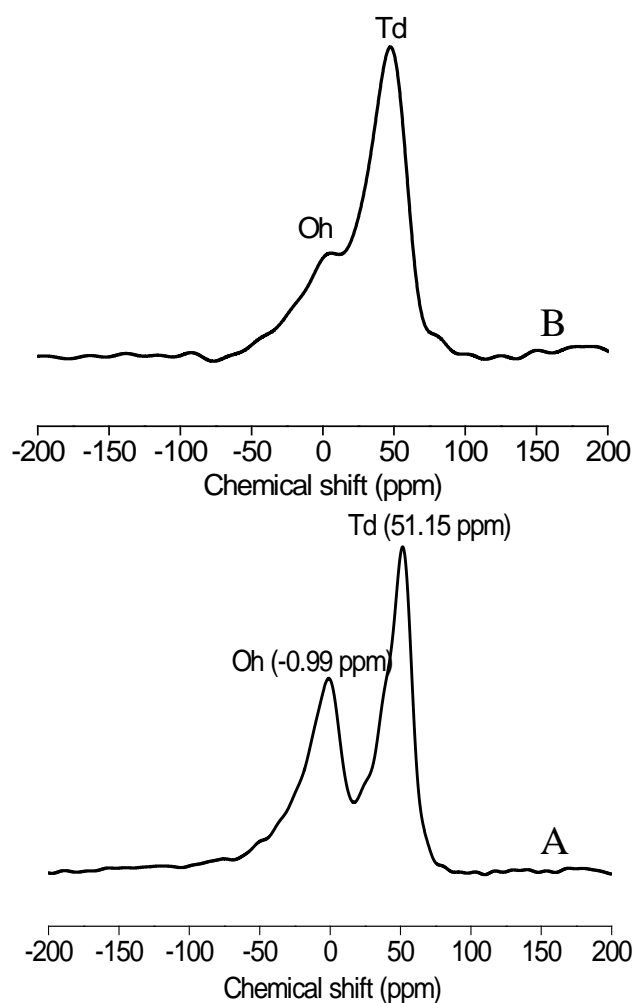


Figure 3B.16. ^{27}Al MAS NMR of $\text{SiO}_2\text{-Al}_2\text{O}_3$ catalyst A) fresh B) spent.

Characterizations revealed that the catalyst undergoes morphological changes however, it is important to note that still those are active in recycle runs. The structural changes happened in the case of spent $\text{SiO}_2\text{-Al}_2\text{O}_3$ catalyst is shown pictorially in the Figure 3B.17.

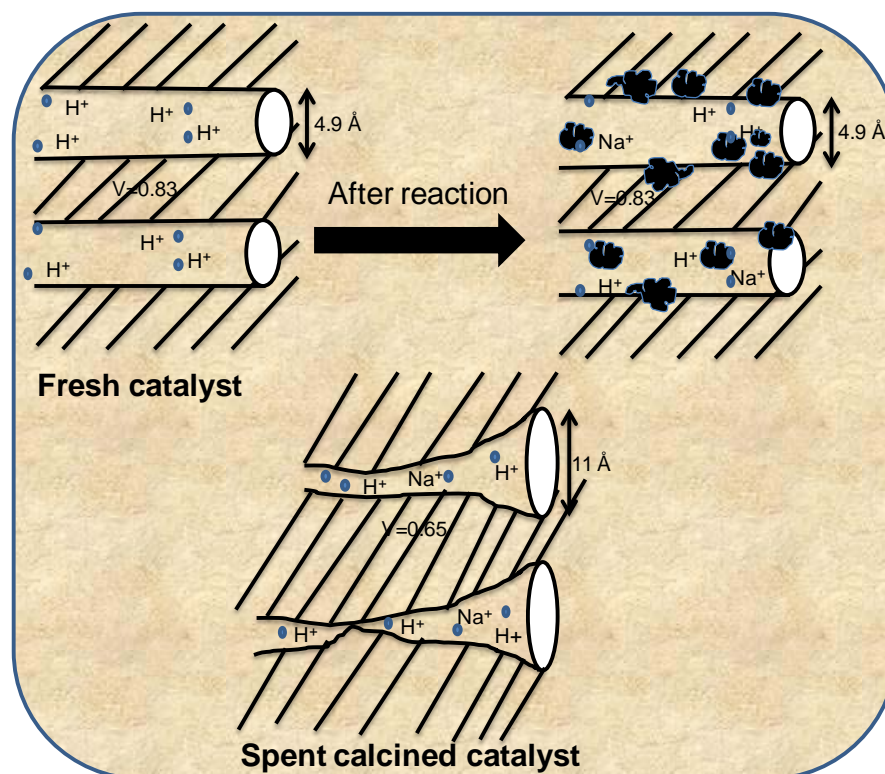


Figure 3B.17. Morphological changes occurred in $\text{SiO}_2\text{-Al}_2\text{O}_3$ catalyst after lignin depolymerization reaction.

3B.3. CONCLUSIONS

In summary, it is demonstrated that various actual lignin substrates can be converted below $250\text{ }^\circ\text{C}$ to aromatic monomers using solid acid catalysts with a very high yield of ca. 60 %. Even the lignin having molecular weight of $60,000\text{ gmol}^{-1}$ was successfully depolymerized into value added aromatic monomers with exceptionally high yield (60 %) over solid acid catalysts ($\text{SiO}_2\text{-Al}_2\text{O}_3$ ($\text{Si/Al} = 5.3$)) under inert atmosphere. All the lignins were completely characterized using various physico-chemical techniques. Confirmation of aromatic monomers formation and retention of functional groups, formation of new groups on products was examined by FTIR and NMR (^1H , ^{13}C) studies. Various types of solid acid catalysts were evaluated in my study ranging from crystalline to amorphous however it was difficult to establish the exact correlation between catalyst property and activity. Catalyst characterization showed the deformation happening in the case of crystalline solid acids. From the study done on lignin substrates like organosolv and ORG lignin it was understood that

SiO₂-Al₂O₃, which is amorphous catalyst, can be effectively recycled with a slight decrease in the activity after each catalytic run. Optimization of reaction conditions was done in order to improve the aromatic monomer yield. Reaction conditions like temperature, pressure, reaction medium, reaction time, stirring speed were studied thoroughly and optimized to obtain selectively aromatic monomers. It was observed that at a temperature of 250 °C with 0.7 MPa N₂ at RT, in H₂O:CH₃OH (1:5 v/v, 30 mL) solvent system, at 30 min., 1000 rpm with SiO₂-Al₂O₃ catalyst maximum amount of aromatic monomers (58 %) can be obtained. The aromatic monomers obtained were isolated in pure form, from the complex mixture using column chromatography (3 nos.) and were well characterized. The optimized reaction conditions were employed for the depolymerization studies of several other kinds of lignin substrates (organosolv, alkali, ORG, EORG and bagasse) and they were also depolymerized successfully to aromatic monomers. Recyclability of SiO₂-Al₂O₃ was studied and it was observed that even the amorphous catalyst was getting deactivated. To study the reason behind deactivation, amorphous SiO₂-Al₂O₃ catalyst was well characterized after each recycle. From XRD and N₂ sorption analysis it was understood that there is an increase in the pore diameter of amorphous SiO₂-Al₂O₃ catalyst after the reaction. Also there was a reduction in surface area and pore volume according to N₂ sorption studies. NH₃-TPD analysis showed a decrease in the acid sites, which was partially due to the poisoning of Brönsted acid sites by the Na ions present in the dealkaline substrate. ICP-OES analysis showed that there was no leaching of Si and Al species from the catalyst even after the reaction, but ²⁹Si and ²⁷Al NMR showed a deformation in both Si and Al environment in the catalyst, which can also adversely affect the activity of the catalyst. From all these studies it was understood that even amorphous catalyst can undergo structural changes under the reaction conditions employed and also catalyst deactivation can be caused due to poisoning of the catalytic active sites by the contamination present in the lignin substrate (dealkaline lignin). Even the amorphous catalysts were undergoing few changes but were still found to be recyclable and gave high yield of aromatic monomers.

It is envisaged that future advancements in this field will be benefited by this study on the complete profile of lignin characterization, catalytic results, products isolation-characterization and catalyst characterizations.

3B.4. REFERENCES

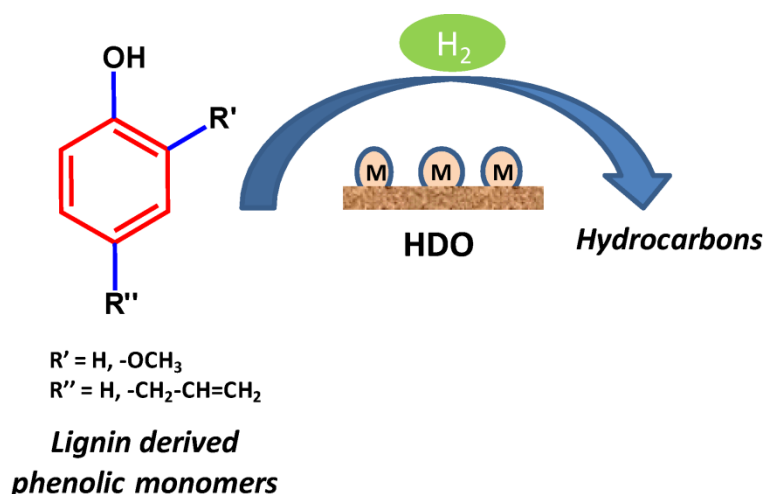
1. Deepa, A. K.; Dhepe, P. L., *RSC Adv.* **2014**, *4*, 12625-12629.
2. Singh, S. K.; Ekhe, J. D., *RSC Advances* **2014**, *4*, 53220-53228.
3. Long, J.; Zhang, Q.; Wang, T.; Zhang, X.; Xu, Y.; Ma, L., *Bioresour. Technol.* **2014**, *154*, 10-17.
4. Toledano, A.; Serrano, L.; Labidi, J.; Pineda, A.; Balu, A. M.; Luque, R., *ChemCatChem* **2013**, *5*, 977-985.
5. Xu, W.; Miller, S. J.; Agrawal, P. K.; Jones, C. W., *ChemSusChem* **2012**, *5*, 667-675.
6. Ye, Y.; Zhang, Y.; Fan, J.; Chang, J., *Ind. Eng. Chem. Res.* **2011**, *51*, 103-110.
7. Yan, N.; Zhao, C.; Dyson, P. J.; Wang, C.; Liu, L.-t.; Kou, Y., *ChemSusChem* **2008**, *1*, 626-629.
8. Li, J.; Henriksson, G.; Gellerstedt, G., *Bioresour. Technol.* **2007**, *98*, 3061-3068.
9. Toledano, A.; Serrano, L.; Labidi, J., *Fuel* **2014**, *116*, 617-624.
10. Fang, Z.; Sato, T.; Smith Jr, R. L.; Inomata, H.; Arai, K.; Kozinski, J. A., *Bioresour. Technol.* **2008**, *99*, 3424-3430.
11. Xu, M.; Lunsford, J. H.; Goodman, D. W.; Bhattacharyya, A., *Appl. Catal., A* **1997**, *149*, 289-301.
12. Khandanl, N. K.; Aghaziarati, M., *Iran. J. Chem. Chem. Eng.* **2009**, *6*, 1-11.
13. Ivanova, S.; Vanhaecke, E.; Louis, B.; Libs, S.; Ledoux, M.-J.; Rigolet, S.; Marichal, C.; Pham, C.; Luck, F.; Pham-Huu, C., *ChemSusChem* **2008**, *1*, 851-857.
14. Voitl, T.; Rudolf von Rohr, P., *ChemSusChem* **2008**, *1*, 763-769.
15. Barta, K.; Warner, G. R.; Beach, E. S.; Anastas, P. T., *Green Chem.* **2014**, *16*, 191-196.
16. Singh, S.; Varanasi, P.; Simmons, B. Renewable aromatics from lignocellulosic lignin. WO2014089574 A1, June 12, 2014.
17. Vigneault, A.; Johnson, D. K.; Chornet, E., *Can. J. Chem. Eng.* **2007**, *85*, 906-916.
18. Sanz, J.; Fornes, V.; Corma, A., *J. Chem. Soc., Faraday Trans. 1* **1988**, *84*, 3113-3119.
19. Gore, K. U.; Abraham, A.; Hegde, S. G.; Kumar, R.; Amoureux, J.-P.; Ganapathy, S., *J. Phys. Chem. B* **2002**, *106*, 6115-6120.
20. McMillan, M.; Brinen, J. S.; Carruthers, J. D.; Haller, G. L., *Colloids Surf.* **1989**, *38*, 133-148.
21. Conner, W. C.; Vincent, R.; Man, P.; Fraissard, J., *Catal. Lett.* **1990**, *4*, 75-83.
22. Klinowski, J., *Annu. Rev. Mater. Res.* **1988**, *18*, 189-218.
23. Samoson, A.; Lippmaa, E.; Engelhardt, G.; Lohse, U.; Jerschke, H. G., *Chem. Phys. Lett.* **1987**, *134*, 589-592.

CHAPTER 4

**HYDRODEOXYGENATION OF
LIGNIN DERIVED AROMATIC
MONOMERS OVER SUPPORTED
METAL CATALYSTS**

4.1. INTRODUCTION

As discussed earlier, in my work depolymerization of lignin into aromatic monomers (60 %) was successfully performed using solid acid catalysts at $T \leq 250$ °C (Refer chapter 3, section 3A.3.1).¹⁻² The main application of these aromatic monomers mixture is that those can be used as fuel additives or octane enhancers. But one of the hurdle associated with these lignin derived aromatic monomers is that they have very high oxygen content (27 %, $(C_{9.5}H_{11}O_3)$ O/C ratio = 0.42) (Refer chapter 3A, section 3A.3.2.3), which may adversely affect their use as fuel additives of octane enhancers. So these aromatic monomers have to be upgraded to reduce the oxygen content by subjecting to hydrodeoxygenation reactions (HDO)³⁻⁸ before those can be used as transportation fuels.⁹⁻¹³ It was observed that most of the lignin derived aromatic monomers consists of several substitutions such as, alkyl, alkoxy, hydroxyl, olefinic double bonds etc. (Refer chapter 3A, Figure 3A.6). Hence in the upgrading reactions of these types of compounds, there exists a competition between HDO and hydrogenation (reduction) of double bond or ring or aldehyde or ketone groups. It is widely assumed that the phenolic compounds such as guaiacol, phenol, syringol, eugenol etc. are best compounds to examine the HDO activity of catalysts (Scheme 4.1) since similar type of compounds are obtained in lignin depolymerization reactions.



Scheme 4.1. Hydrodeoxygenation (HDO) of lignin derived aromatic monomers into hydrocarbons.

Researchers have made several attempts to produce low or no oxygen containing products from lignin derived aromatic monomers. From literature reports it was observed that earlier studies on HDO reactions were performed on model

compounds (aromatic monomers) (e.g. phenol) using conventional sulphided CoMo or NiMo based catalysts above 300 °C. Though effective in giving HDO activity, these catalysts were known to have several drawbacks like coke formation, low water tolerance and sulfur contamination which were responsible to reduce their catalytic activities.¹⁴⁻²⁰ Consequently, instead of these catalysts, supported metal catalysts (metal=Fe, Cu, Ni, Mo, Co, W, Re, Pt, Ru, Pd etc.; support = C, γ -Al₂O₃, H-ZSM-5, SiO₂-Al₂O₃) were evaluated for their HDO activity.^{19, 21-29} From the literature it was understood that HDO activity can be enhanced by the use of mixed catalysts which are combination of supported metals and acid catalysts.³⁰⁻³⁵ Initially homogeneous acids (H₃PO₄) were used in combination with supported metals (Pd/C and H₃PO₄) as HDO catalysts for the conversion of lignin derived aromatic monomers (phenols, guaiacols, and syringols) into hydrocarbons.³¹ But to avoid the drawbacks associated with the homogenous acids those were replaced by solid acids (e.g. Nafion/SiO₂, H-ZSM-5).^{22,35}

Subsequently from literature reports it was understood that bifunctional noble metal catalysts can be a good selection for HDO study of lignin derived compounds. Also it was found that there is a lack of systematic study on HDO reactions (Refer chapter 1, section 1.9). For instance, in guaiacol HDO reactions using Ru/HZSM-5 catalyst after 4 h at 200 °C, cyclohexane was obtained as a main product (93 %),³⁶ but under the same reaction conditions if Ru/C was used as a catalyst then cyclohexanol was obtained as the final product (70 %).³⁷ Also it was observed that if guaiacol HDO is done using Ru/C catalyst at 250 °C the major product observed is methoxy cyclohexanol (60 %).¹⁹ It was also seen that in guaiacol HDO study if a base (MgO) is added along with Ru/C catalyst then at relatively milder reaction condition (160 °C, 2 h) maximum yield for cyclohexanol (80 %) can be obtained.³⁸ These reports shows that variation in temperature, time and support alters the course of reaction.²³ Considering this, it is very important to check the activities of different catalysts under similar reaction conditions to illustrate how catalysts will show difference in their HDO activities.

In this chapter I have made discussions on the HDO studies performed on lignin derived aromatic monomers like phenol, guaiacol, eugenol and mixture of these compounds using bifunctional supported metal catalysts under similar reaction conditions.³⁹ These catalysts were prepared by impregnation method with 2-3.5 wt%

of metal loading (Refer chapter 2B, section 2B.4.2.2 and Table 2B.4). Effect of metal on HDO reactions was studied by impregnating Pt, Pd and Ru on various supports. It was also understood from the earlier reports that depending on the combinations of metals and supports used in the work the course of the reaction was decided to yield either partially hydrogenated or fully hydrogenated products. So I have chosen various supports such as, acidic [Al_2O_3 (AL), $\text{SiO}_2\text{-Al}_2\text{O}_3$ (SA)], neutral [carbon (C)], and basic [hydrotalcite (HT)] and studied their effects in phenol, guaiacol and eugenol HDO reactions. Acidic supports (SA, AL) were chosen since they are known to cleave C-O bonds and that neutral (C), and basic supports (HT) were studied since those can possibly reduce the coke formation on the catalysts. This in turn may increase the catalyst life. In HDO studies of phenol, guaiacol and eugenol compounds, I have purposefully selected 250 °C as the reaction temperature, since lignin depolymerization reactions were also performed at this temperature (Refer chapter 3, section 3A.3.1). Therefore I presume that understanding of the catalytic reactions of lignin derived-aromatic compounds under the same reaction conditions may assist in the better understanding of the reaction network. Also in order to verify which factors influence the course of reaction further investigations on several reaction parameters like temperature (200-250 °C), pressure (1-3 MPa H_2) and time (1-6 h) were carried out.

4.2. EXPERIMENTAL

4.2.1. Catalyst synthesis

All the catalysts were prepared by impregnation method. Pt, Pd and Ru metals were loaded (2-3.5 wt%) on $\text{SiO}_2\text{-Al}_2\text{O}_3$ (Si/Al = 5.3), $\gamma\text{-Al}_2\text{O}_3$, C and HT supports. More details on materials and synthesis procedure used for the preparation of supported metal catalysts are included in chapter 2B (Refer chapter 2B; section 2B.2.2, 2B.3.3). Preparation of hydrotalcite by co-precipitation method was also discussed in chapter 2B (Refer section 2B.3.2).

4.2.2. Hydrodeoxygenation of lignin derived aromatic monomers

Substrates, guaiacol (99 %, Loba Chemie), phenol (99.5 %, Aldrich) and eugenol (99 %, Aldrich), were purchased and used as received. Solvent, n-hexadecane (99 %, Aldrich) was purchased and used as received. Products, 2-methoxy cyclohexanol (99

%, Alfa Aesar), cyclohexane (99 %, Loba Chemie), cyclohexanol (99.5 %, Loba Chemie), 4-propyl phenol (99 %, TCI chemicals) and 4-propyl cyclohexanol (> 98 %, Loba Chemie) were purchased and used as calibration standards for GC analysis.

All the reactions were carried out in a 50 mL batch mode high temperature and high pressure Amar make autoclaves. Supported metal catalysts used were synthesized by impregnation method with 2-3.5 wt% of metal loading (Refer chapter 2B, section 2B.4.2.2., Table 2B.5). For hydrodeoxygenation studies of phenol and eugenol the following reaction procedure was employed. Phenol (2 mmol) or eugenol (2 mmol), catalyst (2-3.5 wt% metal, S/C = 200 mole ratio) and hexadecane (30 mL) were charged in an autoclave. In case of hydrodeoxygenation of guaiacol following procedure was employed. Guaiacol (12 mmol), catalyst (2-3.5 wt% metal, S/C = 214 mole ratio) and hexadecane (30 mL) were charged in an autoclave. In all the reactions, after charging substrate, solvent and catalyst to the autoclave, H₂ gas was charged with Initial pressure of 1-3 MPa (at RT). Reactions were performed at 200-250 °C for 1-6 h. Initially, the rpm was kept at 100 and after attaining the desired reaction temperature it was increased to 1000 and this time was considered as the starting time of the reaction. Online sampling was done at 1 h and 3 h. The reactions were repeated at least 2 times in order to check the reproducibility of results. After the reaction, reactor was cooled and the catalyst was recovered by centrifugation. Further, the recovered catalyst was washed with acetone, dried in oven at 60 °C for 12 h and then again was dried at 150 °C for 2 h under vacuum (10⁻⁴ MPa). After this, the recovered catalyst was calcined (O₂, 20 mLmin⁻¹) and reduced at 400 °C (H₂, 20 mLmin⁻¹) each for 2 h and was used for next reaction.

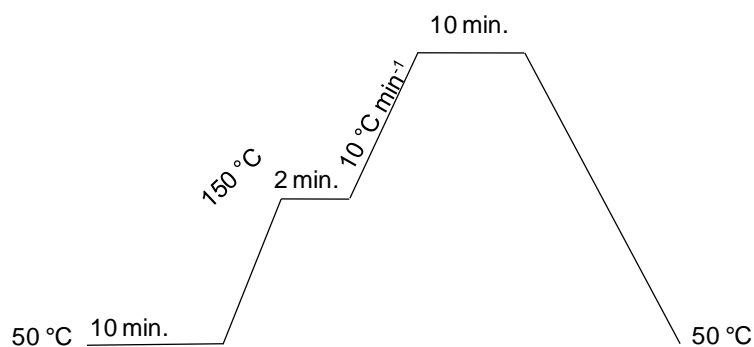
4.2.3. Analysis

Before analysis of reaction mixtures, standard compounds were injected on GC-FID and GC-MS to draw a calibration curve with a ± 2 % error.

4.2.3.1. GC-FID

Reaction mixtures were analyzed using an Agilent Gas Chromatograph (GC) equipped with a HP-5 capillary column (5 % phenyl 95 % dimethyl polysiloxane) (0.32 mm i.d. x 50 m length) and flame ionization detector (FID). N₂ is used as a carrier gas with a flow rate of 0.6 mLmin⁻¹. Injector was maintained at 275 °C and detector temperature

was set at 280 °C. Split mode injector (40:1) was used for sample delivery. Column oven program used was as follows,



4.2.3.2. GC-MS

The molecular weights of the products present in the reaction mixture were checked using Varian 3800 GC-MS, (Saturn 2000MS) equipped with VF-5 capillary column (5 % phenyl 95 % dimethyl polysiloxane) (0.25 mm i.d. x 30 m length). Helium with a flow rate of 0.6 mLmin⁻¹ was used as carrier gas. Column oven program and injector temperature were similar to that used in GC-FID analysis. From the m/z values observed in the fragmentation pattern and also matching those with NIST (version 05) library present in GC-MS, the molecular weights of the corresponding compounds were determined.

4.2.4. Conversion, selectivity and yield calculation

The conversion, selectivity and yields were calculated based on the calibration standards in GC analysis (mol basis) and the formulae used were as follows,

$$\text{Conversion (\%)} = [(\text{Substrate})_{\text{charged}} - (\text{Substrate})_{\text{final}} / (\text{Substrate})_{\text{charged}}] \times 100$$

$$\text{Selectivity (\%)} = [\text{No. of moles of product formed} / \text{No. of moles of substrate converted}] \times 100$$

$$\text{Yield (\%)} = \text{Conversion} \times \text{Selectivity.}$$

4.3. RESULTS AND DISCUSSIONS

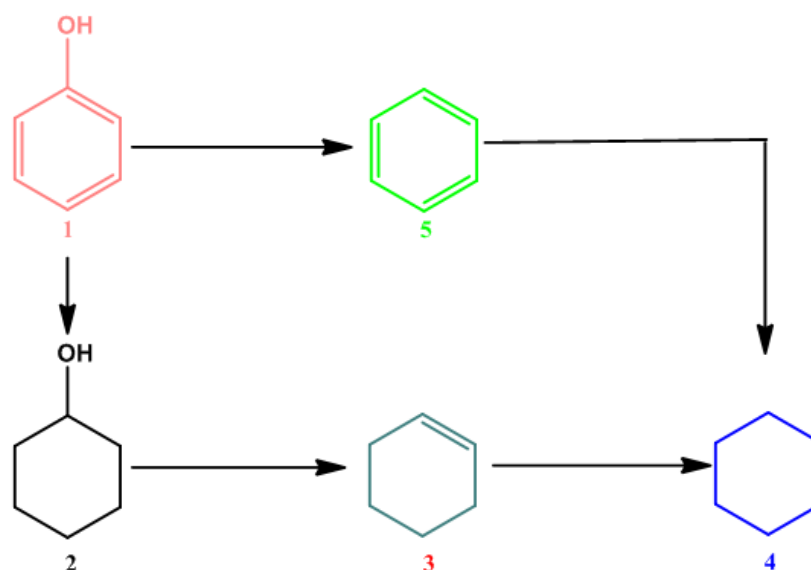
Hydrodeoxygenation (HDO) studies of phenol, guaiacol and eugenol substrates were done using supported metal catalysts. Supported metal catalysts were prepared by impregnating 2-3.5 wt% of noble metals (Pt, Pd and Ru) on various types of supports

like acidic ($\text{SiO}_2\text{-Al}_2\text{O}_3$ (SA), $\gamma\text{-Al}_2\text{O}_3$ (AL), neutral (carbon (C)) and basic (hydrotalcite (HT)) (Refer chapter 2B, section 2B.3.3). All these catalysts were characterized using various physico-chemical techniques. XRD analysis (Refer chapter 2B, Figure 2B.5) showed the characteristic peaks for all metals and supports. In some cases due to higher dispersion, metal peaks were not visible. From ICP-OES analysis it was confirmed that metal loading on supports were 2-3.5 wt% (Refer chapter 2B, section 2B.4.2.2. Table 2B.5). From NH_3 -TPD analysis it was observed that SA support has an acidity of 0.63 mmol g^{-1} and AL support has an acidity of 0.10 mmol g^{-1} . CO_2 -TPD analysis showed a basicity value of 0.88 mmol g^{-1} for HT support and C support was found to be neutral in nature. BET surface area of supported metal catalysts was determined using N_2 sorption analysis (Refer chapter 2B, section 2B.4.2.3). HDO of phenol, guaiacol and eugenol was carried out in hexadecane solvent at $T = 200\text{-}250 \text{ }^\circ\text{C}$, $P = 1\text{-}3 \text{ MPa H}_2$ and $t = 1\text{-}6 \text{ h}$ (Refer chapter 4, section 4.2.2).

4.3.1. Studies on HDO of phenol

Phenol was chosen as model compound to study the HDO reactions since it is a true representative of lignin derived aromatic monomers. Scheme 4.2 shows various possible pathways for phenol to undergo HDO reactions to yield various products. Phenol HDO reactions were performed using Pd and Pt metals loaded on acidic (SA) and neutral (C) supports at $250 \text{ }^\circ\text{C}$, 3 MPa H_2 pressure for 1 h. In the absence of catalyst under these conditions, phenol did not undergo any reaction. But when supported metal catalysts were used ca. 95-99 % phenol conversion was observed (Figure 4.1). All phenol HDO reactions were repeated 2-3 times with an error of $\pm 2 \%$. There was no coke and gas formation under the conditions employed for phenol HDO reactions and $90 \pm 10 \%$ mass balance was observed in all the reactions studied.

Phenol HDO results over supported metal catalysts showed that on acidic supports (SA) both Pd (90 %) and Pt (99 %) catalysts gave selectively cyclohexane (**4**) as major product (Figure 4.1). But with neutral support (C), both Pt (99 %) and Pd (99 %) catalysts gave cyclohexanol (**2**) as the major product. Therefore, cyclohexane (**4**) formation (deoxygenation reaction) happened only in presence of acidity (SA support). It was also important to note that phenol does not yield benzene irrespective of support or metal used for HDO conditions.



Scheme 4.2. Possible products formed in HDO of phenol.

Where ‘1’ is phenol, ‘2’ is cyclohexanol, ‘3’ is cyclohexene, ‘4’ is cyclohexane and ‘5’ is benzene.

It is already reported that deoxygenation happens faster from a saturated ring (cyclohexanol) than from an unsaturated ring (phenol), because C-O bond dissociation energy in phenol (1) (aromatic alcohol) (469 kJmol^{-1}) is greater than that of cyclohexanol (2) (secondary alcohol) (385 kJmol^{-1}).^{14, 40-41} Therefore during HDO reactions, phenol (1) will first undergo hydrogenation to obtain cyclohexanol (2), followed by deoxygenation to obtain cyclohexane (4). It was presumed that cyclohexanol (2) once formed undergoes dehydration to yield cyclohexene (3) in presence of an acidic support and is further hydrogenated to yield cyclohexane (4). Similar observations are also made in few of the earlier studies.^{31, 37} But here I could observe less yields for cyclohexanone and cyclohexene (3) during HDO reactions of phenol, which earlier studies have reported.^{31, 37} This was because hydrogenation of cyclohexene (3) and cyclohexanone formed during the reaction was found to be quite faster than the hydrogenation of phenol (1) and dehydration of cyclohexanol (2).⁴²

Therefore it can be concluded that overall reaction pathway for phenol HDO passes through formation of cyclohexanol (2) but interestingly, it stops at that stage over C supported catalysts (Pt and Pd) which does not have any acidity. This information showed that first step of ring hydrogenation is a metal catalyzed reaction however, further cleavage of C-O bond happens only when the support is acidic (SA).

Complete HDO activity achieved on these catalysts were found to be far better than the earlier works where cyclohexane (**4**) yield was very less (4 %) even when reactions were done at 400 °C over sulphided CoMo catalysts.^{3-4, 6, 8, 14, 43}

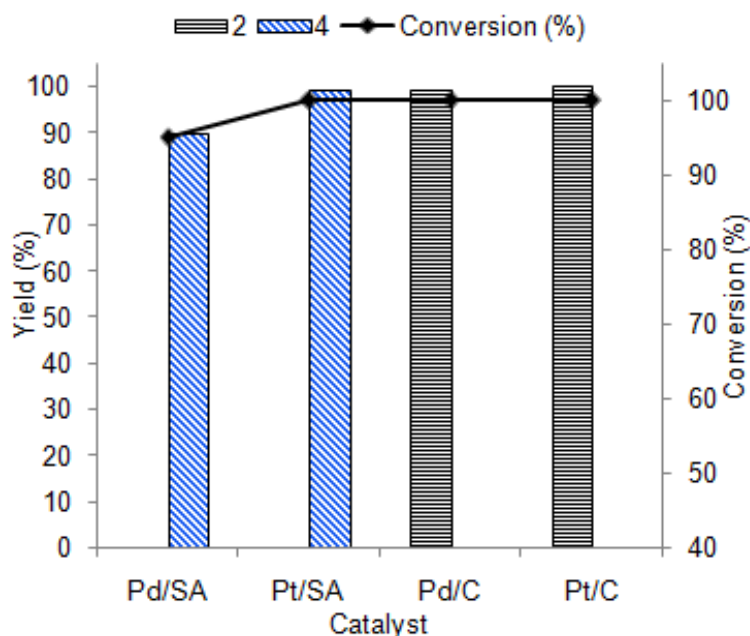


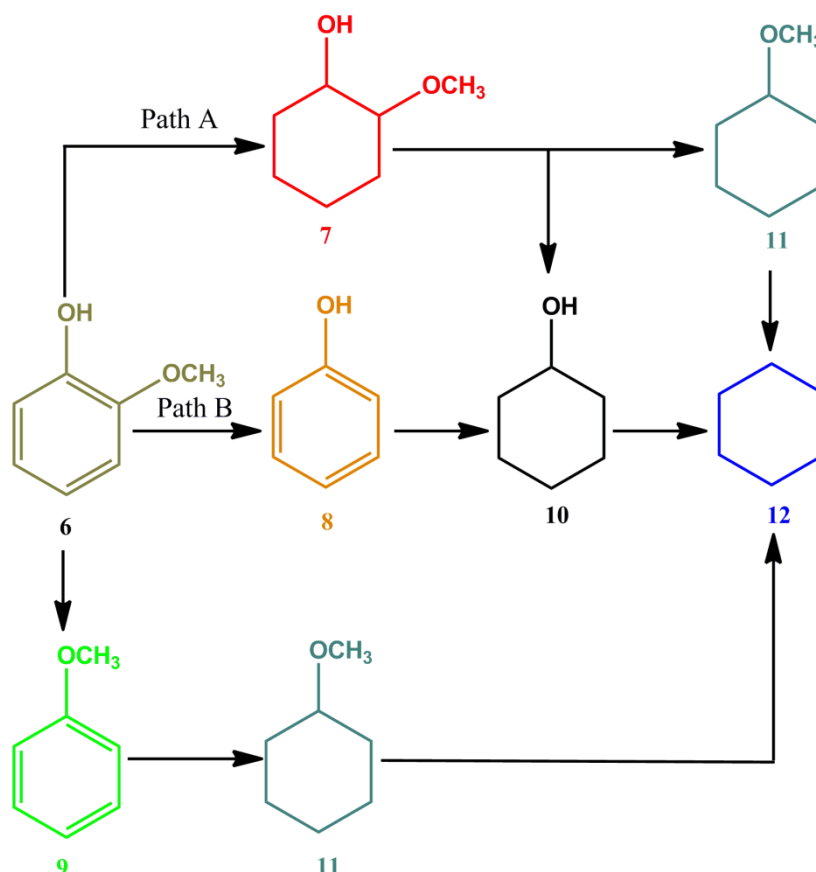
Figure 4.1. Phenol HDO studies over supported metal catalysts.

Where '2' is cyclohexanol and '4' is cyclohexane. Reaction conditions: Phenol (2 mmol), Catalyst (Substrate/Metal = 200 mole ratio), Hexadecane (30 mL), H₂ pressure at RT = 3 MPa, 250 °C, 1h. An error of ±2 % was observed in all the repeated reactions.

4.3.2. Studies on HDO of guaiacol

Hydrodeoxygenation studies over guaiacol were done using supported metal catalysts. Guaiacol substrate was chosen since it is also an example of lignin derived aromatic monomer. Scheme 4.3 represents the possible products formed from guaiacol (**6**) when it undergoes HDO reactions. Guaiacol HDO was performed using Pd, Pt and Ru metals supported on SA, AL, C, HT supports at 200-250 °C, 1-3 MPa H₂ for 1-6 h. According to the results obtained in phenol reactions, it was expected that first ring hydrogenation can happen in guaiacol to yield methoxycyclohexanol (**7**) as a product or else reaction can proceed by the removal of either -OCH₃ or -OH groups to yield products like phenol (**8**) or anisole (**9**), respectively. Further, phenol (**8**) or anisole (**9**) could be converted to cyclohexanol (**10**) and methoxycyclohexane (**11**), respectively.

Eventually, complete hydrodeoxygenation happens resulting in the formation of cyclohexane (**12**) as final product. Similarly, once methoxycyclohexanol (**7**) was formed it can yield methoxycyclohexane (**11**) or cyclohexanol (**10**) which can be further converted to cyclohexane (**12**).



Scheme 4.3. Possible products formed in HDO of guaiacol.

Where '6' is guaiacol, '7' is methoxycyclohexanol, '8' is phenol, '9' is anisole, '10' is cyclohexanol, '11' is methoxycyclohexane and '12' is cyclohexane.

4.3.2.1. Catalytic studies using Pd supported catalysts

Figure 4.2 summarizes the results obtained for guaiacol (**6**) HDO reactions over various supported Pd catalysts. It is very clear from the data that support plays an important role in determining the course of the reaction. For e.g. Over SA supported Pd catalyst, 52 % yield for cyclohexane (**12**) was observed with almost similar conversion of guaiacol (**6**), whereas on Pd/C catalyst, 100 % yield for methoxycyclohexanol (**7**) was observed. Additionally, with Pd/AL as a catalyst formation of cyclohexanol (**10**) (33 %), cyclohexane (**12**) (3 %) and

methoxycyclohexanol (**7**) (57 %) was observed. Pd supported on basic support (HT) gave methoxycyclohexanol (**7**) (86 %) as major product and formation of phenol (**8**), cyclohexane (**12**) was also observed in minor amounts. These results clearly elucidate that the product distribution of Pd supported catalysts varies according to the supports chosen. To understand these results, supports has to be well characterized. It was revealed from the NH₃-TPD and CO₂-TPD characterizations that SA has higher acid amount (0.63 mmol g⁻¹) compared to AL (0.10 mmol g⁻¹) and HT support showed 0.88 mmol g⁻¹ of basicity. Catalytic results imply that when the acidity of supports were increased from 0.10 mmol g⁻¹ (AL) to 0.63 mmol g⁻¹ (SA), formation of cyclohexane (**12**) was improved which means that acidic supports facilitate C-O bond cleavage. It was observed that AL supported catalyst showed formation of compounds in the series, methoxycyclohexanol (**7**) → cyclohexanol (**10**) → cyclohexane (**12**). This was against the general idea in the literature where it was suggested that guaiacol (**6**) was converted to phenol (**8**) and later from it cyclohexanol (**10**) and cyclohexane (**12**) (**8** → **10** → **12**) can be formed.^{20, 26, 44-46} In this work, absence of phenol (**8**) and anisole (**9**) and formation of methoxycyclohexanol (**7**), cyclohexanol (**10**) and cyclohexane (**12**) clearly showed that guaiacol first undergoes ring hydrogenation, followed by C-O bond cleavage. This can be explained on the basis of phenol HDO results where first, phenol undergoes ring hydrogenation to yield cyclohexanol (**2**) over neutral (C) support and afterwards over SA support it was possible to yield cyclohexane (**4**) by the cleavage of C-O bond (refer section 4.3.1). During deoxygenation reactions, a competition may exist between cleavages of -OH and -OCH₃ groups present in guaiacol molecule (**6**) that is which group will cleave first from the aromatic ring. Bond energy of -OH group (469 kJmol⁻¹) attached to ring is more than that of -OCH₃ group (418 kJmol⁻¹), therefore over acidic support, -OCH₃ group is removed first followed by the removal of -OH group but only product **10** (cyclohexanol) was observed and not product **11** (methoxycyclohexane). On contrary to Pd supported on acidic supports (SA and AL), Pd on the neutral support (C) was very selective towards methoxycyclohexanol (**7**) formation and no further conversion of it to cyclohexanol (**10**) or cyclohexane (**12**) happens. These results show that acidity was necessary to further the reactions of methoxycyclohexanol (**7**) but over neutral support only ring hydrogenation is possible. With Pd/HT catalyst also methoxycyclohexanol (**7**) was observed as a main product with very less concentration of products, phenol (**8**) and

cyclohexane (**12**). Absence of cyclohexanol (**10**) indicates that over base support there is no possibility of cleaving C-O bond ($-\text{OCH}_3$ or $-\text{OH}$). Particularly, with the formation of phenol (**8**) seen only with Pd/HT catalyst it seems that the catalyst is capable of taking another route for product formation compared to other catalysts.

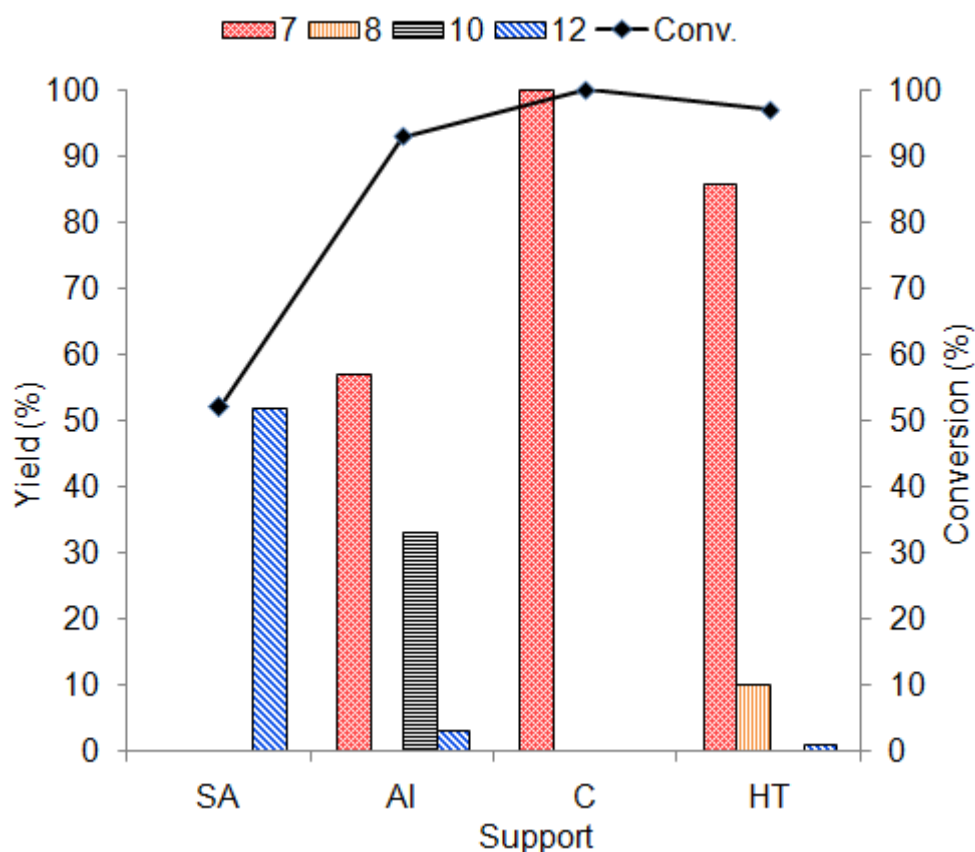


Figure 4.2. Effect of support on supported Pd catalysts in guaiacol HDO reactions.

Where **7** is methoxycyclohexanol, **8** is phenol, **10** is cyclohexanol and **12** is cyclohexane. Reaction conditions: Guaiacol (12 mmol), Catalyst (0.2 g), Hexadecane (30 mL), H_2 pressure at RT = 3 MPa, 250 °C, 1h. An error of ± 2 % was observed in all the repeated reactions.

The above results shows that with neutral (C) and acidic (SA, AL) supports path 'A' is chosen by guaiacol (**6**), but with basic support though main path is 'A' guaiacol can also choose 'path B' which is possible (Scheme 4.3).^{36, 47-51} Unlike in earlier reports where under acid free conditions and conducting reactions at 200 °C, hydrolysis of $-\text{OCH}_3$ group and formation of 1,2-cyclohexanediol was observed by methyl group migration.³⁷ In this work none of these products were observed over C

catalyst but 100 % selectivity to methoxycyclohexanol (**7**) was possible even when reactions were done at 250 °C. It is also possible that guaiacol (**6**) can undergo hydrolysis to form catechol but in this study it was not observed. Besides formation of observed products in all these reactions, there was a possibility of formation of cyclohexene by dehydration of cyclohexanol (**10**). But since the hydrogenation of cyclohexene was probable to happen very fast, hence only formation of product cyclohexane (**12**) was observed.

All the Pd catalysts showed differences in activity which may be due to the differences in the particle size of metal on supports. Hence, the average particle size of Pd on SA, AL, C and HT supports was measured by HRTEM analysis (Refer chapter 2B, section 2B.4.2.4, Table 2B.7). From HRTEM analysis it was understood that same metal on various supports showed variable particle size and dispersion. C supported Pd showed the smallest particle size (5 nm) and other supports like, SA (20 nm), AL (10 nm) and HT (15 nm) showed bigger particle size. However, it seems that the particle size was not playing any major role in these reactions since all the catalysts showed > 99 % conversions within 1 h of reaction and that the product distribution was different for all the catalysts. Additionally, particle size difference was also observed for Pt and Ru metals impregnated on the same support but there was no difference in their activity (Refer chapter 2B, section 2B.4.2.4, Table 2B.7).

The activity of all the catalysts was purposefully studied at definite time period (1 h) in order to compare the results under similar reaction conditions. I would like to highlight here that complete conversions were achieved on C and HT supported Pd catalysts and in both of these reactions methoxycyclohexanol (**7**) was obtained as major product which can still be converted to cyclohexanol (**10**) or cyclohexane (**12**). These products were not formed on Pd/C and Pd/HT catalysts but were observed on Pd/AL and Pd/SA catalysts, so it can be concluded that conversion levels are not important but metal supported on which support is vital to achieve the specific products. Due to this reason regardless of lower conversions on Pd/AL and Pd/SA catalysts further hydrogenation products were observed.

4.3.2.2. Effect of acidic support on guaiacol HDO reactions

To understand the effect of acidic support on the HDO studies, guaiacol reactions were performed using a physical mixture of Pd/C (neutral) and an acidic support (SA or AL). Table 4.1 summarizes the results obtained with the Pd/C + AL and Pd/C + SA catalytic systems. It was observed that if the reaction was performed with Pd/C + SA, the formation of methoxycyclohexanol (**7**), cyclohexanol (**10**), and cyclohexane (**12**) was possible. Similarly, with the Pd/C + AL catalyst also the formation of methoxycyclohexanol (**7**), cyclohexanol (**10**), and cyclohexane (**12**) was observed.

Table 4.1. Role of acidic support on the HDO of guaiacol

Catalyst	Acidic Support	Time [h]	Conversion [%]	Yield [%]			
				7	8	10	12
Pd/C	SA	3	88	2	0	48	36
		6	99	0	0	20	77
	AL	3	100	75	0	13	12
		6	100	42	0	14	44
	—	1	100	100	0	0	0

Where **7** is methoxycyclohexanol, **8** is phenol, **10** is cyclohexanol and **12** is cyclohexane. Reaction conditions: Guaiacol (12 mmol), 3 wt% Pd/C (0.2 g), SA or AL (0.1940 g), Hexadecane (30 mL), H₂ pressure at RT = 3 MPa, 250 °C, 3-6 h. An error of ± 2 % was observed in all the repeated reactions.

But when Pd/C catalyst was used methoxycyclohexanol (**7**) was formed selectively. This clearly indicates that the acidic support plays an important role in deciding the selectivity of the product. Moreover, the data presented in Table 4.1 also reveal that, depending on the acid support used (either AL or SA), the selectivity towards the formation of methoxycyclohexanol (**7**), cyclohexanol (**10**), and cyclohexane (**12**) changes.

4.3.2.3. Catalytic studies using Ru and Pt catalysts

Guaiacol HDO reactions were also studied using Pt and Ru metals loaded on SA, AL, C and HT supports for 1 h (Table 4.2). Pt/SA catalyst gave cyclohexane (**12**) (75 %) as the only product while Pt/C (80 %) and Pt/HT (47 %) showed the formation of methoxycyclohexanol (**7**) as the only product. As discussed earlier (section 4.3.2.1) Pd catalysts also showed product formation pattern similar to Pt catalysts.

Table 4.2. Guaiacol HDO over supported Ru and Pt catalysts

Support	Metal	Conversion [%]	Yield [%]			
			7	8	10	12
SA	Ru	61	0	7	0	54
	Pt	76	0	0	0	75
AL	Ru	66	5	5	11	29
	Pt	41	17	0	14	10
C	Ru	37	19	12	0	5
	Pt	87	80	0	0	0
HT	Ru	38	25	6	0	3
	Pt	49	47	0	0	0
Noncatalytic ^[a]		5	0	0	0	0

Where **7** is methoxycyclohexanol, **8** is phenol, **10** is cyclohexanol and **12** is cyclohexane. Reaction conditions: Guaiacol (12 mmol), Catalyst (0.2 g), Hexadecane (30 mL), H₂ pressure at RT = 3 MPa, 250 °C, 1h, [a]time = 6 h. An error of ± 2 % was observed in all the repeated reactions.

But there was a slight dissimilarity in the activity between Pt/AL and Pd/AL catalysts. Over Pt/AL, the major product observed was methoxycyclohexanol (**7**) (17 %) but formation of cyclohexanol (**10**) (14 %) and cyclohexane (**12**) (10 %) was also observed. But with Pd/AL catalyst, formation of methoxycyclohexanol (**7**) (57 %) was in high concentration whereas formation of cyclohexanol (**10**) (33 %) was lower (relative to formation of methoxycyclohexanol (**7**)) along with the formation of cyclohexane (**12**) (3 %). These results point out that while activity of Pd/AL catalyst for the cleavage of C-O bond resulting in the formation of cyclohexanol (**10**) and cyclohexane (**12**) products was lower but Pt/AL catalyst was active for the same.

A careful look at the Table 4.2 and Figure 4.1 reveals that except Pd/SA catalysts all other Pd supported catalysts were more active than the Pt catalysts for guaiacol HDO reactions. It was claimed in the earlier reports that over Pt/C catalyst, guaiacol (**6**) can give cyclohexanol (**10**) as a major product,³⁷ but under my reaction conditions only the formation of product, methoxycyclohexanol (**7**) was observed. Some reports also show that compared to Pd, Pt catalysts are more active in HDO reactions^{37, 52} but these results show that the Pt catalysts have lower activity than the Pd catalysts.²⁸ It is obvious that disagreements can happen since most of the earlier reports use different methods to synthesize catalysts and use different HDO reaction conditions to check their activities and comment on the activity difference. Due to this reason in this work, HDO activity of all supported metal catalysts was studied under similar reaction conditions.

Another remarkable observation was that supported Ru catalysts have difference in their activity compared to Pd and Pt catalysts (Table 4.2). Formation of phenol (**8**) was observed when Ru metal was supported on SA (7 %), AL (5 %), C (12 %) and HT (6 %) supports, which was absent when Pd and Pt catalysts were used, except for Pd/HT catalyst. This means that Ru catalyst may also follow 'path B' along with 'path A'. Another major activity difference was observed with Ru/AL catalyst. Similar to AL supported Pd and Pt catalysts Ru/AL also showed formation of methoxycyclohexanol (**7**), cyclohexanol (**10**) and cyclohexane (**12**) but difference lies in the fact that with Ru/AL catalyst, cyclohexane (**12**) yield was higher when compared to Pt and Pd based catalysts. This was mostly important since over Pd/AL catalyst only 3 % of cyclohexane (**12**) was formed with 93 % conversion but over Ru/AL catalyst with 66 % conversion 29 % yield for cyclohexane (**12**) was achieved. Guaiacol HDO over Ru/C even without any acidity showed the formation of phenol (**8**) and cyclohexane (**12**) along with formation of methoxycyclohexanol (**7**). This is completely dissimilar to the Pd/C and Pt/C catalysts in which selectively formation of methoxycyclohexanol (**7**) was observed. The formation of phenol (**8**) over Ru/C can be explained on the basis of guaiacol undergoing demethoxylation which was discussed earlier.³⁷ Typically, cleavage of C-O bond is observed over acidic supports but rather surprisingly Ru/C showed an activity towards bond cleavage. From my results it was observed that even in the absence of acidity in the case of Ru supported catalyst deoxygenation happens. This can be explained based on the oxygen binding

energy of Ru metal ($\Delta E_0 = -0.01$ eV) which was higher when compared to Pd and Pt.⁵³ As a result Ru catalysts have greater affinity towards oxygen atom present in the guaiacol support and helps in the easy deoxygenation when compared to Pt and Pd catalysts.

4.3.2.4. Effect of time on the guaiacol HDO reactions

To study the effect of time on guaiacol HDO using supported metal catalysts, reactions were carried out from 1 h to 6 h. Table 4.3 summarizes the time study results for all the catalysts. With increase in time from 1 h to 6 h an increase in guaiacol conversion was observed which may be due to the increase in contact time between reactant and catalyst. SA supported metal catalysts did not show any change in the selectivity with the increase in time as always cyclohexane (**12**) was observed as major product. With AL support, for all the catalysts when time was increased from 1 h to 6 h, the concentration of methoxycyclohexanol (**7**) started increasing. As mentioned earlier, it was possible that first methoxycyclohexanol (**7**) was formed which later was converted into cyclohexanol (**10**) and then to cyclohexane (**12**). This suggestion was supported by the time study where typically concentration of methoxycyclohexanol (**7**) was formed in the reaction mixture which ultimately reduces with increase in concentration of cyclohexanol (**10**) and later cyclohexane (**12**) as time progresses. Similar trend was also observed for Ru/HT catalyst and in case of Pt/HT catalyst with increase in time though conversions increased, product methoxycyclohexanol (**7**) remained stable and gave > 90 % selectivity to the product.

Table 4.3. Time study for guaiacol HDO reactions using various supported metal catalysts

Support	Metal	Time [h]	Conversion [%]	Yield [%]			
				7	8	10	12
SA	Pd	1	52	0	0	0	50
		3	78	0	0	0	75
		6	88	0	0	0	85
	Pt	1	76	0	0	0	75
		3	84	0	0	0	80
		6	96	0	0	0	90
	Ru	1	61	0	7	0	54
		3	68	0	7	0	61
		6	82	0	8	0	73
Al	Pd	1	93	57	0	33	3
		3	96	77	0	17	2
		6	98	34	0	41	24
	Pt	1	41	17	0	14	10
		3	50	14	0	15	20
		6	70	25	0	20	25
	Ru	1	66	5	5	11	29
		3	97	54	0	12	30
		6	98	13	0	51	35
C	Pd	1	100	90	0	0	0
	Pt	1	87	80	0	0	0
	Ru	1	37	19	12	0	5
		3	55	27	17	0	11
		6	95	28	30	0	36
HT	Pd	1	97	85	10	0	1
		1	49	47	0	0	0
	Pt	3	60	50	0	0	0
		6	90	85	0	0	0
	Ru	1	38	25	6	0	3
		3	39	13	2	16	2
		6	90	28	8	39	15

Where **7** is methoxycyclohexanol, **8** is phenol, **10** is cyclohexanol and **12** is cyclohexane. Reaction conditions: Guaiacol (12 mmol), Catalyst (0.2g), Hexadecane (30 mL), H₂ pressure at RT = 3 MPa, 250 °C, 1-6 h. An error of ± 2 % was observed in all the repeated reactions.

4.3.2.5. Effect of temperature and pressure on guaiacol HDO reactions

To probe the effect of temperature on HDO of guaiacol, reactions were carried out at 200-250 °C temperature range and 3 MPa hydrogen pressure using Pd/SA catalyst since it has shown good HDO activity and the results are tabulated in Table 4.4. It was evident from the results that at 200 °C, there was no guaiacol (**6**) conversion (0 %) even after 6 h reaction time. But when temperature was increased to 230 °C guaiacol starts converting (65 %) into cyclohexanol (10 %) which was further converted to cyclohexane (**6**). But at 250 °C whole of cyclohexanol (**11**) was completely converted into cyclohexane (**6**) (Figure 4.3). This was because with increase in temperature (200 °C to 230 °C) the substrate molecules might have gained enough kinetic energy which helps to overcome the energy barrier or activation energy for the reaction to happen and also temperature increase will help to enhance the collision rate of the molecules, as a result reactions happen. In all the reactions, cyclohexane (**12**) was observed as major product. However, at 230 °C a small amount (10 %) of cyclohexanol (**10**) was observed after 3 h reaction. These results are in good correlation with the literature²³ however; there are few reports where it is shown that HDO of guaiacol can happen even at 200 °C using Pd catalyst.^{22, 32-33}

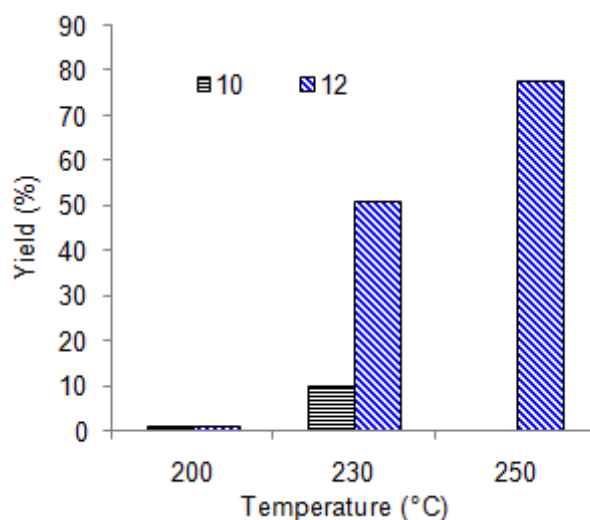


Figure 4.3. Effect of temperature on guaiacol HDO reactions using Pd/SA catalyst.

Where ‘**10**’ is cyclohexanol and ‘**12**’ is cyclohexane. Reaction conditions: Guaiacol (12 mmol), Pd/SA (0.2 g), Hexadecane (30 mL), H₂ pressure at RT = 3 MPa, 200-250 °C, 3 h. An error of ± 2 % was observed in all the repeated reactions.

But in these works large quantities of additional acids (H-ZSM-5, H₃PO₄) were used along with high hydrogen pressures (5 MPa) that may be influencing the catalytic behaviour.^{22, 32-33}

Table 4.4. Effect of temperature on guaiacol HDO reactions using Pd/SA catalyst

Temperature [°C]	Time [h]	Yield [%]			
		7	8	10	12
200	3	0	0	0	0
	6	0	0	0	0
230	3	0	0	10	51
	6	0	0	0	75
250	3	0	0	0	78
	6	0	0	0	88

Where **7** is methoxycyclohexanol, **8** is phenol, **10** is cyclohexanol and **12** is cyclohexane. Reaction conditions: Guaiacol (12 mmol), Pd/SA (0.2g), Hexadecane (30 mL), H₂ pressure at RT = 3 MPa, 200-250 °C, 3-6 h. An error of ± 2 % was observed in all the reactions.

In order to explore the consequences of change in hydrogen pressure on the product formation, guaiacol HDO reactions were carried out at pressures like 1, 2 and 3 MPa using Pd/SA catalyst at 250 °C for 3-6 h. At 1 MPa pressure, cyclohexanol (**10**) was formed along with cyclohexane (**12**). But it was observed that with the increase in pressure from 1 to 2 MPa, cyclohexanol (**10**) formed was completely disappeared and an enhancement in the rate of product formation (**12**) was observed but it remained almost constant when pressure was further increased to 3 MPa (Figure 4.4). It was observed that, increase of hydrogen pressure accelerates the rate of guaiacol conversions into cyclohexanol (**10**) which is further converted to cyclohexane (**12**).

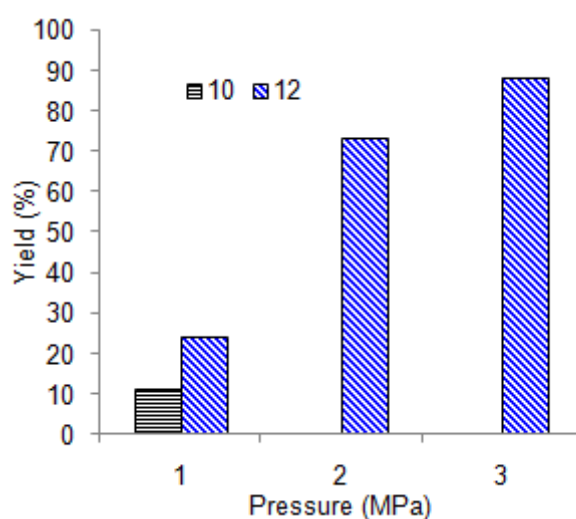


Figure 4.4. Effect of hydrogen pressure on guaiacol HDO reactions using Pd/SA catalyst.

Where '10' is cyclohexanol and '12' is cyclohexane. Reaction conditions: Guaiacol (12 mmol), Pd/SA (0.2 g), Hexadecane (30 mL), H₂ pressure at RT = 1-3 MPa, 250 °C, 3-6 h. An error of ± 2 % was observed in all the repeated reactions.

Table 4.5. Effect of hydrogen pressure on guaiacol HDO reactions using Pd/SA catalyst

Pressure [MPa]	Time [h]	Yield [%]			
		7	8	10	12
1	3	0	0	11	24
	6	0	0	10	52
2	3	0	0	0	73
	6	0	0	0	82
3	3	0	0	0	78
	6	0	0	0	88

Where '7' is methoxycyclohexanol, '8' is phenol, '10' is cyclohexanol and '12' is cyclohexane. Reaction conditions: Guaiacol (12 mmol), Pd/SA (0.2 g), Hexadecane (30 mL), H₂ pressure at RT = 1-3 MPa, 250 °C, 3-6 h. An error of ± 2 % was observed in all the repeated reactions.

4.3.2.6. Catalyst recyclability

The reusability of Pd/SA and Ru/SA catalysts was studied for HDO reaction of guaiacol and the results are presented in Figures 4.5a and 4.5b.

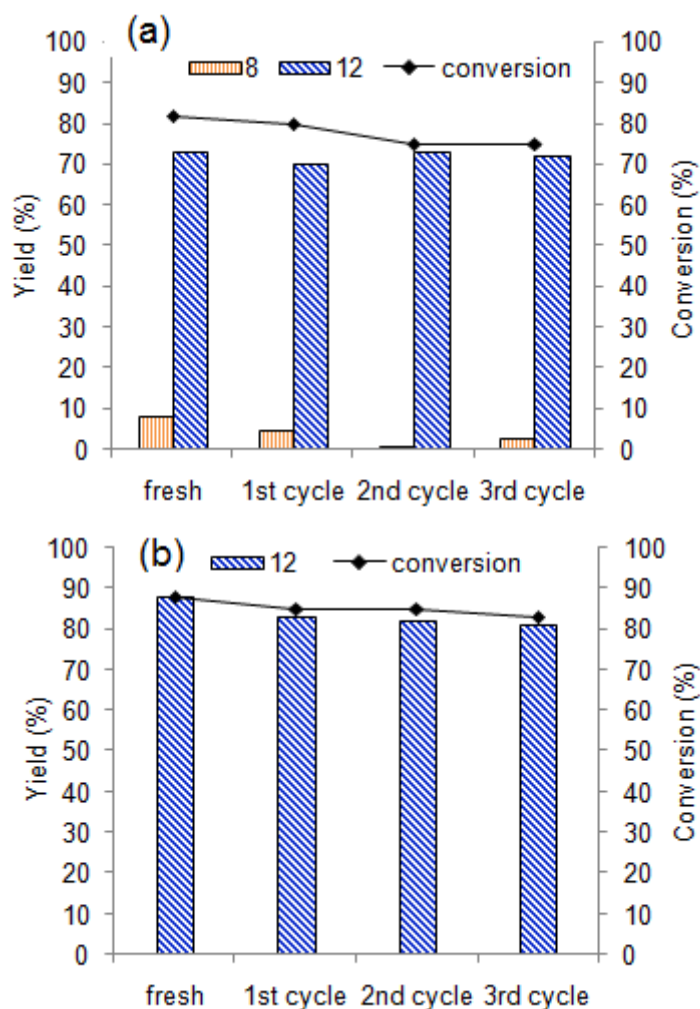


Figure 4.5. Recycle study with (a) Ru/SA and (b) Pd/SA for guaiacol HDO reactions. Where '8' is phenol and '12' is cyclohexane. Reaction conditions: Guaiacol (12 mmol), Ru/SA or Pd/SA (0.2 g), Hexadecane (30 mL), H_2 pressure at RT = 3 MPa, 250 °C, 6 h. An error of ± 2 % was observed in all the reactions.

After reaction, catalyst was recovered by centrifugation, washed with acetone and dried in oven for overnight (12 h), calcined in air (20 mLmin^{-1}), reduced under hydrogen flow (20 mLmin^{-1}) at 400 °C for 2 h and was subjected to the next run. As observed from Figure 4.5a, Ru/SA catalyst showed almost similar activity with the selectivity to product 12 with a yield of 70-72 % which remains constant in all the recycle runs.

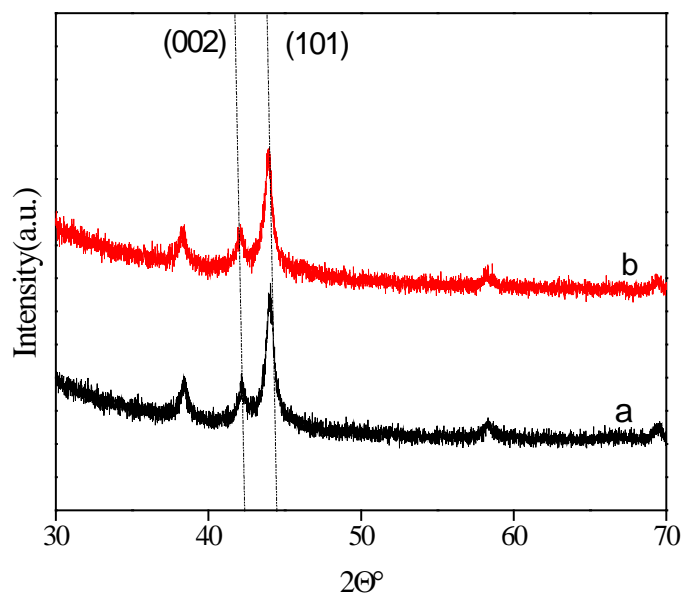


Figure 4.6. XRD patterns of Ru/SA catalyst (a) fresh (b) spent.

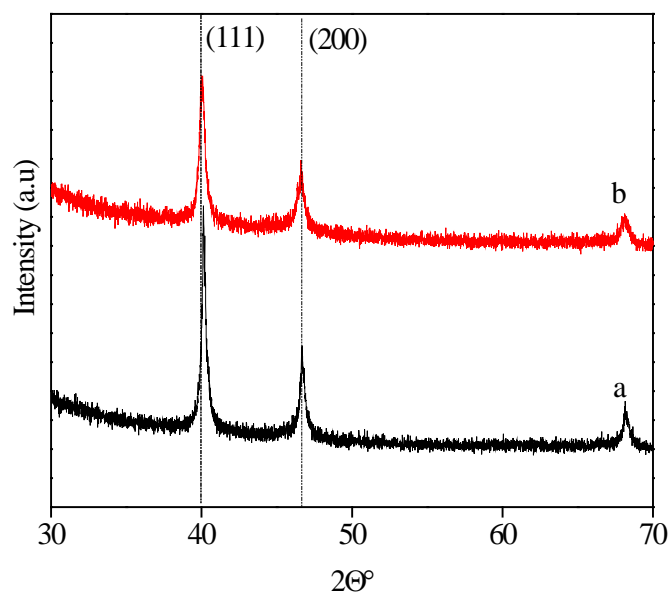


Figure 4.7. XRD patterns of Pd/SA catalyst (a) fresh (b) spent.

Over Pd/SA catalyst also similar activity with ca. 88 % of yield for product was observed in all the runs (Figure 4.5b). These catalytic observations imply that the catalysts are recyclable and are stable under reaction conditions. Also fresh and spent catalysts were characterized by XRD technique and I found no difference in the peak pattern (Figure 4.6 and 4.7). Furthermore by ICP-OES technique it was found out that there was no leaching of the metal from the catalyst.

4.3.2.7. Reaction pathway for guaiacol HDO reactions using supported metals

From the above set of data the reaction network for the Pd, Pt and Ru catalysts (Figures 4.8, 4.9, 4.10) is proposed. As observed, support plays an important role in deciding the course of reaction. Metals dispersed on a strong acidic support, SA gave cyclohexane (**12**) as the main product. Due to less acidity of the support, AL the acid catalyzed C-O bond cleaved products were reduced and methoxycyclohexanol (**7**) and cyclohexanol (**10**) along with cyclohexane (**12**) were observed as products. With a neutral support except for Ru catalyst, both Pd and Pt catalysts gave only methoxycyclohexanol (**7**). These results indicate that higher acidity was required for C-O bond cleavage and that under the reaction conditions it was possible to attain cyclohexane (**12**) with 100 % selectivity. In absence of any acidity (C), catalysts gave product methoxycyclohexanol (**7**) with 100 % selectivity. The mildly acidic support (AL) will surely give mixed products hence may not be the support of preference. The basic support (HT) can also selectively give methoxycyclohexanol (**7**) as a major product. It is reported in the literature³⁸ that in the presence of base, the major product obtained is cyclohexanol (**10**) and that presence of base can suppress hydrolysis of –OCH₃ group and cyclohexane (**12**) formation.

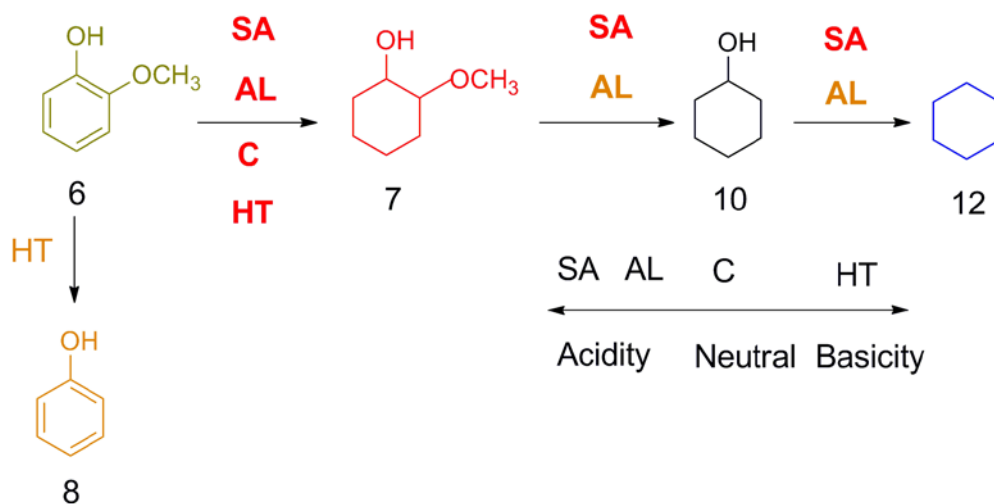


Figure 4.8. Proposed reaction pathway for supported Pd catalysts in guaiacol HDO reactions.

It was also proposed that in presence of base, reaction can proceed through phenol formation to cyclohexanol. However, my experimental results are bit conflicting to these observations. In my work as mentioned earlier, major product is not cyclohexanol (**10**) but it was methoxycyclohexanol (**7**). Nevertheless, my observations

agree with the possibility of formation of phenol (**8**) as a product in presence of base as reported earlier.³⁸

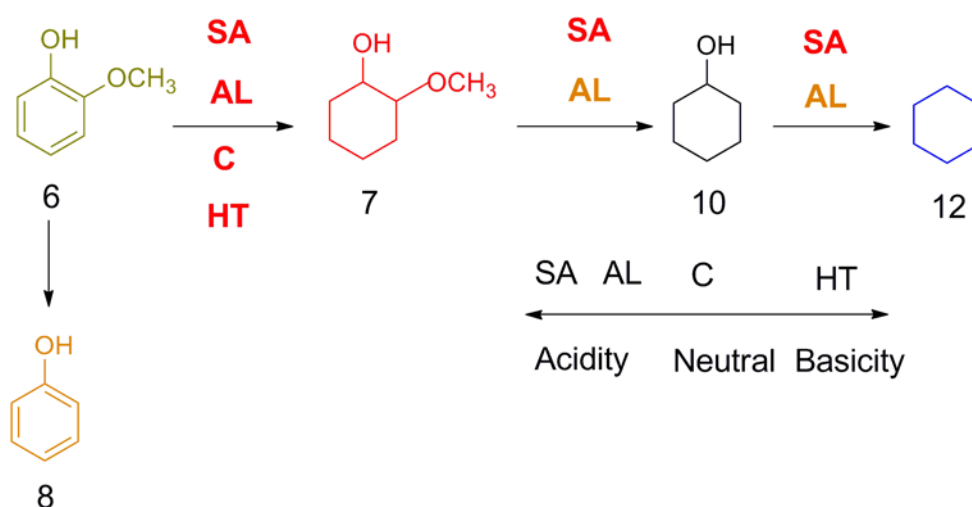


Figure 4.9. Proposed reaction pathway for supported Pt catalysts in guaiacol HDO reactions.

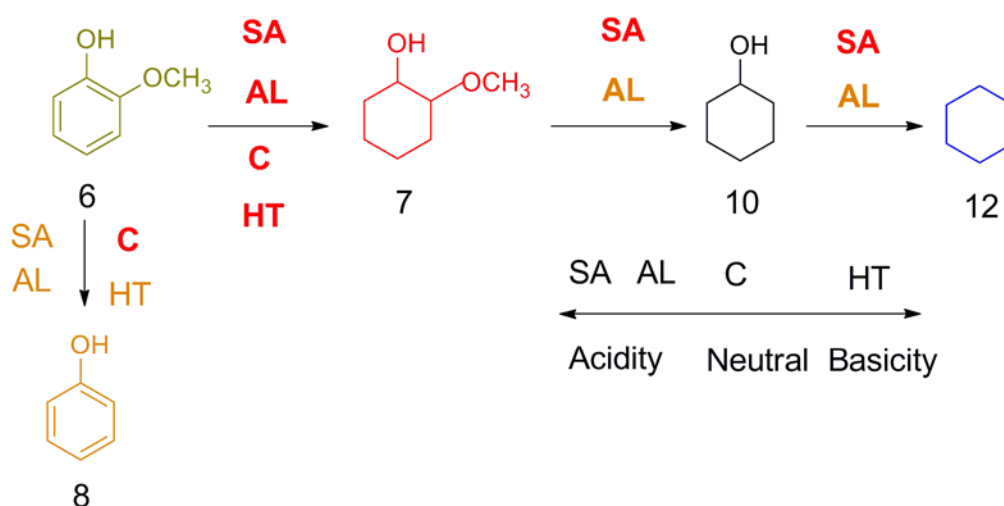
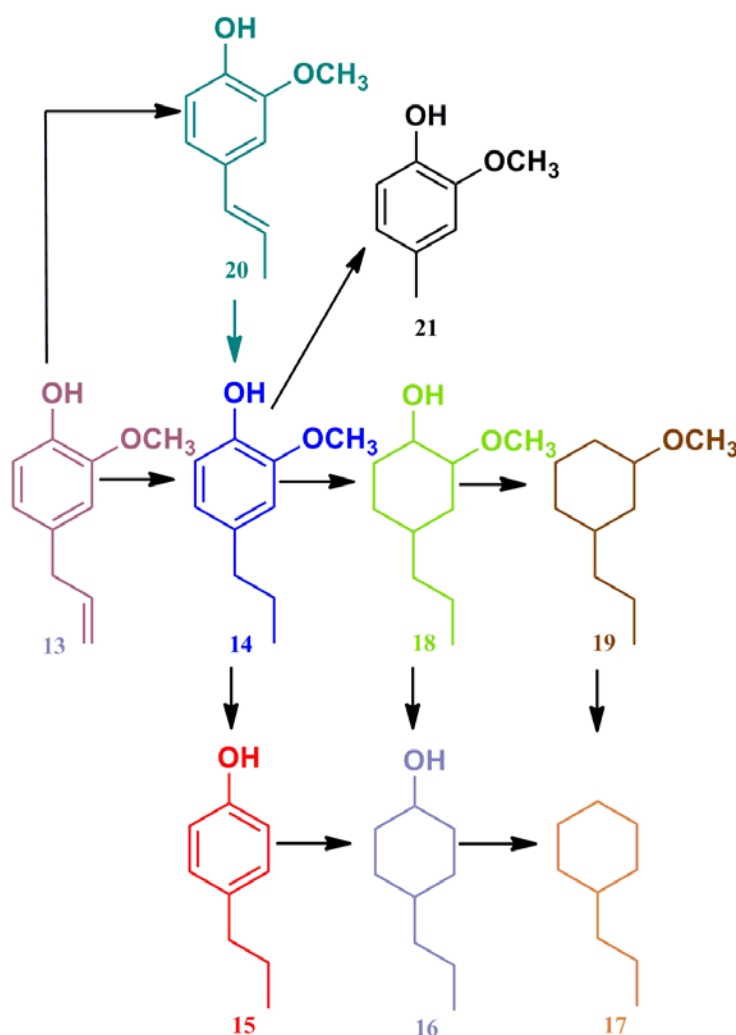


Figure 4.10. Proposed reaction pathway for supported Ru catalysts in guaiacol HDO reactions.

4.3.3. Eugenol HDO studies

In an extension to the work on guaiacol HDO, further complex aromatic monomers derived from lignin, eugenol was studied for HDO reactions over several supported metal catalysts (Scheme 4.4). The purpose of selecting eugenol for this study was that it contains several key functional groups those are similar to lignin and to coniferyl alcohol.



Scheme 4.4. Possible products formed in HDO of eugenol.

Where '13' is eugenol, '14' is propylguaiacol, '15' is propylphenol, '16' is propylcyclohexanol, '17' is propylcyclohexane, '18' is propylmethoxycyclohexanol, '19' is methoxypropylcyclohexane, '20' is isoeugenol and '21' is methylguaiacol.

4.3.3.1. Catalytic studies over Pd catalysts

The catalytic activities of Pd catalysts are shown in Figure 4.11 and it was observed that all the catalysts showed > 99 % conversion for eugenol. As observed over acidic support, (SA), a complete hydrogenation product, propylcyclohexane (17) was possible to obtain similar to what was observed in case of guaiacol substrate. However, unlike in guaiacol case where 100 % selectivity towards cyclohexane (12) was observed, in the case of eugenol almost equal amounts of products 14 (propylguaiacol), propylphenol (15) and propylcyclohexane (17) were formed. A careful look at data suggests that first alkenyl double bond hydrogenation happens and

then it was further converted into propylphenol (**15**) and further into propylcyclohexane (**17**). This was because benzene ring was highly stable due to its delocalisation of π -electrons or due to its resonance energy, whereas the alkenyl double bond was highly reactive towards H_2 addition reactions.

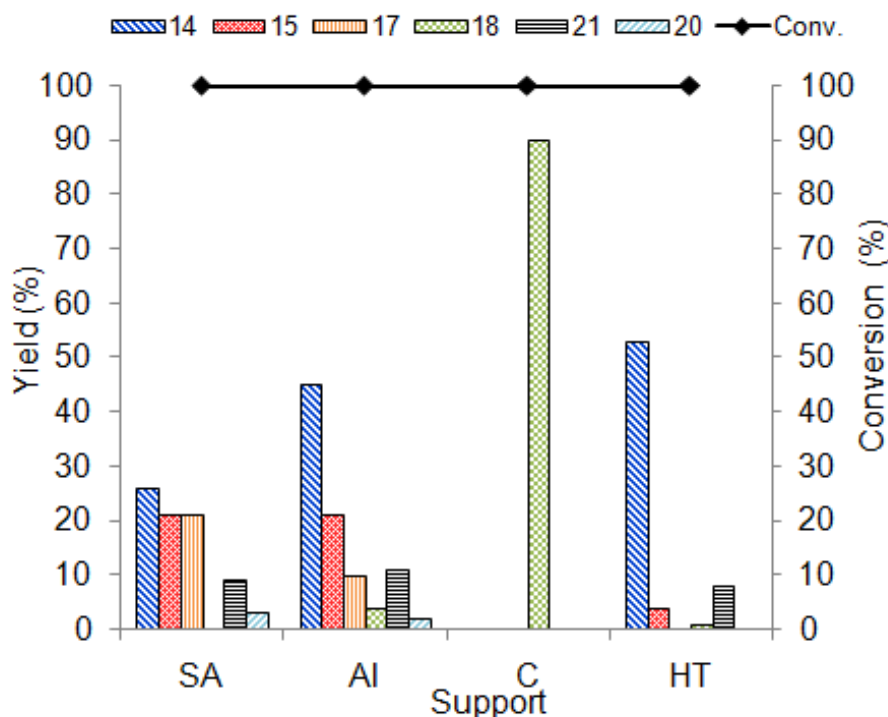


Figure 4.11. Effect of support on supported Pd catalysts in eugenol HDO reactions. Where '**14**' is propylguaiacol, '**15**' is propylphenol, '**17**' is propylcyclohexane, '**18**' is propylmethoxycyclohexanol, '**20**' is isoeugenol and '**21**' is methylguaiacol. Reaction conditions: Eugenol (2 mmol), Catalyst (Substrate/Metal = 200 mole ratio), Hexadecane (30 mL), H_2 pressure at RT = 3 MPa, 250 °C, 1 h. An error of $\pm 2\%$ was observed in all the repeated reactions.

Along with these products, formation of isoeugenol (**20**) and methylguaiacol (**21**) were also observed in minor concentrations. Similar results were observed in earlier studies where Pt/Al_2O_3 catalyst was used for eugenol HDO studies.²⁵ Next, reaction conducted over Pd supported on AL gave complicated product pattern. Similar to SA catalyst, this catalyst also formed propylguaiacol (**14**), propylphenol (**15**) and propylcyclohexane (**17**) products however; concentration of propylguaiacol (**14**) was quite high compared to propylphenol (**15**) and propylcyclohexane (**17**). This was because AL is mildly acidic compared to SA and that cleavage of C-O bond is

difficult over AL although cleavage of relatively weak C-O bond is observed to yield propylphenol (**15**). Over AL catalyst, there seems to be a choice and competition of choosing the path for product propylguaiacol (**14**) as it can form either product propylphenol (**15**) or propylmethoxycyclohexanol (**18**) or methylguaiacol (**21**). Even so, it appears that propylguaiacol (**14**) prefer to form propylphenol (**15**) as a main product since its concentration was quite high compared to propylmethoxycyclohexanol (**18**) and methylguaiacol (**21**). In case of guaiacol HDO reactions, over AL, preferentially methoxy cyclohexanol (**7**) was formed which was similar to propylmethoxycyclohexanol (**18**) product in case of eugenol HDO reactions. Compared to propylmethoxycyclohexanol (**18**), formation of propylcyclohexane (**17**) was higher because of initial higher concentration of propylphenol (**15**) from propylguaiacol (**14**). Yet, while discussing these results it will be important to mention that formation of methylguaiacol (**21**) with 11 % yield was possible. Typically, isomerisation of eugenol was catalyzed by homogeneous base⁵⁴ or solid base⁵⁵⁻⁵⁷ or with metal complexes.⁵⁸ But in this work I observed though in lower concentration formation of isoeugenol, methylguaiacol (**21**) over Pd supported on acidic supports (SA and AL) was possible. Similar observations were also noted by other researchers.^{25, 59}

When neutral support (C) was used for eugenol reactions, selective formation (90 %) of propylmethoxycyclohexanol (**18**) was achieved. This implies that over C support reaction proceeds through propylguaiacol (**14**) to yield propylmethoxycyclohexanol (**18**), and not getting converted to any other product such as propylphenol (**15**) or methylguaiacol (**21**). This was obvious since formation of propylphenol (**15**) and methylguaiacol (**21**) requires acidity and the support in question was neutral. Apparently because of same reason formation of isoeugenol (**20**), an isomerisation product of eugenol was also not possible over C support. To realize what basic support may yield in these reactions, reactions were done with Pd/HT catalyst and the result shows the formation of propylguaiacol (**14**) in major quantity along with the formation of propylphenol (**15**) and propylmethoxycyclohexanol (**18**) products. Since formation of propylphenol (**15**) requires acidity (to cleave C-O bond) its yield was restricted to minimum (4 %). Yet, surprisingly the formation of methylguaiacol (**21**) was observed in very less quantity (8 %) since basic support should be able to isomerize eugenol as anticipated.⁵⁴⁻⁵⁷ Low

carbon balance and change of colour of catalyst to dark brown/black colour suggests that either product propylguaiacol (**14**) or reactant or any other product was strongly adsorbed on the surface of catalyst. However, more studies are necessary to comment further on this. It was also proposed that the acid catalyzed isomerisation may involve carbenium ion chemistry (Figure 4.12). However, it was understood from the earlier studies and from alkane isomerisation reactions that these carbenium ions may also act as a precursor for coke formation on the catalyst surface.⁶⁰⁻⁶³ Thus it is apparent from the catalytic results that in my reactions, I observed no complete carbon balance (without taking into account coke deposited on the catalyst).

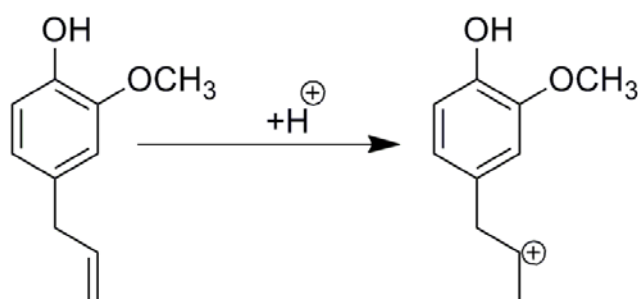


Figure 4.12. Possible formation of carbenium ion.

4.3.3.2. Catalytic studies over Pt and Ru catalysts

To identify and compare the activity of Ru and Pt impregnated on various supports eugenol HDO reactions were conducted under the similar reaction conditions used for Pd catalysts and the results are summarized in Figures 4.13 and 4.14. At hindsight it was clear that in these reactions mostly all the Pt catalysts have shown higher activity than the Pd and Ru catalysts. Moreover, it was clearly visible that Pt catalysts are more selective in yielding propylguaiacol (**14**) as a major product when acidic supports are used. However, when neutral support was used, formation of propylmethoxycyclohexanol (**18**) was observed with 95 % yield. Also the carbon balance in Pt catalyzed reactions is much higher than the other metals. This may be due to the fact that Pt generally shows lower hydrogenation activity compared to Pd. This explanation was reasonable since over SA support, Pt showed (75 %) higher propylguaiacol (**14**) formation compared to Pd (26 %) and further hydrogenation product, propylcyclohexane (**17**) was formed in higher quantity on Pd (21 %) compared to Pt (16 %). Still on AL also partially hydrogenated product, propylguaiacol (**14**) is formed in higher concentration over Pt (92 %) compared to Pd

(45 %) and further hydrogenation product, propylcyclohexane (**17**) was formed in higher amount on Pd (10 %) compared to Pt (0 %). As expected Ru catalysts showed activity in between that of Pd and Pt.

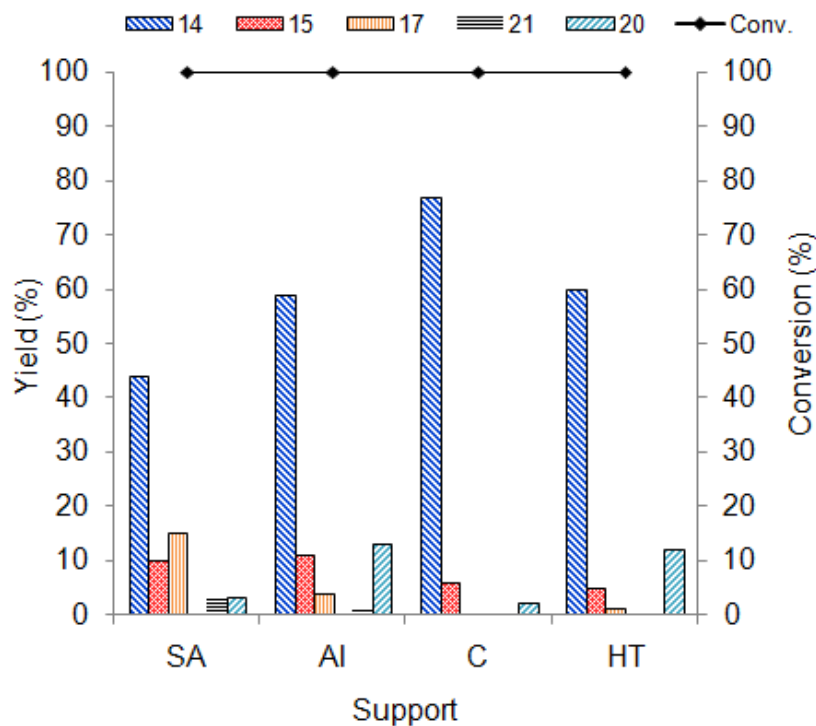


Figure 4.13. Eugenol HDO reactions over Ru supported metal catalysts.

Where '**14**' is propylguaiacol, '**15**' is propylphenol, '**17**' is propylcyclohexane, '**18**' is propylmethoxycyclohexanol, '**20**' is isoeugenol and '**21**' is methylguaiacol. Reaction conditions: Eugenol (2 mmol), Catalyst (Substrate/Metal = 200 mole ratio), Hexadecane (30 mL), H₂ pressure at RT = 3 MPa, 250 °C, 1 h. Conversion was 100 % for all the catalytic reactions. An error of ± 2 % was observed in all the repeated reactions.

Pd/SA and Pd/C catalysts were used repeatedly 3 times to check whether those show similar activities after washing, drying and reducing those under hydrogen flow after each run. It was observed that the Pd/SA catalyst show reproducible activity for the formation of products, propylguaiacol (**14**), propylphenol (**15**) and propylcyclohexane (**17**) along with isoeugenol (**20**) and methylguaiacol (**21**).

Similarly, Pd/C catalyst also gave ca. 90 % yield for product propylmethoxycyclohexanol (**18**) with decrease in ca. 2 % yield in each run may be due to handling loss of catalyst.

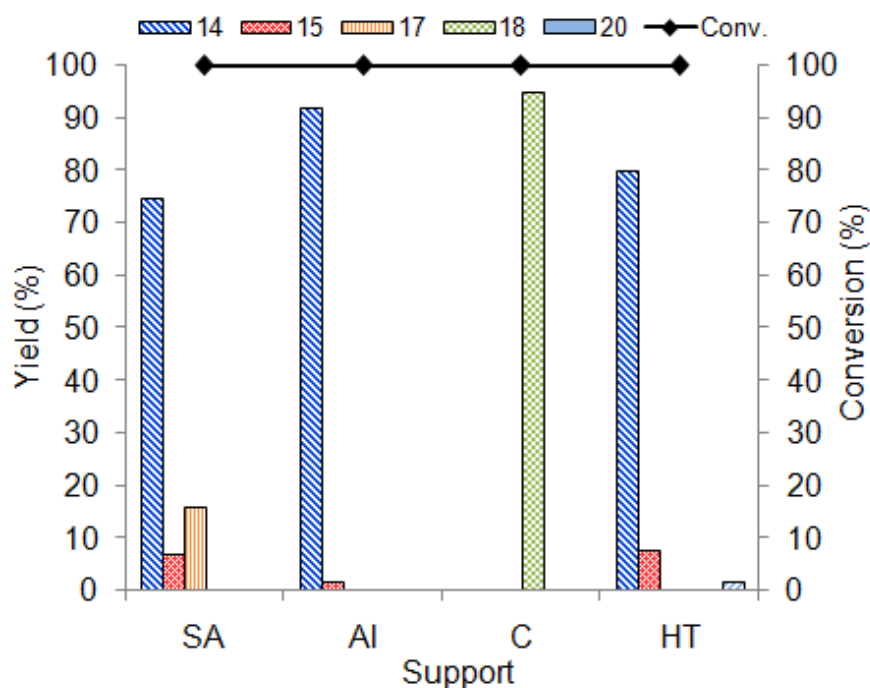


Figure 4.14. Eugenol HDO reactions over Pt supported metal catalysts.

Where '14' is propylguaiacol, '15' is propylphenol, '17' is propylcyclohexane, '18' is propylmethoxycyclohexanol and '20' is isoeugenol. Reaction conditions: Eugenol (2 mmol), Catalyst (Substrate/Metal = 200 mole ratio), Hexadecane (30 mL), H₂ pressure at RT = 3 MPa, 250 °C, 1 h. Conversion was 100 % for all the catalytic reactions. An error of ± 2 % was observed in all the repeated reactions.

4.3.4. The effect of electron density (deficiency or richness) of metal particles on supports

XPS analysis for Pd/SA and Pd/C was performed to explain the effects of surface electronic properties of the metal particles. It is known from literature that when a metal is loaded on an acidic support, there occurs a polarization of electron density of metal atom towards the nearby cations on the acidic support (Brönsted acidity).⁶⁴ So if XPS was done for these metal nanoparticles on acidic support, it was expected that metal nanoparticles will show a higher binding energy due to metal support interaction. XPS studies were done on Pd/SA and Pd/C to explain the metal support interactions, if any.⁶⁵⁻⁶⁷ Studies were performed particularly on SA and C support, since SA has highest acidity among all the supports and C support was used since it was neutral in nature so will not show any surface electronic properties.

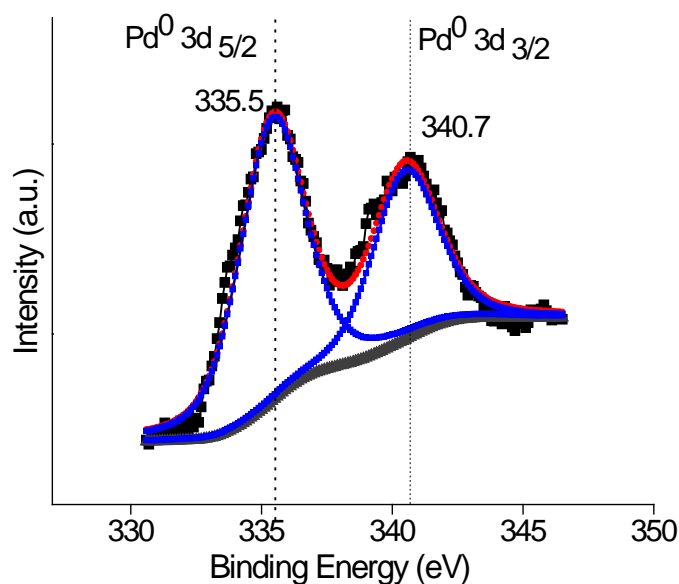


Figure 4.15. XPS analysis of Pd/SA (Pd3d) catalyst.

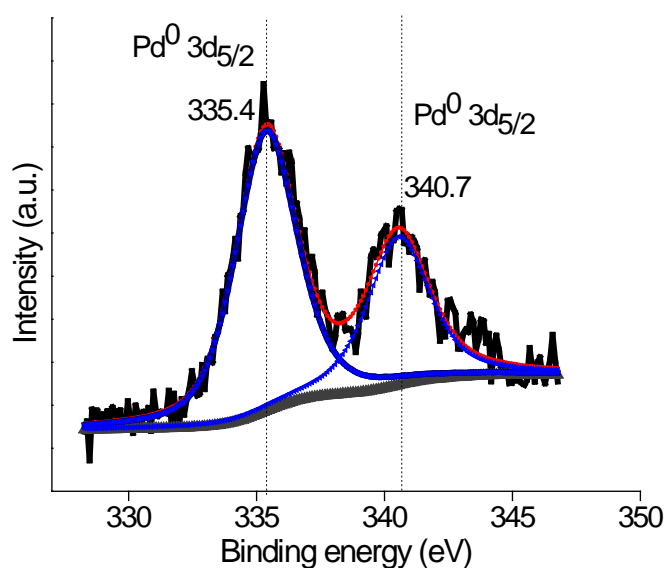


Figure 4.16. XPS analysis of Pd/C (Pd3d) catalyst.

XPS spectra of Pd $3d_{5/2}$ and Pd $3d_{3/2}$ on acidic support (SA) and neutral support (C) are shown in Figures 4.15 and 4.16. The binding energies of both the samples appear at 333.5 and 340.7 eV corresponding to Pd $3d_{5/2}$ and Pd $3d_{3/2}$, respectively which corresponds to fully reduced Pd nanoparticles.⁶⁸⁻⁷⁰ The XPS data shown here for Pd/SA doesn't show a positive shift in the binding energy values of Pd $3d_{5/2}$ and Pd $3d_{3/2}$, which indicates that the metal nanoparticles are less dependent on the support acidity.

4.3.5. Hydrodeoxygenation studies of guaiacol-eugenol mixtures

Since all the above reactions were done using only single aromatic monomer and to understand how catalysts will behave when two substrates, guaiacol and eugenol are mixed together (like in a typical lignin derived mixture of products containing aromatic monomers) reactions were carried out with both these substrates (mixed together) over Pt catalysts. Table 4.6 lists the results obtained when reaction is carried out at 250 °C for 1 h. As expected, Pt supported over acidic support (SA) showed maximum yield for cyclohexane (**12**) when reactions were performed using guaiacol as lone substrate. Along with cyclohexane (**12**), I also observed formation of propylguaiacol (**14**) (80 %), propylphenol (**15**) (4 %) and propylcyclohexane (**17**) (12 %) in HDO reactions of eugenol substrate. These results were also in line with the earlier discussed observations (Figure 4.11 and 4.14, eugenol HDO). When support was changed from acidic (SA) to neutral (C) the product distribution changed and formation of product meyhoxycyclohexanol (**7**) (98 %) probably originating from guaiacol substrate was observed.

Table 4.6. HDO reactions of guaiacol and eugenol mixture over Pt catalysts

Support	Guaiacol					Eugenol						
	Conv. [%] ^[a]	Yield [%] ^[b]				Conv. [%] ^[a]	Yield [%] ^[b]					
		7	8	10	12		14	15	17	18	20	21
SA	88	0	0	0	85	100	80	4	12	0	0	0
C	99	98	0	0	0	100	10	0	0	80	0	0

Reaction conditions: Guaiacol (0.164 g) + Eugenol (0.164 g), Catalyst (0.065 g), hexadecane (30 mL), H₂ pressure at RT = 3 MPa, 250 °C, 1 h. ^[a]Conversions are calculated respective to the charge of the particular substrate. ^[b]Yields are calculated based on the charge of respective substrate. An error of ±2 % was observed in all the repeated reactions.

Besides this, formation of propylmethoxycyclohexanol (**18**) (80 %) derived from eugenol was also observed. However, unlike in lone eugenol substrate where formation of propylguaiacol (**14**) was not seen, here slight quantity (10 %) was seen. Nevertheless, propylguaiacol (**14**) can be eventually converted into propylmethoxycyclohexanol (**18**). These results assure that the catalysts evaluated for

lone substrate for HDO activity are capable of delivering similar performance in mixture of compounds.

4.4. CONCLUSIONS

HDO studies were performed on lignin derived aromatic monomers like phenol, guaiacol and eugenol using supported metal catalysts. Various types of metals like Pd, Pd and Ru impregnated on acidic (SA, AL), basic (HT) and neutral (C) supports were prepared by impregnation method. Catalysts were completely characterized using various physico-chemical techniques. (Refer chapter 2B). Reactions were performed at 200-250 °C, 1-3 MPa H₂ in hexadecane solvent for 1-6 h. HDO studies using supported metal catalysts were first performed on the simplest model compound, phenol using Pd/SA and Pd/C catalysts. Here it was observed that phenol undergoes HDO only in the presence of acidic species (SA support), but in the case of Pd/C catalyst phenol only undergoes hydrogenation reactions. Deoxygenation happened faster from a saturated ring than in an aromatic ring. This was because the bond strength of -OH group attached to sp² carbon (C in the aromatic ring) was stronger than the one attached to sp³ carbon (C attached to saturated ring). So higher amount of energy is required to perform deoxygenation from an aromatic ring (refer section 4.3.1). Similar phenomenon was observed for other compounds (guaiacol and eugenol). Based on the knowledge obtained from phenol HDO reactions, studies were carried out on guaiacol substrate. Here also only in the presence of acidic supports complete HDO happens. Ru and Pt metal also were also studied on SA, AL, C and HT supports. But product distribution depended only on the support acidity irrespective of the metal used. Reaction parameters like temperature, pressure and time was studied which showed that the optimized reaction conditions are 250 °C, 3 MPa H₂, 6 h where obtain maximum hydrogenation or HDO activity can be obtained. Similar trend was observed for eugenol compound also. It was observed that the double bond (outside the aromatic ring) present in eugenol was more susceptible to hydrogenation than the aromatic ring. This was because the double bonds present in the aromatic ring are highly stable, due to the resonance stabilization of the π -electrons in the aromatic ring. It was proposed that the first step of ring hydrogenation in case of guaiacol or double bond hydrogenation with eugenol was metal driven reaction however; further reactions were mostly governed by supports. The removal of oxygen by HDO was

achieved mainly on acidic supports like AL and SA. Nevertheless, SA was proven to be highly active due to high acidity associated with it compared to AL. From the studies it was observed that noble metals facilitated the hydrogenation of aromatic rings and acidic supports helped in the deoxygenation reactions. In guaiacol and eugenol HDO reactions, catalyst recyclability was performed upto 3 runs. From XRD and ICP-OES analysis it was understood that even after 3rd recycle there was no leaching of metal under the conditions employed.

Based on these results a mechanism can be proposed for the ring hydrogenation versus deoxygenation of model compounds with noble metals on neutral and acidic support. For instance it can be concluded that in the case of a catalyst with acidic support, the phenol molecule will approach and adsorb on the catalyst surface in vertical manner resulting in deoxygenation. But in the case of catalyst with neutral support, planar interaction was observed between the aromatic ring and support (Figure 4.17).

Ultimate aim of all these studies was to perform HDO of lignin derived aromatic monomers. Instead of doing studies on this complex mixture a physical mixture of lignin model compounds (guaiacol and eugenol) was prepared which mimicks the aromatic monomer mixture. For these studies Pt catalysts impregnated on SA and C supports at optimized reaction conditions (T = 250 °C, P = 3 MPa H₂, t = 6 h) were employed. It was observed that the catalyst Pt/SA and Pt/C perform similarly like in the case of guaiacol and eugenol substrates when studied individually. These results signify that metal supported on acidic supports can preferably perform maximum HDO under the optimized reaction conditions. The studies performed here will help in designing highly active catalysts for the complete HDO of lignin derived aromatic monomers. Therefore I extend my view towards the complete HDO of lignin derived aromatic monomer mixture using supported metal catalysts which will finally help in the one pot HDO of lignin into hydrocarbon fuels using the best catalytic system.

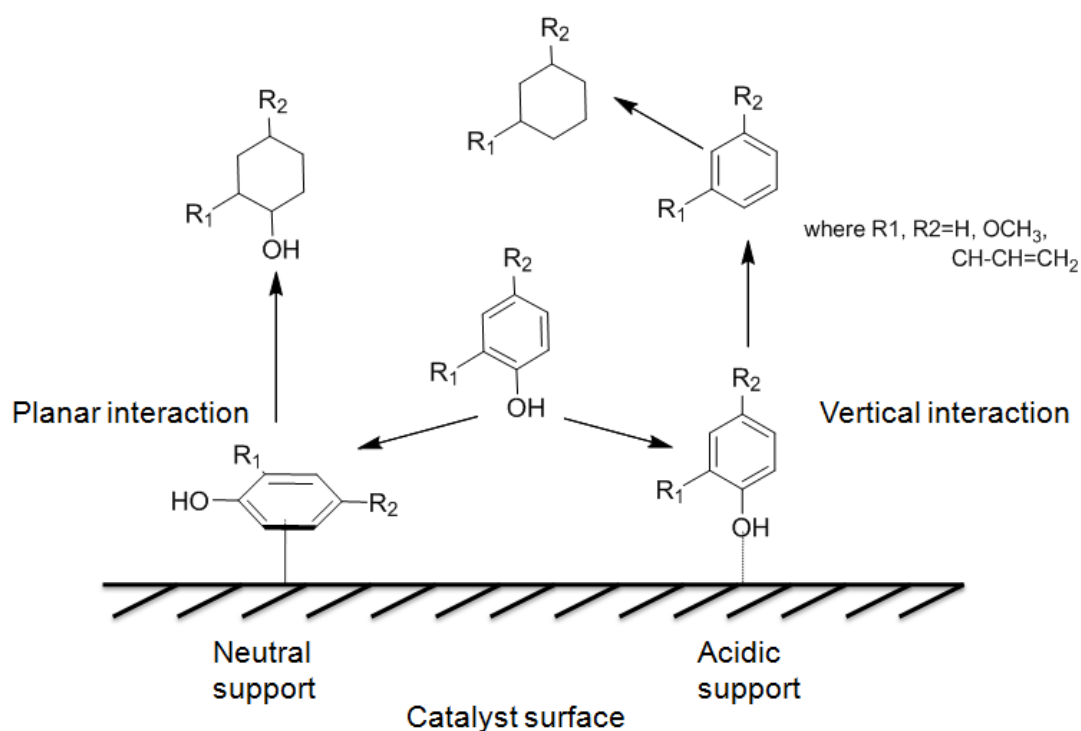


Figure 4.17. Mechanism proposed for ring hydrogenation versus HDO for lignin derived aromatic monomers.

4.5. REFERENCES

1. Deepa, A. K.; Dhepe, P. L., *RSC Adv.* **2014**, *4*, 12625-12629.
2. Deepa, A. K.; Dhepe, P. L. Depolymerization of lignin using solid acid catalysts. U.S. 0302796 A1, November 29, 2012.
3. Laskar, D. D.; Yang, B.; Wang, H.; Lee, J., *Biofuels, Bioprod. Biorefin.* **2013**, *7* 602-626.
4. Bu, Q.; Lei, H.; Zacher, A. H.; Wang, L.; Ren, S.; Liang, J.; Wei, Y.; Liu, Y.; Tang, J.; Zhang, Q.; Ruan, R., *Bioresour. Technol.* **2012**, *124*, 470-477.
5. He, Z.; Wang, X., *Catal. Sustainable Energy Prod.* **2013**, 28-52.
6. Elliott, D. C., *Energy Fuels* **2007**, *21*, 1792-1815.
7. Mortensen, P. M.; Grunwaldt, J. D.; Jensen, P. A.; Knudsen, K. G.; Jensen, A. D., *Appl. Catal., A* **2011**, *407*, 1-19.
8. Oasmaa, A.; Solantausta, Y.; Arpiainen, V.; Kuoppala, E.; Sipil, K., *Energy Fuels* **2010**, 1380-1388.
9. Zakzeski, J.; Bruijninx, P. C. A.; Jongerius, A. L.; Weckhuysen, B. M., *Chem. Rev.* **2010**, *110*, 3552-3599.
10. Elliott, D. C.; Hart, T. R., *Energy Fuels* **2008**, *23*, 631-637.
11. Czernik, S.; Bridgwater, A. V., *Energy Fuels* **2004**, *18*, 590-598.
12. Nowakowski, D. J.; Bridgwater, A. V.; Elliott, D. C.; Meier, D.; de Wild, P., *J. Anal. Appl. Pyrolysis* **2010**, *88*, 53-72.
13. Meier, D.; Faix, O., *Bioresour. Technol.* **1999**, *68*, 71-77.
14. Furimsky, E., *Appl. Catal., A* **2000**, *199*, 147-190.
15. Girgis, M. J.; Gates, B. C., *Ind. Eng. Chem. Res.* **1994**, *33*, 1098-1106.

16. Popov, A.; Kondratieva, E.; Mariey, L.; Goupil, J. M.; Fallah, J. E.; Gilson, J. P.; Travert, A.; Maugé, F., *J. Catal.* **2013**, *297*, 176-186.
17. Choudhary, T. V.; Phillips, C. B., *Appl. Catal. A* **2011**, *39*, 1-12.
18. Jongerius, A. L.; Jastrzebski, R.; Bruijninx, P. C. A.; Weckhuysen, B. M., *J. Catal.* **2012**, *285*, 315-323.
19. Ruiz, P. E.; Frederick, B. G.; De Sisto, W. J.; Austin, R. N.; Radovic, L. R.; Leiva, K.; García, R.; Escalona, N.; Wheeler, M. C., *Catal. Commun.* **2012**, *27*, 44-48.
20. Bui, V. N.; Laurenti, D.; Afanasiev, P.; Geantet, C., *Appl. Catal., B* **2011**, *101*, 239-245.
21. Zhao, C.; Lercher, J. A., *Angew. Chem., Int. Ed.* **2012**, *51*, 5935-5940.
22. Zhao, C.; Lercher, J. A., *ChemCatChem* **2012**, *4*, 64-68.
23. Saidi, M.; Samimi, F.; Karimipourfard, D.; Nimmanwudipong, T.; Gates, B. C.; Rahimpour, M. R., *Energy Environ. Sci.* **2014**, *7*, 103-129.
24. Sun, J.; Karim, A. M.; Zhang, H.; Kovarik, L.; Li, X. S.; Hensely, A. J.; McEwen, J.-S.; Wang, Y., *J. Catal.* **2013**, *306*, 47-57.
25. Nimmanwudipong, T.; Runnebaum, R. C.; Ebeler, S. E.; Block, D. E.; Gates, B. C., *Catal. Lett.* **2012**, *142*, 151-160.
26. Yan, N.; Zhao, C.; Dyson, P. J.; Wang, C.; Liu, L.-t.; Kou, Y., *ChemSusChem* **2008**, *1*, 626-629.
27. Yan, N.; Yuan, Y.; Dykeman, R.; Kou, Y.; Dyson, P. J., *Angew. Chem., Int. Ed.* **2010**, *49*, 5549-5553.
28. Gutierrez, A.; Kaila, R. K.; Honkela, M. L.; Slioor, R.; Krause, A. O. I., *Catal. Today* **2009**, *147*, 239-246.
29. Deutsch, K. L.; Shanks, B. H., *Appl. Catal.* **2012**, *144*, 447-448.
30. Zhao, C.; Camaioni, D. M.; Lercher, J. A., *J. Catal.* **2012**, *12*-23.
31. Zhao, C.; Kou, Y.; Lemonidou, A. A.; Li, X.; Lercher, J. A., *Angew. Chem., Int. Ed.* **2009**, *48*, 3987-3990.
32. Zhao, C.; He, J.; Lemonidou, A. A.; Li, X.; Lercher, J. A., *J. Catal.* **2011**, *280*, 8-16.
33. Jongerius, A. L.; Bruijninx, P. C. A.; Weckhuysen, B. M., *Green Chem.* **2013**, *15*, 3049-3056.
34. Sergeev, A. G.; Hartwig, J. F., *Science* **2011**, *332*, 439-443.
35. Zhao, C.; Kou, Y.; Lemonidou, A. A.; Li, X. B.; Lercher, J. A., *Chem. Commun.* **2010**, *46*, 412-414.
36. Zhang, W.; Chen, J.; Liu, R.; Wang, S.; Chen, L.; Li, K., *ACS Sustainable Chem. Eng.* **2013**, *2*, 683-691.
37. Nimmanwudipong, T.; Runnebaum, R. C.; Block, D. E.; Gates, B. C., *Catal. Lett.* **2011**, *141*, 779-783.
38. Nakagawa, Y.; Ishikawa, M.; Tamura, M.; Tomishige, K., *Green Chem.* **2014**, *16*, 2197-2203.
39. Deepa, A. K.; Dhepe, P. L., *ChemPlusChem* **2014**, DOI: 10.1002/cplu.201402145.
40. Mortensen, P. M.; Grunwaldt, J. D.; Jensen, P. A.; Knudsen, K. G.; Jensen, A. D., *Appl. Catal., A* **2011**, *407*, 1-19.
41. Venderbosch, R. H.; Ardiyanti, A. R.; Wildschut, J.; Oasmaa, A.; Heeres, H. J., *J. Chem. Technol. Biotechnol.* **2010**, *85*, 674-686.
42. Mortensen, P. M.; Grunwaldt, J.-D.; Jensen, P. A.; Jensen, A. D., *ACS Catal.* **2013**, *3*, 1774-1785.
43. Furimsky, E., *Catal. Today* **2013**, *217*, 13-56.
44. Lin, Y.-C.; Li, C.-L.; Wan, H.-P.; Lee, H.-T.; Liu, C.-F., *Energy Fuels* **2011**, *25*, 890-896.
45. Pinheiro, A.; Hudebine, D.; Dupassieux, N.; Geantet, C., *Energy Fuels* **2009**, *23*, 1007-1014.
46. Viljva, T. R.; M., S. E. R.; Krause, A. O. I., *Appl. Catal., A* **2001**, *209*, 1007-1014.

47. Lee, C. R.; Yoon, J. S.; Suh, Y.-W.; Choi, J.-W.; Ha, J.-M.; Suh, D. J.; Park, Y.-K., *Catal. Commun.* **2012**, *17*, 54-58.
48. Prochazkova, D.; Zamostny, P.; Bejblova, M.; Cerveny, L.; Cejka, J., *Appl. Catal. A* **2007**, *332*, 56-64.
49. Wildschut, J.; Mahfud, F. H.; Venderbosch, R. H.; Heeres, H. J., *Ind. Eng. Chem. Res.* **2009**, *48* 10324-10334.
50. Zhao, C.; Kou, Y.; Lemonidou, A. A.; Li, X.; Lercher, J. A., *Angew. Chem., Int. Ed.* **2009**, *121*, 4047-4050.
51. Pham, T. T.; Lobban, L. L.; Resasco, D. E.; Mallinson, R. G., *J. Catal.* **2009**, *266*, 9-14.
52. Ohta, H.; Kobayashi, H.; Hara, K.; Fukuoka, A., *Chem. Commun.* **2011**, *47*, 12209-12211.
53. Nørskov, J. K.; Rossmeisl, J.; Logadottir, A.; Lindqvist, L.; Kitchin, J. R.; Bligaard, T.; Jonsson, H., *J. Phys. Chem. B* **2004** *108*, 17886-17892
54. Cerveny, L.; Krejčíková, A.; Marhouf, A.; Ružička, *React Kinet Catal Lett.* **1987**, *33*, 471-476.
55. Kishore, D.; Kannan, S., *App Catal A Gen* **2004**, *270*, 227-235.
56. Kishore, D.; Kannan, S., *Green Chem.* **2002**, *4*, 607-610.
57. Jinesh, C. M.; Churchil, A.; Antonyaraj, S. K., *Catal. Today* **2009**, *141*, 176-181.
58. Sharma, S. K.; Sivastava, V. K.; Jasra, R. V., *J Mol Catal A: Chem* **2006**, *245*, 200-209.
59. Binder, J. B.; Gray, M. J.; White, J. F.; Zhang, Z. C.; Holladay, J. E., *Biomass Bioenergy* **2009**, *33*, 1122-1130.
60. Ertl, G.; Knözinger, H.; Weitkamp, J., *Handbook of Heterogeneous Catalysis*. Wiley-VCH: 1997.
61. Ko, A. N.; Wojciechowski, B. W., *Int J Chem Kinet.* **1983**, *15*, 1249-1274.
62. Venuto, P. B.; Hamilton, L. A.; Landis, P. S., *J Catal.* **1966** *5*,484-493.
63. Zhou, X.; Chen, T.; Yang, B.; Jiang, X.; Zhang, H.; Wang, L., *Energy Fuels* **2011**, *25*, 2427-2437.
64. Mojet, B. L.; Miller, J. T.; Ramaker, D. E.; Koningsberger, D. C., *J. Catal.* **1999**, *186*, 373-386.
65. Huang, J.; Jiang, Y.; van Vegten, N.; Hunger, M.; Baiker, A., *Title J. Catal.* **2011**, *281*, 352-360.
66. Hoxha, F.; Schmidt, E.; Mallat, T.; Schimmoeller, B.; Pratsinis, S. E.; Baiker, A., *J. Catal.* **2011**, *278*, 94-101.
67. Schmidt, E.; Hoxha, F.; Mallat, T.; Baiker, A., *J. Catal.* **2010**, *274*, 117-120.
68. Wagner, C. D.; Muilenberg, G. E., *Handbook of X-ray photoelectron spectroscopy: a reference book of standard data for use in X-ray photoelectron spectroscopy*. Physical Electronics Division, Perkin-Elmer Corp.: 1979.
69. Brun, M.; Berthet, A.; Bertolini, J. C., *J. Electron Spectrosc. Relat. Phenom.* **1999**, *104*, 55-60.
70. Briggs, D.; Seah, M. P., *Practical Surface Analysis*. Wiley: Chichester, 1990; Vol. 1.

CHAPTER 5

SUMMARY AND CONCLUSIONS

SUMMARY AND CONCLUSIONS

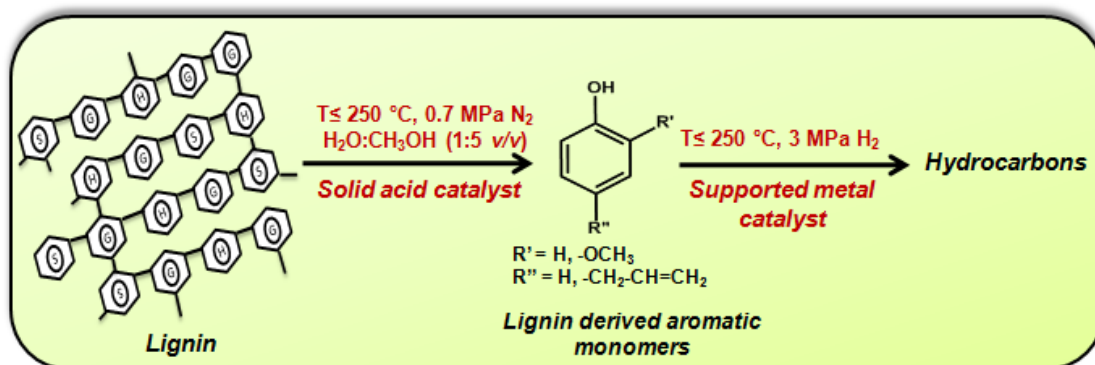
Fossil feedstocks constitute one of the major resources for our modern civilization. But they are limited and cannot be replenished within an acceptable period of time. Lignocellulosic biomass is abundant and is a renewable resource, which can act as a better alternative for fossil feedstocks and can also play an important role in reducing global warming. Hence, in recent times application of lignocellulosic biomass in the production of fuels and chemicals has gained lot of interest. Lignin, an amorphous aromatic polymer comprises 15-25 % of lignocellulosic biomass. Due to its abundant availability and aromatic nature, lignin can be efficiently valorized into aromatic monomers which can be used as fuel additives or octane enhancers and chemicals. In view of these points, I have focused my studies on developing a method for depolymerizing lignin into aromatic monomers using solid acid catalysts (structured and amorphous). But the high oxygen content of lignin derived aromatic monomers will reduce the efficiency of fuels derived from it. So additionally, I have performed hydrodeoxygenation (HDO) reactions using supported metal catalysts on lignin derived aromatic monomers like phenol, guaiacol and eugenol.

Considering the above points, work has been carried out and hence my Ph.D. thesis is divided into 5 chapters. The main points of all the chapters are summarized below.

Chapter 1 includes a general introduction on how lignocellulosic biomass can act as a good alternative to fossil feedstocks. In this chapter I have discussed about the details on the composition of lignocellulosic biomass (cellulose, hemicellulose and lignin). Lignin composition in lignocellulosic biomass is ca. 15-25 % and is considered as a source of fuel and chemicals if can be depolymerized into aromatic monomers. Lignin is a complex three dimensional amorphous biopolymer having an aromatic nature which provides rigidity to the plant. A general structure, linkages and functional groups present in lignin are discussed in this chapter. The availability of lignin from various sources and their present valorization methods were also described. In this chapter, I have also discussed about various techniques like Kraft, Organosolv, Lignosulfonate, Steam explosion used for the isolation of lignin from lignocellulosic biomass. It was understood that the structural and functional properties of lignin depend on type of extraction technique used for isolation. Based on the literature reports it was observed that several attempts were made for the efficient valorization

of lignin. Some of the important pathways for depolymerizing lignin include pyrolysis, gasification, base catalysed, acid catalysed, metal catalysed, ionic liquid assisted and supercritical fluid assisted methods. But it was understood that most of the earlier reports on depolymerization of lignin have several drawbacks like either they use homogenous catalysts (acids or bases) or precious metals (Pd, Pt, Ru) for their studies, which is not economically viable. Another drawback is that most of the processes operate under harsh reaction conditions ($T > 340\text{ }^{\circ}\text{C}$) which will result in the formation of higher amount of degradation products (coke, char and gas) and hence reduce the aromatic monomer formation. Additionally, one of the major drawbacks with the conventional processes for depolymerization of lignin was that most of the studies are done using lignin model compounds like dimers and trimers instead of using actual lignin substrates. Considering the drawbacks associated with the known methods it is vital to develop a distinct method to convert actual lignin substrates selectively into aromatic monomers under milder reaction conditions ($T \leq 250\text{ }^{\circ}\text{C}$) using heterogeneous catalysts. Moreover, it will be advantageous to use solid acid catalysts as they are already known to convert cellulose and hemicelluloses into sugars and sugar derivatives. The development of a methodology employing milder conditions and solid acid catalysts for depolymerization of actual lignin substrates will help in the production of maximum amount of aromatic monomers. Furthermore, the hydrodeoxygenation (HDO) study of lignin derived aromatic monomers in presence of supported metal catalysts will help to reduce the oxygen content and upgrade the efficiency of the fuels derived from these products. Considering above discussions, following were the objectives of my work (Scheme 5.1),

- ❖ To develop a method for the depolymerization of actual lignin substrates into aromatic monomers using solid acid catalysts under milder reaction conditions ($T \leq 250\text{ }^{\circ}\text{C}$).
- ❖ Isolation of aromatic monomers obtained after solid acid catalysed depolymerization of lignin using column chromatography.
- ❖ To perform HDO reactions of lignin derived aromatic monomers into hydrocarbons over supported metal catalysts.



Scheme 5.1. Solid acid catalysed depolymerization of lignin into aromatic monomers and their further hydrodeoxygenation over supported metal catalysts.

Chapter 2A includes the details on various types of actual lignin substrates namely dealkaline, organosolv, alkali, ORG, EORG and bagasse lignin used in the study for solid acid catalysed depolymerization of lignin. Structural and functional properties of all these lignin were performed using various physico-chemical techniques. Major findings in this chapter are summarized below.

- Isolation of lignin (bagasse lignin) from sugarcane bagasse was performed using organosolv method and its properties were studied using various characterization techniques.
- Molecular weights of all the lignin were determined using MALDI-TOF and GPC analysis. It was observed that dealkaline lignin was having the highest molecular weight ($60,000\text{ gmol}^{-1}$) amongst the lignin substrates studied.
- Elemental composition (CHNS) showed the presence of 60-65 % C and 5-8 % H in all the lignin, except in case of ORG and bagasse lignin having 57 % and 51 % of C, respectively. In the case of dealkaline lignin and alkali lignin S contamination (ca. 1 %) was observed, which was due to the type of extraction process (Kraft) used in lignin (dealkaline and alkali lignin) isolation, where NaOH and Na_2S are used as reagents.
- Based on elemental analysis, a general molecular formula was derived for the lignin substrates studied. Typically, all the lignin have the general formula, $\text{C}_x\text{H}_y\text{O}_z$ ($x: 7.9\text{-}9.0$; $y: 10\text{-}10.62$; $z: 2.89\text{-}4.5$).
- ICP-OES and SEM-EDAX analysis performed on lignin confirmed the Na contamination in dealkaline lignin (ca. 967 ppm) and alkali lignin (ca. 2333 ppm), due to the type of (Kraft) process used for their extraction. All other

lignin which were isolated by organosolv method and were free of Na contamination.

- From FT-IR, ^1H and ^{13}C NMR analysis presence of C-C, C-O-C linkages in all the lignin was confirmed. Presence of various types of functional groups like hydroxyl, carbonyl, alkyl and alkoxy groups was also identified in lignin using the above techniques.
- Amorphous nature and purity of lignin was confirmed using XRD analysis. Peaks corresponding to Na and S were detected using this technique.
- UV-Vis analysis of all the lignin substrates showed a λ maximum at 270 nm which confirmed its aromatic nature.
- Thermal degradation studies of lignin were performed using TGA-DTA analysis in N_2 and air atmosphere. It was observed that even when thermal degradation studies were performed at 1000 °C in N_2 atmosphere, 35-40 % of unburnt residues were observed for all the lignin. But, when studies were performed in presence of oxygen, minimal quantity (0-3 %) of unburnt residue was observed. But in the case of dealkaline lignin even burnt in oxygen at 1000 °C almost 17 % residue was observed which is in line with the manufactures (TCI Chemicals) specifications.
- Several solvents from polar to nonpolar (polarity index, 0-9) were checked for lignin solubility. From the results it was found that water-methanol (1:5 v/v) mixture would be the best solvent system for carrying out the reactions since in this solvent system all the six different types of lignin have maximum solubility.

Chapter 2B deals with the synthesis and characterization of solid acid catalysts and supported metal catalysts used for depolymerization of lignin and HDO of lignin derived aromatic monomers, respectively.

- Solid acid catalysts studied here include, structured solid acid catalysts ((H-USY (Si/Al = 15), H-ZSM-5 (Si/Al = 11.5), H-BEA (Si/Al = 19), H-MOR (Si/Al = 10), Montmorillonite, K10 clay and Al pillared clay) and amorphous solid acid catalysts ($\text{SiO}_2\text{-Al}_2\text{O}_3$ (Si/Al = 5.3), 10 wt % $\text{MoO}_3/\text{SiO}_2$).
- Amorphous solid acid catalyst, 10 wt % $\text{MoO}_3/\text{SiO}_2$ was synthesized using sol-gel method and was well characterized using various techniques.

- Synthesis of various types of supported metal catalysts for HDO of lignin derived aromatic monomers was performed by conventional impregnation method. These catalysts include Pt, Pd, Ru metals loaded on SiO₂-Al₂O₃, γ -Al₂O₃, C and hydrotalcite supports.

All solid acid catalysts and supported metal catalysts were characterized using various physico-chemical techniques.

- XRD analysis was performed to determine the crystalline or amorphous nature of the solid acids, while the metal peaks were identified for supported metal catalysts.
- N₂ sorption studies were performed to determine the surface area, pore diameter and pore volume of solid acids and supported metals.
- NH₃-TPD technique determined the amount of acid sites (weak and strong) in solid acid catalysts. It was observed that among the solid acids used H-MOR (Si/Al=10) was having the highest amount of total acid sites (1.15 mmol g⁻¹).
- ICP-OES analysis confirmed the Si/Al ratio of zeolites, percentage of metal loading in MoO₃/SiO₂ and supported metal catalysts. ICP-OES of MoO₃/SiO₂ suggests that theoretical metal loading and experimental metal loading is 10 wt% and 9 wt% respectively.
- HRTEM analysis determined the average particle size and the percentage of dispersion of metal nanoparticles over various supports. It was understood from this analysis that metals loaded on carbon supports were showing the highest percentage of dispersion (20 %) when compared to other supported metal catalysts employed in the study.

Chapter 3A discusses the depolymerization of dealkaline lignin substrate into aromatic monomers using various solid acid catalysts.

- Various types of solid acid catalysts were evaluated for the depolymerization of dealkaline lignin substrate into aromatic monomers. Reactions were performed at 250 °C with 0.7 MPa N₂ for 30 min. in H₂O:CH₃OH (1:5 v/v, 30 mL) solvent.
- Aromatic monomers were extracted using THF solvent from dealkaline lignin reaction mixture.

- Structured solid acid catalysts ((H-USY (Si/Al = 15), H-ZSM-5 (Si/Al = 11.5), H-BEA (Si/Al = 19), H-MOR (Si/Al = 10), Montmorillonite, K10 clay and Al pillared clay) and amorphous solid acid catalysts ($\text{SiO}_2\text{-Al}_2\text{O}_3$ (Si/Al = 5.3), 10 wt % of $\text{MoO}_3/\text{SiO}_2$) were evaluated in depolymerization studies of dealkaline lignin substrate.
- Among the solid acid catalysts tested H-USY (Si/Al = 15) was found to give maximum amount of THF soluble aromatic monomers (60 %) (Figure 5.1).

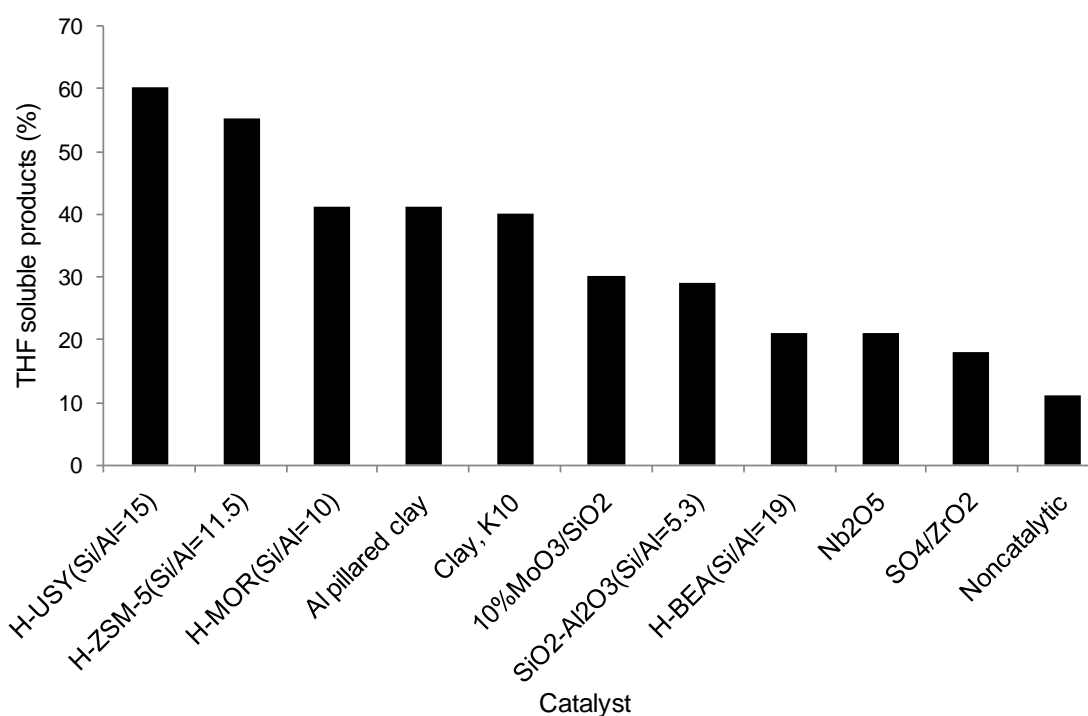


Figure 5.1. Catalyst evaluation study of dealkaline lignin depolymerization reaction. Reaction conditions: dealkaline lignin (0.5 g), catalyst (0.5 g), $\text{H}_2\text{O}:\text{CH}_3\text{OH}$ (1:5 v/v, 30 mL), 250 °C, 30 min., 500 rpm, 0.7 MPa N_2 at RT.

- The aromatic monomers formed were identified and confirmed using various techniques like GC-FID, GC-MS, HPLC, LC-MS, GPC, MALDI-TOF and CHNS analysis.
- FTIR and NMR (^1H and ^{13}C) analysis were performed to assign a correlation between structure of lignin and aromatic monomers.
- Catalytic activities of solid acids were compared with homogeneous acid catalysts (HCl and H_2SO_4). It was observed that large amount of oligomeric

products were formed when homogeneous acids were used as catalyst for depolymerization reactions of lignin.

- Correlation between acidity and activity of solid acid catalysts in depolymerization reactions were determined. It was observed that as the amount of acid sites increases there is a possibility for degradation reactions (char, coke and gas) to happen rather than getting aromatic monomer after depolymerization of lignin.
- Recycle studies performed over H-USY (Si/Al=15) catalysts showed drastic decrease in the activity of the catalyst. This decrease in the catalytic activity can be expected, since dealkaline lignin contains ca. 967 ppm of Na which can possibly poison the Brönsted acid sites present in the H-USY (Si/Al = 15) catalyst which was confirmed by NH₃-TPD and ICP-OES analysis.
- Additionally, from XRD analysis it was observed that there was a decrease in crystallinity of H-USY (Si/Al = 15) catalyst after reaction.
- ²⁹Si and ²⁷Al NMR analysis of spent H-USY (Si/Al = 15) showed a change in the Si and Al environment of the catalyst during the course of the reaction, but ICP-OES showed that there was no leaching of Si and Al from the catalyst.
- N₂ sorption studies of the spent H-USY (Si/Al = 15) catalyst showed a reduction in the surface area of the catalyst, decrease in pore volume and increase in pore diameter.
- All these characterizations supports the fact that the structured solid acid catalysts (having definite pore and channel structure) like H-USY (Si/Al = 15) even though capable of giving a very high yield for aromatic monomers (ca. 60 %), are not stable under the reaction conditions.
- Therefore amorphous solid acid catalysts (SiO₂-Al₂O₃ (Si/Al = 5.3)) can be suggested as a better catalyst for performing further studies on depolymerization of lignin into aromatic monomers.

Chapter 3B discusses the solid acid catalysed depolymerization of six different types of actual lignin substrates (dealkaline, organosolv, alkali, ORG, EORG and bagasse) into aromatic monomers using amorphous solid acid catalysts (SiO₂-Al₂O₃ (Si/Al = 5.3))

- It was observed that $\text{SiO}_2\text{-Al}_2\text{O}_3$ ($\text{Si}/\text{Al} = 5.3$) catalyst could give a very high yield of aromatic monomers (ca. 58 %) even for dealkaline lignin having molecular weight of $60,000 \text{ gmol}^{-1}$ (Figure 5.2).

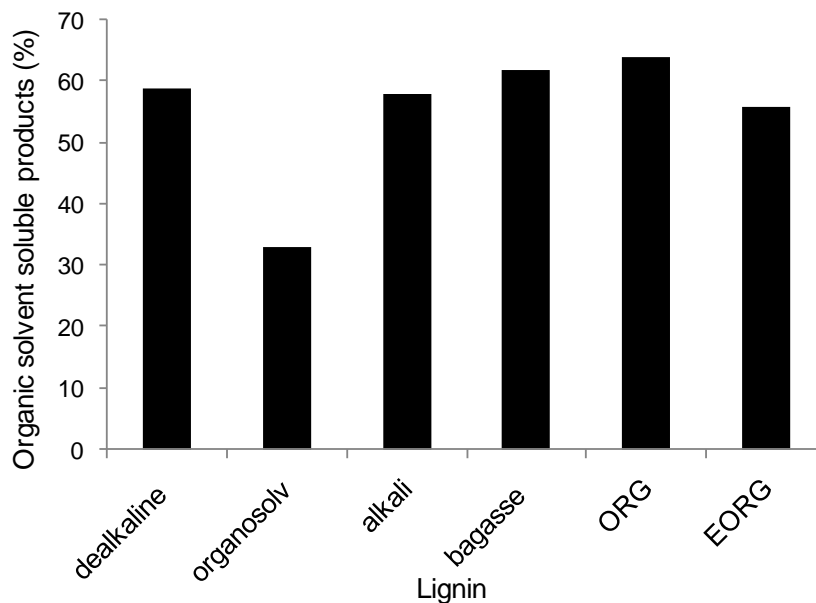


Figure 5.2. Effect of various lignin substrates. Reaction conditions: Lignin (0.5 g), $\text{SiO}_2\text{-Al}_2\text{O}_3$ (0.5 g), $\text{H}_2\text{O}:\text{CH}_3\text{OH}$ (1:5 v/v, 30 mL), 250 °C, 30 min., 1000 rpm, 0.7 MPa N_2 at RT. Products are extracted in THF for dealkaline lignin, in DEE for organosolv lignin, in EtOAc for alkali/EORG/ bagasse lignin and CHCl_3 for ORG lignin.

- Optimization of reaction conditions was done in order to improve the aromatic monomer yield. Reaction conditions like temperature, pressure, reaction medium, reaction time, stirring speed were optimized to obtain maximum amount of aromatic monomers. It was observed that at a temperature of 250 °C with 0.7 MPa N_2 at RT, in $\text{H}_2\text{O}:\text{CH}_3\text{OH}$ (1:5 v/v, 30 mL) solvent system, at 30 min., 1000 rpm with $\text{SiO}_2\text{-Al}_2\text{O}_3$ ($\text{Si}/\text{Al} = 5.3$) catalyst maximum amount of aromatic monomers (58 %) can be obtained.
- The optimized reaction conditions were employed for the depolymerization of several other kinds of lignin substrates (organosolv, alkali, ORG, EORG and bagasse) and they were also depolymerized successfully to aromatic monomers (40-60 %).

- The aromatic monomers obtained were isolated in pure form, from the complex mixture using column chromatography (3 nos.) and were well characterized using NMR, GC-MS and CHNS analysis.
- From the study done on lignin substrates like organosolv and ORG lignins, it was understood that $\text{SiO}_2\text{-Al}_2\text{O}_3$ ($\text{Si/Al} = 5.3$), an amorphous catalyst, can be effectively recycled with a slight decrease in the activity after each catalytic run (3 runs).
- From the study done on dealkaline lignin substrate using $\text{SiO}_2\text{-Al}_2\text{O}_3$ ($\text{Si/Al} = 5.3$) it was observed that the catalyst was getting deactivated. To study the reason behind deactivation, catalyst was well characterized after each recycle. From XRD and N_2 sorption analysis it was understood that there is an increase in the pore diameter of amorphous $\text{SiO}_2\text{-Al}_2\text{O}_3$ catalyst after the reaction. Also there is a reduction in surface area and pore volume according to N_2 sorption studies. $\text{NH}_3\text{-TPD}$ analysis showed a decrease in the acid sites, which was partially due to the poisoning of Brönsted acid sites by the Na ions present in the dealkaline substrate. ICP-OES analysis also showed that there was no leaching of Si and Al species from the catalyst even after the reaction, but ^{29}Si and ^{27}Al NMR showed a deformation in both Si and Al environment in the catalyst, which can also adversely affect the activity of the catalyst.
- From all these studies it was understood that even amorphous catalyst can undergo structural changes under the reaction conditions employed and also catalyst deactivation can be caused due to poisoning of the catalytic active sites by the Na metal ion contamination present in the lignin substrate (dealkaline lignin). Even the amorphous catalysts were undergoing few changes but were still found to be recyclable and gave high yields of aromatic monomers.

Chapter 4 describes the HDO studies of lignin derived aromatic monomers like phenol, guaiacol and eugenol using supported metal catalysts prepared by impregnation method.

- Role of metal and support in HDO reactions were studied using supported metal catalysts. Various types of metals like Pd, Pt and Ru supported on acidic ($\text{SiO}_2\text{-Al}_2\text{O}_3$, $\gamma\text{-Al}_2\text{O}_3$), basic (hydrotalcite) and neutral (carbons) supports were synthesized using impregnation method.

- Catalysts were characterized using various physico-chemical techniques like XRD, N₂ sorption and HRTEM analysis.
- HDO reactions for lignin derived aromatic monomers such as phenol, guaiacol and eugenol were performed at 200-250 °C using 1-3 MPa H₂ in hexadecane solvent for 1-6 h using supported metal catalysts (Figure 5.3).

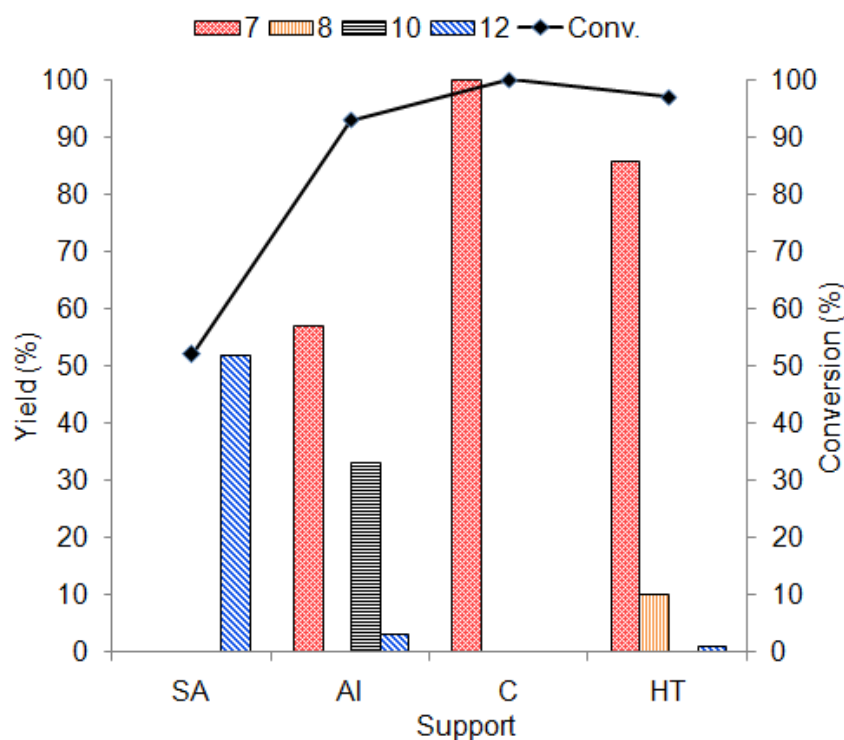


Figure 5.3. Effect of support on supported Pd catalysts in guaiacol HDO reactions.

Where '7' is methoxycyclohexanol, '8' is phenol, '10' is cyclohexanol and '12' is cyclohexane. Reaction conditions: Guaiacol (12 mmol), Catalyst (0.2 g), Hexadecane (30 mL), H₂ pressure at RT = 3 MPa, 250 °C, 1h. An error of ± 2 % was observed in all the repeated reactions.

- Reaction parameters like temperature, pressure and time were studied which showed that the optimized reaction conditions are 250 °C, 3 MPa H₂, 6 h where maximum hydrogenation or HDO activity could be obtained.
- Reusability of the supported metal catalysts in both the substrates (guaiacol and eugenol) was proven beyond doubt by subjecting the catalysts for reaction at least for 3 times. From XRD and ICP-OES analysis it was understood that there was no leaching of metal under the conditions employed.

- From HDO studies it was observed that noble metals facilitated the hydrogenation of aromatic rings and acidic supports helped in the deoxygenation reactions. It was also understood that irrespective of metal, HDO reactions happened only if the support has acidity.
- Also HDO studies of physical mixture of model compounds (guaiacol and eugenol compounds), which mimicks the lignin derived aromatic monomer mixture, was performed using supported metal catalysts. These studies will help in the complete HDO of lignin derived aromatic monomer using supported metal catalysts which will finally help in the one pot HDO of lignin into hydrocarbon fuels with a high efficiency.

List of Publications and Patents

1. Solid acid catalysed depolymerization of lignin into value added aromatic monomers.
Deepa, A. K.; Dhepe, P. L., *RSC Adv.*, **2014**, *4*, 12625-12629.
2. Value addition to lignocellulosics and biomass-derived sugars: An insight into solid acid based catalytic methods.
Bhaumik, P.; Deepa, A. K.; Kane, T.; Dhepe, P. L., *J. Chem. Sci.* **2014**, *126*, 373- 385.
3. Function of metals and supports on the hydrodeoxygenation of phenolic compounds.
Deepa, A. K.; Dhepe, P. L., *ChemPlusChem*, **2014**, DOI: 10.1002/cplu.201402145.
4. Lignin depolymerization into aromatic monomers over solid acid catalysts.
Deepa A. K.; Dhepe, P. L., *Manuscript under revision*.
5. Depolymerization of lignin using solid acid catalysts.
Deepa, A. K., Dhepe, P. L. Patent Application no: IN 2889 DEL 2010, US 13/467,128, AU 2012202602, BR 102012017987-3, ES 201300399.

Contributions to National/International Symposia/Conferences

1. Poster presented entitled “*Synthesis, Characterization & Catalysis of Sulfonated Mesoporous Silica*” during 20th National Symposium on Catalysis (2010) held at IIT, Madras, Chennai, India.
2. Poster presented entitled “Depolymerization of lignin using heterogeneous catalysts” during “*Current trends in Industrial catalysis*” (2012) held at National Chemical Laboratory (NCL), Pune, India.
3. Poster presented entitled “Heterogeneous catalysts in the conversion of lignocelluloses” during “2nd International Indo German Symposium on Green Chemistry and Catalysis for Sustainable Development” (2012) held at UDCT, Mumbai, India.
4. Poster presented entitled “*Heterogeneous catalysts in the conversion of lignocelluloses*” during “*Workshop on Industrial Catalysis & Catalysis Processes*” (2012) held at National Chemical Laboratory (NCL), Pune, India.
5. Oral presentation entitled “*Heterogeneous catalysts in the conversion of lignocelluloses*” during 21st National Symposium on Catalysis (2013) held at IICT, Hyderabad, India.
6. Poster presented entitled “*Heterogeneous catalysts in the depolymerization of lignin to aromatic monomers and their further hydrodeoxygenation*” during 16th International Symposium on Homogeneous & Heterogeneous Catalysis (ISHHC-16) (2013) held at Sapporo, Japan.
7. Poster presented entitled “*Hydrodeoxygenation of lignin derived aromatic monomers using supported metal catalysts*” during “*Post conference of ISHHC-16*” (2013) held at Jozanki, Japan.

Notes

Notes

Notes
